

Stony Brook University



OFFICIAL COPY

The official electronic file of this thesis or dissertation is maintained by the University Libraries on behalf of The Graduate School at Stony Brook University.

© All Rights Reserved by Author.

Soft Leptogenesis as a Viable Model of Baryogenesis

A Dissertation Presented

by

Chee Sheng Fong

to

The Graduate School

in Partial Fulfillment of the Requirements

for the Degree of

Doctor of Philosophy

in

Physics

Stony Brook University

August 2011

Stony Brook University

The Graduate School

Chee Sheng Fong

We, the dissertation committee for the above candidate for the Doctor of Philosophy degree, hereby recommend acceptance of this dissertation.

Maria Concepcion Gonzalez-Garcia - Advisor
Associate Professor, Department of Physics and Astronomy

George Sterman - Committee Chair
Professor, Department of Physics and Astronomy

Matthew Dawber
Assistant Professor, Department of Physics and Astronomy

Hooman Davoudiasl
Physicist, the Physics Department,
Brookhaven National Laboratory

This dissertation is accepted by the Graduate School

Lawrence Martin
Dean of the Graduate School

Abstract of the Dissertation

Soft Leptogenesis as a Viable Model of Baryogenesis

by

Chee Sheng Fong

Doctor of Philosophy

in

Physics

Stony Brook University

2011

The fact that we live in a matter-antimatter asymmetric universe is a deep mystery which the Standard Model of particle physics falls short of explaining. Imposing supersymmetry on the Standard Model plus right-handed neutrinos with lepton-number-violating Majorana masses results in the stability of the Higgs mass under quantum corrections, small active neutrino masses and generation of baryon asymmetry of the universe (baryogenesis) through leptogenesis. If supersymmetry is realized in nature, it has to be broken. The existence of soft supersymmetry-breaking terms introduce additional CP violating sources which can be utilized in leptogenesis in a scenario termed *soft leptogenesis*.

In the first part of this dissertation we study the contributions to CP violation in soft leptogenesis paying special attention to the role of thermal corrections. Using both field-theoretical and quantum mechanical approaches, we compute the CP asymmetries

and conclude that for all soft supersymmetry-breaking sources of CP violation considered, an exact cancellation between the leading order asymmetries produced in the fermionic and bosonic channels occurs at $T = 0$ and hence thermal effects are needed to prevent this cancellation.

Motivated by the relevance of quantum effects in resonant leptogenesis, we further investigate the impact of the use of quantum Boltzmann equations in soft leptogenesis. Then we study the lepton flavor effects in the temperature range relevant for soft leptogenesis $10^5 \text{ GeV} \lesssim T \lesssim 10^9 \text{ GeV}$ and show that they could enhance the efficiency of soft leptogenesis up to an order of 1000 from the unflavored scenario. This enhancement permits larger values of the required lepton-violating soft bilinear term up to a natural supersymmetric scale (TeV).

Finally, we discuss the effective theory appropriate for studying soft leptogenesis at temperatures $T > 10^7 \text{ GeV}$ where the main source of $B - L$ asymmetry is the CP asymmetry of a new anomalous R -charge. This results in baryogenesis through R -genesis with an efficiency that can be up to two orders of magnitude larger than in the usual estimates. Contrary to common belief, a sizable baryon asymmetry is generated also when thermal effects are neglected.

To my family.

Contents

List of Figures	x
List of Tables	xvii
Acknowledgements	xviii
List of Publications	xx
1 Introduction	1
1.1 Matter-Antimatter Asymmetric Universe	1
1.1.1 Sakharov’s three conditions for baryogenesis	4
1.1.2 The need to go beyond the Standard Model	6
1.2 Baryogenesis through Leptogenesis	9
1.2.1 Example: Type I seesaw and leptogenesis	9
1.2.2 Supersymmetry and leptogenesis	15
2 Soft Leptogenesis	19
2.1 Introduction	19
2.2 The Lagrangian	21
2.3 CP Asymmetries	24
2.3.1 Definition	24
2.3.2 Thermal effects	25
2.3.3 Field theoretical approach	28
2.3.4 Quantum mechanical approach	34
2.3.5 Vanishing of the CP asymmetry in decays	41
2.4 Unflavored Scenario	43
2.4.1 Relevant parameters and scenarios	43

2.4.2	Unflavored Boltzmann equations	47
2.4.2.1	Neglecting CP asymmetry in scatterings	53
2.4.2.2	Assuming superequilibration	54
2.4.3	Results	55
2.5	Discussion and Conclusions	58
3	Quantum Effects	63
3.1	The Possible Role of Quantum Effects	63
3.2	The Modification to the CP Asymmetry	64
3.3	Results	67
3.4	Discussion and Conclusions	74
4	The Role of Lepton Flavors	75
4.1	Introduction	75
4.2	Introducing Flavor Effects	77
4.2.1	Flavored CP asymmetries and reaction densities	77
4.2.2	Flavor structure	78
4.2.3	Lepton flavor equilibration interactions	80
4.3	Flavored Boltzmann Equations	85
4.4	Results	87
4.4.1	Universal trilinear scenario (UTS)	87
4.4.1.1	Gaugino contributions to the CP asymmetries	91
4.4.2	Simplified misaligned scenario (SMS)	94
4.4.3	Natural B values	98
4.4.4	Lepton flavor equilibration and low energy constraints	99
4.5	Discussion and Conclusions	102
5	Non-superequilibration and R-genesis	105
5.1	Introduction	105
5.2	Soft Leptogenesis Above the Superequilibration Temperature	108
5.2.1	Anomalous and non-anomalous symmetries	109
5.2.2	Chemical equilibrium conditions and conservation laws	112
5.2.2.1	General Constraints	114
5.2.2.2	Above the superequilibration temperature	117

5.2.3	Case I: Electron and down-quark Yukawa reactions in equilibrium	119
5.2.4	Case II: Electron and down-quark Yukawa reactions out of equilibrium	119
5.3	R-genesis Boltzmann Equations	120
5.3.1	NSE Regime: R-genesis in a simple case	124
5.4	Results	127
5.5	Discussion and Conclusions	133
6	Conclusions and Outlook	137
	Bibliography	140
A	Phase Conventions and Feynman Rules	152
B	Boltzmann Equations	158
B.1	General Boltzman Equations	158
B.1.1	Particle a not in kinetic equilibrium and $\mu_a = 0$	164
B.1.2	All particles in kinetic equilibrium with nonzero chemical potentials	166
B.1.3	Relation between chemical potential and particle density asymmetry	168
B.2	Boltzmann Equations for Soft Leptogenesis	168
B.2.1	Definitions	169
B.2.2	Derivations of unflavored Boltzmann equations	172
B.2.2.1	Approximations: integrated Boltzmann equations	179
B.2.3	Subtracted $2 \leftrightarrow 2$ scatterings	183
B.2.4	Lepton flavor and lepton flavor equilibration	187
B.2.5	Boltzmann equations in the superequilibration regime	191
B.2.6	Boltzmann equations in the non-superequilibration regime	196
C	Conditions in the Superequilibration Regime	201
C.1	Flavor charges	202
C.2	All Yukawa reactions in equilibrium	204
C.3	Electron and up-quark Yukawa reactions out of equilibrium	205

C.4	First generation Yukawa reactions out of equilibrium	206
-----	--	-----

List of Figures

- 1.1 The late thermal history of our Universe is pretty well-understood. Assuming that we start with a baryon-antibaryon symmetric Universe, the baryon density $n_B(T)$ and antibaryon density $n_{\bar{B}}(T)$ normalized to the total entropy density of the Universe $s(T)$ will freeze out (i.e. the baryon-antibaryon annihilation rate becomes much slower than the expansion rate of the Universe and the annihilations simply do not occur) at around $T \sim 22 \text{ MeV}$ resulting in $\frac{n_B}{s} \Big|_{T=T_0} = \frac{n_{\bar{B}}}{s} \Big|_{T=T_0} \sim 7 \times 10^{-20}$ where T_0 denote “the current temperature/time”. However, from the measurements of light element abundances generated during Big Bang nucleosynthesis as well as from the temperature anisotropies in the cosmic microwave background (CMB), we determine $\frac{n_B}{s} \Big|_{T=T_0} \sim 10^{-10}$ while the amount of $\frac{n_{\bar{B}}}{s} \Big|_{T=T_0}$ is negligibly small. 2

1.2	The extrapolation of the current known physics to early thermal history of the Universe. Inflation (a period of exponential expansion of the Universe) provides explanation to the flatness, isotropy and homogeneity of the Universe while reheating is the period at the end of inflation in which matter and radiation are produced by converting the energy stored in the vacuum. In order to generate the current observed baryon asymmetry $Y_{\Delta B}^0 \sim \mathcal{O}(10^{-10})$ of the Universe, some mechanism to generate nonzero $Y_{\Delta B}$ i.e. <i>baryogenesis</i> (or baryogenesis through <i>leptogenesis</i> which is the mechanism we will focus on in this thesis) has to happen after inflation but at $T > 38$ MeV. Notice that once baryogenesis is complete (there is no more asymmetry being generated), $Y_{\Delta B} = Y_{\Delta B}^0$ will be constant. In order to solve the hierarchy problem, we usually require some new physics at TeV scale. One of the most popular ones being supersymmetry which will be considered in this thesis.	5
1.3	The CP asymmetry in type I leptogenesis results from the interference between tree and loop wave and vertex diagrams. For the one loop wave diagram, there is an additional contribution from L conserving diagram to the CP asymmetry which vanishes when summing over the lepton flavor α	11
2.1	The CP asymmetries in the decays of \tilde{N}_{\pm} into scalars and fermions arise from the interference between tree and loop diagrams. The blob on the \tilde{N}_{\pm} line contains a sum over all possible self-energy correction diagrams while the blob on the vertex indicates sum over all possible vertex correction diagrams.	25
2.2	Feynman diagrams contributing to the RHSN self-energies at one-loop.	30
2.3	Feynman diagrams contributing to the RHSN decay vertex at one-loop.	30
2.4	Δ_{BF} (black solid curve), Δ^s (blue dashed curve) and Δ^f (red dotted curve) as a function of $z \equiv M/T$	33
2.5	Soft leptogenesis diagrams for sneutrino decays into scalars (1a), (1b), (1c) and into fermions (2a), (2b), (2c).	42

2.6	Evolution of $Y_{\tilde{N}_{\text{tot}}}$ (black solid curve) and $Y_{\Delta_{B-L}}$ (red dashed curve) assuming thermal initial RHSN abundance $Y_{\tilde{N}_{\text{tot}}}(z \rightarrow 0) = 2Y_{\tilde{N}}^{\text{eq}}(z \rightarrow 0)$ for $m_{\text{eff}} = 10^{-4}$ eV (top) and $m_{\text{eff}} = 10^{-2}$ eV (bottom). The equilibrium RHSN abundance $Y_{\tilde{N}_{\text{tot}}}^{\text{eq}}$ is given by the grey dotted curve.	60
2.7	Evolution of $Y_{\tilde{N}_{\text{tot}}}$ (black solid curve) and $Y_{\Delta_{B-L}}$ (red dashed curve) assuming zero initial RHSN abundance $Y_{\tilde{N}_{\text{tot}}}(z \rightarrow 0) = 0$ for $m_{\text{eff}} = 10^{-4}$ eV (top) and $m_{\text{eff}} = 10^{-2}$ eV (bottom). The equilibrium RHSN abundance $Y_{\tilde{N}_{\text{tot}}}^{\text{eq}}$ is given by the grey dotted curve.	61
2.8	Efficiency factor $ \eta $ as a function of m_{eff} for $M = 10^7$ GeV and $\tan \beta = 30$. The two curves correspond to vanishing initial RHSN abundance (solid black curve) and thermal initial RHSN abundance, (dashed red curve).	62
2.9	B, m_{eff} regions in which successful SL can be achieved considering only the contribution to CP asymmetry from mixing i.e. $\epsilon^S(T)$ as in eq. (2.93). We take $ \text{Im}A = 10^3$ GeV and different values of M as labeled in the figure. The two panels correspond to vanishing initial RHSN abundance (left) and thermal initial RHSN abundance (right).	62
3.1	Absolute value of the lepton asymmetry with the quantum time dependence of the CP asymmetry (solid) and without it (dashed) as a function of z for different values of m_{eff} as labeled in the figure. In each panel the two upper curves (black) correspond to the resonant case $R = 1$ while the lower two curves (red) correspond to the very degenerate case $R = 2 \times 10^{-4}$. The left (right) panels correspond to vanishing (thermal) initial RHSN abundance. The figure is shown for $M = 10^7$ GeV and $\tan \beta = 30$ though as discussed in the text, the results as normalized in the figure are very weakly dependent on those two parameters. . .	68

3.2	Absolute value of the lepton asymmetry with the quantum time dependence of the CP asymmetry (solid) and without it (dashed) for vanishing initial RHSN abundance. For comparison in the right panel we show the result that would be obtained with $\Delta_{BF}(z) = 1$	70
3.3	Efficiency factor as a function of m_{eff} and R for $M = 10^7$ GeV and $\tan \beta = 30$. The left (right) panels correspond to vanishing (thermal) initial RHSN abundance. In the upper panels the different curves correspond to $R = 1$ (black thick solid) , 0.1 (dashed), 10^{-2} (dotted), 10^{-3} (dash-dotted) and 10^{-4} (thin solid). For comparison we also show the results without including the quantum effects (purple thick solid line). In the lower panels we plot the ratio of the efficiency factor with and without quantum corrections as a function of R . The different curves from top to bottom correspond to $m_{\text{eff}} = 10^{-1}$ eV (thick solid), 10^{-2} eV (dashed), 10^{-3} eV (dotted), 10^{-4} eV (dot-dashed), and 10^{-5} eV (thin solid).	72
3.4	B, m_{eff} regions in which successful SL can be achieved with (left panels) and without (right panels) quantum effects. We take $ \text{Im}A = 10^3$ GeV and $\tan \beta = 30$ and different values of M as labeled in the figure. The upper (lower) panels correspond to vanishing (thermal) initial RHSN abundance.	73
4.1	The lepton flavor violating lepton-slepton scatterings through the exchange of $SU(2)_L$ and $U(1)_Y$ gauginos $\tilde{\lambda}_G$	81
4.2	The top panel shows the ratio of $\bar{\Gamma}_{\text{LFE}}$ to the Hubble expansion rate H at z_{dec} as a function of \tilde{m}_{od} for $m_{\text{eff}} = 0.1$ eV and $\tan \beta = 30$ and three values of M . The bottom panel shows in the $(P_\alpha m_{\text{eff}}, M)$ plane, contours of constant values of \tilde{m}_{od} (in GeV) for which $\bar{\Gamma}_{\text{LFE}}(z_{\text{dec}}^\alpha) \geq P_\alpha \bar{\Gamma}_{\text{ID}}(z_{\text{dec}}^\alpha)$	83
4.3	Efficiency factor $ \eta_{\text{fla}}/\eta_0 $ as a function of m_{eff} for $M = 10^7$ GeV and $\tan \beta = 30$. The two curves correspond to vanishing initial RHSN abundance (solid black curve) and thermal initial RHSN abundance, (dashed red curve).	88

4.4	<p>B, m_{eff} regions in which successful SL can be achieved when flavor effects are included with $P_e = P_\mu = P_\tau = 1/3$ We take $\text{Im}A = 10^3$ GeV and $\tan\beta = 30$ and different values of M as labeled in the figure. The dashed contours are the corresponding ones when flavor effects are not included. The two panels correspond to vanishing initial RHSN abundance (left) and thermal initial RHSN abundance (right).</p>	90
4.5	<p>Maximum baryon asymmetry as a function of B (left) and M (right). The solid (dashed) lines are for no flavor effects and vanishing (thermal) initial RHSN abundance. The dotted (dash-dotted) lines are the corresponding asymmetries after including flavor effects with $P_e = P_\mu = P_\tau = 1/3$. The horizontal line correspond to the 1σ WMAP measurements in the ΛCDM model eq. (1.2).</p>	91
4.6	<p>B, m_{eff} regions in which successful SL can be achieved when flavor effects are included with $P_e = P_\mu = P_\tau = 1/3$ and for different sources of CP violation. In all cases we take $A = m_2 = 10^3$ GeV and $\tan\beta = 30$ and different values of M and ϕ_A and ϕ_g as labeled in the figure (see text for details). The left (right) panels correspond to vanishing (thermal) initial RHSN abundance</p>	93
4.7	<p>The dependence of the efficiency – normalized to the flavor equipartition case $P = (1/3, 1/3, 1/3)$ – on the values of the lepton flavor projections (top) and on m_{eff} (bottom). The figures correspond to $M = 10^6$ GeV and $\tan\beta = 30$.</p>	96
4.8	<p>Maximum values of B and M which can lead to SL as a function of the flavor projections (we plot both as a function of P_τ or $1 - P_\tau$ for clarity when either P_τ or $1 - P_\tau$ is very small). The figure corresponds to $A \sin\phi_A = 1$ TeV and $\tan\beta = 30$.</p>	99
4.9	<p>The dependence of the efficiency (normalized to the flavor equipartition case $P = (1/3, 1/3, 1/3)$) on the off-diagonal soft slepton mass parameter \tilde{m}_{od}, for different values of M and of the flavor projections (see text for details).</p>	100

- 4.10 This figure shows the excluded region (shaded in yellow) of $\tilde{m}_{od} \cos \beta$ versus $m_{SUSY}(\cos \beta)^{\frac{3}{4}}/(\sin \beta)^{\frac{1}{4}}$ arising from the present bound on $BR(\mu \rightarrow e\gamma) \leq 1.2 \times 10^{-11}$, together with the minimum value of $\tilde{m}_{od} \cos \beta$ for which LFE effects start damping out flavor effects in SL. Three bands are shown corresponding to $M = 10^5$ GeV, $M = 10^6$ GeV and $M = 10^7$ GeV. The width of the bands represents the range associated with variations of $P_\alpha m_{\text{eff}}$ in the range 0.003 eV–10 eV, where P_α is the largest of the three flavor projections. The vertical dashed line represents the value of $m_{SUSY}/(\tan \beta)^{\frac{1}{2}}$ (for $\tan \beta = 1$) required to explain the discrepancy between the SM prediction and the measured value of a_μ . [129] 101
- 5.1 The lepton-slepton scatterings induced by soft gaugino masses $m_{\tilde{g}}$ through the exchange of $SU(2)_L$ and $U(1)_Y$ gauginos $\tilde{\lambda}_G$. Notice that the amplitude squared of these processes are proportional to $m_{\tilde{g}}^2$ and vanish in the limit of vanishing $m_{\tilde{g}}$ 107
- 5.2 Evolution of $Y_{\Delta_{B-L}}$. The solid continuous (red) line depict the complete results in the $m_{\tilde{g}} = \mu \rightarrow 0$ limit. The dashed (blue) line correspond to the same limit but with all thermal corrections to the CP asymmetries neglected. The dotted (black) line gives $Y_{\Delta_{B-L}}$ with thermal effects when SE is assumed. Panels on the left and right sides are respectively for Case I ($h_{e,d}$ Yukawa equilibrium) and Case II ($h_{e,d}$ Yukawa non-equilibrium). Upper and lower panels are respectively for $m_{\text{eff}} = 0.05$ eV and $m_{\text{eff}} = 0.20$ eV. 129
- 5.3 Efficiency factor η as a function of the washout parameter m_{eff} for Case I ($h_{e,d}$ Yukawa equilibrium) and different values of $m_{\tilde{g}} = \mu$. The red continuous line corresponds to the $m_{\tilde{g}} = \mu = 100$ GeV which is still in the full NSE regime, while the dashed blue line to the same limit but with thermal corrections neglected. The red dash-dotted line corresponds respectively to $m_{\tilde{g}} = \mu = 500$ GeV, and the black dotted line to SE with $m_{\tilde{g}}, \mu \rightarrow \infty$ 130

5.4	The final value of $Y_{\Delta_{B-L}}$ normalized to the SE result $Y_{\Delta_{B-L}}^{SE}$ as a function of $m_{\tilde{g}}$ and μ for Case I ($h_{e,d}$ Yukawa equilibrium) and $m_{\text{eff}} = 0.20$ eV. The red continuous line corresponds to varying simultaneously both parameters holding $m_{\tilde{g}} = \mu$. The blue dashed line corresponds to varying only $m_{\tilde{g}}$ in the limit $\mu \rightarrow \infty$. The green dotted line corresponds to varying only μ in the limit $m_{\tilde{g}} \rightarrow \infty$	131
5.5	Final values of the charge density asymmetries as a function of $m_{\tilde{g}} = \mu$ for Case I ($h_{e,d}$ Yukawa equilibrium) and $m_{\text{eff}} = 0.20$ eV. Thick red line: $Y_{\Delta_{B-L}}$; thick blue line: $3Y_{\Delta_{R_\chi}} - Y_{\Delta_{R_B}}$; thin dashed purple line: $Y_{\Delta_{R_B}}$; thin dotted purple line: $Y_{\Delta_{R_\chi}}$	132
A.1	Vertex factors involving $SU(2)_L$ and $U(1)_Y$ gauginos	156
A.2	Vertex factors involving \tilde{N}_\pm	157

List of Tables

- 5.1 B, L, PQ and R charges for the particle supermultiplets that are labeled in the top row by their L-handed fermion component. Note that we use chemical potentials for the R-handed $SU(2)_L$ singlet fields u, d, e that have opposite charges with respect to the ones for u^c, d^c, e^c given in the table. The R charges for bosons are determined by $R(b) = R(f) + 1$ 109
- 5.2 Charges for the fermionic and bosonic components of the SUSY multiplets under the R -symmetries defined in eqs.(5.5), (5.6) and (5.9). Supermultiplets are labeled in the top row by their L-handed fermion component. We use chemical potentials for the R-handed $SU(2)_L$ singlet fields u, d, e that have opposite charges with respect to the ones for u^c, d^c, e^c given in the table. 111

Acknowledgements

First of all, I would like to express my greatest gratitude to my thesis advisor Concha Gonzalez-Garcia. This thesis would not be possible without her patient guidance, support and critique all throughout my PhD years. I also thank her for carefully and painstakingly going over the draft of this thesis numerous times! Otherwise, it would not be half as readable as it is now. Any remaining confusion is solely due to my own blunder.

Next, I would like to thank the Department of Physics and Astronomy at Stony Brook University for admitting me and giving me the opportunity to teach in the first two years. For the rest of the four years, I would like to acknowledge the C. N. Yang Institute for Theoretical Physics for the generous financial support and providing a stimulating environment to do physics. I especially thank Prof. George Sterman, Betty Gasparino, Doreen Matesich and Emily Vance who have managed the institute in such an ordered manner. I want to take this chance to thank George for carefully reading my thesis and providing many corrections to my (poor) grammar and useful suggestions to make some confusing statements clearer. I would also like to thank the computer system manager Chi Ming Hung who has helped to solve my numerous computer-related issues. During my stay at the institute, I am fortunate to have met the friends who have helped, advised and inspired me. They are Ilmo Sung, Yu-tin Huang, Peng Dai, Itai Ryb, Leo Almeida, Zuowei Liu and Ning Chen. I would also like to take this opportunity to thank my considerate and thoughtful officemates Dharmesh Jain, Wenbin Yan, Ahmet Ozan Erdogan, Pedro Liendo and Prerit Jaiswal who help to make this office a comfortable environment to work in.

Part of this work was done with my collaborators Juan Racker, Enrico Nardi, Juan Gonzalez-Fraile and Oscar Eboli to whom I thank for patiently

putting up with my ignorance and stubbornness. I would like to take this opportunity to thank Enrico for carefully going over the final draft of this thesis and providing many corrections (even in the bibliography!).

I am indebted to the professors who taught me the joy of learning and doing physics. I thank Prof. Peter van Nieuwenhuizen, George Sterman, Robert Shrock, Barry McCoy, Warren Siegel, Edward Shuryak, Ismail Zahed and Alexandre Abanov.

This section would not be complete without thanking my dear friends whom we shared both fun and difficult times during my years in graduate school. I thank Bryan Kim, Chris Malone, Manas Kulkarni, Prasad Hegde, Abhijit Gadde, Tom Berlijn, Ritwik Mukherjee, Rik Sarkar, Somnath Basu, Marija Kotur, Prerit Jaiswal, Soumya Mohapatra, Mithun Bhattacharya, Qingzhou Jiang, Clare Tao, Heli Vora, Divya Bhatnagar and Sriram Ganeshan. During the autumns of my PhD years, I am fortunate (thanks to Concha) to have the opportunity to travel to beautiful Barcelona (Universitat de Barcelona) for one or two months to carry out my research. Needless to say, most of the big progress in this work happened during my stay in Barcelona. I especially thank my good friends Jordi Salvado and Johanna Fuks who made my annual short stay at Barcelona felt at home.

I would also like to thank all the people whom I have met in the Buddhism Study and Practice group at Stony Brook University. I especially thank Hai-Dee Lee, Sheila Sussman, Jen-Chih Hsieh, Richard Rocco, and Chunmei Tang for sharing their experiences in meditation. Practicing mindfulness and awareness have been helpful to keep my blood pressure in check especially while completing this thesis.

To my dear friends who are physically far away, I thank them for being there all the time and keeping me up-to-date about their well-being and interesting lives. They are always sources of motivation and inspiration to me. They are Kim Hang Do, Louis Wong, Pick Wei Lau, King Hong Yeo, Teng Ean Tan, Chen Yong Pang, Jacky Tong, Michael Lim and the rest. Due to limited space (and time), it is impossible to list all of you but I sincerely thank you all.

Last but not least, I would like to thank the people who are most dear to me, my family: my beloved grandma, my parents, my three sisters and my brother-in-law for their continuous and selfless love and support.

List of Publications

This thesis is mainly based on the following publications:

1. Chee Sheng Fong and M. C. Gonzalez-Garcia, “Flavoured Soft Leptogenesis,” *JHEP* **0806**, 076 (2008) [arXiv:0804.4471 [hep-ph]].
2. Chee Sheng Fong and M. C. Gonzalez-Garcia, “On Quantum Effects in Soft Leptogenesis,” *JCAP* **0808**, 008 (2008) [arXiv:0806.3077 [hep-ph]].
3. Chee Sheng Fong and M. C. Gonzalez-Garcia, “On Gaugino Contributions to Soft Leptogenesis,” *JHEP* **0903**, 073 (2009) [arXiv:0901.0008 [hep-ph]].
4. Chee Sheng Fong, M. C. Gonzalez-Garcia, Enrico Nardi, and J. Racker, “Flavoured soft leptogenesis and natural values of the B term,” *JHEP* **1007**, 001 (2010) [arXiv:1004.5125 [hep-ph]].
5. Chee Sheng Fong, M. C. Gonzalez-Garcia, and Enrico Nardi, “Early Universe effective theories: The soft leptogenesis and R-genesis case,” *JCAP* **1102**, 032 (2011) [arXiv:1012.1597 [hep-ph]].

Additional work completed in the duration of the author’s PhD career:

1. O. J. P. Eboli, Chee Sheng Fong, J. Gonzalez-Fraile and M. C. Gonzalez-Garcia, “Determination of the Spin of New Resonances in Electroweak Gauge Boson Pair Production at the LHC,” *Phys. Rev. D* **83**, 095014 (2011) [arXiv:1102.3429 [hep-ph]].

2. Chee Sheng Fong, M. C. Gonzalez-Garcia, and J. Racker, “CP violation from Scatterings with Gauge Bosons in Leptogenesis,” *Phys. Lett. B* **697**, 463-470 (2011) [arXiv:1010.2209 [hep-ph]].
3. Chee Sheng Fong, M. C. Gonzalez-Garcia, Enrico Nardi, and J. Racker, “Supersymmetric Leptogenesis,” *JCAP* **1012**, 013 (2010) [arXiv:1009.0003 [hep-ph]].
4. Chee Sheng Fong and J. Racker, “On fast CP violating interactions in leptogenesis,” *JCAP* **1007**, 001 (2010) [arXiv:1004.2546 [hep-ph]].

Chapter 1

Introduction

1.1 Matter-Antimatter Asymmetric Universe

We can define matter as *substance* that is made of baryons (mostly protons and neutrons) and leptons (mostly electrons) while antimatter as substance that is made of antibaryons and antileptons. If we assign baryon number $B = 1$ and lepton number $L = 1$ to baryon and lepton respectively, then antibaryon and antilepton carry $B = -1$ and $L = -1$ respectively. On the Earth, we have only a very tiny amount of antimatter that comes from the cosmic rays. Other than that, antiparticles exist mainly in the human-made particle colliders. Even for the Universe as a whole, there are various sources of evidence which show that antimatter is very rare (see e.g. [1]). While it is hard to determine the lepton density of the Universe, there are several probes to measure (indirectly) the baryon density of the Universe. In particular, the late thermal history of the Universe as illustrated in Figure 1.1 (from time $t \sim 10^{-2}$ s after the beginning of the Universe until *today*) is considered pretty well-understood due to these measurements.

The experimental determination of the baryon content of the Universe at the earliest time comes from the measurement of light element abundances (D, ^3He , ^4He and ^7Li) generated during primordial nucleosynthesis (also known as Big Bang nucleosynthesis or BBN) that took place at around $t \sim 10^{-2}$ to 100 s ($T \sim 10$ to 0.1 MeV). These abundances crucially depend upon the baryon density of the Universe during that period. The measured abundances imply that the baryon density n_B normalized to the total entropy density of the

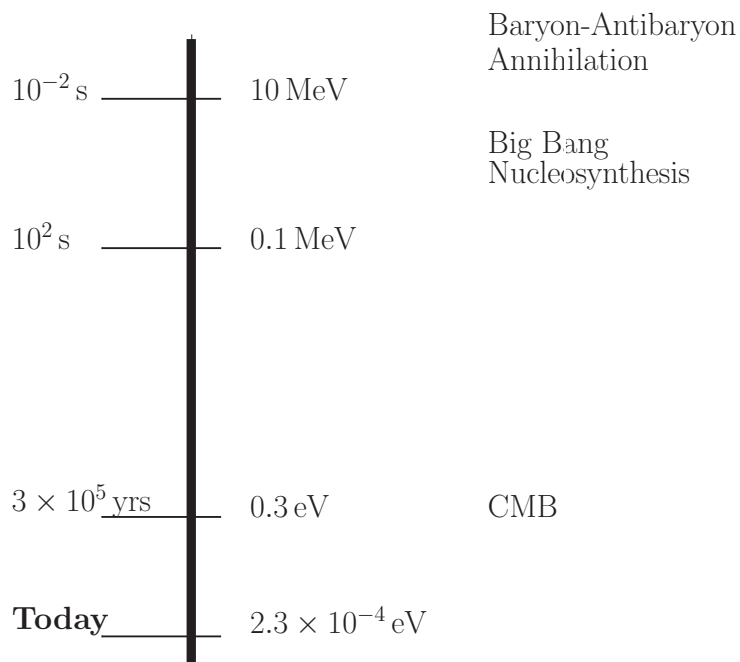


Figure 1.1: The late thermal history of our Universe is pretty well-understood. Assuming that we start with a baryon-antibaryon symmetric Universe, the baryon density $n_B(T)$ and antibaryon density $n_{\bar{B}}(T)$ normalized to the total entropy density of the Universe $s(T)$ will freeze out (i.e. the baryon-antibaryon annihilation rate becomes much slower than the expansion rate of the Universe and the annihilations simply do not occur) at around $T \sim 22 \text{ MeV}$ resulting in $\frac{n_B}{s} \Big|_{T=T_0} = \frac{n_{\bar{B}}}{s} \Big|_{T=T_0} \sim 7 \times 10^{-20}$ where T_0 denote “the current temperature/time”. However, from the measurements of light element abundances generated during Big Bang nucleosynthesis as well as from the temperature anisotropies in the cosmic microwave background (CMB), we determine $\frac{n_B}{s} \Big|_{T=T_0} \sim 10^{-10}$ while the amount of $\frac{n_{\bar{B}}}{s} \Big|_{T=T_0}$ is negligibly small.

Universe s has to be [2]¹

$$Y_B^{BBN} = \frac{n_B}{s} \Big|_{T=T_0} = (7.92 \pm 1.35) \times 10^{-11}, \quad (1.1)$$

where T_0 means “the present temperature/time”².

The second probe is the precise determination of the temperature fluctuations of the cosmic microwave background (CMB). The CMB photons originated at the time $t \sim 3 \times 10^5$ years (or $T \sim 0.3$ eV) when the Universe first became transparent (i.e. photons were decoupled from the baryonic plasma and started to propagate freely). The anisotropies in the CMB depend upon the period of oscillations of the photon-baryon fluid which is determined by the baryon density. The five-year measurement of the CMB with the Wilkinson Microwave Anisotropy Probe (WMAP) spacecraft determined that [3]

$$Y_B^{CMB} = \frac{n_B}{s} \Big|_{T=T_0} = (8.78 \pm 0.24) \times 10^{-11}. \quad (1.2)$$

The agreement between the two measurements (1.1) and (1.2) at two different periods (and different physics) of the Universe is one of the great successes of modern cosmology.

From the theoretical side, one could question if our current understanding of particle physics and cosmology is able to predict (‘postdict’ to be precise) $n_B/s|_{T=T_0} \sim \mathcal{O}(10^{-10})$ as in eqs. (1.1) and (1.2). In fact, due to the expansion of the Universe, the annihilations between baryons and antibaryons will not be “perfect”. At some point, the annihilations rate will be slower than the expansion rate of the Universe and the annihilations become ineffective, resulting in some leftover baryons and antibaryons (these leftovers are known as the *freeze-out* values). If we assume that the Universe starts with equal amount of baryons and antibaryons, the baryon-antibaryon annihilations become ineffective at $T \sim 22$ MeV and the number densities of baryons and antibaryons will freeze out to be $n_B/s|_{T=T_0} = n_{\bar{B}}/s|_{T=T_0} \sim 7 \times 10^{-20}$ [1], which is much

¹It is an excellent approximation to treat the expansion of the Universe as adiabatic with the total entropy $S = sV$ being constant. Hence, if there is no interaction which changes the number of baryons, n_B/s will be constant.

²In principle, T_0 should be the temperature when nucleosynthesis took place. However, at quite before this temperature at $T \sim 22$ MeV, the number of baryons and antibaryons had already frozen out and from that time onwards there is no interaction which violates B , hence the ratio n_B/s will be fixed and T_0 can be taken as “the present temperature”.

too small compared to the current observed value of $n_B/s|_{T=T_0} \sim \mathcal{O}(10^{-10})$. In order to avoid this “annihilation catastrophe”, some mysterious mechanism has to separate baryons and antibaryons when $n_B/s = n_{\bar{B}}/s \sim 8 \times 10^{-11}$ which occurs at $T \sim 38 \text{ MeV}$. Nonetheless, the horizon at that moment only contained about 10^{-7} solar masses and hence this possibility is totally precluded by causality [1].

In brief, we need to explain two facts: $n_B/s|_{T=T_0} \sim \mathcal{O}(10^{-10})$ and the absence of $n_{\bar{B}}/s|_{T=T_0}$. One possibility is to have a baryon asymmetry $Y_{\Delta B} \equiv (n_B - n_{\bar{B}})/s \sim \mathcal{O}(10^{-10})$ as an initial condition. However if we accept inflation (a period of exponential expansion of the Universe) as an explanation to the flatness, isotropy, and homogeneity of the Universe, any preexisting baryon asymmetry would have been diluted to a very negligible value after inflation. Hence, the most reasonable conclusion is that a nonzero $Y_{\Delta B}$ is dynamically generated in the early Universe after inflation but at $T > 38 \text{ MeV}$ as illustrated in Figure 1.2. In fact, $Y_{\Delta B} \sim \mathcal{O}(10^{-10})$ implies a very small imbalance between the number of baryons and antibaryons in the early Universe. For example if we translate this into the asymmetry between number density of quarks and antiquarks at $t \sim 10^{-6} \text{ s}$, we have [1]

$$\frac{n_q - n_{\bar{q}}}{n_q} \sim 3 \times 10^{-8}. \quad (1.3)$$

That is, for every 30 million and 1 quarks, there was about 30 million antiquarks, a very small excess indeed. However as we will see to generate this small excess is a nontrivial problem in particle physics.

1.1.1 Sakharov’s three conditions for baryogenesis

As first pointed out by Sakharov in 1967 [4], we can list down three necessary conditions in order to dynamically generate a nonzero $Y_{\Delta B}$:

1. Baryon number (B) violation
2. Charge (C) and charge-parity (CP) violation
3. Departure from thermal equilibrium

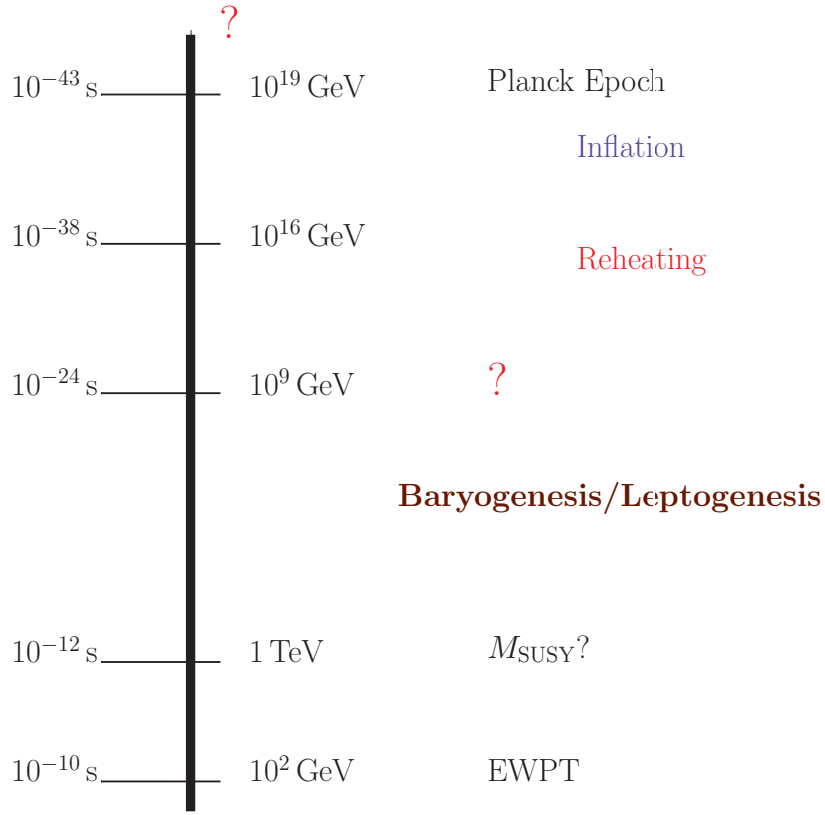


Figure 1.2: The extrapolation of the current known physics to early thermal history of the Universe. Inflation (a period of exponential expansion of the Universe) provides explanation to the flatness, isotropy and homogeneity of the Universe while reheating is the period at the end of inflation in which matter and radiation are produced by converting the energy stored in the vacuum. In order to generate the current observed baryon asymmetry $Y_{\Delta B}^0 \sim \mathcal{O}(10^{-10})$ of the Universe, some mechanism to generate nonzero $Y_{\Delta B}$ i.e. *baryogenesis* (or baryogenesis through *leptogenesis* which is the mechanism we will focus on in this thesis) has to happen after inflation but at $T > 38$ MeV. Notice that once baryogenesis is complete (there is no more asymmetry being generated), $Y_{\Delta B} = Y_{\Delta B}^0$ will be constant. In order to solve the hierarchy problem, we usually require some new physics at TeV scale. One of the most popular ones being supersymmetry which will be considered in this thesis.

The first condition is fairly obvious. We need to have at least an interaction that violates B .

As for the second condition, we can understand it as follows. Let us assume that there is a B -violating interaction which produces a final state with $B = b$. In order to generate a net $B \neq 0$, we need to have C violation such that the charge conjugate interaction which produces the final state with $B = -b$ occurs at a different rate. If we take into account the left and right chiralities of the states, we could have B -violating interactions as follows: $X \rightarrow B_L B_L$ and $X \rightarrow B_R B_R$ with CP conjugate interactions $\bar{X} \rightarrow \bar{B}_R \bar{B}_R$ and $\bar{X} \rightarrow \bar{B}_L \bar{B}_L$ where X is a boson that has $B = 0$ while $B_{L,R}$ are respectively left- and right-handed fermions that carry $B = 1$. If only C is violated while CP is conserved, even though $\Gamma(X \rightarrow B_L B_L) \neq \Gamma(\bar{X} \rightarrow \bar{B}_L \bar{B}_L)$ and $\Gamma(X \rightarrow B_R B_R) \neq \Gamma(\bar{X} \rightarrow \bar{B}_R \bar{B}_R)$, we would have $\Gamma(X \rightarrow B_L B_L) = \Gamma(\bar{X} \rightarrow \bar{B}_R \bar{B}_R)$ and $\Gamma(X \rightarrow B_R B_R) = \Gamma(\bar{X} \rightarrow \bar{B}_L \bar{B}_L)$. As a result, we have $\Gamma(X \rightarrow B_L B_L) + \Gamma(X \rightarrow B_R B_R) = \Gamma(\bar{X} \rightarrow \bar{B}_R \bar{B}_R) + \Gamma(\bar{X} \rightarrow \bar{B}_L \bar{B}_L)$ and the net baryon number is still zero. Hence we conclude that both C and CP violation are necessary.

As for the third condition, the need to depart from thermal equilibrium follows from the fact that in chemical equilibrium, the chemical potentials associated with all non-conserved quantum numbers e.g. B , L vanish. Also, particle and antiparticle masses are guaranteed to be equal by CPT invariance. Hence the phase space density of baryons and antibaryons are identical $(e^{E/T} + 1)^{-1}$ implying that $n_B = n_{\bar{B}}$ [1].

1.1.2 The need to go beyond the Standard Model

In principle, the Standard Model (SM) fulfills all three Sakharov's conditions. Due to non-trivial vacuum gauge configurations, both B and L are anomalous under the SM electroweak (EW) gauge group and hence are not conserved at the quantum level. It turns out that only the linear combination of the form $B - L$ is anomaly-free and hence is absolutely conserved (taking into account the lepton flavors, the conserved charges are $B/3 - L_\alpha$ with $\alpha = e, \mu, \tau$). At zero temperature, the rate for $B + L$ -violating interactions is associated with the instanton solution that describes the tunneling between EW vacua of different B (also L). This rate is proportional to $\exp(-16\pi^2/g_W^2)$ where $g_W =$

$g_2/\sin\theta_W$ and hence is very suppressed [5]. However, at finite temperature when $T > \text{few} \times 10^2 \text{ GeV}$, Kuzmin, Rubakov, and Shaposhnikov showed that these processes would have enough energy to climb over (instead of tunnel through) the barriers that separate these vacua [6]. The maximum free energy for this transition is that of a static field configuration called *sphaleron*. In the rest of the thesis, we will call these $B + L$ -violating processes simply as EW sphaleron processes. For $T \gg \mathcal{O}(100) \text{ GeV}$, the rate of EW sphaleron processes is estimated to be³

$$\Gamma_{B+L} \simeq 250\alpha_W^5 T, \quad (1.4)$$

where $\alpha_W = g_W^2/(4\pi)$. Comparing this to the expansion rate of the Universe, we obtain that for $T \lesssim 10^{12} \text{ GeV}$, the EW sphaleron interactions are in thermal equilibrium.

In the SM, C is maximally violated while CP is violated via the nonzero phase δ_{CP} in the Cabbibo-Kobayashi-Maskawa (CKM) [8, 9] matrix that has been experimentally observed in the K and B mesons system. Finally, the out of thermal equilibrium condition could happen during the electroweak phase transition (EWPT) if it is first-order. The realization of baryogenesis with the ingredients above is termed EW baryogenesis [10].

Nonetheless, it turns out that EW baryogenesis in the SM fails in two aspects. Firstly the experimentally measured CP violation which is proportional to the Jarlskog invariant J_{CP} [11] is too small to explain the baryon asymmetry [12]. Secondly the lower bound on the Higgs mass from LEP ($m_H > 114 \text{ GeV}$) [2] precludes the required first order EWPT [13]. Hence, we need to go beyond the SM. In the following, we will give an incomplete list of possible mechanisms to generate the cosmic baryon asymmetry⁴.

One of the most popular extensions to the SM is supersymmetry (SUSY) because it has many nice features like stabilizing the quantum correction to the Higgs mass, providing a dark matter candidate, giving unification of the gauge couplings at the Grand Unification Theory (GUT) scale etc⁵. In the

³Please refer to Section 3 of the review [7] and the references therein for the details on $B + L$ -violating interactions.

⁴The reader can also refer to Section 1.2 of ref. [7] and references therein for a more complete list.

⁵A detailed discussion on supersymmetry is beyond the scope of this thesis. The author

Minimal Supersymmetric Standard Model (MSSM), there is actually a narrow window in the SUSY parameter space that allows EW baryogenesis to be successful [16].

On the other hand, GUT baryogenesis [4, 17–21] (including its supersymmetric extension) could directly generate the baryon asymmetry in the out of equilibrium decays of heavy GUT bosons which violate both B and L , with the required CP phases from the gauge and Yukawa couplings. However in $SU(5)$ or any grand unification model with higher symmetries that contains $U(1)_{B-L}$ as a subgroup, $B + L$ is violated but not $B - L$. Hence, the $B + L$ -violating EW sphaleron interactions which come into equilibrium at $T \lesssim 10^{12}$ GeV as discussed earlier, would completely deplete this asymmetry. Furthermore, the non-observation of proton decay also puts a lower bound on the mass of the decaying GUT boson to be at $M_{GUT} \sim 10^{16}$ GeV. In summary, a high reheating temperature $T_{RH} \gg 10^{12}$ GeV after inflation is required in order to thermally produce sufficient heavy GUT bosons for baryogenesis. But such high T_{RH} is not desirable from the point of view of producing unwanted relics like monopoles or gravitinos as we will discuss in more detail in Section 1.2.2.

There is yet another, bigger window for baryogenesis, which is to make use of the EW sphaleron process which is in thermal equilibrium at $T \gtrsim 100$ GeV together with a new interaction that violates L , C and CP . The basic idea is to have a L , C and CP violating interaction that occurs out of thermal equilibrium (i.e. proceeds slower than the expansion rate of the Universe⁶) resulting in a nonzero lepton asymmetry which is then transformed into baryon asymmetry with the help of EW sphaleron processes. This scenario was first conceived by Fukugita and Yanagida in 1986 [22] and is termed baryogenesis through *leptogenesis* or leptogenesis for short⁷. This is the mechanism we will focus on in this thesis.

has learned most of his knowledge on supersymmetry phenomenology from the two excellent textbooks by Baer and Tata [14] and by Drees, Godbole and Roy [15].

⁶This can happen, for example, in the decays of a sufficiently massive particle.

⁷For comprehensive reviews please refer to refs. [7, 23].

1.2 Baryogenesis through Leptogenesis

The discovery of neutrino oscillations has promoted leptogenesis to a very attractive scenario to explain the origin of the cosmic baryon asymmetry. This is because as we will explain below without any fine-tuning of the model parameters, a neutrino mass scale naturally compatible with the solar and atmospheric neutrino mass square differences would be optimal to yield the correct value of the baryon asymmetry. The possibility of explaining two apparently unrelated experimental facts (neutrino oscillations and the baryon asymmetry) within a single framework has boosted the interest in leptogenesis studies, leading to important developments in the field, as for example the inclusion of thermal corrections [24, 25], spectator processes [26, 27], flavor effects [28–32], CP asymmetries in scatterings [33], lepton asymmetries from the decays of the heavier Majorana neutrinos [34, 35], and many more.

1.2.1 Example: Type I seesaw and leptogenesis

The simplest realization of leptogenesis is in the type I seesaw framework [36–39] where heavy SM gauge singlet fermions ν_{R_i} (also known as right-handed neutrinos or RHN) are added to the SM. They have L violating Majorana masses M_i and when decay out of thermal equilibrium produce dynamically a lepton asymmetry which is partially converted into a baryon asymmetry due to fast EW sphaleron processes.

By adding n generations of RHN to the SM⁸, the Lagrangian of type I seesaw is given by

$$\mathcal{L}_I = \mathcal{L}_{SM} - \frac{1}{2}M_i\overline{\nu_{R_i}^c}\nu_{R_i} - \epsilon_{ab}Y_{i\alpha}\overline{\ell_\alpha^a}H^b\nu_{R_i} + \text{h.c.}, \quad (1.5)$$

where \mathcal{L}_{SM} is the SM Lagrangian, $i = 1, \dots, n$ the generation index of RHN, $\alpha = e, \mu, \tau$ the lepton flavor index and $a, b = 0, 1$ the $SU(2)_L$ indices with $\epsilon_{01} = -\epsilon_{10} = 1$. In eq. (1.5), $\ell_\alpha = (\nu_{L_\alpha}, \alpha_L^-)^T$ and $H = (H^+, H^0)^T$ are the $SU(2)_L$ left-handed lepton and Higgs doublets respectively. In eq. (1.5), we define the Lorentz invariant complex conjugation for a fermion field Ψ as

⁸As we will see later, in order to have leptogenesis, $n \geq 2$. Coincidentally, current neutrino oscillation experiments require $n \geq 2$ since at least two neutrinos are known to be massive.

$\Psi^c = C\bar{\Psi}^T$ with C the charge conjugation matrix which satisfies

$$C^\dagger = C^{-1}, \quad C^T = -C, \quad C^{-1}\Gamma_i C = \eta_i \Gamma_i^T, \quad (1.6)$$

where $\eta_i = +1$ for $\Gamma_i = 1, i\gamma_5, \gamma_\mu\gamma_5$ and $\eta_i = -1$ for $\Gamma_i = \gamma_\mu, \frac{1}{2}i[\gamma_\mu, \gamma_\nu]$.

Without loss of generality, we have chosen the basis where the Majorana mass matrix M is diagonal in eq. (1.5) while the neutrino Yukawa couplings $Y_{i\alpha}$ are in general complex and non-diagonal. After EWPT, the neutral component of the Higgs doublet develops a vacuum expectation value (VEV) $v = 174$ GeV and generates the neutrino Dirac masses $(m_D)_{i\alpha} = Y_{i\alpha}v$. The mass terms for neutrinos can be written down as

$$\begin{aligned} \mathcal{L}_{M\nu} &= -\frac{1}{2}\bar{\nu}_L m_D^T \bar{\nu}_R - \frac{1}{2}\bar{\nu}_R^c m_D \bar{\nu}_L^c - \frac{1}{2}\bar{\nu}_R^c M \bar{\nu}_R + \text{h.c.} \\ &= -\frac{1}{2}\bar{\nu} M_\nu \bar{\nu}^c + \text{h.c.}, \end{aligned} \quad (1.7)$$

where $\bar{\nu} = (\bar{\nu}_L, \bar{\nu}_R^c)^T$ is a $(3+n)$ -dimensional vector and M_ν is the $(3+n) \times (3+n)$ mass matrix given by

$$M_\nu = \begin{pmatrix} 0 & m_D^T \\ m_D & M \end{pmatrix}. \quad (1.8)$$

Assuming $m_D \ll M$, we can diagonalize the M_ν and obtain at leading order, the light and heavy neutrino masses respectively as

$$m_\nu \simeq -U_\nu^T m_D^T M^{-1} m_D U_\nu, \quad (1.9)$$

$$m_N \simeq M, \quad (1.10)$$

with the respective light and heavy mass eigenstates given by

$$\bar{\nu} \simeq U_\nu^\dagger \bar{\nu}_L^c + (U_\nu^\dagger \bar{\nu}_L^c)^c, \quad (1.11)$$

$$\bar{N} \simeq \bar{\nu}_R + \bar{\nu}_R^c. \quad (1.12)$$

where U_ν is a 3×3 unitary matrix. From eqs. (1.11) and (1.12), we see that both light and heavy neutrinos are Majorana fermions which satisfy $\Psi^c = \Psi$. Notice that in the basis where the charged lepton Yukawas are diagonal, U_ν

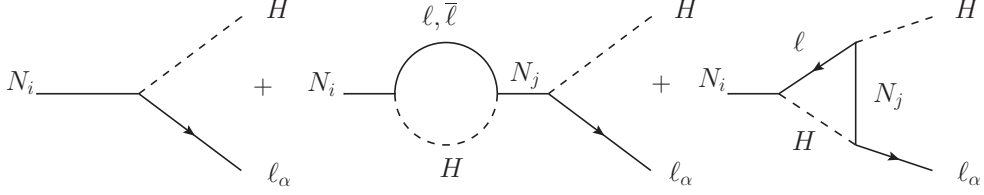


Figure 1.3: The CP asymmetry in type I leptogenesis results from the interference between tree and loop wave and vertex diagrams. For the one loop wave diagram, there is an additional contribution from L conserving diagram to the CP asymmetry which vanishes when summing over the lepton flavor α .

is the lepton mixing matrix which is also known as the Pontecorvo-Maki-Nakagawa-Sakata (PMNS) mixing matrix [40–42]. The light neutrino masses given by eq. (1.9) shows that the heavier the M (and hence m_N in eq. (1.10)), the lighter are the m_ν and vice versa and hence the name *seesaw* mechanism.

Let us rewrite the Lagrangian (1.5) in terms of the Majorana RHN $N_i \equiv \nu_{Ri} + \nu_{Ri}^c$ which satisfies $\nu_{Ri} = P_R N_i$ and $\nu_{Ri}^c = P_L N_i$ where $P_{L,R} = \frac{1}{2}(1 \mp \gamma_5)$ are respectively the left and right chiral projectors:

$$\mathcal{L}_I = \mathcal{L}_{SM} - \frac{1}{2} M_i \bar{N}_i N_i - (\epsilon_{ab} Y_{i\alpha} \bar{\ell}_\alpha^a H^b P_R N_i + \text{h.c.}). \quad (1.13)$$

We will define the CP asymmetry in the decays of RHN as

$$\epsilon_{i\alpha} = \frac{\gamma(N_i \rightarrow \ell_\alpha H^*) - \gamma(N_i \rightarrow \bar{\ell}_\alpha H)}{\gamma(N_i \rightarrow \ell_\alpha H^*) + \gamma(N_i \rightarrow \bar{\ell}_\alpha H)}, \quad (1.14)$$

where $\gamma(i \rightarrow f)$ is the thermally averaged decay rate (the general definition of thermally averaged reaction density is given by eq. (B.21)). Ignoring thermal effects [24, 25], it can be shown that eq. (1.14) is equivalent to

$$\epsilon_{i\alpha} = \frac{|\mathcal{A}(N_i \rightarrow \ell_\alpha H^*)|^2 - |\mathcal{A}(N_i \rightarrow \bar{\ell}_\alpha H)|^2}{|\mathcal{A}(N_i \rightarrow \ell_\alpha H^*)|^2 + |\mathcal{A}(N_i \rightarrow \bar{\ell}_\alpha H)|^2}, \quad (1.15)$$

where $\mathcal{A}(i \rightarrow f)$ is the decay amplitude. At tree-level, it is clear that $\epsilon_{i\alpha}$ vanishes. CP violation, however, can be induced at loop level through the interference between tree and 1-loop diagrams as shown in Figure 1.3. There are two types of contributions from the 1-loop diagrams: the self-energy or

wave diagram (middle) and the vertex diagram (right). We can construct wave and vertex diagrams which are L -violating for which the flow of fermion number for lepton is not continuous but gets reversed due to the Majorana nature in the RHN propagator. However for the wave diagram, we can also construct an additional diagram which is L -conserving (see the second digram in Figure 1.3). At leading order, we obtain the CP asymmetry as [43]

$$\begin{aligned} \epsilon_{i\alpha} = & \frac{1}{8\pi} \frac{1}{(YY^\dagger)_{ii}} \sum_{j \neq i} \text{Im} [(YY^\dagger)_{ji} Y_{i\alpha}^* Y_{j\alpha}] g \left(\frac{M_j^2}{M_i^2} \right) \\ & + \frac{1}{8\pi} \frac{1}{(YY^\dagger)_{ii}} \sum_{j \neq i} \text{Im} [(YY^\dagger)_{ij} Y_{i\alpha}^* Y_{j\alpha}] \frac{M_i^2}{M_i^2 - M_j^2}, \end{aligned} \quad (1.16)$$

where

$$g(x) = \sqrt{x} \left[\frac{1}{1-x} + 1 - (1+x) \ln \left(\frac{1+x}{x} \right) \right]. \quad (1.17)$$

In eq. (1.16), the first term results from the L -violating wave and vertex diagrams while the second term is from the L -conserving wave diagram. The terms of the form $(M_i^2 - M_j^2)^{-1}$ in eq. (1.16) are from L -violating and L -conserving wave diagrams which will resonantly enhance the CP asymmetry if $M_i \approx M_j$ resulting in resonant leptogenesis scenario [44–48]⁹. Notice that if we sum over lepton flavor α , the second term vanishes because the combination of the Yukawa couplings is real. In addition, we can also see that we need to have at least two RHN or the CP asymmetry vanishes because the combination of the Yukawa couplings is real.

For illustration purposes below, we will sum over lepton flavor and obtain

$$\epsilon_i = \sum_{\alpha} \epsilon_{i\alpha} = \frac{1}{8\pi} \frac{1}{(YY^\dagger)_{ii}} \sum_{j \neq i} \text{Im} [(YY^\dagger)_{ji}^2] g \left(\frac{M_j^2}{M_i^2} \right). \quad (1.18)$$

Assuming a hierarchical spectrum of the RHN ($M_1 \ll M_{i>1}$), only the CP asymmetry from the decays of N_1 will be important since the lepton asymmetries generated from the decays of heavier $N_{i>1}$ will be washed out by the N_1

⁹Notice that the resonant term becomes singular in the degenerate limit $M_i = M_j$ and an effective field-theoretical approach based on resummation formalism has to be used (see Section 2.3.3) [44].

interactions. In this limit, the CP asymmetry from N_1 decay is

$$\epsilon_1 = -\frac{3}{16\pi} \frac{1}{(YY^\dagger)_{11}} \sum_{j \neq 1} \text{Im} [(YY^\dagger)_{j1}^2] \frac{M_1}{M_j}. \quad (1.19)$$

Assuming three generations of RHN ($n = 3$) and using the Casas-Ibarra parametrization [49] for the Yukawa couplings

$$Y_{i\alpha} = \frac{1}{v} \left(\sqrt{D_{m_N}} R \sqrt{D_{m_\nu}} U_\nu^\dagger \right)_{i\alpha}, \quad (1.20)$$

where $D_{m_N} = \text{diag}(M_1, M_2, M_3)$, $D_{m_\nu} = \text{diag}(m_{\nu_1}, m_{\nu_2}, m_{\nu_3})$ and R any complex orthogonal matrix satisfying $R^T R = R R^T = 1$, eq. (1.19) becomes

$$\epsilon_1 = -\frac{3}{16\pi} \frac{M_1}{v^2} \frac{\sum_i m_{\nu_i} \text{Im}(R_{1i}^2)}{\sum_i m_{\nu_i} |R_{1i}|^2}. \quad (1.21)$$

Then using the orthogonality condition $\sum_i R_{1i}^2 = 1$, we obtain the Davidson-Ibarra bound [50]

$$|\epsilon_1| \leq \epsilon^{DI} = \frac{3}{16\pi} \frac{M_1}{v^2} (m_{\nu_3} - m_{\nu_1}), \quad (1.22)$$

where m_{ν_3} (m_{ν_1}) is the heaviest (lightest) light neutrino mass.

Now, let us see how one can relate the CP asymmetry ϵ_1 to the lepton asymmetry (and later to the baryon asymmetry). Qualitatively, assume that we have an initial thermal abundance of N_1 i.e. $Y_{N_1}(T \gg M_1) \sim Y_{N_1}^{eq}(T \gg M_1)$ and that the decay of N_1 is very out of equilibrium (hence the inverse decay reaction $\ell H \rightarrow N_1$ which would wash out the lepton asymmetry is negligible), eventually when all the N_1 decay away, the final lepton asymmetry is simply given by

$$Y_{\Delta L}^0 \equiv \left. \frac{n_\ell - n_{\bar{\ell}}}{s} \right|_{T=T_0} \sim \epsilon_1 Y_{N_1}^{eq}(T \gg M_1), \quad (1.23)$$

where $Y_{N_1}^{eq}(T \gg M_1) \equiv \frac{n_{N_1}^{eq}(T \gg M_1)}{s(T)} = 45/(\pi^4 g_{*s})$ is the equilibrium number density of N_1 when it is relativistic (assuming Maxwell-Boltzmann distribution), normalized over entropy density of the Universe $s(T) = \frac{2\pi^2}{45} g_{*s} T^3$ with the entropy degrees of freedom $g_{*s} = 106.75$ for the SM (see elaboration around

eq. (B.6) and eq. (B.12)).

To be more precise, assuming no pre-existing lepton asymmetry, the final lepton asymmetry generated from the decays of N_1 can be parametrized as

$$Y_{\Delta L}^0 = \epsilon_1 \eta Y_{N_1}^{eq}(T \gg M_1), \quad (1.24)$$

where we have defined the *efficiency* η with $0 \leq |\eta| \leq 1$ as a quantity which measures the number density of N_1 with respect to the equilibrium value, the out of equilibrium condition at decay, the washout from inverse decay (i.e. $\ell H \rightarrow N_1$), the effects from spectator processes and thermal corrections and so on. To obtain η , we have to solve a set of Boltzmann equations which describe the evolution of the number densities of relevant particles i.e. N_1 , leptons and antileptons.

Assuming there is no other interaction which violates B and/or L (besides the L -violating RHN decays), the final $B - L$ asymmetry $Y_{\Delta B-L}^0$ can be approximated by

$$Y_{\Delta B-L}^0 \approx -Y_{\Delta L}^0, \quad (1.25)$$

assuming no pre-existing $B - L$ asymmetry. This relation does not hold in general because when in thermal equilibrium, EW sphaleron interactions do violate both B and L . In fact, one also has to take into account the reactions which come into equilibrium at different temperature regimes to get the correct factor which relates $Y_{\Delta B-L}$ and $Y_{\Delta L}$ (which is usually of the order of 1) [27]. In this section, we will just use the approximation eq. (1.25). The reason why we would like to express the asymmetry in term of $Y_{\Delta B-L}$ over $Y_{\Delta L}$ is because after leptogenesis is complete, $Y_{\Delta B-L}$ will be absolutely conserved while L and B are continuously being violated by the EW sphaleron processes. The final baryon asymmetry $Y_{\Delta B}^0$ will then be determined at the time when the EW sphaleron processes fall out of equilibrium either before or after EWPT through the following relation [51]

$$Y_{\Delta B}^0 = \begin{cases} \frac{28}{79} Y_{\Delta B-L}^0 & T > T_{EWPT}, \\ \frac{12}{37} Y_{\Delta B-L}^0 & T < T_{EWPT}, \end{cases} \quad (1.26)$$

where the numerical factors come from solving the chemical equilibrium condi-

tions and conservation laws for the particles which constitutes the relativistic degrees of freedom at the time of EW sphaleron decoupling.

Using eqs. (1.22)–(1.26), and requiring that $Y_{\Delta B}^0 \geq Y_B^{CMB}$ eq. (1.2), we obtain

$$M_1 \gtrsim \frac{5 \times 10^8 \text{ GeV}}{\eta}, \quad (1.27)$$

where we assume the EW sphaleron interactions decouple before EWPT and normally ordered hierarchical neutrinos, $m_{\nu_3} - m_{\nu_1} \simeq \sqrt{\Delta m_{atm}^2}$ where the latest fit from neutrino oscillation data gives $\Delta m_{atm}^2 = 2.46 \pm 0.12(\pm 0.37) \times 10^{-3} \text{ eV}^2$ [52]. Many careful numerical studies have been done to determine η and it was found that for a hierarchical spectrum of the RHN, successful leptogenesis requires generically quite heavy RHN masses [50] with $M_1 \gtrsim 10^9 \text{ GeV}$ [50, 53, 54] (although flavour effects [30–32, 55–57] and/or extended scenarios [58–60] may affect this limit). This bound implies that the RHN must be produced at temperature $T \gtrsim 10^9 \text{ GeV}$ which in turn implies the reheating temperature after inflation has to be $T_{RH} \gtrsim 10^9 \text{ GeV}$ in order to have sufficient RHN. As we will see in next section, this will result in the so-called “gravitino problem” [61–65] in the SUSY scenario.

1.2.2 Supersymmetry and leptogenesis

We know that the minimal extension to SM which incorporates neutrino masses e.g. the type I seesaw mechanism described above, is not satisfactory in itself due to the large hierarchy between this new scale and the EW one. Low-energy SUSY $\Lambda_{\text{susy}} \sim \text{TeV}$ can be invoked to naturally stabilize this hierarchy and this provides a sound motivation for studying leptogenesis in the framework of the supersymmetrized version of the seesaw mechanism. Supersymmetric leptogenesis has been studied, both in dedicated studies [66] or in conjunction with the SM leptogenesis [25]. In these studies, the order of magnitude of the baryon asymmetry generated are shown to be the same as in the non-supersymmetric case. The differences between the SM and supersymmetric leptogenesis can be resumed by means of simple counting of a few numerical factors [7, 67, 68], like for example the number of relativistic degrees of freedom in the thermal bath, the number of loop diagrams contributing to the CP asymmetries, the multiplicities of the final states in the decays of the

heavy neutrinos and sneutrinos. However, several features that are specific of SUSY in the high temperature regime relevant for leptogenesis, in which soft SUSY-breaking parameters¹⁰ can be effectively set to zero resulting in new anomalous global symmetries, have been overlooked or neglected in these studies. In ref. [69], we performed a detailed study taking into account these new effects were carried out. Nonetheless, the numerical corrections with respect to the case when all new effects are neglected remain at the $\mathcal{O}(1)$ level.

Once SUSY has been introduced, at the same time, we also introduce another problem: there is a certain conflict between the upper bound on the T_{RH} such that gravitinos are not overproduced and the lower bound on the T_{RH} required for the thermal production of RHN [50, 53, 54]. On one hand, if gravitino is stable i.e. it is a dark matter candidate, its abundance cannot be greater than the measured dark matter abundance. Depending on the masses of gravitino and gaugino, this implies a constraint on T_{RH} such that gravitinos are not overproduced [70–76]

$$T_{RH} \lesssim 10^7 - 10^9 \text{ GeV}. \quad (1.28)$$

On the other hand if gravitino is unstable and if it is lighter than ~ 10 TeV, it will decay after the BBN starts and hence completely spoil the successful prediction of BBN for light element abundances [77–80]. For example, the latest study in ref. [80] gives an upper bound for gravitino mass ranging from 300 GeV to 30 TeV to be

$$T_{RH} \lesssim 10^5 - 10^{10} \text{ GeV}. \quad (1.29)$$

For the unstable gravitino with mass larger than ~ 30 TeV, its decay to the lightest neutralino (dark matter candidate) also imposes an upper bound $T_{RH} \sim 10^{10}$ GeV such that the Universe is not overclosed i.e. producing more lightest neutralinos than the measured dark matter abundance [80]. Hence, there is a serious conflict between successful thermal leptogenesis which as seen in previous section requires $T_{RH} \gtrsim 10^9$ GeV and the upper bound on T_{RH} imposed by gravitino consideration.

¹⁰These are the explicit SUSY-breaking terms which do not reintroduce quadratic divergences to the scalar mass corrections.

Nevertheless, we don't have to look far for a solution¹¹. For the fact that we haven't seen any of the superpartners (sparticles), if SUSY is realized in nature, it must be broken. Hence, introducing the soft SUSY-breaking terms¹² is unavoidable. With the addition of these soft terms, we also introduce potential new sources of CP violation which could be utilized in leptogenesis [81–84]. Given that the new effects are generically suppressed by powers of the ratio between the soft scale and the RHN masses, Λ_{susy}/M , we can estimate the characteristic temperature window in which the new contributions can give relevant effects. For example if we estimate the CP asymmetry to be $\epsilon \sim \Lambda_{\text{susy}}/M$ where $\Lambda_{\text{susy}} \sim \text{TeV}$ while generically successful leptogenesis requires $\epsilon \gtrsim 10^{-5}$, then the relevant mass scale will be $M \sim 10^4 - 10^8 \text{ GeV}$. Hence, this low temperature realization of supersymmetric leptogenesis with CP violation from the soft terms allow to relax or evade the gravitino problem altogether.

In this thesis, we will follow a particular realization of such a scenario first proposed independently by two groups: Grossman, Kashti, Nir and Roulet [82], and D'Ambrosio, Giudice and Raidal [83] in 2003. This scenario is realized by simply adding to the MSSM some gauge singlets and the corresponding soft terms. Following ref. [83], we will term this scenario as *soft leptogenesis*.

The outline of this thesis is as follows:

In Chapter 2, we will review the basis of soft leptogenesis and recap the main results from the previous studies (e.g. [82, 83, 85, 86]). Then we will derive the corresponding CP asymmetries in soft leptogenesis using two different approaches: field theoretical and quantum mechanical. In particular, we will show that thermal effects are always needed to prevent a vanishing total CP asymmetry [87]. As shown in refs. [88, 89], there is an important quantitative differences between the classical and the quantum approaches in the case of resonant leptogenesis [44–48]. Since the self energy contribution to the CP asymmetry in soft leptogenesis is produced resonantly, we dedicated Chapter 3 to study in detail the role of quantum effects in this scenario. In particular, we show that because of the thermal nature of soft leptogenesis, the dependence

¹¹In fact, many solutions have been proposed, either to lower the scale of successful leptogenesis or relax the bound on T_{RH} from overproducing gravitinos. However in this thesis we are going to focus on the former and in particular the one that is readily available in the MSSM.

¹²We will simply denote the soft SUSY-breaking as 'soft' from here onwards. For example, the soft SUSY-breaking mass will be termed soft mass.

of the quantum effects on the washout regime for soft leptogenesis is quantitatively different than in the usual seesaw resonant leptogenesis scenario [90]. In Chapter 4, we will show that in the temperature regime relevant for soft leptogenesis, lepton flavors have to be taken into account. In particular, we will consider how different flavor structures in the couplings could enhance the efficiency of leptogenesis [91, 92]. Recently in ref. [69], we show that in supersymmetric leptogenesis, several new qualitative features that are specific of SUSY in the high temperature regime relevant for leptogenesis appear. Nevertheless, in the same paper, we also show that for the standard type-I seesaw leptogenesis, the quantitative corrections with respect to the case when all new effects are neglected remain at the $\mathcal{O}(1)$ level. On the other hand, in soft leptogenesis, as we will study in Chapter 5, these new features will not only yield far reaching qualitative differences but also very large quantitative effects [93]. In particular, baryogenesis could be realized through R -genesis and contrary to common belief, a sizable baryon asymmetry is generated also when thermal effects are neglected. Finally in Chapter 6, we will conclude.

In Appendix A, we will describe the phase convention and Feynman rules we use in this thesis. In Appendix B, we derive the complete Boltzmann equations for soft leptogenesis. In Appendix C, we will list down the chemical equilibrium conditions appropriate for $T \lesssim 10^7$ GeV that is relevant for soft leptogenesis.

Chapter 2

Soft Leptogenesis

2.1 Introduction

In the usual type I seesaw leptogenesis reviewed in Section 1.2.1, the heavy particle involved in L -violating decay with CP violation is the RHN. In the supersymmetrized version as briefly discussed in Section 1.2.2, this role is played by both the RHN and its superpartner the right-handed sneutrino (RHSN). On the other hand, in soft leptogenesis (SL) [82, 83], since the relevant CP violation sources are from the soft terms which only involve the RHSN, the decaying heavy particle which is responsible for leptogenesis will be solely the RHSN.

In the original papers on soft leptogenesis (SL) [82, 83] only one type of contribution to the CP asymmetries in RHSN decays was identified: the so called CP violation in mixing. CP violation in mixing is induced by the soft bilinear sneutrino B term that removes the mass degeneracy between the two real RHSN states. As for the case of resonant leptogenesis [44–48], the RHSN self-energy contributions to the CP asymmetries can be resonantly enhanced and give rise to sufficiently large CP violation in sneutrino decays. In order to satisfy the resonant condition, the bilinear B coupling has to be of the same order of the decay width of RHSN, $\Gamma_{\tilde{N}}$ i.e. $B \sim \Gamma_{\tilde{N}}$. In the parameter spaces relevant for SL, this translates into unconventionally small values of $B \ll \text{TeV}$ [82, 83, 90, 91]. Extended scenarios were proposed to alleviate this problem [86, 94–99]. In the SL induced by CP violation in mixing as discussed above, an exact cancellation occurs between the asymmetries in the

fermionic and bosonic channels at temperature $T = 0$. Thermal effects, thus, play a fundamental role in this mechanism: final state Fermi-blocking and Bose-enhancement as well as effective masses for the particle excitations in the plasma break SUSY and effectively remove this degeneracy.

On the other hand, it was also realized that besides CP violation in RHSN mixing, additional sources of CP violation can arise from vertex corrections to the decay amplitudes, and from the interference between mixing and decay [85, 87]. These new sources of CP violation (the so-called “new ways to soft leptogenesis” [85]) are induced by gaugino soft masses that appear in vertex corrections to the RHSN decays. With respect to the mixing contributions, these corrections are suppressed by more powers of Λ_{susy}/M and thus they can be sizable only at relatively low temperatures $T \lesssim 10^5 \text{ GeV}$ [85]. Although in this regime they can allow for more conventional values of $B \sim \text{TeV}$, such a low seesaw scale implies that the suppression of the light neutrino masses is mainly due to very small values of the neutrino Yukawa couplings $Y^2 \sim 10^{-10}$ rather than to the seesaw scale. Furthermore it was found that, unlike for CP violation in mixing, these contributions did not require thermal effects as they did not vanish at $T = 0$ [85]. However we will show in this chapter that this result is not correct¹ and that for all soft SUSY-breaking sources of CP violation considered, at $T = 0$, an exact cancellation between the asymmetries produced in the fermionic and scalar channels holds up to second order in soft parameters.

The organization of this chapter is as follows: In Section 2.2, we will write down the Lagrangian and identify the CP-violating phases. In Section 2.3, we will derive explicit expressions of the CP asymmetries from mixing, decay, and interference between decay and mixing using both field-theoretical and quantum mechanical approaches, paying special attention to thermal effects. Then in Section 2.4, we will present the result of soft leptogenesis by numerically solving Boltzmann equations and finally conclude in Section 2.5.

¹As agreed upon by the authors of ref. [85].

2.2 The Lagrangian

The superpotential for the supersymmetric seesaw model is:

$$W = W_{\text{MSSM}} + Y_{i\alpha}\epsilon_{ab}\hat{N}_i^c\hat{\ell}_\alpha^a\hat{H}_u^b + \frac{1}{2}M_i\hat{N}_i^c\hat{N}_i^c, \quad (2.1)$$

where $a, b = 0, 1$ are the $SU(2)_L$ indices with $\epsilon_{01} = -\epsilon_{10} = 1$, $\alpha = e, \mu, \tau$ being the lepton flavor index and $i = 1, 2, \dots$ labels the generations of RHN chiral superfields defined according to usual convention in terms of their left-handed Weyl spinor components (\hat{N}_i^c contains scalar component $\tilde{N}_i \equiv \tilde{\nu}_{R_i}^*$ and fermion component $(\nu_{R_i})^c$). We also have $\hat{\ell}_\alpha = (\hat{\nu}_{L_\alpha}, \hat{\alpha}_L^-)^T$, $\hat{H}_u = (\hat{H}_u^+, \hat{H}_u^0)^T$ as the left chiral superfields of the lepton and up-type Higgs $SU(2)_L$ doublets respectively. Without loss of generality, we have chosen to work in the basis where the Majorana mass matrix M is diagonal. Notice that due to the Majorana mass term, we cannot consistently assign lepton number to \hat{N}_i such that the superpotential (2.1) remains invariant under global $U(1)_{L_\alpha}$. In other words, both L and L_α are broken by the superpotential (2.1).

From eq. (2.1), we can write down the interaction Lagrangian density involving $N_i \equiv \nu_{R_i} + (\nu_{R_i})^c$ and \tilde{N}_i as follows

$$-\mathcal{L}_{\text{int}} = Y_{i\alpha}\epsilon_{ab} \left(M_i^* \tilde{N}_i^* \tilde{\ell}_\alpha^a H_u^b + \overline{\tilde{H}_u^{c,b}} P_L \ell_\alpha^a \tilde{N}_i + \overline{\tilde{H}_u^{c,b}} P_L N_i \tilde{\ell}_\alpha^a + \overline{N}_i P_L \ell_\alpha^a H_u^b \right) + \text{h.c.}, \quad (2.2)$$

where $P_{L,R} = \frac{1}{2}(1 \mp \gamma_5)$ are respectively the left and right chiral projectors. In eq. (2.2) the $SU(2)_L$ doublets are given by $\tilde{\ell}_\alpha = (\tilde{\nu}_{L_\alpha}, \tilde{\alpha}_L^-)^T$, $H_u = (H_u^+, H_u^0)^T$, $\ell_\alpha = (\nu_{L_\alpha}, \alpha_L^-)^T$, and $\tilde{H}_u^c = (\tilde{H}_u^{+,c}, \tilde{H}_u^{0,c})^T$. Notice that since $\tilde{H}_u^+ = \tilde{H}_{u,L}^+$ is left-handed positively charged Weyl higgsino, $\tilde{H}_u^{+,c} = \tilde{H}_{u,R}^-$ is right-handed negatively charged Weyl higgsino.

In principle, we need to know the SUSY-breaking mechanism at high scale that determines the soft terms at TeV scale. Alternatively we can parametrize our ignorance of the exact SUSY-breaking mechanism by writing down the relevant soft terms in the Lagrangian and simply treating them as free parameters. Working in the basis where charged lepton Yukawa couplings are diagonal, the relevant soft terms involving \tilde{N}_i , $SU(2)_L$ gauginos $\tilde{\lambda}_2^{\pm,0}$, $U(1)_Y$

gauginos $\tilde{\lambda}_1$ and slepton $\tilde{\ell}_\alpha$ are given by

$$\begin{aligned}
-\mathcal{L}_{\text{soft}} &= \widetilde{M}_{ij}^2 \widetilde{N}_i^* \widetilde{N}_j + \left(AY_{i\alpha} \epsilon_{ab} \widetilde{N}_i \tilde{\ell}_\alpha^a H_u^b + \frac{1}{2} BM_i \widetilde{N}_i \widetilde{N}_i + \text{h.c.} \right) \\
&+ \frac{1}{2} \left(m_2 \overline{\widetilde{\lambda}_2^{\pm,0}} P_L \widetilde{\lambda}_2^{\pm,0} + m_1 \overline{\widetilde{\lambda}_1} P_L \widetilde{\lambda}_1 + \text{h.c.} \right), \tag{2.3}
\end{aligned}$$

where we assume for simplicity the proportionality of the bilinear and trilinear couplings: $B_i = BM_i$ and $A_{i\alpha} = AY_{i\alpha}$. In Chapter 4, however, we will study the consequence of having a more general trilinear coupling $A_{i\alpha} = AZ_{i\alpha}$ and show that its flavor structure will play an important role.

Even if we assume the off-diagonal terms of \widetilde{M}_{ij} to be negligible $\widetilde{M}_{ij} \ll \widetilde{M}_{ii}$ for $i \neq j$, the presence of the B term implies that the RHSN and anti-RHSN states mix in mass matrix with mass eigenvectors

$$\begin{aligned}
\widetilde{N}_{+i} &= \frac{1}{\sqrt{2}} \left(e^{i\Phi_i/2} \widetilde{N}_i + e^{-i\Phi_i/2} \widetilde{N}_i^* \right), \\
\widetilde{N}_{-i} &= -\frac{i}{\sqrt{2}} \left(e^{i\Phi_i/2} \widetilde{N}_i - e^{-i\Phi_i/2} \widetilde{N}_i^* \right), \tag{2.4}
\end{aligned}$$

where $\Phi_i \equiv \arg(BM_i)$. The corresponding mass eigenvalues are

$$M_{i\pm}^2 = M_i^2 + \widetilde{M}_{ii}^2 \pm |BM_i|. \tag{2.5}$$

In the following, we will choose without loss of generality $\Phi_i = 0$ which is equivalent to assigning the phases only to A and $Y_{i\alpha}$. Including the soft terms from eq. (2.3), the interaction Lagrangian involving the RHSN mass eigenstates $\widetilde{N}_{\pm i}$ and N_i together with the $SU(2)_L$ and $U(1)_Y$ gauginos interactions with

(s)leptons and higgs(inos), is given by

$$\begin{aligned}
- \mathcal{L}_{SL} = & \frac{Y_{i\alpha}}{\sqrt{2}} \epsilon_{ab} \left\{ \tilde{N}_{+i} \left[\overline{\tilde{H}_u^{c,b}} P_L \ell_\alpha^a + (A + M_i) \tilde{\ell}_\alpha^a H_u^b \right] \right. \\
& + i \tilde{N}_{-i} \left[\overline{\tilde{H}_u^{c,b}} P_L \ell_\alpha^a + (A - M_i) \tilde{\ell}_\alpha^a H_u^b \right] \left. \right\} \\
& + Y_{i\alpha} \epsilon_{ab} \left(\overline{\tilde{H}_u^{c,b}} P_L N_i \tilde{\ell}_\alpha^a + \overline{N}_i P_L \ell_\alpha^a H_u^b \right) \\
& + g_2 (\sigma_\pm)_{ab} \left(\overline{\tilde{\lambda}_2^\pm} P_L \ell_\alpha^a \tilde{\ell}_\alpha^{b*} + \overline{\tilde{H}_u^{c,a}} P_L \tilde{\lambda}_2^\pm H_u^{b*} \right) \\
& + \frac{g_2}{\sqrt{2}} (\sigma_3)_{ab} \left(\overline{\tilde{\lambda}_2^0} P_L \ell_\alpha^a \tilde{\ell}_\alpha^{b*} + \overline{\tilde{H}_u^{c,a}} P_L \tilde{\lambda}_2^0 H_u^{b*} \right) \\
& + \frac{g_Y}{\sqrt{2}} \delta_{ab} \left[\overline{\tilde{\lambda}_1} (y_{\ell L} P_L - y_{\ell R} P_R) \ell_\alpha^a \tilde{\ell}_\alpha^{b*} + \overline{\tilde{H}_u^{c,a}} P_L \tilde{\lambda}_1 H_u^{b*} \right] + \text{h.c.}, \quad (2.6)
\end{aligned}$$

where g_2 and g_Y are respectively the $SU(2)_L$ and $U(1)_Y$ gauge couplings, $y_{\ell L} = -1$ and $y_{\ell R} = 2$ being respectively the hypercharges of the left- and right-handed (s)leptons and $\sigma_\pm = (\sigma_1 \pm i\sigma_2)/2$ with σ_i being the Pauli matrices².

All the parameters appearing in the superpotential (2.1) and in the Lagrangian (2.3) (or equivalently in the first three lines of eq. (2.6)) are in principle complex quantities. However, superfield phase redefinition allows to remove several complex phases. In the following, for simplicity, we will concentrate on SL arising from a single RHSN generation $i = 1$ and in what follows we will drop that index ($Y_\alpha \equiv Y_{1\alpha}$, $Z_\alpha \equiv Z_{1\alpha}$, $B = B_{11}$, etc.). Thus we will only be interested in the physical phases involving the RHSN of the first generation. After superfield phase rotations, the relevant Lagrangian terms restricted to $i = 1$ are characterized by only three independent physical phases that are

$$\phi_A \equiv \arg(AB^*), \quad (2.7)$$

$$\phi_{g_2} \equiv \frac{1}{2} \arg(Bm_2^*), \quad (2.8)$$

$$\phi_{g_Y} \equiv \frac{1}{2} \arg(Bm_1^*), \quad (2.9)$$

which we choose to assign to the A , and to the gaugino coupling operators g_2 , g_Y respectively³. So for the CP asymmetry calculations below we will take M , B , m_2 , m_1 and Y_α to be positive real while A , g_2 and g_Y to be complex

²The Feynman rules we used are collected in Appendix A.

³For details of the phase convention we use, please refer to Appendix A.

with respective phase ϕ_A , ϕ_{g_2} and ϕ_{g_Y} .

The tree-level RHSN decay width is given by

$$\Gamma_{\tilde{N}_\pm} = \frac{M}{4\pi} \sum_\alpha Y_\alpha^2 \left[1 \pm \frac{\text{Re}(A)}{M} \left(1 - \frac{B}{2M} \right) + \frac{|A|^2}{2M^2} + \frac{B^2}{8M^2} + \mathcal{O}(\delta_S^3) \right], \quad (2.10)$$

where

$$\delta_S \equiv \frac{A}{M}, \frac{B}{M}, \frac{m_2}{M}, \frac{\tilde{M}}{M}, \quad (2.11)$$

and we have assumed $\delta_S \ll 1$. Neglecting SUSY-breaking effects in the RHSN masses and in the vertex, we have

$$\Gamma_{\tilde{N}_+} \simeq \Gamma_{\tilde{N}_-} \simeq \Gamma \equiv \frac{M}{4\pi} \sum_\alpha Y_\alpha^2. \quad (2.12)$$

2.3 CP Asymmetries

2.3.1 Definition

We will define the total CP asymmetry in the decays of \tilde{N}_\pm as

$$\epsilon_\alpha = \frac{\sum_{i=\pm, a_\alpha} \left[\gamma(\tilde{N}_i \rightarrow a_\alpha) - \gamma(\tilde{N}_i \rightarrow \bar{a}_\alpha) \right]}{\sum_{i=\pm, a_\beta, \beta} \left[\gamma(\tilde{N}_i \rightarrow a_\beta) + \gamma(\tilde{N}_i \rightarrow \bar{a}_\beta) \right]}, \quad (2.13)$$

where $\gamma(\tilde{N}_i \rightarrow a_\alpha)$ is the thermally averaged decay rate for the decay of \tilde{N}_i into final state a_α ($a_\alpha \equiv s_\alpha, f_\alpha$ with $s_\alpha = \tilde{\ell}_\alpha^a H_u^b$ and $f_\alpha = \ell_\alpha^a \tilde{H}_u^{c,b}$) defined in Appendix B.2.1. Ignoring thermal effects⁴ and only taking into account the mass splitting in the decay width and amplitudes, eq. (2.13) becomes

$$\epsilon_\alpha^0 = \frac{\sum_{i=\pm, a_\alpha} \left(|\hat{\mathcal{A}}_i^{a_\alpha}|^2 - |\overline{\hat{\mathcal{A}}}_i^{\bar{a}_\alpha}|^2 \right) / M_i}{\sum_{i=\pm, a_\beta, \beta} \left(|\hat{\mathcal{A}}_i^{a_\beta}|^2 + |\overline{\hat{\mathcal{A}}}_i^{\bar{a}_\beta}|^2 \right) / M_i}, \quad (2.14)$$

⁴In the next section, we will be explicit about the thermal effects which are important and cannot be ignored.

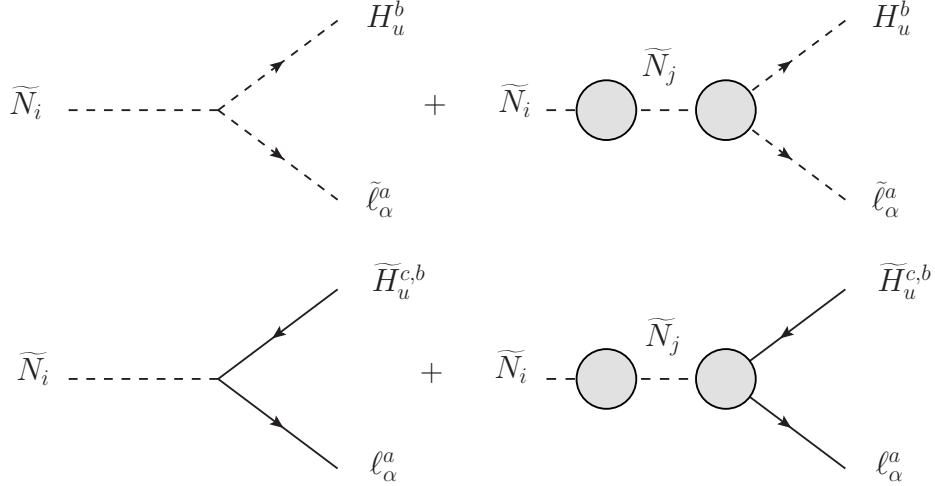


Figure 2.1: The CP asymmetries in the decays of \tilde{N}_\pm into scalars and fermions arise from the interference between tree and loop diagrams. The blob on the \tilde{N}_\pm line contains a sum over all possible self-energy correction diagrams while the blob on the vertex indicates sum over all possible vertex correction diagrams.

where $\hat{\mathcal{A}}_i^{a_\alpha}$ is the decay amplitude of \tilde{N}_i into a_α .

At tree level, it is clear that ϵ_α^0 vanishes because the amplitude squared $|\hat{\mathcal{A}}_i^{a_\alpha}|^2$ is equal to that of its conjugate $|\hat{\mathcal{A}}_i^{\bar{a}_\alpha}|^2$. Hence, CP asymmetry has to be induced at loop level from the interference between tree and loop diagrams as shown in Figure 2.1. There are two kind sources of CP violation: the first one arises from the self-energy corrections while the second arises from vertex corrections (see Figure 2.1). Furthermore, as we will see in Section 2.3.3, 2.3.4 and 2.3.5, ignoring the thermal effects, there is a cancellation between the CP asymmetries for the decays of \tilde{N}_i to scalars and fermions i.e. $|\hat{\mathcal{A}}_i^{s_\alpha}|^2 - |\hat{\mathcal{A}}_i^{\bar{s}_\alpha}|^2 = -|\hat{\mathcal{A}}_i^{f_\alpha}|^2 + |\hat{\mathcal{A}}_i^{\bar{f}_\alpha}|^2$, resulting in $\epsilon_\alpha^0 = 0$. Hence in order to spoil this cancellation, thermal effects have to be taken into account.

2.3.2 Thermal effects

Thermal effects come into play in several aspects:

- (A) Thermal corrections to (s)lepton and higgs(inos) propagators

- (B) Final state statistical factors
- (C) Thermal masses of (s)leptons and higgs(inos)
- (D) Thermal corrections to gauge and Yukawa couplings
- (E) Particle motion in the thermal bath

In the thermal bath where the RHSN decays ($T/M \sim 0.1 - 10$), scalar and fermionic particles have different occupation numbers due to their different statistics. In the two pioneering papers [82, 83], the most relevant thermal effect in SL was shown to be (B) which arises from the final state Bose-enhancement and Fermi-blocking for the RHSN decays into scalars and fermions, respectively. This effect partially lifts the cancellation between the scalar and fermionic asymmetries at the relevant temperature. In ref. [82], only effect (B) was taken into account. In ref. [83], on top of (B), the effects (C) and (D) were taken into account although this additional effects did not significantly change the overall picture. Later, the full-fledged thermal effects (A)-(D) in SL were taken into account in ref. [25] which showed that they did not introduce significant changes. In all these studies, effect (E) has always been ignored. As shown in refs. [24, 25], in the case of SM type I leptogenesis, the effect is at most $\sim 20\%$ with respect to the $T = 0$ case and hence it is assumed justified to ignore this effect in SL as well.

In this thesis, we are going to consider only thermal effects (B), (C) and (D). Taking into account of the aforementioned effects and keeping the mass splitting only in the decay widths and the amplitudes, the total CP asymmetry (2.13) simplifies to:

$$\epsilon_\alpha = \epsilon_{+\alpha}^s + \epsilon_{-\alpha}^s + \epsilon_{+\alpha}^f + \epsilon_{-\alpha}^f, \quad (2.15)$$

where

$$\epsilon_{\pm\alpha}^s = \frac{\left(|\hat{\mathcal{A}}_{\pm}^{s_\alpha}|^2 - |\overline{\hat{\mathcal{A}}_{\pm}^{s_\alpha}}|^2\right) c_{\pm}^{s_\alpha}/M_i}{\sum_{i=\pm, a_\beta, \beta} \left(|\hat{\mathcal{A}}_i^{a_\beta}|^2 + |\overline{\hat{\mathcal{A}}_i^{a_\beta}}|^2\right) c_i^{a_\beta}/M_i}, \quad (2.16)$$

$$\epsilon_{\pm\alpha}^f = \frac{\left(|\hat{\mathcal{A}}_{\pm}^{f_\alpha}|^2 - |\overline{\hat{\mathcal{A}}_{\pm}^{f_\alpha}}|^2\right) c_{\pm}^{f_\alpha}/M_i}{\sum_{i=\pm, a_\beta, \beta} \left(|\hat{\mathcal{A}}_i^{a_\beta}|^2 + |\overline{\hat{\mathcal{A}}_i^{a_\beta}}|^2\right) c_i^{a_\beta}/M_i}. \quad (2.17)$$

In eqs. (2.16) and (2.17), we have explicitly factorized out the thermal factors $c_i^{s\alpha}, c_i^{f\alpha}$ which contain thermal phase-space factors and final state Bose-enhancement and Fermi-blocking factors of the scalar and fermionic channels, respectively. Hence the amplitudes $\hat{\mathcal{A}}_i^{a\alpha}$ and $\overline{\hat{\mathcal{A}}}_i^{\bar{a}\alpha}$ refer to zero temperature ones. As long as we neglect the zero temperature lepton and slepton masses and small neutrino Yukawa couplings, these phase-space factors are flavor independent. Ignoring also the mass splitting between \tilde{N}_+ and \tilde{N}_- , they are the same for $i = \pm$. After including finite temperature effects in the approximation of decay at rest of the \tilde{N}_\pm , they are given by:

$$c_+^f(T) = c_-^f(T) \equiv c^f(T) = (1 - x_\ell - x_{\tilde{H}_u})\lambda(1, x_\ell, x_{\tilde{H}_u}) \times [1 - f_\ell^{eq}] [1 - f_{\tilde{H}_u}^{eq}], \quad (2.18)$$

$$c_+^s(T) = c_-^s(T) \equiv c^s(T) = \lambda(1, x_{H_u}, x_{\tilde{\ell}}) [1 + f_{H_u}^{eq}] [1 + f_{\tilde{\ell}}^{eq}], \quad (2.19)$$

where

$$f_{H_u, \tilde{\ell}}^{eq} = \frac{1}{\exp[E_{H_u, \tilde{\ell}}/T] - 1}, \quad (2.20)$$

$$f_{\tilde{H}_u, \ell}^{eq} = \frac{1}{\exp[E_{\tilde{H}_u, \ell}/T] + 1}, \quad (2.21)$$

are the Bose-Einstein and Fermi-Dirac equilibrium distributions, respectively, and

$$E_{\ell, \tilde{H}_u} = \frac{M}{2}(1 + x_{\ell, \tilde{H}_u} - x_{\tilde{H}_u, \ell}), \quad E_{H_u, \tilde{\ell}} = \frac{M}{2}(1 + x_{H_u, \tilde{\ell}} - x_{\tilde{\ell}, H_u}), \quad (2.22)$$

$$\lambda(1, x, y) = \sqrt{(1 + x - y)^2 - 4x}, \quad x_a \equiv \frac{m_a(T)^2}{M^2}. \quad (2.23)$$

In Section 2.3.3, we will derive explicit expressions of the CP asymmetries resulted from mixing, decay, and the interference between decay and mixing using a field-theoretical approach, explicitly showing the need to include thermal effects for non-vanishing CP asymmetries. In Section 2.3.4 we recompute the CP asymmetries using a quantum mechanical approach, based on an effective non-hermitian Hamiltonian and find the same T dependence of the CP asymmetries. Finally in Section 2.3.5, we will present a general argument proving that at $T = 0$ the direct leptonic CP violation due to vertex corrections in

RHSN decays vanishes at one loop, due to an exact cancellation between the scalar and fermion contributions confirming the explicit calculations from the previous sections.

2.3.3 Field theoretical approach

As discussed in ref. [83], when $\Gamma \gg \Delta M_{\pm} \equiv M_+ - M_-$, the two RHSN states are not well-separated particles. In this case, the result for the asymmetry depends on how the initial state is prepared. In what follows we will assume that the RHSN are in a thermal bath with a thermalization time Γ^{-1} shorter than the typical oscillation times, ΔM_{\pm}^{-1} , therefore coherence is lost and it is appropriate to compute the CP asymmetries in terms of the mass eigenstates (2.4).

We compute the relevant decay amplitudes following the effective field-theoretical approach described in ref. [44–48], which takes into account the CP violation due to mixing and decay (as well as their interference) of nearly degenerate states by using resummed propagators for unstable mass eigenstate particles. The decay amplitude $\hat{A}_i^{a\alpha}$ of the unstable external state \tilde{N}_i into final state a_α ($a_\alpha \equiv s_\alpha, f_\alpha$ with $s_\alpha = \tilde{\ell}_\alpha^a H_u^b$ and $f_\alpha = \ell_\alpha^a \tilde{H}_u^{c,b}$) is described by a superposition of amplitudes with stable final states:

$$\begin{aligned} \hat{A}_{\pm}^{a\alpha} &= (A_{\pm}^{a\alpha} + i\mathcal{V}_{\pm}^{a\alpha \text{abs}}(p^2)) - (A_{\mp}^{a\alpha} + i\mathcal{V}_{\mp}^{a\alpha \text{abs}}(p^2)) \\ &\quad \times \frac{i\Sigma_{\mp\pm}^{\text{abs}}}{M_{\pm}^2 - M_{\mp}^2 + i\Sigma_{\mp\mp}^{\text{abs}}}, \end{aligned} \quad (2.24)$$

$$\begin{aligned} \overline{\hat{A}}_{\pm}^{\bar{a}\alpha} &= (A_{\pm}^{a\alpha*} + i\mathcal{V}_{\pm}^{a\alpha \text{abs}*}(p^2)) - (A_{\mp}^{a\alpha*} + i\mathcal{V}_{\mp}^{a\alpha \text{abs}*}(p^2)) \\ &\quad \times \frac{i\overline{\Sigma}_{\mp\pm}^{\text{abs}}}{M_{\pm}^2 - M_{\mp}^2 + i\overline{\Sigma}_{\mp\mp}^{\text{abs}}}. \end{aligned} \quad (2.25)$$

$A_{\pm}^{a\alpha}$ are the tree amplitudes:

$$A_+^{s\alpha} = \frac{Y_\alpha}{\sqrt{2}}(A^* + M)\epsilon_{ab}, \quad A_-^{s\alpha} = -i\frac{Y_\alpha}{\sqrt{2}}(A^* - M)\epsilon_{ab}, \quad (2.26)$$

$$A_+^{f\alpha} = \frac{Y_\alpha}{\sqrt{2}}[\bar{u}(p_\ell)P_R v(p_{\tilde{H}_c^a})]\epsilon_{ab}, \quad A_-^{f\alpha} = -i\frac{Y_\alpha}{\sqrt{2}}[\bar{u}(p_\ell)P_R v(p_{\tilde{H}_c^a})]\epsilon_{ab}. \quad (2.27)$$

Σ_{ij}^{abs} are the absorptive parts of the $\tilde{N}_i \rightarrow \tilde{N}_j$ self-energies (see Figure 2.2):

$$\Sigma_{\mp\mp}^{(1)\text{abs}} = \Gamma M \left[\frac{1}{2} + \frac{M_{\mp}^2}{2M^2} + \frac{|A|^2}{2M^2} \mp \frac{\text{Re}(A)}{M} \right], \quad (2.28)$$

$$\Sigma_{\mp\pm}^{(1)\text{abs}} = -\Gamma \text{Im}(A). \quad (2.29)$$

$\mathcal{V}_{\pm}^{\alpha\text{abs}}$ are the absorptive parts of the vertex corrections (see Figure 2.3)⁵:

$$\mathcal{V}_{+}^{s\alpha\text{abs}}(p^2) = \epsilon_{ab} \frac{Y_{\alpha}}{\sqrt{2}} \frac{3m_2}{32\pi} (g_2)^2 \ln \frac{m_2^2}{p^2 + m_2^2}, \quad (2.30)$$

$$\mathcal{V}_{-}^{s\alpha\text{abs}}(p^2) = -i\epsilon_{ab} \frac{Y_{\alpha}}{\sqrt{2}} \frac{3m_2}{32\pi} (g_2)^2 \ln \frac{m_2^2}{p^2 + m_2^2}, \quad (2.31)$$

$$\begin{aligned} \mathcal{V}_{+}^{f\alpha\text{abs}}(p^2) &= \epsilon_{ab} \frac{Y_{\alpha}}{\sqrt{2}} \frac{3m_2}{32\pi p^2} (A^* + M) (g_2^*)^2 \ln \frac{m_2^2}{p^2 + m_2^2} \\ &\quad \times [\bar{u}(p_{\ell}) P_R v(p_{\tilde{H}_c^c})], \end{aligned} \quad (2.32)$$

$$\begin{aligned} \mathcal{V}_{-}^{f\alpha\text{abs}}(p^2) &= -i\epsilon_{ab} \frac{Y_{\alpha}}{\sqrt{2}} \frac{3m_2}{32\pi p^2} (A^* - M) (g_2^*)^2 \ln \frac{m_2^2}{p^2 + m_2^2} \\ &\quad \times [\bar{u}(p_{\ell}) P_R v(p_{\tilde{H}_c^c})], \end{aligned} \quad (2.33)$$

where we only consider the contribution from $SU(2)_L$ gauginos. The contribution from $U(1)_Y$ gaugino can be obtained by simply substituting $\alpha_2 \rightarrow \alpha_Y \equiv \frac{|g_Y|^2}{4\pi}$ and $3 \rightarrow 1$ in eqs. (2.30)–(2.33). We would like to point out that eqs. (2.28)–(2.33) have been computed and verified both by directly evaluating the imaginary part of the Feynman integral and by using Cutkosky's cutting rules [100].

Substituting (2.24) and (2.25) into (2.16) and (2.17) we get in the numerators:

$$\begin{aligned} |\hat{\mathcal{A}}_{\pm}^{a_{\alpha}}|^2 - |\overline{\hat{\mathcal{A}}}_{\pm}^{a_{\alpha}}|^2 &\simeq -4 \left\{ -\text{Im} [A_{\pm}^{a_{\alpha}*} A_{\mp}^{a_{\alpha}} \Sigma_{\mp\pm}^{\text{abs}}] \frac{M_{\pm}^2 - M_{\mp}^2}{(M_{\pm}^2 - M_{\mp}^2)^2 + |\Sigma_{\mp\mp}^{\text{abs}}|^2} \right. \\ &\quad + \text{Im} [A_{\pm}^{a_{\alpha}*} \mathcal{V}_{\pm}^{a_{\alpha}\text{abs}}(M_{\pm}^2)] \\ &\quad + \text{Im} [\mathcal{V}_{\pm}^{a_{\alpha}\text{abs}*}(M_{\pm}^2) A_{\mp}^{a_{\alpha}} \Sigma_{\mp\pm}^{\text{abs}} - A_{\pm}^{a_{\alpha}*} \mathcal{V}_{\mp}^{a_{\alpha}\text{abs}}(M_{\pm}^2) \Sigma_{\mp\pm}^{\text{abs}}] \\ &\quad \left. \times \frac{\Sigma_{\mp\mp}^{\text{abs}}}{(M_{\pm}^2 - M_{\mp}^2)^2 + |\Sigma_{\mp\mp}^{\text{abs}}|^2} \right\}, \end{aligned} \quad (2.34)$$

⁵There is an irrelevant global i factor in the tree level $A_{\pm}^{a_{\alpha}}$ and one-loop $\mathcal{V}_{\pm}^{a_{\alpha}\text{abs}}$ amplitudes compared to $A_{\mp}^{a_{\alpha}}$ and $\mathcal{V}_{\mp}^{a_{\alpha}\text{abs}}$ arising from the particular choice of global phase in the definition of \tilde{N}_{\pm} in eq. (2.4).

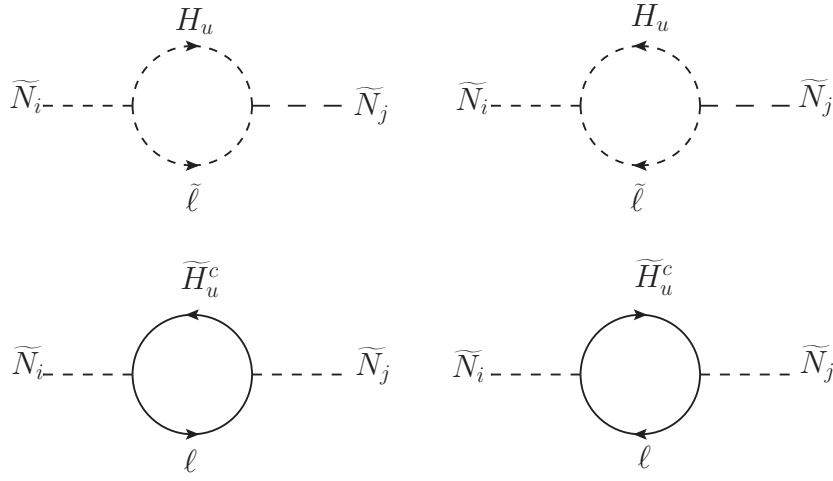


Figure 2.2: Feynman diagrams contributing to the RHSN self-energies at one-loop.

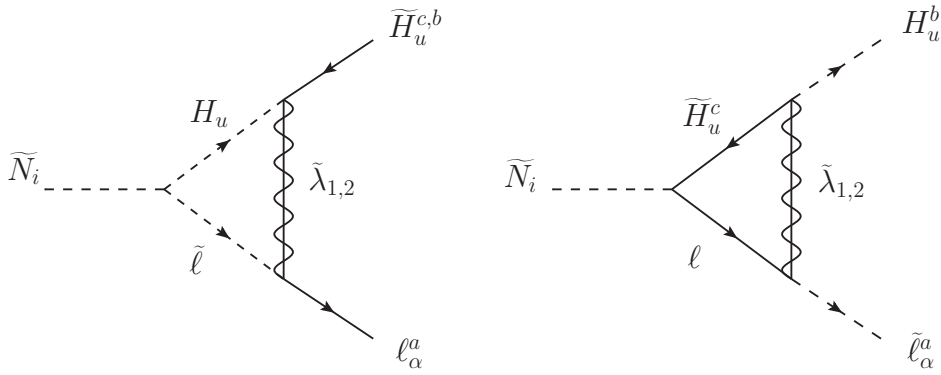


Figure 2.3: Feynman diagrams contributing to the RHSN decay vertex at one-loop.

where we have used the relations $\Sigma_{\mp\mp}^{\text{abs}} = \overline{\Sigma}_{\mp\mp}^{\text{abs}}$ and $\Sigma_{\mp\pm}^{\text{abs}*} = \overline{\Sigma}_{\mp\pm}^{\text{abs}}$. The \simeq sign means that terms of order δ_S^3 and higher are ignored with δ_S defined in eq. (2.11). The three lines in (2.34) correspond respectively to (S=‘self-energy’) CP violation in \tilde{N} mixing from the off-diagonal one-loop self-energies (this corresponds to the effects originally considered in refs. [82, 83]), (V=‘vertex’) CP violation due to the gaugino-mediated one-loop vertex corrections to the \tilde{N} decay [85], and (I=‘interference’) CP violation in the interference of vertex and self-energies.

In the denominator of (2.16) and (2.17) we consider only the tree amplitudes $|\hat{\mathcal{A}}_{\pm}^{a_\alpha}|^2 + |\hat{\mathcal{A}}_{\pm}^{\bar{a}_\alpha}|^2 = 2|A_{\pm}^{a_\alpha}|^2$, with $|A_{\pm}^{s_\alpha}|^2 = Y_\alpha^2 [|A|^2 + M^2 \pm 2M\text{Re}(A)]$ and $|A_{\pm}^{f_\alpha}|^2 = Y_\alpha^2 M_\pm^2$.

Using the explicit forms in eqs. (2.26) – (2.33) we find that up to order δ_S^2 , the three contributions to the CP asymmetry from scalar and fermionic decays satisfy:

$$\begin{aligned} \epsilon_{\pm\alpha}^{sS} &= \Delta^s(T) \epsilon_{\pm\alpha}^S, & \epsilon_{\pm\alpha}^{fS} &= -\Delta^f(T) \epsilon_{\pm\alpha}^S, \\ \epsilon_{\pm\alpha}^{sV} &= \Delta^s(T) \epsilon_{\pm\alpha}^V, & \epsilon_{\pm\alpha}^{fV} &= -\Delta^f(T) \epsilon_{\pm\alpha}^V, \\ \epsilon_{\pm\alpha}^{sI} &= \Delta^s(T) \epsilon_{\pm\alpha}^I, & \epsilon_{\pm\alpha}^{fI} &= -\Delta^f(T) \epsilon_{\pm\alpha}^I, \end{aligned} \quad (2.35)$$

with

$$\epsilon_{\pm\alpha}^S = -P_\alpha \frac{|A|}{M} \sin(\phi_A) \frac{2B\Gamma}{4B^2 + \Gamma^2}, \quad (2.36)$$

$$\begin{aligned} \epsilon_{\pm\alpha}^V &= -\frac{3P_\alpha \alpha_2 m_2}{8} \frac{m_2}{M} \ln \frac{m_2^2}{m_2^2 + M^2} \left[\frac{|A|}{M} \sin(\phi_A + 2\phi_g) \right. \\ &\quad \left. - \frac{B}{M} \sin(2\phi_g) \pm \sin(2\phi_g) \right], \end{aligned} \quad (2.37)$$

$$\epsilon_{\pm\alpha}^I = \frac{3P_\alpha \alpha_2 m_2}{4} \frac{|A|}{M} \frac{1}{M} \ln \frac{m_2^2}{m_2^2 + M^2} \sin(\phi_A) \cos(2\phi_g) \frac{\Gamma^2}{4B^2 + \Gamma^2}, \quad (2.38)$$

and

$$\Delta_{s,f}(T) \equiv \frac{c^{s,f}(T)}{c^s(T) + c^f(T)}. \quad (2.39)$$

In the above we have defined $\phi_g \equiv \phi_{g_2}$, $\alpha_2 = \frac{|g_2|^2}{4\pi}$ and the flavor projectors as

$$P_\alpha = \frac{Y_\alpha^2}{\sum_\beta Y_\beta^2}, \quad (2.40)$$

which are constrained by the conditions

$$\sum_\alpha P_\alpha = 1 \quad \text{and} \quad 0 \leq P_\alpha \leq 1. \quad (2.41)$$

Summing up the contributions from the decays of \tilde{N}_+ and \tilde{N}_- to scalars and fermions, one gets the three contributions to the total CP asymmetry in eq. (2.13) as

$$\epsilon_\alpha^S(T) = P_\alpha \bar{\epsilon}^S \Delta_{BF}(T), \quad (2.42)$$

$$\epsilon_\alpha^V(T) = P_\alpha \bar{\epsilon}^V \Delta_{BF}(T), \quad (2.43)$$

$$\epsilon_\alpha^I(T) = P_\alpha \bar{\epsilon}^I \Delta_{BF}(T), \quad (2.44)$$

where we have defined

$$\bar{\epsilon}^S \equiv -\frac{|A|}{M} \sin(\phi_A) \frac{4B\Gamma}{4B^2 + \Gamma^2}, \quad (2.45)$$

$$\bar{\epsilon}^V \equiv -\frac{3\alpha_2}{4} \frac{m_2}{M} \ln \frac{m_2^2}{m_2^2 + M^2} \left[\frac{|A|}{M} \sin(\phi_A + 2\phi_g) - \frac{B}{M} \sin(2\phi_g) \right], \quad (2.46)$$

$$\bar{\epsilon}^I \equiv \frac{3\alpha_2}{2} \frac{m_2}{M} \frac{|A|}{M} \ln \frac{m_2^2}{m_2^2 + M^2} \sin(\phi_A) \cos(2\phi_g) \frac{\Gamma^2}{4B^2 + \Gamma^2}, \quad (2.47)$$

and the *thermal factor*

$$\Delta_{BF}(T) \equiv \Delta^s(T) - \Delta^f(T). \quad (2.48)$$

As mentioned earlier the CP asymmetries from the contribution of $U(1)_Y$ gaugino can be obtained by substituting $\alpha_2 \rightarrow \alpha_Y = \frac{|g_Y|^2}{4\pi}$ and $3 \rightarrow 1$ in eqs. (2.46) and (2.47). Since they do not exhibit any new feature besides the multiplicative factors mentioned here, we will neglect them in the rest of this thesis.

In Figure 2.4, we plot Δ_{BF} (black solid curve), Δ^s (blue dashed curve) and

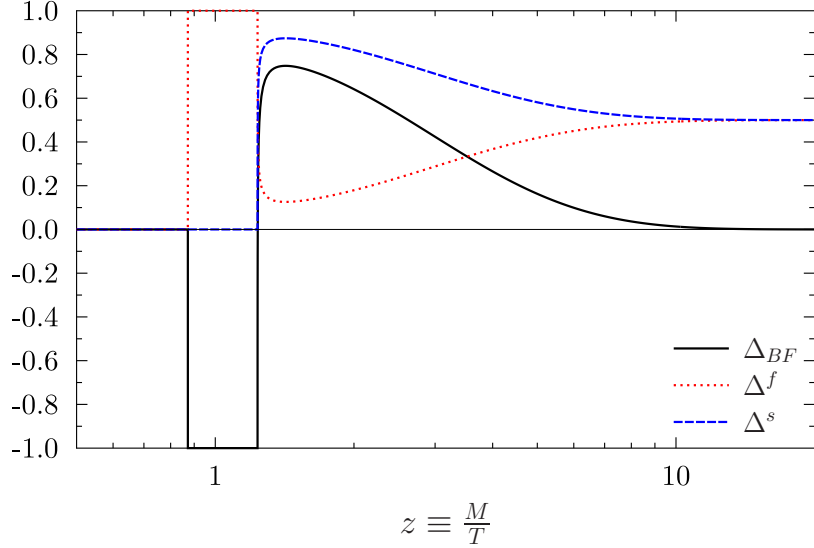


Figure 2.4: Δ_{BF} (black solid curve), Δ^s (blue dashed curve) and Δ^f (red dotted curve) as a function of $z \equiv M/T$.

Δ^f (red dotted curve) as a function of $z \equiv M/T$. For $z \lesssim 0.8$, the decays of RHSN to scalars and fermions are kinematically forbidden. For a brief period $0.8 \lesssim z \lesssim 1.2$, the fermionic channel becomes accessible although the scalar channel is still closed. For $z \gtrsim 1.2$, the scalar channel opens up as well and we can clearly see that a significant non-cancellation between Δ^s and Δ^f till $z \sim 10$.

The CP asymmetry in eq. (2.42) is the contribution to the lepton asymmetry due to CP violation in RHSN mixing discussed in refs. [82, 83, 91]. Eqs. (2.43) and (2.44) give the contribution to the lepton asymmetry related to CP violation in decay and in the interference of mixing and decay. They have similar parametric dependences as the ones derived in ref. [85]. However as explicitly shown in eqs. (2.35), the scalar and fermionic CP asymmetries cancel each other at zero temperature because as $T \rightarrow 0$, both $c^s(T), c^f(T) \rightarrow 1$. Consequently we find that, up to second order in the soft parameters, all contributions to the lepton asymmetry in the soft SUSY scenario require thermal effects in order to be significant. In fact, $\epsilon_\alpha^S(T)$ does not vanish at the order of $\mathcal{O}(\delta_S^3)$ at $T = 0$ although $\epsilon_\alpha^V(T)$ and $\epsilon_\alpha^I(T)$ still vanish exactly at $T = 0$ in agreement with the general proof presented in Section 2.3.5.

We finish by noticing that in this derivation we have neglected thermal corrections to the CP asymmetry from the loops, i.e., we have computed the imaginary part of the one-loop graphs by directly evaluating the imaginary part of the Feynman integrals or Cutkosky's cutting rules at $T = 0$ [100].

2.3.4 Quantum mechanical approach

In this section we recompute the asymmetry using a quantum mechanical (QM) approach, based on an effective (non hermitian) Hamiltonian [82, 83, 85]. In this language an analogy can be drawn between the $\tilde{N}-\tilde{N}^*$ system and the system of neutral mesons such as $K^0-\bar{K}^0$ and its time evolution is determined in the non-relativistic limit by the Hamiltonian:

$$H = \begin{pmatrix} M & \frac{B}{2} \\ \frac{B}{2} & M \end{pmatrix} - \frac{i}{2} \begin{pmatrix} \Gamma & \frac{\Gamma A^*}{M} \\ \frac{\Gamma A}{M} & \Gamma \end{pmatrix}, \quad (2.49)$$

with Γ given in eq. (2.12).

In refs.[82, 83, 85] the QM formalism was applied for weak initial states \tilde{N} and \tilde{N}^* . In practice it is possible to use the formalism to study the evolution of either initially weak or mass eigenstates. So in order to study the dependence of the results on the choice of physical initial conditions we will compute the asymmetry in this formalism assuming either of the two possibilities for initial states. So we define the basis:

$$\begin{aligned} \tilde{N}_1 &= (g\tilde{N} + h\tilde{N}^*), \\ \tilde{N}_2 &= e^{i\theta} (h\tilde{N} - g\tilde{N}^*). \end{aligned} \quad (2.50)$$

The mass basis, eq. (2.4) corresponds to $(g, h, \theta) = (\frac{1}{\sqrt{2}}, \frac{1}{\sqrt{2}}, -\frac{\pi}{2})$. Assuming that the physical initial states were pure \tilde{N} and \tilde{N}^* corresponds to $(g, h, \theta) = (1, 0, \pi)$.

The decay amplitudes of \tilde{N}_1 and \tilde{N}_2 into fermions $f_\alpha = \ell_\alpha^a \tilde{H}_u^{c,b}$ including

the one-loop contribution from gaugino exchange are:

$$\begin{aligned}
A_1^{f\alpha} &= \left\{ Y_\alpha h - \frac{3Y_\alpha}{2M^2} (gM + hA^*) (g_2^*)^2 \frac{m_2}{16\pi} I_f \right\} [\bar{u}(p_\ell) P_{R\nu}(p_{\tilde{H}_u^c})] \epsilon_{ab}, \\
\overline{A_1^{f\alpha}} &= \left\{ Y_\alpha g - \frac{3Y_\alpha}{2M^2} (hM + gA) (g_2)^2 \frac{m_2}{16\pi} I_f \right\} [\bar{u}(p_{\tilde{H}_u^c}) P_{L\nu}(p_\ell)] \epsilon_{ab}, \\
A_2^{f\alpha} &= -e^{-i\theta} \left\{ Y_\alpha g - \frac{3Y_\alpha}{2M^2} (hM - gA^*) (g_2^*)^2 \frac{m_2}{16\pi} I_f \right\} [\bar{u}(p_\ell) P_{R\nu}(p_{\tilde{H}_u^c})] \epsilon_{ab}, \\
\overline{A_2^{f\alpha}} &= e^{-i\theta} \left\{ Y_\alpha h - \frac{3Y_\alpha}{2M^2} (hA - gM) (g_2)^2 \frac{m_2}{16\pi} I_f \right\} \\
&\quad \times [\bar{u}(p_{\tilde{H}_u^c}) P_{L\nu}(p_\ell)] \epsilon_{ab}, \tag{2.51}
\end{aligned}$$

where the \overline{A} denotes the decay amplitudes into antifermions. The corresponding decay amplitudes into scalar $s_\alpha = \tilde{\ell}_\alpha^a H_u^b$ are:

$$\begin{aligned}
A_1^{s\alpha} &= \left\{ Y_\alpha (gM + hA^*) - \frac{3Y_\alpha}{2} h (g_2)^2 \frac{m_2}{16\pi} I_s \right\} \epsilon_{ab}, \\
\overline{A_1^{s\alpha}} &= \left\{ Y_\alpha (hM + gA) - \frac{3Y_\alpha}{2} g (g_2^*)^2 \frac{m_2}{16\pi} I_s \right\} \epsilon_{ab}, \\
A_2^{s\alpha} &= e^{-i\theta} \left\{ Y_\alpha (hM - gA^*) + \frac{3Y_\alpha}{2} g (g_2)^2 \frac{m_2}{16\pi} I_s \right\} \epsilon_{ab}, \\
\overline{A_2^{s\alpha}} &= e^{-i\theta} \left\{ Y_\alpha (hA - gM) - \frac{3Y_\alpha}{2} h (g_2^*)^2 \frac{m_2}{16\pi} I_s \right\} \epsilon_{ab}. \tag{2.52}
\end{aligned}$$

In eqs. (2.51) and (2.52), we have

$$\begin{aligned}
\text{Re}(I_f) &\equiv f_R = -\frac{1}{\pi} \left[\frac{1}{2} \left(\ln \frac{m_2^2}{m_2^2 + M^2} \right)^2 + \text{Li}_2 \left(\frac{m_2^2}{m_2^2 + M^2} \right) - \zeta(2) \right], \\
\text{Re}(I_s) &\equiv s_R = \frac{1}{\pi} \left[\frac{1}{2} \left(\ln \frac{m_2^2}{m_2^2 + M^2} \right)^2 + \text{Li}_2 \left(\frac{m_2^2}{m_2^2 + M^2} \right) - \zeta(2) \right. \\
&\quad \left. + B_0(M^2, m_2, 0) + B_0(M^2, 0, m_2) \right], \\
\text{Im}(I_f) &\equiv f_I = \text{Im}(I_s) \equiv s_I = -\ln \frac{m_2^2}{m_2^2 + M^2}. \tag{2.53}
\end{aligned}$$

The eigenvectors of the Hamiltonian in terms of the states \tilde{N}_1 and \tilde{N}_2 are:

$$\begin{aligned} |\tilde{N}_L\rangle &= (gp + hq) |\tilde{N}_1\rangle + e^{-i\theta} (hp - gq) |\tilde{N}_2\rangle, \\ |\tilde{N}_H\rangle &= (gp - hq) |\tilde{N}_1\rangle + e^{-i\theta} (hp + gq) |\tilde{N}_2\rangle, \end{aligned} \quad (2.54)$$

where

$$\frac{q}{p} = -1 - \frac{\Gamma|A|}{BM} \sin(\phi_A) - \frac{\Gamma^2|A|^2}{M^2B^2} \cos^2(\phi_A) - \frac{i}{2} \frac{\Gamma^2|A|^2}{M^2B^2} \sin(2\phi_A). \quad (2.55)$$

At time t the states \tilde{N}_1 and \tilde{N}_2 evolve into

$$\begin{aligned} |\tilde{N}_{1,2}(t)\rangle &= \frac{1}{2} \left\{ [e_L(t) + e_H(t) \pm C_0 (e_L(t) - e_H(t))] |\tilde{N}_{1,2}\rangle \right. \\ &\quad \left. + e^{\mp i\theta} C_{1,2} (e_L(t) - e_H(t)) |\tilde{N}_{2,1}\rangle \right\}, \end{aligned} \quad (2.56)$$

where

$$C_0 = gh \left(\frac{p}{q} + \frac{q}{p} \right), \quad C_1 = h^2 \frac{p}{q} - g^2 \frac{q}{p}, \quad C_2 = h^2 \frac{q}{p} - g^2 \frac{p}{q}, \quad (2.57)$$

and

$$e_{H,L}(t) \equiv e^{-i(M_{H,L} - \frac{i}{2}\Gamma_{H,L})t}. \quad (2.58)$$

The total time integrated CP asymmetry is

$$\epsilon_\alpha^{QM} = \frac{\sum_{i=1,2,a_\alpha} \Gamma(\tilde{N}_i \rightarrow a_\alpha) - \Gamma(\tilde{N}_i \rightarrow \bar{a}_\alpha)}{\sum_{i=1,2,a_\beta,\beta} \Gamma(\tilde{N}_i \rightarrow a_\beta) + \Gamma(\tilde{N}_i \rightarrow \bar{a}_\beta)}, \quad (2.59)$$

where $\Gamma(\tilde{N}_i \rightarrow a_\alpha)$ are the time integrated decay rates which from eq. (2.56) are found to be

$$\begin{aligned} \Gamma(\tilde{N}_i \rightarrow a_\alpha) &= \frac{1}{4} \frac{c^{a_\alpha}}{16\pi M} \left(|A_i^{a_\alpha}|^2 G_{i+} + |A_{j \neq i}^{a_\alpha}|^2 G_{j-} \right. \\ &\quad \left. + 2 [\operatorname{Re}(A_i^{a_\alpha*} A_{j \neq i}^{a_\alpha}) G_{ii}^R - \operatorname{Im}(A_i^{a_\alpha*} A_{j \neq i}^{a_\alpha}) G_{ii}^I] \right). \end{aligned} \quad (2.60)$$

$\Gamma(\tilde{N}_i \rightarrow \bar{a}_\alpha)$ can be obtained from eq. (2.60) with the replacement $A_i^{a_\alpha} \rightarrow \overline{A_i^{a_\alpha}}$. We have defined the time integrated projections

$$G_{1(2)+} = 2 \left(\frac{1}{1-y^2} + \frac{1}{1+x^2} \right) + 2|C_0|^2 \left(\frac{1}{1-y^2} - \frac{1}{1+x^2} \right) \pm 8 \left[\text{Re}(C_0) \frac{y}{1-y^2} - \text{Im}(C_0) \frac{x}{1+x^2} \right], \quad (2.61)$$

$$G_{1(2)-} = 2|C_{1,2}|^2 \left(\frac{1}{1-y^2} - \frac{1}{1+x^2} \right), \quad (2.62)$$

$$G_{11(22)}^R = 2 \left\{ \text{Re} [e^{\mp i\theta} C_{1(2)}] \frac{y}{1-y^2} - \text{Im} [e^{\mp i\theta} C_{1(2)}] \frac{x}{1+x^2} \right\} \pm 2 \text{Re} [e^{\mp i\theta} C_0^* C_{1(2)}] \left(\frac{1}{1-y^2} - \frac{1}{1+x^2} \right), \quad (2.63)$$

$$G_{11(22)}^I = 2 \left\{ \text{Im} [e^{\mp i\theta} C_{1(2)}] \frac{y}{1-y^2} + \text{Re} [e^{\mp i\theta} C_{1(2)}] \frac{x}{1+x^2} \right\} \pm 2 \text{Im} [e^{\mp i\theta} C_0^* C_{1(2)}] \left(\frac{1}{1-y^2} - \frac{1}{1+x^2} \right), \quad (2.64)$$

in terms of masses and width differences coefficients⁶:

$$x = \frac{M_H - M_L}{\Gamma} = \frac{B}{\Gamma} - \frac{1}{2} \frac{\Gamma |A|^2}{B M^2} \sin^2(\phi_A), \quad (2.65)$$

$$y = \frac{\Gamma_H - \Gamma_L}{2\Gamma} = \frac{|A|}{M} \cos(\phi_A) - \frac{B}{2M}. \quad (2.66)$$

Substituting eqs. (2.60)–(2.64) one can write the numerator in eq. (2.59) as

$$\sum_i \Gamma(\tilde{N}_i \rightarrow a_\alpha) - \Gamma(\tilde{N}_i \rightarrow \bar{a}_\alpha) \equiv \Delta\Gamma^{a_\alpha, R} + \Delta\Gamma^{a_\alpha, NR} + \Delta\Gamma^{a_\alpha, I}, \quad (2.67)$$

⁶We use the expression of $\Gamma_H - \Gamma_L$ from ref. [85]. Notice that with this definition $\Gamma_H - \Gamma_L \neq \Gamma_{\tilde{N}_+} - \Gamma_{\tilde{N}_-}$ where $\Gamma_{\tilde{N}_\pm}$ is defined in eq. (2.10).

with

$$\begin{aligned}
\Delta\Gamma^{a_\alpha,R} &= \frac{1}{2} \frac{c^{a_\alpha}}{16\pi M} \frac{x^2 + y^2}{(1-y^2)(1+x^2)} \\
&\quad \left\{ |C_0|^2 \left(|A_1^{a_\alpha}|^2 - |\overline{A_1^{a_\alpha}}|^2 + |A_2^{a_\alpha}|^2 - |\overline{A_2^{a_\alpha}}|^2 \right) \right. \\
&\quad - \frac{(|C_1|^2 - |C_2|^2)}{2} \left(|A_1^{a_\alpha}|^2 - |\overline{A_1^{a_\alpha}}|^2 - |A_2^{a_\alpha}|^2 + |\overline{A_2^{a_\alpha}}|^2 \right) \\
&\quad + 2 \left[\operatorname{Re} \left(A_1^{a_\alpha*} A_2^{a_\alpha} - \overline{A_1^{a_\alpha*}} \overline{A_2^{a_\alpha}} \right) \operatorname{Re} \left(e^{-i\theta} C_0^* C_1 \right) \right. \\
&\quad \left. - \operatorname{Re} \left(A_2^{a_\alpha*} A_1^{a_\alpha} + \overline{A_2^{a_\alpha*}} \overline{A_1^{a_\alpha}} \right) \operatorname{Re} \left(e^{i\theta} C_0^* C_2 \right) \right] \\
&\quad - 2 \left[\operatorname{Im} \left(A_1^{a_\alpha*} A_2^{a_\alpha} - \overline{A_1^{a_\alpha*}} \overline{A_2^{a_\alpha}} \right) \operatorname{Im} \left(e^{-i\theta} C_0^* C_1 \right) \right. \\
&\quad \left. \left. - \operatorname{Im} \left(A_2^{a_\alpha*} A_1^{a_\alpha} + \overline{A_2^{a_\alpha*}} \overline{A_1^{a_\alpha}} \right) \operatorname{Im} \left(e^{i\theta} C_0^* C_2 \right) \right] \right\}, \tag{2.68}
\end{aligned}$$

$$\begin{aligned}
\Delta\Gamma^{a_\alpha,NR} &= \frac{c^{a_\alpha}}{16\pi M} \frac{1}{(1-y^2)} \left\{ 2y \operatorname{Re}(C_0) \left(|A_1^{a_\alpha}|^2 - |\overline{A_1^{a_\alpha}}|^2 - |A_2^{a_\alpha}|^2 + |\overline{A_2^{a_\alpha}}|^2 \right) \right. \\
&\quad + \left(|A_1^{a_\alpha}|^2 - |\overline{A_1^{a_\alpha}}|^2 + |A_2^{a_\alpha}|^2 - |\overline{A_2^{a_\alpha}}|^2 \right) \\
&\quad + y \left[\operatorname{Re} \left(A_1^{a_\alpha*} A_2^{a_\alpha} - \overline{A_1^{a_\alpha*}} \overline{A_2^{a_\alpha}} \right) \operatorname{Re} \left(e^{-i\theta} C_1 \right) \right. \\
&\quad \left. + \operatorname{Re} \left(A_2^{a_\alpha*} A_1^{a_\alpha} - \overline{A_2^{a_\alpha*}} \overline{A_1^{a_\alpha}} \right) \operatorname{Re} \left(e^{i\theta} C_2 \right) \right] \\
&\quad - y \left[\operatorname{Im} \left(A_1^{a_\alpha*} A_2^{a_\alpha} - \overline{A_1^{a_\alpha*}} \overline{A_2^{a_\alpha}} \right) \operatorname{Im} \left(e^{-i\theta} C_1 \right) \right. \\
&\quad \left. \left. + \operatorname{Im} \left(A_2^{a_\alpha*} A_1^{a_\alpha} - \overline{A_2^{a_\alpha*}} \overline{A_1^{a_\alpha}} \right) \operatorname{Im} \left(e^{i\theta} C_2 \right) \right] \right\}, \tag{2.69}
\end{aligned}$$

$$\begin{aligned}
\Delta\Gamma^{a_\alpha, I} = & \frac{c^{a_\alpha}}{16\pi M} \frac{x}{(1+x^2)} \left\{ -2\text{Im}(C_0) \left(|A_1^{a_\alpha}|^2 - |A_1^{\bar{a}_\alpha}|^2 - |A_2^{a_\alpha}|^2 + |A_2^{\bar{a}_\alpha}|^2 \right) \right. \\
& - \left[\text{Re} \left(A_1^{a_\alpha*} A_2^{a_\alpha} - \overline{A_1^{\bar{a}_\alpha*} A_2^{\bar{a}_\alpha}} \right) \text{Re} (e^{-i\theta} C_1) \right. \\
& + \text{Re} \left(A_2^{a_\alpha*} A_1^{a_\alpha} - \overline{A_2^{\bar{a}_\alpha*} A_1^{\bar{a}_\alpha}} \right) \text{Re} (e^{i\theta} C_2) \left. \right] \\
& - \left[\text{Im} \left(A_1^{a_\alpha*} A_2^{a_\alpha} - \overline{A_1^{\bar{a}_\alpha*} A_2^{\bar{a}_\alpha}} \right) \text{Im} (e^{-i\theta} C_1) \right. \\
& \left. \left. + \text{Im} \left(A_2^{a_\alpha*} A_1^{a_\alpha} - \overline{A_2^{\bar{a}_\alpha*} A_1^{\bar{a}_\alpha}} \right) \text{Im} (e^{i\theta} C_2) \right] \right\}. \tag{2.70}
\end{aligned}$$

In writing the above equations we have classified the contributions as *resonant*, (*non-resonant*), *R* (*NR*), depending on whether they present an overall factor $\frac{x^2+y^2}{1+x^2}$ (or no $\frac{1}{1+x^2}$ at all). We have labeled the remainder as *interference* term *I*.

After substituting the explicit values for the amplitudes and the coefficients and neglecting all those terms which cancel in both basis we get that

$$\begin{aligned}
\Delta\Gamma^{f_\alpha, R} &= -c^f \Delta\Gamma_\alpha^R, & \Delta\Gamma^{s_\alpha, R} &= c^s \Delta\Gamma_\alpha^R, \\
\Delta\Gamma^{f_\alpha, NR} &= -c^f \Delta\Gamma_\alpha^{NR}, & \Delta\Gamma^{s_\alpha, NR} &= c^s \Delta\Gamma_\alpha^{NR}, \\
\Delta\Gamma^{f_\alpha, I} &= -c^f \Delta\Gamma_\alpha^I, & \Delta\Gamma^{s_\alpha, I} &= c^s \Delta\Gamma_\alpha^I, \tag{2.71}
\end{aligned}$$

with

$$\begin{aligned}
\Delta\Gamma_\alpha^R &= -\frac{1}{4\pi} Y_\alpha^2 [(g^2 - h^2)^2 + (2gh)^2 \cos(2\theta)] |A| \sin(\phi_A) \\
&\times \frac{1}{x} \frac{x^2 + y^2}{(1-y^2)(1+x^2)}, \tag{2.72}
\end{aligned}$$

$$\begin{aligned}
\Delta\Gamma_\alpha^{NR} &= \frac{3}{16\pi} Y_\alpha^2 \alpha_2 \ln \frac{m_2^2}{m_2^2 + M^2} \frac{m_2}{M} \frac{1}{1-y^2} [-|A| \sin(\phi_A + 2\phi_g) \\
&+ yM (2(2gh)^2 + (g^2 - h^2)^2 \cos(2\theta)) \sin(2\phi_g)], \tag{2.73}
\end{aligned}$$

$$\begin{aligned}
\Delta\Gamma_\alpha^I &= \frac{3}{16\pi} Y_\alpha^2 \alpha_2 \ln \frac{m_2^2}{m_2^2 + M^2} \frac{m_2}{M} \frac{1}{1+x^2} |A| \\
&\times \sin(\phi_A) \cos(2\theta) \cos(2\phi_g). \tag{2.74}
\end{aligned}$$

Eqs. (2.71) explicitly display that the cancellation of the CP asymmetries at $T = 0$ occurs also in this formalism whether the RHSN are initial mass or weak eigenstates. We have traced the discrepancy with ref. [85] to a missing

$\cos(\phi_f - \phi_s)$ factor in their expression for $\sin \delta_s$ in their eq.(19). Once that factor is included, ϵ_2^m in their eq.(22) cancels against ϵ_2^{mdi} in their eq.(25), and ϵ^i in their eq.(23) cancels against ϵ^d in their eq.(24) so that the total asymmetry is zero at $T = 0$.

Introducing the explicit values for the coefficients for initial weak RHSN and the expressions for x and y and expanding at order δ_S^2 we get

$$\epsilon_\alpha^{R,QMw}(T) = -P_\alpha \frac{|A|}{M} \sin(\phi_A) \frac{B\Gamma}{B^2 + \Gamma^2} \Delta_{BF}(T), \quad (2.75)$$

$$\begin{aligned} \epsilon_\alpha^{NR,QMw}(T) &= -\frac{3P_\alpha \alpha_2 m_2}{4 M} \ln \frac{m_2^2}{m_2^2 + M^2} \left[\frac{|A|}{M} \sin(\phi_A) \cos(2\phi_g) \right. \\ &\quad \left. + \frac{B}{2M} \sin(2\phi_g) \right] \Delta_{BF}(T), \end{aligned} \quad (2.76)$$

$$\begin{aligned} \epsilon_\alpha^{I,QMw}(T) &= \frac{3P_\alpha \alpha_2 m_2}{4 M M} \ln \frac{m_2^2}{m_2^2 + M^2} \sin(\phi_A) \cos(2\phi_g) \\ &\quad \times \frac{\Gamma^2}{B^2 + \Gamma^2} \Delta_{BF}(T). \end{aligned} \quad (2.77)$$

Correspondingly for initial \tilde{N}_\pm states one gets

$$\epsilon_\alpha^{R,QMm}(T) = P_\alpha \frac{|A|}{M} \sin(\phi_A) \frac{B\Gamma}{B^2 + \Gamma^2} \Delta_{BF}(T), \quad (2.78)$$

$$\begin{aligned} \epsilon_\alpha^{NR,QMm}(T) &= -\frac{3P_\alpha \alpha_2 m_2}{4 M} \ln \frac{m_2^2}{m_2^2 + M^2} \left[\frac{|A|}{M} \sin(\phi_A) \cos(2\phi_g) \right. \\ &\quad \left. + \frac{B}{2M} \sin(2\phi_g) \right] \Delta_{BF}(T), \end{aligned} \quad (2.79)$$

$$\begin{aligned} \epsilon_\alpha^{I,QMm}(T) &= -\frac{3P_\alpha \alpha_2 m_2}{4 M M} \ln \frac{m_2^2}{m_2^2 + M^2} \sin(\phi_A) \cos(2\phi_g) \\ &\quad \times \frac{\Gamma^2}{B^2 + \Gamma^2} \Delta_{BF}(T). \end{aligned} \quad (2.80)$$

Comparing eqs. (2.78)–(2.80) with eqs. (2.75)–(2.77) and eqs. (2.42)–(2.44) we find that they show very similar parametric dependence though there are some differences in the numerical coefficients. In particular we find that $\epsilon_\alpha^{R,QM}$, $\epsilon_\alpha^{I,QM}$ and the B -dependent (second term) in either the weak or mass basis $\epsilon_\alpha^{NR,QM}$ coincide with ϵ_α^S , ϵ_α^I and the B -dependent term in ϵ_α^V derived in the previous section after the redefinition $A \rightarrow 2A$, $B \rightarrow 2B$ and $\sin(\phi_A) \rightarrow \pm \sin(\phi_A)$. We find only some differences in the phase combination which appears in the B independent term in the asymmetries $\epsilon_\alpha^{I,QM}$ and ϵ_α^V as seen

in eqs. (2.43), (2.76) and (2.79). So, we conclude that the choice of initial state can only lead to these minor differences but the role of thermal effects for the non-vanishing of the CP asymmetry holds independent of the chosen basis as well as of the approach (QM or field theoretical) chosen for evaluating the CP asymmetry.

2.3.5 Vanishing of the CP asymmetry in decays

While it was claimed in ref. [85] that the new sources of direct CP violation from vertex corrections involving the gauginos do not require thermal effects to produce a sizable lepton asymmetry in the plasma, as we have seen in the previous two sections, there is actually a zero temperature cancellation between the CP asymmetries for decays into scalars and into fermions also when the vertex corrections are included. This issue is of some interest, because if thermal corrections are necessary for SL to work, then non-thermal scenarios, like the ones in which sneutrinos are produced by inflaton decays and the thermal bath remains at a temperature $T \ll M$ during the following leptogenesis epoch, would be completely excluded. In the following, we will present a simple but general argument proving that at $T = 0$ the direct leptonic CP violation in sneutrinos decays vanishes at one loop, due to an exact cancellation between the scalar and fermion contributions.

Let us take for simplicity $\Phi = 0$ in eq. (2.4) (this amounts to assign the phases ϕ_A and ϕ_g in eqs. (2.7) and (2.8) respectively to A and m_2)⁷. Since the lepton flavor α won't play a role in this proof, we will suppress it in this section. Let us introduce for the various amplitudes the shorthand notation $A_\ell^\pm \equiv A(\tilde{N}_\pm \rightarrow \ell \tilde{H}_u^c)$, $A_\ell^{\tilde{N}(\tilde{N}^*)} \equiv A(\tilde{N}(\tilde{N}^*) \rightarrow \ell \tilde{H}_u^c)$ with similar expressions for the other final states. From eq. (2.4) we can write

$$2 |A_\ell^\pm|^2 = |A_\ell^{\tilde{N}}|^2 + |A_\ell^{\tilde{N}^*}|^2 \pm 2 \operatorname{Re} \left(A_\ell^{\tilde{N}} \cdot A_\ell^{\tilde{N}} \right), \quad (2.81)$$

$$2 |A_\ell^\pm|^2 = |A_\ell^{\tilde{N}}|^2 + |A_\ell^{\tilde{N}^*}|^2 \pm 2 \operatorname{Re} \left(A_\ell^{\tilde{N}} \cdot A_\ell^{\tilde{N}} \right), \quad (2.82)$$

where the complex conjugate amplitudes in the last terms of both these equations have been rewritten as follows: $(A_\ell^{\tilde{N}^*})^* = A_{\tilde{N}^*}^\ell = A_\ell^{\tilde{N}}$ and $(A_\ell^{\tilde{N}})^* =$

⁷Here we only consider the contributions from $SU(2)_L$ gauginos since the proof with $U(1)_Y$ gaugino will be exactly parallel.

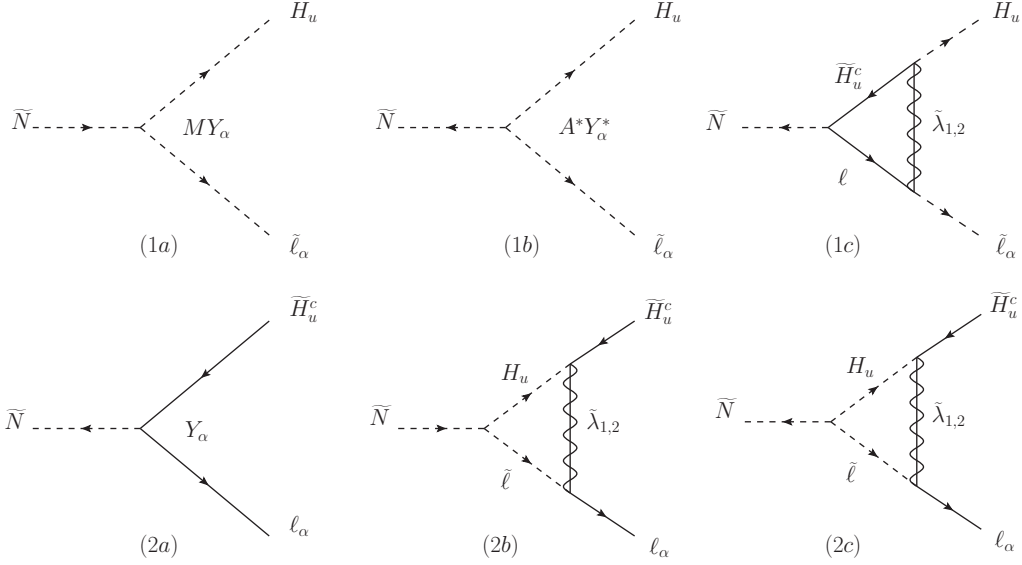


Figure 2.5: Soft leptogenesis diagrams for sneutrino decays into scalars (1a), (1b), (1c) and into fermions (2a), (2b), (2c).

$A_{\tilde{N}^*}^{\tilde{\ell}} = A_{\tilde{\ell}}^{\tilde{N}}$ by using CPT invariance in the second step. The direct CP asymmetry for \tilde{N}_{\pm} decays into fermions is given by the difference between eq. (2.81) and eq. (2.82):

$$2 \left(|A_{\tilde{\ell}}^{\pm}|^2 - |A_{\tilde{\ell}}^{\mp}|^2 \right) = \left(|A_{\tilde{\ell}}^{\tilde{N}^*}|^2 - |A_{\tilde{\ell}}^{\tilde{N}^*}|^2 \right) + \left(|A_{\tilde{\ell}}^{\tilde{N}}|^2 - |A_{\tilde{\ell}}^{\tilde{N}}|^2 \right). \quad (2.83)$$

With the replacements $\ell \rightarrow \tilde{\ell}$ and $\bar{\ell} \rightarrow \tilde{\ell}^*$, a completely equivalent expression holds also for the decays into scalars.

The tree level and one loop diagrams for the various decay amplitudes into scalars and fermions are given in Figure 2.5. We note at this point that $A_{\tilde{\ell}}^{\tilde{N}}$ has no one-loop amplitude to interfere with (see diagram (1a)) and thus, up to one-loop, the full amplitude coincides with the tree level result, and is CP conserving. $A_{\tilde{\ell}}^{\tilde{N}}$ is a pure one-loop amplitude (see diagram (2c)) and therefore is also CP conserving. This implies:

$$\left| A_{\tilde{\ell}}^{\tilde{N}} \right|^2 = \left| A_{\tilde{\ell}^*}^{\tilde{N}^*} \right|^2, \quad (2.84)$$

$$\left| A_{\tilde{\ell}}^{\tilde{N}} \right|^2 = \left| A_{\tilde{\ell}}^{\tilde{N}^*} \right|^2. \quad (2.85)$$

We can thus change simultaneously the signs of $|A_{\tilde{\ell}}^{\tilde{N}}|^2$ and $|A_{\tilde{\ell}}^{\tilde{N}^*}|^2$ in eq. (2.83) without affecting the equality, and the same we can do in the analogous equation for the scalars. This gives:

$$2 \left(|A_{\tilde{\ell}}^{\pm}|^2 - |A_{\tilde{\ell}^*}^{\pm}|^2 \right) = \left(|A_{\tilde{\ell}}^{\tilde{N}^*}|^2 + |A_{\tilde{\ell}}^{\tilde{N}}|^2 \right) - \left(|A_{\tilde{\ell}}^{\tilde{N}}|^2 + |A_{\tilde{\ell}}^{\tilde{N}^*}|^2 \right), \quad (2.86)$$

$$2 \left(|A_{\tilde{\ell}}^{\pm}|^2 - |A_{\tilde{\ell}^*}^{\pm}|^2 \right) = \left(|A_{\tilde{\ell}}^{\tilde{N}^*}|^2 + |A_{\tilde{\ell}^*}^{\tilde{N}^*}|^2 \right) - \left(|A_{\tilde{\ell}}^{\tilde{N}}|^2 + |A_{\tilde{\ell}^*}^{\tilde{N}}|^2 \right). \quad (2.87)$$

Using CPT invariance

$$|A_{\tilde{\ell}}^{\tilde{N}^*}|^2 + |A_{\tilde{\ell}}^{\tilde{N}}|^2 = |A_{\tilde{N}}^{\tilde{\ell}}|^2 + |A_{\tilde{N}}^{\tilde{\ell}^*}|^2, \quad (2.88)$$

$$|A_{\tilde{\ell}}^{\tilde{N}^*}|^2 + |A_{\tilde{\ell}^*}^{\tilde{N}^*}|^2 = |A_{\tilde{N}}^{\tilde{\ell}^*}|^2 + |A_{\tilde{N}}^{\tilde{\ell}}|^2, \quad (2.89)$$

and unitarity

$$|A_{\tilde{N}}^{\tilde{\ell}}|^2 + |A_{\tilde{N}}^{\tilde{\ell}^*}|^2 + |A_{\tilde{N}}^{\tilde{\ell}^*}|^2 + |A_{\tilde{N}}^{\tilde{\ell}}|^2 = |A_{\tilde{\ell}}^{\tilde{N}}|^2 + |A_{\tilde{\ell}}^{\tilde{N}^*}|^2 + |A_{\tilde{\ell}^*}^{\tilde{N}}|^2 + |A_{\tilde{\ell}^*}^{\tilde{N}^*}|^2, \quad (2.90)$$

we can readily see that the sum of zero temperature fermionic CP asymmetry eq. (2.86) and scalar CP asymmetry eq. (2.87) vanishes. We have thus proved that for \tilde{N}_+ and \tilde{N}_- independently, at one loop there is an exact cancellation between the scalars and fermions final state contributions, and thus at $T = 0$ the direct decay CP asymmetries vanish.

2.4 Unflavored Scenario

2.4.1 Relevant parameters and scenarios

Here we will look at SL in the unflavored scenario. In this case, since lepton flavor is irrelevant, the CP asymmetries (2.42)-(2.44) have to be summed over

lepton flavor:

$$\epsilon^S(T) = \sum_{\alpha} \epsilon_{\alpha}^S(T) = \bar{\epsilon}^S \Delta_{BF}(T), \quad (2.91)$$

$$\epsilon^V(T) = \sum_{\alpha} \epsilon_{\alpha}^V(T) = \bar{\epsilon}^V \Delta_{BF}(T), \quad (2.92)$$

$$\epsilon^I(T) = \sum_{\alpha} \epsilon_{\alpha}^I(T) = \bar{\epsilon}^I \Delta_{BF}(T). \quad (2.93)$$

In this case, the relevant parameters that appear in the CP asymmetries (2.91)-(2.93) are $|A|$, m_2 , B , M and the two CP violating phases ϕ_A and ϕ_g .

Next we will discuss the parameters which characterize the decay of RHSN, namely its mass M and the neutrino Yukawa couplings Y_{α} which appear in the RHSN decay width Γ eq. (2.12). We will define a convenient parameter, the decay parameter K to compare Γ to the expansion rate of the Universe $H(T) = \sqrt{\frac{4g_*\pi^3}{45} \frac{T^2}{M_{pl}}}$ as follows

$$K = \frac{\Gamma}{H(M)} \equiv \frac{m_{\text{eff}}}{m^*}, \quad (2.94)$$

where we define the effective neutrino mass parameter [101]

$$m_{\text{eff}} \equiv \frac{\sum_{\alpha} Y_{\alpha}^2 v_u^2}{M}, \quad (2.95)$$

and the equilibrium mass $m^* \equiv \frac{8\pi v_u^2}{9M_{pl}} \sqrt{\frac{g_*\pi^3}{45}}$ with $M_{pl} = 1.22 \times 10^{19}$ GeV being the Planck mass and g_* the total number of relativistic degrees of freedom. Taking $g_* = 228.75$ in the MSSM, we have $m^* = 7.83 \times 10^{-4}$ eV. In eq. (2.95) $v_u = v \sin \beta$ (with $v=174$ GeV) is the vacuum expectation value (VEV) of the up-type Higgs doublet and the angle β is defined as follows: $\tan \beta \equiv v_u/v_d$ where v_d is the VEV of the down-type Higgs doublet. In the following, we will use m_{eff} (or equivalently K) as a free parameter to characterize the out of equilibrium condition of the RHSN decays.

The *strong* washout regime is defined as the regime where $K \gg 1$, the *weak* washout regime as where $K \ll 1$ while the *intermediate* washout regime as where $K \sim 1$. In the following, we will discuss two scenarios regarding the initial abundance of RHSN $Y_{\tilde{N}_{\pm}}(T \gg M) \equiv \frac{n_{\tilde{N}_{\pm}}}{s}(T \gg M)$:

1. Zero initial abundance of RHSN, $Y_{\tilde{N}_{\pm}}(T \gg M) = 0$. In this scenario, the population of RHSN is assumed to be created only through neutrino Yukawa interactions in thermal bath.
2. Thermal initial abundance of RHSN, $Y_{\tilde{N}_{\pm}}(T \gg M) = Y_{\tilde{N}_{\pm}}^{eq}(T \gg M)$. In this scenario, we assume there are some additional fast interactions in early times which generated a thermal abundance of RHSN.

The following discussion is a generic feature of leptogenesis. However, for definiteness, we will use the decays of \tilde{N} as the example. Assuming that the decays of \tilde{N} generate a lepton asymmetry $Y_{\Delta\ell} = Y_{\ell} - Y_{\bar{\ell}}$, we can write down the simplified Boltzmann equations to describe the evolution of $Y_{\tilde{N}}$ and $Y_{\Delta\ell}$ (detailed discussion will be given in the next Section), taken into account of only decay and inverse decay as follows:

$$\frac{dY_{\tilde{N}}}{dz} = D \left(Y_{\tilde{N}} - Y_{\tilde{N}}^{eq} \right), \quad (2.96)$$

$$\frac{dY_{\Delta\ell}}{dz} = \epsilon D \left(Y_{\tilde{N}} - Y_{\tilde{N}}^{eq} \right) - W Y_{\Delta\ell}, \quad (2.97)$$

where we define $z \equiv M/T$ as a convenient variable, ϵ is the CP asymmetry parameter, $Y_{\tilde{N}}^{eq}$ the equilibrium abundance of \tilde{N} , and the decay and washout (inverse decay) terms are respectively given by

$$D = K \frac{z \mathcal{K}_1(z)}{\mathcal{K}_2(z)}, \quad (2.98)$$

$$W = D \frac{Y_{\tilde{N}}^{eq}}{Y_{\ell}^{eq}}, \quad (2.99)$$

with \mathcal{K}_n the modified Bessel function of the second kind of order n . As can be observed from eq. (2.97), in thermal equilibrium $Y_{\tilde{N}} = Y_{\tilde{N}}^{eq}$ and no asymmetry can be generated. The final lepton asymmetry $Y_{\Delta\ell}^0$ generated can be parametrized as follows

$$Y_{\Delta\ell}^0 = \epsilon \eta Y_{\tilde{N}}^{eq}(T \gg M), \quad (2.100)$$

where the efficiency $0 \leq |\eta| \leq 1$ takes into account the departure from thermal equilibrium condition and the erasure of the lepton asymmetry through inverse decay and its value can be determined from solving eqs. (2.96)–(2.97).

Qualitatively, when $K \gg 1$, while the generation of lepton asymmetry is fast, so is its erasure (washout) through inverse decays. In this case, irrespectively of the initial abundance, $Y_{\tilde{N}}$ will approach its thermal abundance value very early, and any possible lepton asymmetry which could have been created in the early times during the \tilde{N} production phase (i.e. $Y_{\tilde{N}} < Y_{\tilde{N}}^{eq}$) or being created from other mechanism (e.g. from the decays of heavier generation of \tilde{N}) will be efficiently washout. The final lepton asymmetry is determined by the amount generated when \tilde{N} starts decaying away (i.e. when $Y_{\tilde{N}} > Y_{\tilde{N}}^{eq}$) and until the end of leptogenesis. Hence the final lepton asymmetry (i.e. η) is expected to decrease with increasing washout (i.e. K) that erases the lepton asymmetry during this \tilde{N} decaying period.

On the other hand, when $K \ll 1$, the washout of the lepton asymmetry is negligible. In this scenario, the initial condition plays an important role. With thermal initial abundance of \tilde{N} , $Y_{\tilde{N}}(T \gg M) = Y_{\tilde{N}}^{eq}(T \gg M)$ and assuming the CP asymmetry ϵ to be constant⁸, the final lepton asymmetry generated should saturate to the maximum possible value $\epsilon Y_{\tilde{N}}^{eq}(T \gg M)$ that is $\eta = 1$. On the other hand, for zero initial abundance of \tilde{N} , $Y_{\tilde{N}}(T \gg M) = 0$, a “wrong” sign lepton asymmetry⁹ is created while \tilde{N} are being populated (i.e. $Y_{\tilde{N}} < Y_{\tilde{N}}^{eq}$). Due to the weak washout, such lepton asymmetry remains. Eventually when \tilde{N} starts decaying away (i.e. $Y_{\tilde{N}} > Y_{\tilde{N}}^{eq}$) until the end of leptogenesis, the “right” sign lepton asymmetry is generated. The final lepton asymmetry is determined from the imperfect cancellation between these two opposite sign lepton asymmetries. Since the total \tilde{N} population is created solely through its Yukawa interactions in the initial phase, smaller K implies that lesser \tilde{N} will be created. Hence we expect the final lepton asymmetry to fall off with decreasing K as we are having less \tilde{N} to generate the lepton asymmetry. For the intermediate regime $K \sim 1$, the precise value of η can be obtained by solving the Boltzmann equations.

We now turn to discuss what are the expected values for K (i.e. m_{eff}). Using the Casas-Ibarra parameterization for three generations of RHN [49] as in eq. (1.20), it can be shown that $m_{\text{eff}} \geq m_1$ where m_1 is the mass of

⁸As we will see later, the temperature dependent CP asymmetry in SL does have crucial qualitative and quantitative effects.

⁹Notice that the “right” or “wrong” sign is arbitrary since the sign of ϵ can be changed by choice of the CP violating phase.

the lightest active neutrino. Barring any strong phase cancellations between different matrix elements, we have $m_{\text{eff}} \lesssim m_3$ where m_3 is the mass of the heaviest active neutrino. Data on solar and atmospheric neutrinos indicate $m_3 \gtrsim 0.05 \text{ eV}$ and the second heaviest active neutrino has mass $m_2 \gtrsim 0.01 \text{ eV}$ (for a recent fit see ref. [52]). The tightest bound from recent cosmology fit indicates the sum of light neutrino masses $\sum_i m_i \leq 0.35 \text{ eV}$ [102]. The latter hints that it is natural to have $m_{\text{eff}} \lesssim 0.35 \text{ eV}$. Assuming that m_{eff} is around $0.01 - 0.05 \text{ eV}$, we would fall in the strong washout regime. In fact, in two RHN model with normal hierarchy, it can be shown that $m_{\text{eff}} \geq \sqrt{m_3^2 - m_1^2} \simeq 0.05 \text{ eV}$ which implies that we are always in the strong washout regime. In principle, the out of thermal equilibrium condition (Sakharov's third condition in Section 1.1.1) by definition implies $K < 1$ i.e. in the weak washout regime. However, as we will see later, successful leptogenesis could be possible even in the very strong washout regime due to inefficiency of the washout and various enhancements e.g. lepton flavor effects. But generically there is nothing concrete that we can say about m_{eff} , so in our study, we will treat it as a free parameter.

2.4.2 Unflavored Boltzmann equations

In this section, we will write down the relevant Boltzmann equations (BEs) necessary to describe the evolution of particle abundances in SL scenario. In order to do so, in principle, we have to write down a BE for each type of particle that is in the thermal bath (which is a lot!). Nevertheless, by comparing the characteristic time scale τ of a particle physics interaction with the age of the Universe $t_U(T)$ at a given temperature T , we can cut down immensely the number of particle types which have to be described by BE which we will discuss in the following.

At each specific temperature T , particle reactions must be treated in a different way depending if their characteristic time scale τ (given by inverse of their their thermally averaged rates) is

- (i) much shorter than the age of the Universe: $\tau \ll t_U(T)$;
- (ii) much larger than the age of the Universe: $\tau \gg t_U(T)$;
- (iii) comparable with the Universe age: $\tau \sim t_U(T)$.

The first type of reactions (i) occur very frequently during one expansion time $1/H(T)$ and their effects can be simply ‘resummed’ by imposing on the thermodynamic system the chemical equilibrium condition appropriate for each specific reaction, that is $\sum_I \mu_I = \sum_F \mu_F$, where μ_I denote the chemical potential of an initial state particle, and μ_F that of a final state particle. The numerical values of the parameters that are responsible for these reactions only determine the precise temperature T when chemical equilibrium is attained and the resummation of all effects into chemical equilibrium conditions holds. But apart from this, they have no other relevance, and do not appear explicitly in the effective formulation of the problem.

Reactions of the second type (ii) cannot have any effect on the system, since they basically do not occur. Then all physical processes are blind to the corresponding parameters, that can be set to zero in the effective Lagrangian. In most cases (but not in *all* cases) this results in exact global symmetries that correspond to conservation laws for the corresponding charges, that must be respected by the equations describing the dynamics of the system.

Reactions of the third type (iii) in general violate some symmetries, and thus spoil the corresponding conservation conditions, but are not fast enough to enforce chemical equilibrium conditions. Only reactions of this type appear explicitly in the formulation of the problem (they generally enter into a set of BEs for the evolution of the system) and only the corresponding parameters represent fundamental quantities in the specific effective theory.

In SL, the reactions of type (iii) are the ones which involve the neutrino Yukawa coupling Y^2 since by definition the decays of RHSN have rate comparable to the expansion rate of the Universe. Hence we need BEs to describe the evolution of the abundances of RHN Y_N and RHSN $Y_{\tilde{N}}$. By the same argument, the decays of RHSN which violate L also belong to the reaction of type (iii) and hence we need to use BEs to describe the evolution of lepton and slepton asymmetries defined respectively as $Y_{\Delta\ell} \equiv Y_\ell - Y_{\tilde{\ell}}$ and $Y_{\Delta\tilde{\ell}} \equiv Y_{\tilde{\ell}} - Y_{\tilde{\ell}^*}$.

Here we assume that the RHSN are in a thermal bath with a thermalization time shorter than the oscillation time. Under this assumption the initial states can be taken as being the mass eigenstates in eq. (2.4) and we will write the corresponding equations for those states and the scalar and fermion lepton numbers.

The BE describing the evolution of the number density of particles n_X in the plasma are (see Appendix B.1 or textbook [1] for more details)

$$\begin{aligned} \frac{dn_X}{dt} + 3Hn_X = & \sum_{j,l,m} \Lambda_{lm\dots}^{Xj\dots} [f_l f_m \dots (1 \pm f_X)(1 \pm f_j) \dots W(lm \dots \rightarrow Xj \dots) - \\ & - f_X f_j \dots (1 \pm f_l)(1 \pm f_m) \dots W(Xj \dots \rightarrow lm \dots)] \end{aligned}$$

where

$$\begin{aligned} \Lambda_{lm\dots}^{Xj\dots} & \equiv \int d\Pi_X d\Pi_j \dots d\Pi_l d\Pi_m \dots (2\pi)^4 \delta^{(4)}(p_X + p_j + \dots - p_l - p_m - \dots), \\ d\Pi_x & \equiv \frac{d^3 p_x}{(2\pi)^3 2E_x}, \end{aligned}$$

and $W(lm \dots \rightarrow Xj \dots)$ is the squared transition amplitude summed over initial and final spins (also summed over the gauge multiplicity i.e. $SU(2)_L$ degrees of freedom). In the above, f_X is the distribution function of particle X and is related to its number density n_X through

$$n_X = g_X \int \frac{d^3 p}{(2\pi)^3} f_X, \quad (2.101)$$

where g_X is the number of spin degrees of freedom of particle X . In this section, we will neglect the so-called ‘‘spectator effects’’ which are related to the finite chemical potentials of the Higgs, higgsino, quark and squark fields[26, 27] by assuming that they follow either Bose-Einstein or Fermi-Dirac distribution with vanishing chemical potential i.e. $f = (e^{E/T} \mp 1)^{-1}$. We will include all spectator processes in the later chapters. Including them gives an extra suppression of $\mathcal{O}(1)$ in the strong washout regime. For the leptons and sleptons we assume that they are in kinetic equilibrium and we account for their asymmetries by introducing a chemical potential for the leptons, μ_ℓ , and sleptons, $\mu_{\tilde{\ell}}$:

$$f_\ell = \frac{1}{e^{(E_\ell - \mu_\ell)/T} + 1}, \quad f_{\tilde{\ell}} = \frac{1}{e^{(E_{\tilde{\ell}} - \mu_{\tilde{\ell}})/T} - 1}, \quad (2.102)$$

and the corresponding ones for the antiparticles with the exchange $\mu_\ell \rightarrow -\mu_\ell$ and $\mu_{\tilde{\ell}} \rightarrow -\mu_{\tilde{\ell}}$ respectively. Furthermore in order to eliminate the dependence

in the expansion of the Universe we write the equations in terms of the abundances Y_X , where $Y_X = n_X/s$ where $s = \frac{2\pi^2}{45} g_{s*} T^3$ is the entropy density of the Universe.

We are interested in the evolution of $Y_{\tilde{N}_i}$, and the fermionic $Y_{\Delta\ell}$ and scalar $Y_{\Delta\tilde{\ell}}$ lepton asymmetries where the sum over $SU(2)_L$ degrees of freedom is assumed. In fact, we can relate $Y_{\Delta\ell}$ and $Y_{\Delta\tilde{\ell}}$ to their respective chemical potential (see Appendix B.1.3). Finally, in order to account for all the $\Delta L = 1$ terms we also need to consider the evolution of Y_N .

Neglecting SUSY-breaking effects in the RHSN masses and in the vertices, all the amplitudes for N_+ and N_- are equal as well as their corresponding equilibrium number densities, $n_{\tilde{N}_+}^{eq} = n_{\tilde{N}_-}^{eq} \equiv n_{\tilde{N}}^{eq}$. So we can define a unique BE for $Y_{\tilde{N}_{\text{tot}}} \equiv Y_{\tilde{N}_+} + Y_{\tilde{N}_-}$. Thus, in total, in this unflavored case, we have a set of four BEs.

The derivation of the factorization of the relevant CP asymmetries including the thermal effects is somehow lengthy but straightforward. In particular, keeping up to leading order in the CP asymmetry parameter we can neglect the difference between $f_{\tilde{N}_\pm}$ and $f_{\tilde{N}_\pm}^{eq}$ in the definitions of the thermal average widths (see Appendix B.2.1). Many of the terms in the equations are equivalent to the ones given for example in ref. [66] for supersymmetric type I seesaw leptogenesis¹⁰.

Altogether we find¹¹:

$$\dot{Y}_N = - \left(\frac{Y_N}{Y_N^{eq}} - 1 \right) \left(\gamma_N + 4\gamma_t^{(0)} + 4\gamma_t^{(1)} + 4\gamma_t^{(2)} + 2\gamma_t^{(3)} + 4\gamma_t^{(4)} \right), \quad (2.103)$$

$$\begin{aligned} \dot{Y}_{\tilde{N}_{\text{tot}}} = & - \left(\frac{Y_{\tilde{N}_{\text{tot}}}}{Y_{\tilde{N}}^{eq}} - 2 \right) \left(\frac{\gamma_{\tilde{N}}}{2} + \gamma_{\tilde{N}}^{(3)} + 3\gamma_{22} + 2\gamma_t^{(5)} \right. \\ & \left. + 2\gamma_t^{(6)} + 2\gamma_t^{(7)} + \gamma_t^{(8)} + 2\gamma_t^{(9)} \right), \end{aligned} \quad (2.104)$$

¹⁰However, some care has to be taken as the eqs. in ref. [66] are given in the weak basis for the \tilde{N} while we give here the corresponding equations in the mass basis.

¹¹For a detailed derivation of the BEs in SL, please refer to Appendix B.2.

$$\begin{aligned}
\dot{Y}_{\Delta\ell} &= \epsilon_f(T) \left(\frac{Y_{\tilde{N}_{\text{tot}}}}{Y_{\tilde{N}}^{eq}} - 2 \right) \frac{\gamma_{\tilde{N}}}{2} - \frac{Y_{\Delta\ell}}{Y_{\ell}^{eq}} \gamma_{\tilde{N}}^f \\
&\quad - \frac{Y_{\Delta\ell}}{Y_{\ell}^{eq}} \left(\frac{1}{4} \gamma_N + \frac{Y_{\tilde{N}_{\text{tot}}}}{Y_{\tilde{N}}^{eq}} \gamma_t^{(5)} + 2\gamma_t^{(6)} + 2\gamma_t^{(7)} + \frac{Y_N}{Y_{\tilde{N}}^{eq}} \gamma_t^{(3)} + 2\gamma_t^{(4)} \right) \\
&\quad + \left(\frac{Y_{\Delta\ell}}{Y_{\ell}^{eq}} - \frac{Y_{\Delta\tilde{\ell}}}{Y_{\tilde{\ell}}^{eq}} \right) \gamma_{\tilde{g}}^{\text{eff}}, \tag{2.105}
\end{aligned}$$

$$\begin{aligned}
\dot{Y}_{\Delta\tilde{\ell}} &= \epsilon_s(T) \left(\frac{Y_{\tilde{N}_{\text{tot}}}}{Y_{\tilde{N}}^{eq}} - 2 \right) \frac{\gamma_{\tilde{N}}}{2} - \frac{Y_{\Delta\tilde{\ell}}}{Y_{\tilde{\ell}}^{eq}} \gamma_{\tilde{N}}^s \\
&\quad - \frac{Y_{\Delta\tilde{\ell}}}{Y_{\tilde{\ell}}^{eq}} \left(\frac{1}{4} \gamma_N + \gamma_{\tilde{N}}^{(3)} + \frac{1}{2} \frac{Y_{\tilde{N}_{\text{tot}}}}{Y_{\tilde{N}}^{eq}} \gamma_t^{(8)} + 2\gamma_t^{(9)} \right. \\
&\quad \left. + 2 \frac{Y_N}{Y_{\tilde{N}}^{eq}} \gamma_t^{(0)} + 2\gamma_t^{(1)} + 2\gamma_t^{(2)} \right) \\
&\quad - \frac{Y_{\Delta\tilde{\ell}}}{Y_{\tilde{\ell}}^{eq}} \left(2 + \frac{1}{2} \frac{Y_{\tilde{N}_{\text{tot}}}}{Y_{\tilde{N}}^{eq}} \right) \gamma_{22} - \left(\frac{Y_{\Delta\ell}}{Y_{\ell}^{eq}} - \frac{Y_{\Delta\tilde{\ell}}}{Y_{\tilde{\ell}}^{eq}} \right) \gamma_{\tilde{g}}^{\text{eff}}, \tag{2.106}
\end{aligned}$$

where we have defined $\dot{Y}_X \equiv sH z \frac{dY_X}{dz}$ and $2Y_{\ell}^{eq} = Y_{\tilde{\ell}}^{eq} = \frac{15}{2\pi^2 g_{*s}}$ (see Appendix B.1.3). Assuming Maxwell-Boltzmann equilibrium distribution, we also have

$$Y_{\tilde{N}}^{eq} = \frac{45}{4\pi^4 g_{*s}} z^2 \mathcal{K}_2(z), \quad Y_N^{eq} = \frac{45}{2\pi^4 g_{*s}} z^2 \mathcal{K}_2(z). \tag{2.107}$$

The CP asymmetries in the BEs (2.105) and (2.106) are defined as

$$\epsilon^s(T) = \sum_{q=S,V,I} \bar{\epsilon}^q \Delta^s(T), \quad \epsilon^f(T) = - \sum_{q=S,V,I} \bar{\epsilon}^q \Delta^f(T). \tag{2.108}$$

The different γ 's are the thermally averaged reaction densities (they are

defined in Appendix B.2.1) for the following processes:

$$\begin{aligned}
\gamma_{\tilde{N}} &= \gamma_{\tilde{N}}^f + \gamma_{\tilde{N}}^s = \sum_{i=\pm} \left[\gamma(\tilde{N}_i \leftrightarrow \tilde{H}_u \ell) + \gamma(\tilde{N}_i \leftrightarrow H_u \tilde{\ell}) \right] , \\
\gamma_{\tilde{N}}^{(3)} &= \sum_{i=\pm} \gamma(\tilde{N}_\pm \leftrightarrow \tilde{\ell}^* \tilde{u}^* \tilde{Q}) , \\
\gamma_{22} &= \sum_{i=\pm} \gamma(\tilde{N}_i \tilde{\ell} \leftrightarrow \tilde{u}^* \tilde{Q}) = \sum_{i=\pm} \gamma(\tilde{N}_i \tilde{Q}^* \leftrightarrow \tilde{\ell}^* \tilde{u}^*) = \sum_{i=\pm} \gamma(\tilde{N}_i \tilde{u} \leftrightarrow \tilde{\ell}^* \tilde{Q}) , \\
\gamma_N &= \gamma(N \leftrightarrow \ell H_u) + \gamma(N \leftrightarrow \tilde{\ell} \tilde{H}_u) , \\
\gamma_t^{(0)} &= \gamma(N \tilde{\ell} \leftrightarrow Q \tilde{u}^*) = \gamma(N \tilde{\ell} \leftrightarrow \tilde{Q} \bar{u}) , \\
\gamma_t^{(1)} &= \gamma(N \bar{Q} \leftrightarrow \tilde{\ell}^* \tilde{u}^*) = \gamma(N \leftrightarrow \tilde{\ell}^* \tilde{Q}) , \\
\gamma_t^{(2)} &= \gamma(N \tilde{u} \leftrightarrow \tilde{\ell}^* Q) = \gamma(N \tilde{Q}^* \leftrightarrow \tilde{\ell}^* \bar{u}) , \\
\gamma_t^{(3)} &= \gamma(N \ell \leftrightarrow Q \bar{u}) , \\
\gamma_t^{(4)} &= \gamma(N u \leftrightarrow \bar{\ell} Q) = \gamma(N \bar{Q} \leftrightarrow \bar{\ell} \bar{u}) , \\
\gamma_t^{(5)} &= \sum_{i=\pm} \gamma(\tilde{N}_i \ell \leftrightarrow Q \tilde{u}^*) = \sum_{i=\pm} \gamma(\tilde{N}_i \ell \leftrightarrow \tilde{Q} \bar{u}) , \\
\gamma_t^{(6)} &= \sum_{i=\pm} \gamma(\tilde{N}_i \tilde{u} \leftrightarrow \bar{\ell} Q) = \sum_{i=\pm} \gamma(\tilde{N}_i \tilde{Q}^* \leftrightarrow \bar{\ell} \bar{u}) , \\
\gamma_t^{(7)} &= \sum_{\pm} \gamma(\tilde{N}_i \bar{Q} \leftrightarrow \bar{\ell} \tilde{u}^*) = \sum_{i=\pm} \gamma(\tilde{N}_i u \leftrightarrow \bar{\ell} \tilde{Q}) , \\
\gamma_t^{(8)} &= \sum_{i=\pm} \gamma(\tilde{N}_i \tilde{\ell}^* \leftrightarrow \bar{Q} u) , \\
\gamma_t^{(9)} &= \sum_{i=\pm} \gamma(\tilde{N}_i Q \leftrightarrow \tilde{\ell} u) = \sum_{i=\pm} \gamma(\tilde{N}_i \bar{u} \leftrightarrow \tilde{\ell} \bar{Q}) , \tag{2.109}
\end{aligned}$$

where in all cases a sum over gauge multiplicity, the CP conjugate final states and lepton flavors is implicit.

The explicit expressions for the γ 's in eq. (2.109) can be found, for example, in ref. [66] for the case of Boltzmann-Maxwell distribution functions and neglecting Pauli-blocking and Bose-enhancement statistical factors as well as the relative motion of the particles with respect to the plasma¹². With these

¹²Neglecting SUSY-breaking effects in the RHSN masses and in the vertices, it can be shown that the thermal widths for the RHSN mass eigenstates and weak eigenstates are the same.

approximations, for example:

$$\gamma_{\tilde{N}} = 2n_{\tilde{N}}^{eq} \Gamma_{\tilde{N}} \frac{\mathcal{K}_1(z)}{\mathcal{K}_2(z)}, \quad \gamma_N = n_N^{eq} \Gamma_N \frac{\mathcal{K}_1(z)}{\mathcal{K}_2(z)}, \quad (2.110)$$

where $\Gamma_N = \Gamma_{\tilde{N}} = \Gamma$ are the zero temperature widths eq. (2.12). The factor of 2 in the first equation above is due to the sum over of \tilde{N}_+ and \tilde{N}_- states. In our calculation we keep the thermal masses and statistical factors on the CP asymmetries but we neglect them in the rest of the thermal widths, with the exception of the Higgs mass in the $\Delta L = 1$ processes involving a Higgs boson exchange in the t -channel to regularize the infrared divergence.

We have included in eqs. (2.103)–(2.106) the \tilde{N}_\pm and N decay and inverse decay processes as well as all the $\Delta L = 1$ scattering processes induced by the *top* Yukawa coupling. We ignore $\Delta L = 1$ scattering involving gauge bosons. They are infrared divergent and there is still not a consensus in the literature on how to regularize them [25, 47, 103].

$\Delta L = 2$ processes involving the on-shell exchange of N or \tilde{N}_\pm are already accounted for by the decay and inverse decay processes. The $\Delta L = 2$ off-shell scattering processes involving the pole-subtracted s-channel and the u- and t-channel, as well as the L -conserving processes from N and \tilde{N} pair creation and annihilation have not been included. The reaction rates for these processes are quartic in the neutrino Yukawa couplings and therefore can be safely neglected as long as the neutrino Yukawa couplings are much smaller than one, as it is the case for the relevant mass range for successful SL which is $M \lesssim 10^9$ GeV as we will see in the next section. The effect of non-resonant $\Delta L = 2$ processes only become important and will strongly suppress the asymmetry generated when $M \gtrsim 10^{14}$ GeV as the neutrino Yukawa couplings become the order of 1 (see e.g. ref. [25]).

2.4.2.1 Neglecting CP asymmetry in scatterings

We have accounted for the dominant CP asymmetry in the mixing as generated by the thermal effects in the \tilde{N}_\pm two body decays but we have not included the possible CP violating effects induced by mixing in its three body decays or in its scattering processes [30, 33, 45, 47, 104].

Strictly speaking, when scatterings are included, for consistency one should

include also the corresponding CP asymmetries. In the type I seesaw leptogenesis, contributions to the total CP asymmetry from scatterings have been shown to dominate only at high temperature $z \lesssim 0.5$ [33]. Hence it is only relevant in the weak washout regime with zero initial RHN abundance [30, 33]. In this case, the inclusion of CP asymmetry in scatterings suppresses the total lepton asymmetry generated due to the strong cancellation between opposite sign lepton asymmetries generated during the RHN production phase and when they eventually decay away (which in the limit of zero washout will actually yield a zero final lepton asymmetry [30]).

In SL, however, the inclusion of CP asymmetry in scatterings cannot be done in a straightforward way because their thermal factors constitute a new set of non trivial quantities. Hence, a careful quantitative study in this direction is still needed and is also beyond the scope of this thesis and will be left as future work.

2.4.2.2 Assuming superequilibration

In eqs. (2.105) and (2.106) γ_g^{eff} represents processes which transform leptons into scalar leptons and vice versa (for example $[e + e \leftrightarrow \tilde{e} + \tilde{e}]$). The rates for these reactions are larger than the ones in eq. (2.109) because they do not involve the neutrino Yukawa couplings. Consequently they will try to equilibrate the chemical potentials of lepton and slepton i.e. $\mu_\ell \approx \mu_{\tilde{\ell}} \implies \frac{Y_{\Delta\ell}}{Y_\ell^{eq}} \approx \frac{Y_{\Delta\tilde{\ell}}}{Y_{\tilde{\ell}}^{eq}}$ a condition known as *superequilibration* or superequilibrium [105] (please refer to Appendix C for further discussion). In Chapter 5, we will see that at temperature $T \gtrsim 10^7$ GeV, γ_g^{eff} actually falls out of equilibrium and this can have interesting consequences but as of now we will work with the assumption of superequilibration.

Assuming superequilibration $\frac{Y_{\Delta\ell}}{Y_\ell^{eq}} \approx \frac{Y_{\Delta\tilde{\ell}}}{Y_{\tilde{\ell}}^{eq}}$ and using the fact that $Y_{\tilde{\ell}}^{eq} = 2Y_\ell^{eq}$ (the expression is given below eq. 2.106), we can combine the BEs for $Y_{\Delta\ell}$ and $Y_{\Delta\tilde{\ell}}$ by defining

$$Y_{L_{\text{tot}}} \equiv Y_{\Delta\ell} + Y_{\Delta\tilde{\ell}} = 3Y_{\Delta\ell}, \quad (2.111)$$

$$\epsilon(T) \equiv \epsilon^s(T) + \epsilon^f(T), \quad (2.112)$$

and obtain the BE:

$$\begin{aligned}
\dot{Y}_{L_{\text{tot}}} &= \left[\epsilon(T) \left(\frac{Y_{\tilde{N}_{\text{tot}}}}{Y_{\tilde{N}}^{\text{eq}}} - 2 \right) - \frac{Y_{L_{\text{tot}}}}{Y_c^{\text{eq}}} \right] \frac{\gamma_{\tilde{N}}}{2} \\
&\quad - \frac{Y_{L_{\text{tot}}}}{Y_c^{\text{eq}}} \left(\frac{1}{4} \gamma_N + \frac{Y_{\tilde{N}_{\text{tot}}}}{Y_{\tilde{N}}^{\text{eq}}} \gamma_t^{(5)} + 2\gamma_t^{(6)} + 2\gamma_t^{(7)} + \frac{Y_N}{Y_N^{\text{eq}}} \gamma_t^{(3)} + 2\gamma_t^{(4)} \right) \\
&\quad - \frac{Y_{L_{\text{tot}}}}{Y_c^{\text{eq}}} \left(\frac{1}{4} \gamma_N + \gamma_{\tilde{N}}^{(3)} + \frac{1}{2} \frac{Y_{\tilde{N}_{\text{tot}}}}{Y_{\tilde{N}}^{\text{eq}}} \gamma_t^{(8)} + 2\gamma_t^{(9)} \right. \\
&\quad \left. + 2 \frac{Y_N}{Y_N^{\text{eq}}} \gamma_t^{(0)} + 2\gamma_t^{(1)} + 2\gamma_t^{(2)} \right) \\
&\quad - \frac{Y_{L_{\text{tot}}}}{Y_c^{\text{eq}}} \left(2 + \frac{1}{2} \frac{Y_{\tilde{N}_{\text{tot}}}}{Y_{\tilde{N}}^{\text{eq}}} \right) \gamma_{22},
\end{aligned} \tag{2.113}$$

where we have defined $Y_c^{\text{eq}} \equiv \frac{45}{4\pi^2 g_{*s}}$. So in total we are left with three BEs for Y_N , $Y_{\tilde{N}_{\text{tot}}}$, and $Y_{L_{\text{tot}}}$.

2.4.3 Results

As discussed in Section 1.2.1, it is convenient to follow the evolution of the $B - L$ asymmetry, $Y_{\Delta_{B-L}}$ since it is absolutely conserved once leptogenesis is complete. At temperature $T > 10^{12}$ GeV when EW sphaleron interactions are not in equilibrium (reactions of type (ii)), we simply have $Y_{L_{\text{tot}}} = -Y_{\Delta_{B-L}}$ because there is no other interactions which violates B and L . However, at lower temperatures relevant for SL when EW sphaleron interactions come into equilibrium, this relation does not hold¹³. In fact, one has to take into account the reactions which come into equilibrium (reactions of type (i)) at the different temperature regimes and in general one cannot ignore lepton flavor effects (the subject of Chapter 4). Here we will simply approximate $Y_{L_{\text{tot}}} \approx -Y_{\Delta_{B-L}}$.

Assuming no pre-existing asymmetry, the final $Y_{\Delta_{B-L}}^0$ can be parametrized as¹⁴

$$Y_{\Delta_{B-L}}^0 = -Y_{L_{\text{tot}}}^0 = -2\bar{\epsilon}\eta Y_{\tilde{N}}^{\text{eq}}(T \gg M), \tag{2.114}$$

¹³A careful analysis was carried out for example in refs. [27, 28].

¹⁴The factor 2 in eq. (2.114) arises from the fact that there are two RHN states while we have defined $Y_{\tilde{N}}^{\text{eq}}$ for one degree of freedom. Defined this way, η has the standard normalization $\eta \rightarrow 1$ for perfect out of equilibrium decay.

where

$$\bar{\epsilon} \equiv \sum_{q=S,V,I} \bar{\epsilon}^q, \quad (2.115)$$

and $Y_{\tilde{N}}^{eq}(T \gg M) = 45/(2\pi^4 g_{*s})$ which follows eq. (2.107) by taking the limit $T \gg M$. The efficiency factor η takes into account the possible inefficiency in the production of RHSN, the erasure of the generated asymmetry by L -violating scattering processes and the temperature dependence of the CP asymmetry and it is obtained by solving the array of BEs above. Here η mainly depends on m_{eff} defined in eq. (2.95). There is a very mild dependence on M due to the running of couplings and the thermal factor $\Delta_{BF}(T)$ in eq. (2.48). Also notice that η defined in this way is independent of the type of CP asymmetries responsible for lepton asymmetry generation.

To relate the current baryon asymmetry $Y_{\Delta B}^0$ to the $Y_{\Delta B-L}^0$ generated from the decays of RHSN, in principle we have to know the rate of EW sphaleron processes. However since $B - L$ is absolutely conserved by EW sphaleron processes which are in equilibrium for $100 \text{ GeV} \lesssim T \lesssim 10^{12} \text{ GeV}$ (see Section 1.1.2), what really matters is the moment right before EW sphaleron falls out of equilibrium (before it stops converting $B - L$ to B). Assuming only the SM particles, up-type and down-type Higgs doublets constitute the relativistic degrees of freedom in the thermal bath at the time just before EW sphaleron processes decouple (while all sparticles are too heavy and disappear from the thermal bath), the relation between $Y_{\Delta B}^0$ and $Y_{\Delta B-L}^0$ before EWPT is given by

$$Y_{\Delta B}^0 = \frac{8}{23} Y_{\Delta B-L}^0. \quad (2.116)$$

The relation above will change if the EW sphaleron processes decouple after EWPT [51, 106] or if the threshold effects for heavy particles namely sparticles and/or top quarks and Higgs are taken into account [106, 107].

Solving the BEs (2.103), (2.104) and (2.113) with parametrization (2.114), we can determine the efficiency η as a function of m_{eff} and M . In Figure 2.8 we plot $|\eta|$ as a function of m_{eff} for $M = 10^7 \text{ GeV}$. Following refs. [25, 83] we consider two different initial conditions for the RHSN abundance. In one case, one assumes that the RHSN population is created by their Yukawa interactions with the thermal plasma, and set $Y_{\tilde{N}_{\text{tot}}}(z \rightarrow 0) = 0$. The other case corresponds to an initial RHSN abundance equal to the thermal one, $Y_{\tilde{N}_{\text{tot}}}(z \rightarrow 0) =$

$2Y_{\tilde{N}}^{eq}(z \rightarrow 0)$. As we can see from Figure 2.8, in the strong washout regime, the efficiency is independent of the initial condition as discussed in Section 2.4.1. We can also see this behavior by looking at the evolution of Y_{B-L} in the strong regime for both thermal and zero initial RHSN abundances (bottom panels of Figure 2.6 and Figure 2.7).

Notice that with thermal initial RHSN abundance and in the weak washout regime, the efficiency does not flatten out to a maximum value as we would have expected if the CP asymmetry were constant i.e. temperature independent (see discussion in Section 2.4.1). What we observe in Figure 2.8 is that, in this case, the efficiency (dashed red curve) decreases with decreasing m_{eff} due to time (i.e. temperature T) dependence of the CP asymmetry. As m_{eff} decreases, due to weaker Yukawa interactions, the RHSN will become overabundant at a later time (see the top panel of Figure 2.6) and hence decay at a time when the CP asymmetry is smaller (see Figure 2.4), resulting in smaller efficiency. In the strong washout regime, the efficiency decreases with increasing m_{eff} due to increasing washout (see the bottom panel of Figure 2.6). If the CP asymmetry were constant, the efficiency will decrease as $\sim 1/m_{\text{eff}}$ (see e.g. ref. [108] for the discussion on leptogenesis in the strong washout regime). However, due to the strong temperature dependence of the CP asymmetry in SL, there is an additional dependence of final efficiency on m_{eff} and as a result, the efficiency in the strong washout regime does not decrease as $\sim 1/m_{\text{eff}}$ but according to Figure 2.8 it decreases slightly faster.

On the other hand, with zero initial RHSN abundance (solid black curve in Figure 2.8), we notice that there is a sign change in the efficiency somewhere around intermediate washout regime. The reason is the following. During the RHSN production phase (i.e. $Y_{\tilde{N}_{\text{tot}}} < 2Y_{\tilde{N}}^{eq}$), the “wrong” sign lepton asymmetry is generated. In the weak washout regime, a large part of “wrong” sign asymmetry survives due to weak washout and also the RHSN will decay late when the CP asymmetry is smaller. As a result, the “right” sign lepton asymmetry generated when eventually all the RHSN decay away could not overcome the “wrong” sign one (see the top panel of Figure 2.7). In the strong washout regime, the washout of the initial “wrong” sign lepton asymmetry is more efficient and also the RHSN will decay earlier when the CP asymmetry is larger. The combination of these two effects result in a final “right” sign

lepton asymmetry (see the bottom panel of Figure 2.7).

In the intermediate regime, a perfect cancellation between the “wrong” and “right” sign lepton asymmetries results in the dip (where the efficiency curve changes the sign) observed in Figure 2.8. It is important to notice that “right” or “wrong” sign lepton asymmetry discussed here is arbitrary since the sign of $\bar{\epsilon}$ can be changed by choice of the CP phases in eqs. (2.45)–(2.47).

Considering only the contribution to CP asymmetry from the mixing [82, 83] i.e. $\epsilon^S(T)$ as in eq. (2.91), we plot in Figure 2.9 the range of parameters B and m_{eff} for which enough baryon asymmetry is generated, $|Y_{\Delta B}^0| \geq 8.54 \times 10^{-11}$. We show the ranges for several values of M and for the characteristic value of $|\text{Im}A| = 1$ TeV. The figure illustrates our quantification of the known result that independently of the initial RHSN distributions, successful SL requires $M \lesssim 10^9$ GeV as well as $B \ll \mathcal{O}(\text{TeV})$ [82, 83]. This justifies the omission of the non-resonant $\Delta L = 2$ processes in the BEs which are only relevant when $M \gtrsim 10^{14}$ GeV.

In the next section, we will briefly discuss the contributions to the CP asymmetry due to gaugino soft masses [85] i.e. $\epsilon^V(T)$ and $\epsilon^I(T)$ (eq. (2.92) and eq. (2.93)) and leave the detailed study to Chapter 4 when we consider the lepton flavor effects.

2.5 Discussion and Conclusions

In this chapter, we have quantified in detail the contributions to CP violation in RHSN decays induced by soft terms: the soft bilinear B , trilinear A and gaugino mass terms paying special attention to the role of thermal effects. Using a field-theoretical as well as a quantum mechanical approach we conclude that for all the soft SUSY-breaking sources of CP violation considered, an exact cancellation between the asymmetries produced in the fermionic and bosonic channels occurs at $T = 0$ up to second order in soft SUSY-breaking parameters. However, once thermal effects are included, this cancellation is partially lifted.

Considering the CP asymmetry from mixing eq. (2.91), our results show good agreement with the ones in ref. [83]. In particular we reproduce that for zero initial conditions, η can take both signs depending on the value of

m_{eff} , thus it is possible to generate the right sign asymmetry with either sign of $\text{Im}A$. For thermal initial conditions, on the contrary, $\eta > 0$ and the right asymmetry can only be generated for $\text{Im}A > 0$. In particular, independently of the initial RHSN distributions, successful SL requires $M \lesssim 10^9$ GeV as well as $B \ll \mathcal{O}(\text{TeV})$. From eq. (2.45), we see that resonantly enhanced CP asymmetry require $B \sim \Gamma/2$ which is an unconventionally small B value ¹⁵.

Although we do not quantify the contributions to the CP asymmetry due to gaugino soft masses [85] i.e. $\epsilon^V(T)$ (eq. (2.92)) and $\epsilon^I(T)$ (eq. (2.93)) in this chapter, we will comment on their contributions in the following. From eqs. (2.46) and (2.47), assuming non-vanishing and non-cancellation between phases, we have

$$\begin{aligned}\bar{\epsilon}^V &\sim \frac{m_2}{M} \frac{|A|, B}{M}, \\ \bar{\epsilon}^I &\sim \frac{m_2}{M} \frac{|A|}{M} \frac{\Gamma^2}{4B^2 + \Gamma^2}.\end{aligned}\tag{2.117}$$

In general, successful SL requires $|\bar{\epsilon}| \gtrsim \mathcal{O}(10^{-5})$. Hence for $\bar{\epsilon}^V$ with $M \sim \mathcal{O}(10^5)$ GeV we can have all the soft couplings m_2 , $|A|$ and in particular B to be at the TeV scale. However for $\bar{\epsilon}^I$, we always need to have $B \lesssim \Gamma$ much smaller than the TeV scale. The quantitative result from the gaugino contribution is presented in Section 4.4.1.1 where we also consider the lepton flavor effects.

¹⁵SL based on specific models which naturally generate small B values are considered in refs. [86, 96, 99, 109].

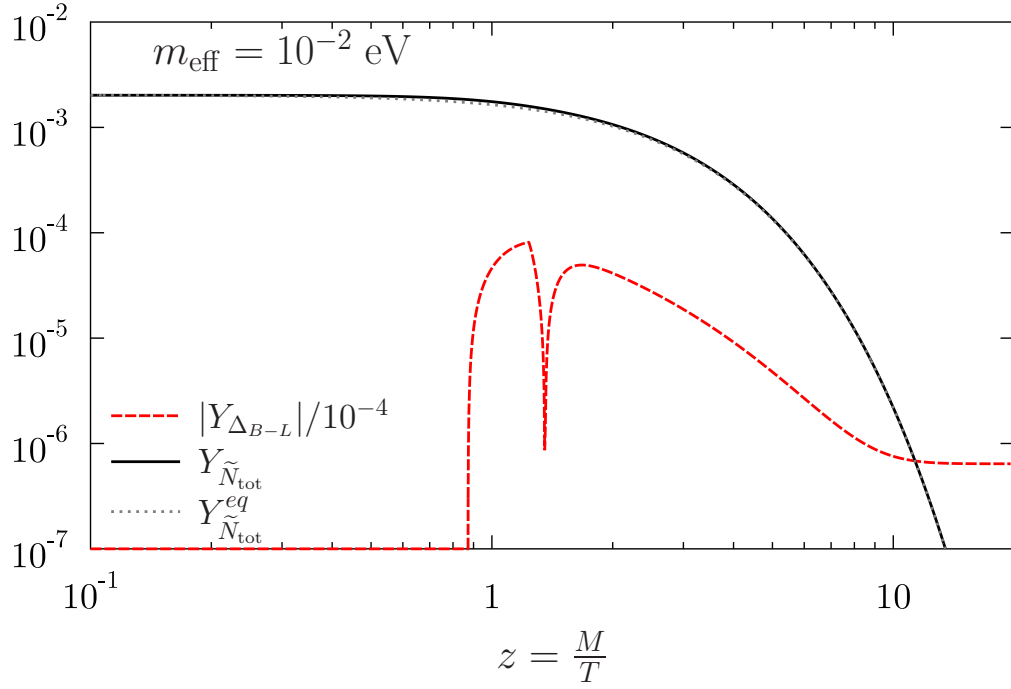
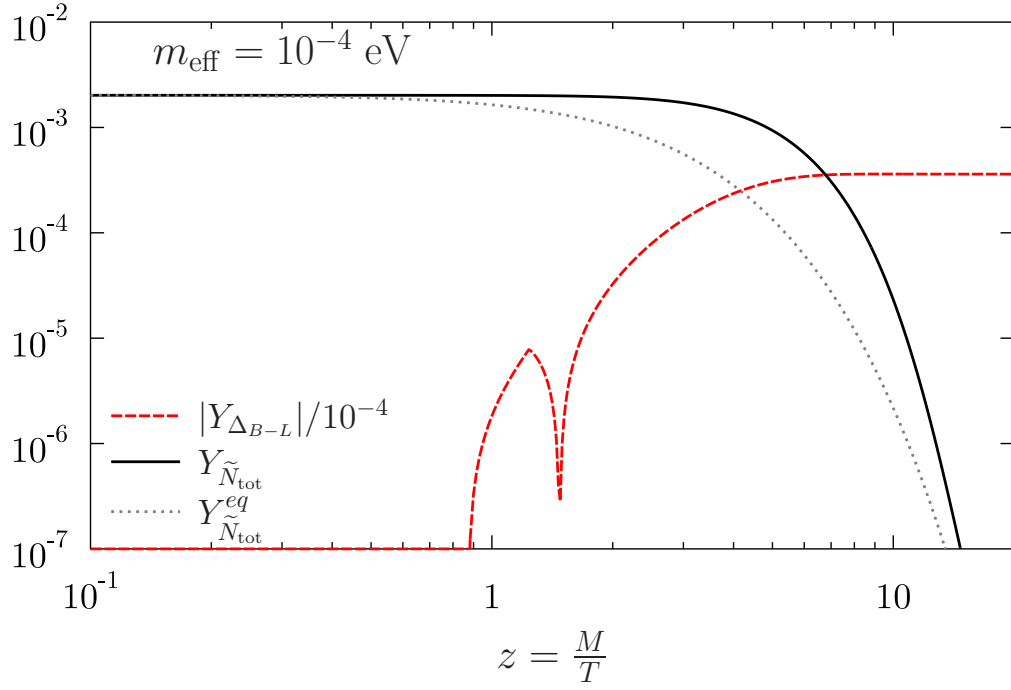


Figure 2.6: Evolution of $Y_{\tilde{N}_{\text{tot}}}$ (black solid curve) and $Y_{\Delta_{B-L}}$ (red dashed curve) assuming thermal initial RHSN abundance $Y_{\tilde{N}_{\text{tot}}}(z \rightarrow 0) = 2Y_{\tilde{N}}^{\text{eq}}(z \rightarrow 0)$ for $m_{\text{eff}} = 10^{-4} \text{ eV}$ (top) and $m_{\text{eff}} = 10^{-2} \text{ eV}$ (bottom). The equilibrium RHSN abundance $Y_{\tilde{N}_{\text{tot}}}^{\text{eq}}$ is given by the grey dotted curve.

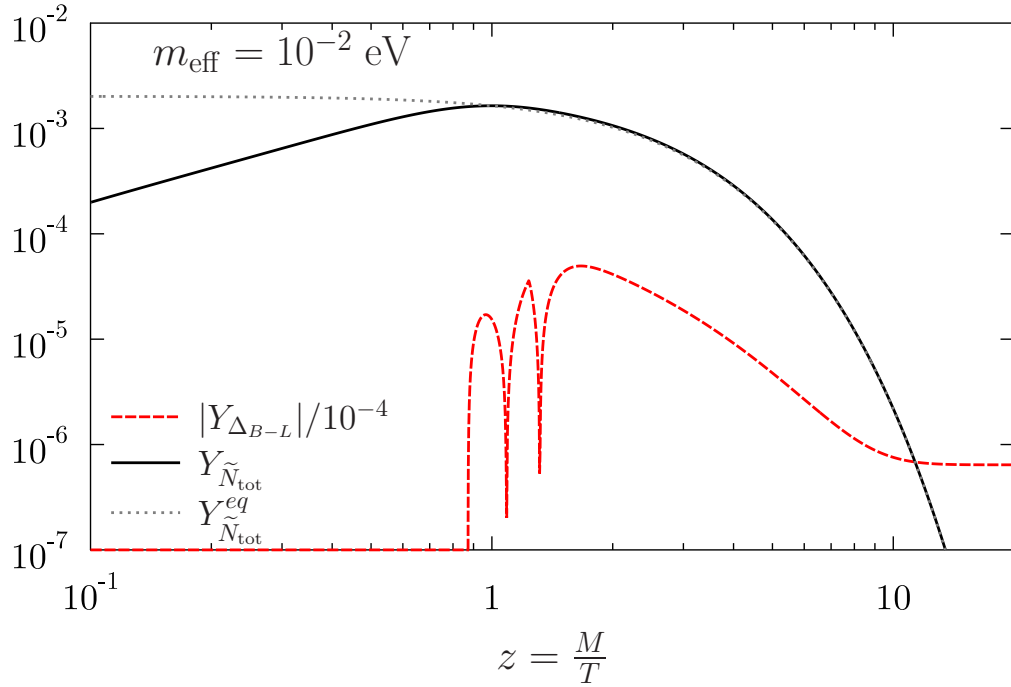
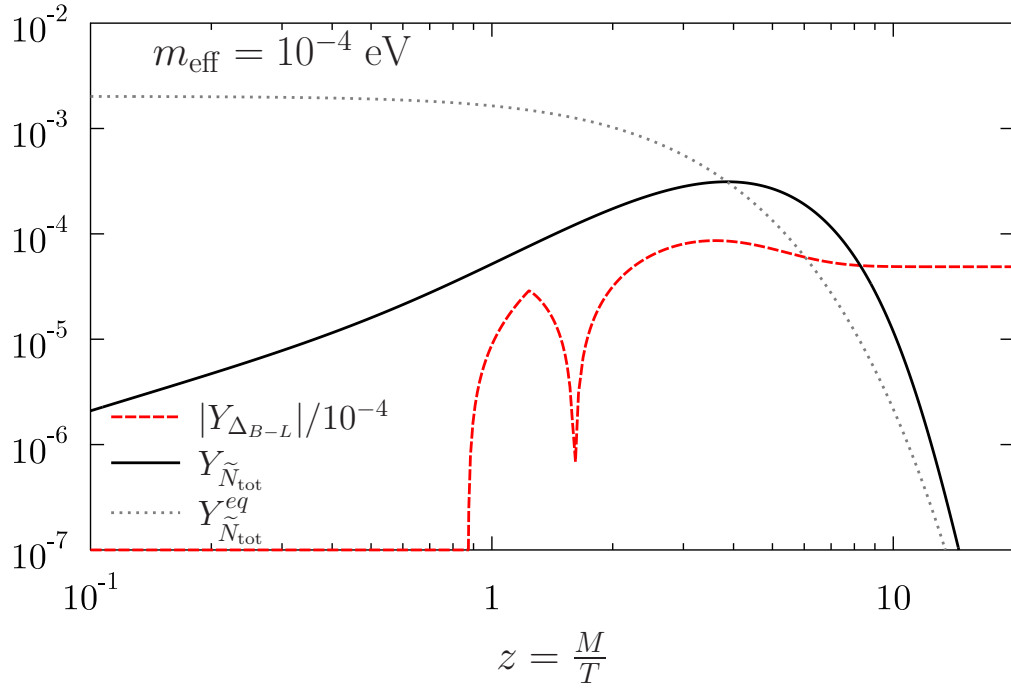


Figure 2.7: Evolution of $Y_{\tilde{N}_{\text{tot}}}$ (black solid curve) and $Y_{\Delta_{B-L}}$ (red dashed curve) assuming zero initial RHSN abundance $Y_{\tilde{N}_{\text{tot}}}(z \rightarrow 0) = 0$ for $m_{\text{eff}} = 10^{-4}$ eV (top) and $m_{\text{eff}} = 10^{-2}$ eV (bottom). The equilibrium RHSN abundance $Y_{\tilde{N}_{\text{tot}}}^{\text{eq}}$ is given by the grey dotted curve.

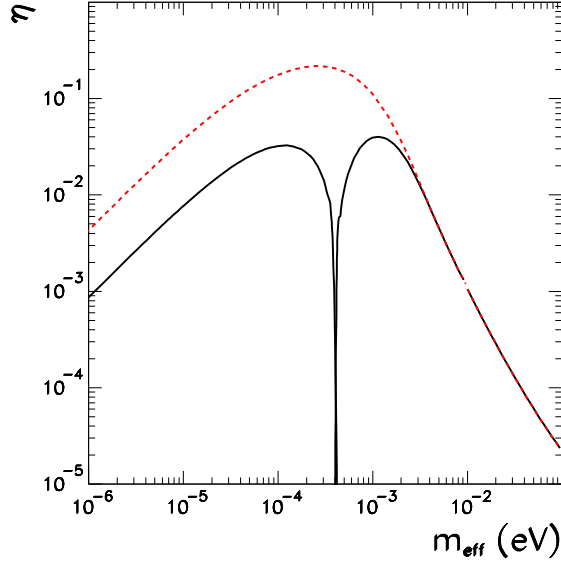


Figure 2.8: Efficiency factor $|\eta|$ as a function of m_{eff} for $M = 10^7$ GeV and $\tan\beta = 30$. The two curves correspond to vanishing initial RHSN abundance (solid black curve) and thermal initial RHSN abundance, (dashed red curve).

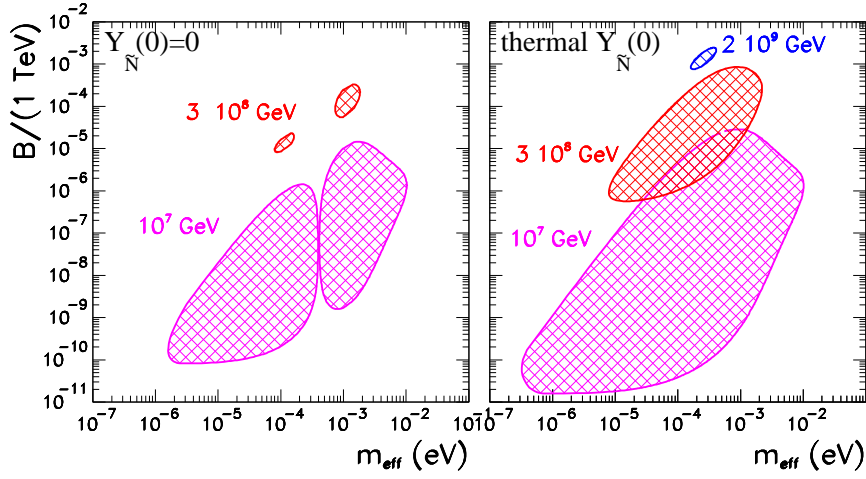


Figure 2.9: B, m_{eff} regions in which successful SL can be achieved considering only the contribution to CP asymmetry from mixing i.e. $\epsilon^S(T)$ as in eq. (2.93). We take $|\text{Im}A| = 10^3$ GeV and different values of M as labeled in the figure. The two panels correspond to vanishing initial RHSN abundance (left) and thermal initial RHSN abundance (right).

Chapter 3

Quantum Effects

3.1 The Possible Role of Quantum Effects

In most studies, the dynamics of thermal leptogenesis (both for the standard seesaw case, as well as for the SL scenario) is studied using the approach of classical BE as described in the previous chapter. The possibility of using quantum BE (QBE) in leptogenesis was first discussed in ref. [110] and more recently derived in detail in ref. [111–117]. Following ref. [111], QBE were obtained starting from the non-equilibrium quantum field theory based on the Closed Time-Path (CTP) formulation. They differ from the classical BE in that they contain integrals over the past times unlike in the classical kinetic theory in which the scattering terms do not include any integral over the past history of the system which is equivalent to assume that any collision in the plasma does not depend upon the previous ones. In the CTP formalism, the energy conservation delta functions which appear in the evaluation of the reaction rates are substituted by retarded time integrals of time-dependent kernels and cosine functions whose arguments are the energy involved in the reactions. In the limit in which the time range of the kernels is shorter than the relaxation time of the particle abundances and the time integrals are taken over an infinite time (i.e. neglecting memory effects), the standard time-independent reaction rates (see for e.g. those defined in Appendix B.2.1) are recovered. Furthermore, the CP asymmetry also acquires an additional time-dependent piece with its value at a given instant depending upon the previous history of the system. According to ref. [111], quantitatively, this is the most relevant ef-

fect for leptogenesis. If the time variation of the CP asymmetry is shorter than the relaxation time of the particles abundances, the solutions to the quantum and the classical Boltzmann equations are expected to differ only by terms of the order of the ratio of the time-scale of the CP asymmetry to the relaxation time-scale of the distribution. This is typically the case in thermal leptogenesis with hierarchical RHN. However, as discussed in refs. [88, 89], in the resonant leptogenesis scenario, $(M_j - M_i)$ is of the order of the decay rate of the RH neutrinos. As a consequence the typical time-scale to build up coherently the time-dependent CP asymmetry, which is of the order of $(M_j - M_i)^{-1}$, can be larger than the time-scale for the change of the abundance of the RHN. This, as shown in refs. [88, 89], leads to quantitative differences between the classical and the quantum approach in the case of resonant leptogenesis and, in particular, in the weak washout regime they enhance the produced asymmetry.

Motivated by these results and by the fact that in SL the CP asymmetry in mixing (eq. (2.42)) is produced resonantly, we perform a detailed study of the role of quantum effects in the SL scenario. Our results show that, because of the thermal nature of SL, the dependence of the quantum effects on the washout regime for SL is quantitatively different than in the seesaw resonant scenario. In particular in the weak washout regime quantum effects do not enhance but suppress the produced baryon asymmetry. Quantum effects are most quantitatively important for extremely degenerate RHSN (that is far away from the resonant condition), $\Delta M \ll \Gamma$, and in the strong washout regime they can lead to an enhancement, as well as change of sign, of the produced asymmetry. But altogether, for a given M the required values of the lepton violating soft bilinear term B to achieve successful leptogenesis are not substantially modified.

3.2 The Modification to the CP Asymmetry

As discussed in ref. [83], when $\Gamma \gg \Delta M \equiv M_+ - M_-$, the two singlet sneutrino states \tilde{N}_\pm are not well-separated particles. In this case, the result for the CP asymmetry depends on how the initial state is prepared. In what follows we will assume that the RHSN are in a thermal bath with a thermalization time Γ^{-1} shorter than the typical oscillation times, $(\Delta M)^{-1}$, therefore coherence is

lost and it is appropriate to compute the CP asymmetry in terms of the mass eigenstates.

As we have seen in the previous chapter, the relevant CP asymmetry in SL is temperature T (i.e. time) dependent even in the *classical* regime. This is so because the CP asymmetry is generated by the SUSY-breaking thermal effects which make the relevant decay CP asymmetries into scalars and fermions different. In the absence of these thermal corrections, no significant asymmetry can be generated (one exception is the non-superequilibration scenario discussed in Chapter 5).

The inclusion of quantum effects (for technical details see refs. [88, 89, 111]) introduces an additional time dependence in the CP asymmetry. As shown in refs. [88, 89, 111] quantum effects are flavor independent as long as the damping rates of the leptons are taken to be flavor independent. Neglecting also the difference in the width between the two RHSN which is the same for all flavors, we obtain

$$\epsilon(T) = \bar{\epsilon} \times \Delta_{BF}(T) \times QC(t), \quad (3.1)$$

where

$$QC(t) = 2 \sin^2 \left(\frac{M_+ - M_-}{2} t \right) - \frac{\Gamma}{M_+ - M_-} \sin((M_+ - M_-)t). \quad (3.2)$$

The factor $QC(t)$ is the one which remains after taking the corresponding past time integral to large time such that only on-shell decay processes contribute to the CP asymmetry (i.e. neglecting memory effects in decay processes). We see that this factor grows for $t \lesssim 1/\Delta M$ and starts oscillating for $t \gtrsim 1/\Delta M$. This oscillation pattern originates from the CP violating decays of two mixed states N_+ and N_- analogous to the CP violation in neutral meson systems. If the timescale for the decay $t \sim 1/\Gamma$ is much larger than $1/\Delta M$, the CP asymmetry should average to the *classical* value. However, if the decay timescale $t \sim 1/\Gamma$ is shorter $1/\Delta M$, this additional time dependence on CP asymmetry may not be negligible.

Next we have to change the variable from time t of eq. (3.2) to a more convenient variable $z = M/T$ as we do when writing down the BE. As a reminder to the readers, we will write a few lines illustrating this change. For

a universe undergoing adiabatic expansion, the entropy per comoving volume is constant i.e. $sR^3 = \text{constant}$. Since $s \propto z^{-3}$, we have $R \propto z$. Then, the Hubble constant is given by $H \equiv R^{-1}dR/dt = z^{-1}dz/dt$. After integration, we get

$$t = \frac{1}{H(M)} \frac{z^2 - z_0^2}{2}, \quad (3.3)$$

where z_0 is the temperature at $t = 0$. Substituting eq. 3.3 into eq. (3.2), we obtain

$$\begin{aligned} QC(z) &= 2 \sin^2 \left(\frac{1}{2} \frac{M_+ - M_-}{2H(M)} z^2 \right) - \frac{\Gamma}{M_+ - M_-} \sin \left(\frac{M_+ - M_-}{2H(M)} z^2 \right), \\ &= 2 \sin^2 \left(\frac{m_{\text{eff}}}{m^*} R \frac{z^2}{8} \right) - \frac{2}{R} \sin \left(\frac{m_{\text{eff}}}{m^*} R \frac{z^2}{4} \right). \end{aligned} \quad (3.4)$$

where we set $z_0 = 0$ (i.e. at very high initial temperature). In writing the second equality we have used that $M_+ - M_- = B$ assuming $\widetilde{M} \ll M$ (see eq. (2.5)), and we have defined the degeneracy parameter R ,

$$R = \frac{2(M_+ - M_-)}{\Gamma} = \frac{2B}{\Gamma}. \quad (3.5)$$

In summary, the final CP asymmetry consists of three factors. The first one is the temperature independent piece $\bar{\epsilon}$ defined in eq. (2.115). Since we are interested in studying the case where the CP asymmetry is produced resonantly (i.e. from mixing), we will only look at $\bar{\epsilon} = \bar{\epsilon}^S$ (eq. (2.45)) which can be rewritten as follows¹:

$$\bar{\epsilon}^S = \frac{\text{Im}A}{M} \frac{2R}{R+1}. \quad (3.6)$$

Notice $\bar{\epsilon}^S$ is resonantly enhanced for $R = 1$. The second one is the thermal factor $\Delta_{BF}(T)$ which is only non-vanishing for $z \gtrsim 0.8$ (see Figure 2.4). The third one is the quantum correction factor, $QC(T)$ discussed earlier.

Next we turn to quantify the impact of this last additional quantum time-dependence of the CP asymmetry on the final lepton asymmetry and study

¹Studying quantum effects for $\bar{\epsilon}^V$ (2.46) and $\bar{\epsilon}^I$ (2.47) is straightforward. In any case, in the interesting parameter space for $\bar{\epsilon}^V$ where $R \gg 1$, quantum effects will be irrelevant while the quantum effects on $\bar{\epsilon}^I$ for the relevant parameter space where $R \ll 1$ can be inferred from the current study e.g. from Figure 3.3.

of the relevance of the quantum effects using the BEs (2.103), (2.104) and (2.113). Following ref. [111], we neglect quantum effects in the thermally averaged reaction densities and keep them only in the CP asymmetry.

3.3 Results

We show in Figure 3.1 the evolution of the lepton asymmetry with and without the quantum correction factor in the CP asymmetry for several values of the washout factor m_{eff} and for the resonant case $R = 1$ and the very degenerate case $R = 2 \times 10^{-4}$. The two upper panels correspond to strong and moderate washout regimes, while the lower two correspond to weak and very weak washout regimes. We consider two different initial conditions for the RHSN abundance. In one case, one assumes that the RHSN population is created by their Yukawa interactions with the thermal plasma, and set $Y_{\tilde{N}_{\text{tot}}}(z \rightarrow 0) = 0$. The other case corresponds to an initial RHSN abundance equal to the thermal one, $Y_{\tilde{N}_{\text{tot}}}(z \rightarrow 0) = 2Y_{\tilde{N}}^{\text{eq}}(z \rightarrow 0)$. The initial condition on the RHSN abundances can lead to differences in the weak washout regime. On the contrary, as seen in Section 2.4.3, in the strong washout regime any asymmetry generated in the early time (e.g. in the RHSN production phase) is efficiently washed out (contrary to what happens in the weak washout regime). Consequently, in the strong washout regime the generated lepton asymmetry is independent of the initial conditions. This behavior is explicitly displayed on the upper panel of Figure 3.1. It can also be observed on the right hand side of the upper panels as well as on the upper curves of the lower panels of Figure 3.3, and on the right hand side of Figure 3.4.

First we notice that, as expected, for strong washout and large degeneracy parameter R (see the upper curves in the upper panels), the quantum effects lead to the oscillation of the produced asymmetry till it finally averages out to the *classical* value.

The figure also illustrates that for very small values of R and in the strong washout regime, quantum effects enhance the final asymmetry. For small enough R the arguments in the periodic functions in $QC(T)$ are very small for all relevant values of z and m_{eff} . So the \sin^2 term in $QC(T)$ is negligible and

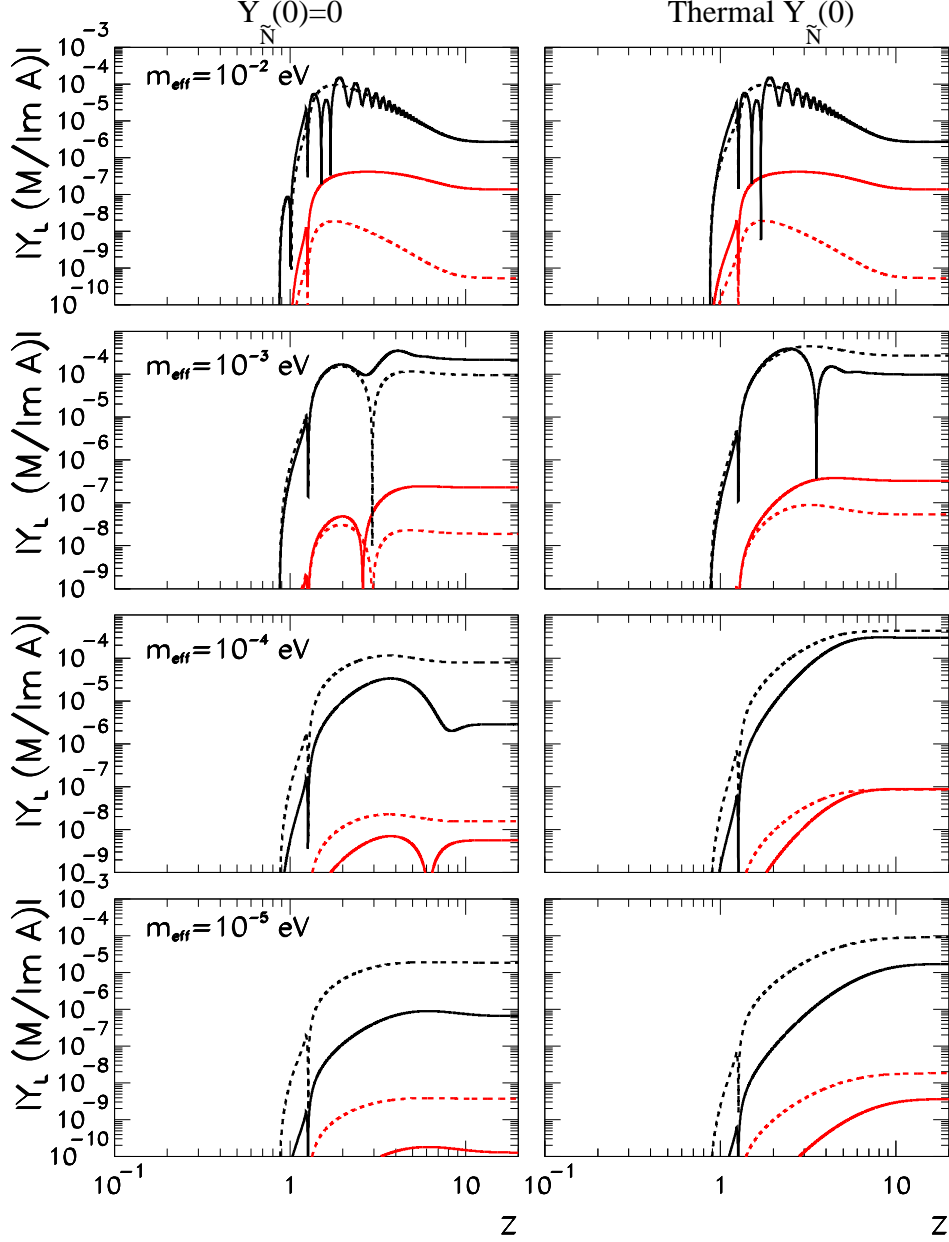


Figure 3.1: Absolute value of the lepton asymmetry with the quantum time dependence of the CP asymmetry (solid) and without it (dashed) as a function of z for different values of m_{eff} as labeled in the figure. In each panel the two upper curves (black) correspond to the resonant case $R = 1$ while the lower two curves (red) correspond to the very degenerate case $R = 2 \times 10^{-4}$. The left (right) panels correspond to vanishing (thermal) initial RHSN abundance. The figure is shown for $M = 10^7$ GeV and $\tan \beta = 30$ though as discussed in the text, the results as normalized in the figure are very weakly dependent on those two parameters.

expanding the sin term we get

$$QC(T) \simeq -\frac{m_{\text{eff}}}{m_*} \frac{z^2}{2}, \quad (3.7)$$

which, in the strong regime, is always larger than 1.

Also we see that, independently of the initial conditions, and of the value of the degeneracy parameter R , the quantum effects always lead to a suppression of the final produced lepton asymmetry in the weak washout regime. This is different from what happens in type-I seesaw resonant leptogenesis in which quantum effects lead to an enhancement of the produced asymmetry in weak washout and $R \sim 1$ and for zero initial RHN abundances [88]².

The origin of the difference is in the additional time dependence of the CP asymmetry in SL Δ_{BF} . In order to understand this, we must remember that in type-I seesaw resonant leptogenesis, in the weak washout regime, the final lepton asymmetry results from a cancellation between the opposite sign asymmetry generated when RH neutrinos are initially produced and the lepton asymmetry produced when they finally decay. When the time-dependent quantum corrections are included, this near-cancellation does not hold or it occurs at earlier times. As a consequence the asymmetry grows larger once these corrections are included as discussed in ref. [88].

But in SL, even in the classical regime the thermal factor Δ_{BF} already prevents the cancellation to occur. Therefore the inclusion of the time dependent quantum effects only amounts to an additional multiplicative factor which, in this regime, is smaller than one.

This behavior is explicitly displayed in Figure 3.2 where we compare the absolute value of the lepton asymmetry with the quantum time dependence of the CP asymmetry and without it in SL with what would be obtained if the thermal factor $\Delta_{BF}(z)$ was not included (so that the CP asymmetry takes a form similar to the one for resonant seesaw). As seen in Figure 3.2, without the $\Delta_{BF}(z)$ the asymmetry starts being produced at lower z and it changes

²We notice in passing that for the type-I seesaw resonant leptogenesis the weak washout regime is physically unreachable as long as flavor effects are not included. This is so because there is a lower bound on the washout parameter once the washout associated to the two quasi-degenerate heavy neutrinos contributes, which implies that $m_{\text{eff}} \geq \sqrt{\Delta m_{\text{solar}}^2} \sim 8 \times 10^{-3}$ [118]. Such a bound does not apply to SL as long as, as assumed in this work, only the lightest RHSN generation contributes.

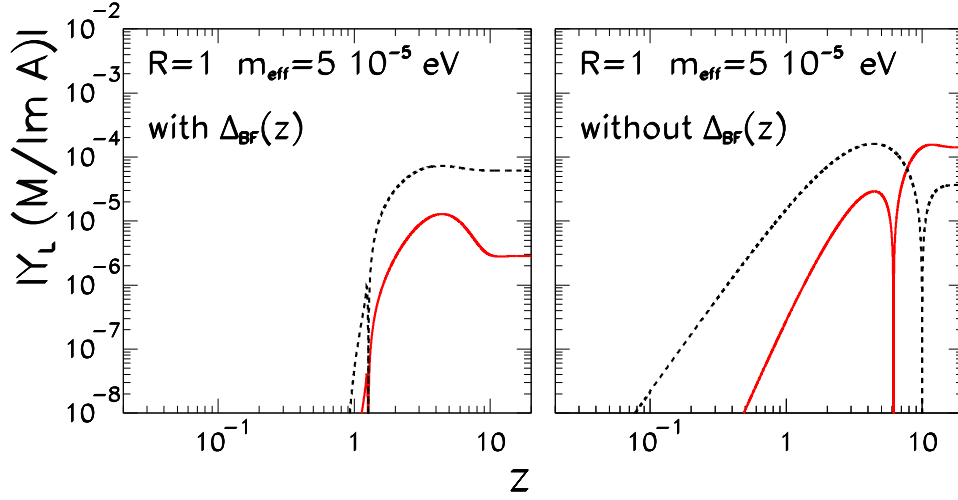


Figure 3.2: Absolute value of the lepton asymmetry with the quantum time dependence of the CP asymmetry (solid) and without it (dashed) for vanishing initial RHSN abundance. For comparison in the right panel we show the result that would be obtained with $\Delta_{BF}(z) = 1$.

sign in the classical regime. This change of sign is due to the cancellation between the opposite sign asymmetry generated when RH neutrinos are initially produced and the lepton asymmetry produced when they finally decay. Inclusion of the $QC(T)$ factor reduces the asymmetry at small z and this makes the cancellation to occur at lower z and consequently the final asymmetry is larger.

In the full calculation (left panel in Figure 3.2) the asymmetry only starts being non-negligible for larger z , i.e. $z \gtrsim 0.8$, and it changes sign for $z \sim 1$, both features due to the Δ_{BF} factor. Inclusion of the quantum correction, $QC(T)$ amounts for a suppression of the initial asymmetry by a factor given in eq. (3.7). As a consequence the final asymmetry is suppressed (and it also has the opposite sign) after including the quantum corrections.

A more systematic dependence of the results with the washout and degeneracy parameters, m_{eff} and R is shown in Figure 3.3 where we plot the efficiency factor η as a function of m_{eff} and R . We remind the reader that within our approximations for the thermal widths, in the classical regime, η

is mostly a function of m_{eff} exclusively³. Inclusion of the quantum correction $QC(T)$ makes η to depend both on m_{eff} and R but still remains basically independent of M .

From Figure 3.3 we see that for small enough values of the product of the washout parameter and the degeneracy parameter the arguments of the periodic functions in $QC(T)$ are always small in the range of z where the lepton asymmetry is generated. As explained above, in this regime the \sin^2 term in $QC(T)$ is negligible while the \sin term is multiplied by an amplitude proportional to $1/R$. Therefore, the dependence on R cancels in this limit and the resulting correction is given in eq. (3.7). This explains the plateaux observed at low values of the degeneracy parameter R in the lower panels of Figure 3.3. Similar behavior is found in ref. [89] for the resonant leptogenesis scenario. Also, as seen in eq. (3.7), the correction grows with m_{eff} which leads to the considerable enhancement of the efficiency seen in the upper curves of the lower panel in Figure 3.3. However we must notice that this enhancement occurs in a regime where the CP asymmetry is very small due to the small value of R since $\bar{\epsilon}$ is proportional to R .

Finally, in Figure 3.4 we compare the range of parameters B and m_{eff} for which enough asymmetry is generated, $Y_{\Delta B}^0 \geq 8.54 \times 10^{-11}$ with and without inclusion of the quantum corrections. We show the ranges for several values of M and for the characteristic value of $|\text{Im}A| = 1$ TeV. From the figure we see that due to the suppression of the asymmetry for the weak washout regime discussed above, for a given value of M the regions extend only up to larger values of m_{eff} once the quantum corrections are included. Also, because of the enhancement in the very degenerate, strong washout regime, the regions tend to extend to lower values of B and larger values of m_{eff} for a given value of M . Furthermore, once quantum effects are included, η can take both signs (depending on the value of m_{eff}), independently of the initial RHSN abundance. Thus it is possible to generate the right sign asymmetry with either sign of $\text{Im}A$ for both thermal and zero initial RHSN abundance. On the contrary without quantum corrections, for thermal initial conditions

³There is a residual dependence on M due to the running of the top Yukawa coupling as well as the thermal effects included in Δ_{BF} although it is very mild. For $\tan\beta \sim \mathcal{O}(1)$ there is also an additional (very weak) dependence due to the associated change in the top Yukawa coupling.

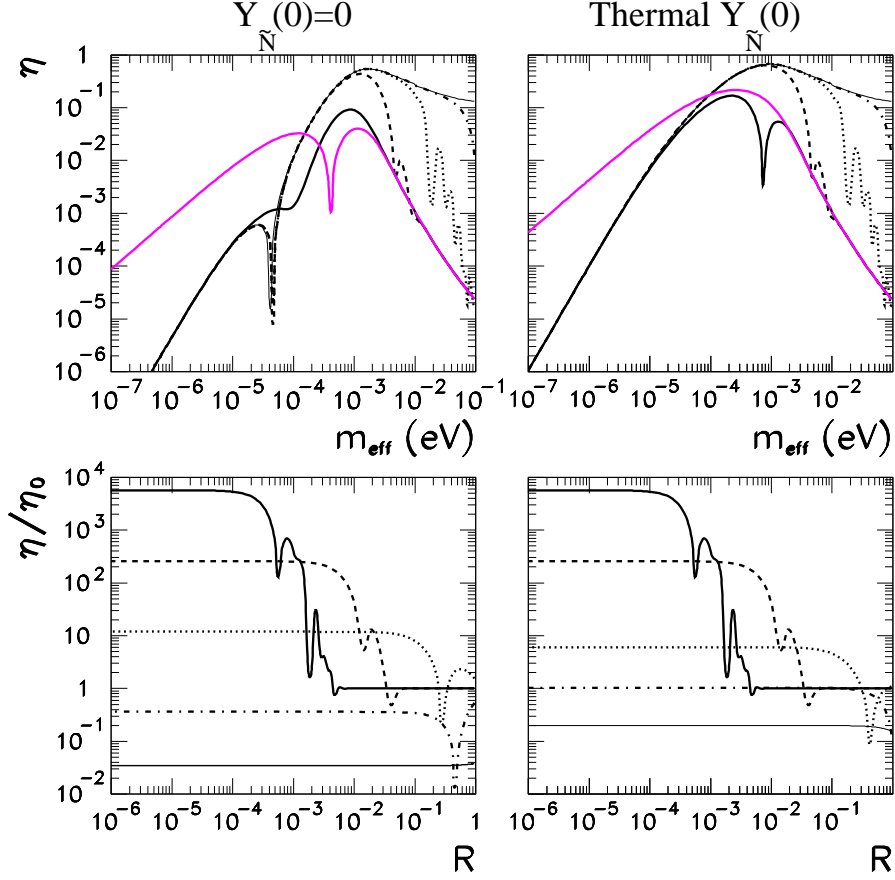


Figure 3.3: Efficiency factor as a function of m_{eff} and R for $M = 10^7$ GeV and $\tan \beta = 30$. The left (right) panels correspond to vanishing (thermal) initial RHSN abundance. In the upper panels the different curves correspond to $R = 1$ (black thick solid), 0.1 (dashed), 10^{-2} (dotted), 10^{-3} (dash-dotted) and 10^{-4} (thin solid). For comparison we also show the results without including the quantum effects (purple thick solid line). In the lower panels we plot the ratio of the efficiency factor with and without quantum corrections as a function of R . The different curves from top to bottom correspond to $m_{\text{eff}} = 10^{-1}$ eV (thick solid), 10^{-2} eV (dashed), 10^{-3} eV (dotted), 10^{-4} eV (dot-dashed), and 10^{-5} eV (thin solid).

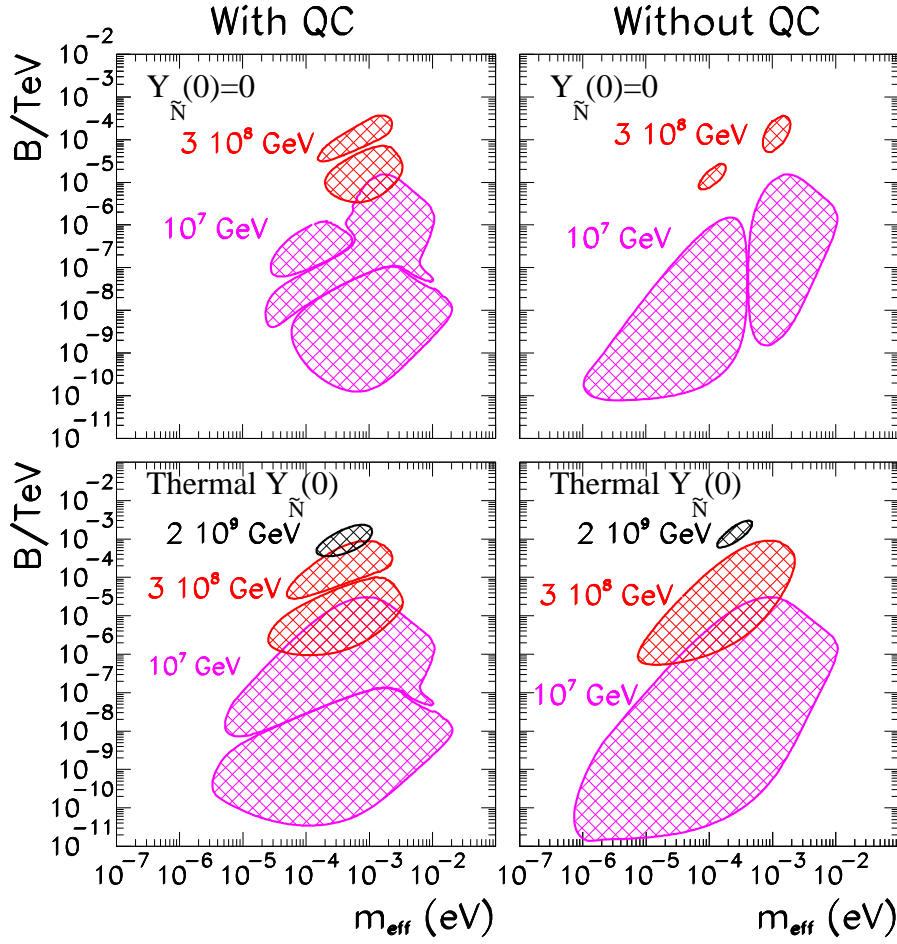


Figure 3.4: B, m_{eff} regions in which successful SL can be achieved with (left panels) and without (right panels) quantum effects. We take $|\text{Im}A| = 10^3 \text{ GeV}$ and $\tan\beta = 30$ and different values of M as labeled in the figure. The upper (lower) panels correspond to vanishing (thermal) initial RHSN abundance.

$\eta > 0$ and the right asymmetry can only be generated for $\text{Im}A > 0$.

3.4 Discussion and Conclusions

In this chapter we have studied the possible role of quantum effects in the SL scenario. In particular, we studied the effects on the produced asymmetry as a function of the washout parameter m_{eff} and the degeneracy parameter $R = 2\Delta M/\Gamma$. Our results show that, because of the thermal nature of SL, the characteristic time for the building of the asymmetry is larger than in the seesaw resonant leptogenesis which leads to quantitative differences on the dependence of the effect on the washout regime between the two scenarios.

In particular, in the weak washout regime, quantum effects do not enhance but suppress the produced lepton asymmetry in SL. Quantum effects are most quantitatively important for extremely degenerate RHSN, $\Delta M \ll \Gamma$. In this case and in the strong washout regime quantum effects can enhance the absolute value of the produced asymmetry as well as induce a change of its sign.

Nevertheless, altogether our results show that the required values of the Majorana mass M and the lepton violating soft bilinear coefficient B to achieve successful leptogenesis are not substantially modified by the inclusion of these quantum effects. Consequently in the rest of this thesis they will be ignored.

Chapter 4

The Role of Lepton Flavors

4.1 Introduction

In the original works, SL [82, 83] was addressed within the one-flavor approximation which consists of studying the evolutions of Y_N , $Y_{\tilde{N}_{tot}}$, $Y_{\Delta\ell}$ and $Y_{\Delta\tilde{\ell}}$ with the BEs eqs. (2.103)–(2.106). This approximation is valid as long as the interactions mediated by charged lepton Yukawa couplings are negligible (reactions of type (ii) discussed in Section 2.4.2) so that we can consider the lepton asymmetry to be concentrated on the $|\ell\rangle$ and $|\tilde{\ell}\rangle$ states defined as

$$\begin{aligned} |\ell\rangle &\equiv \frac{1}{\sqrt{\sum_{\beta} Y_{\beta}^2}} \sum_{\alpha} Y_{\alpha} |\ell_{\alpha}\rangle, \\ |\tilde{\ell}\rangle &\equiv \frac{1}{\sqrt{\sum_{\beta} Y_{\beta}^2}} \sum_{\alpha} Y_{\alpha} |\tilde{\ell}_{\alpha}\rangle, \end{aligned} \tag{4.1}$$

that is the left-handed lepton and slepton doublets to which \tilde{N}_{\pm} couples.

This one-flavor approximation is rigorously correct only at $T \gtrsim 10^{12}$ GeV when all the charged lepton Yukawa interactions are out of equilibrium. This is not the case in SL since successful leptogenesis in this scenario requires a relatively low RHN mass scale $M \sim 10^4 - 10^9$ GeV as we have seen in previous chapters. Thus the characteristic T is such that the rates of processes mediated by the τ and μ (and even e) Yukawa couplings are not negligible.

In order to understand the role of lepton flavors qualitatively, let us assume that SL happens at certain temperature below $T \sim 10^8$ GeV where both the interactions mediated by τ and μ -lepton Yukawa couplings are in thermal equilibrium (i.e. they are reactions of type (i) discussed in Section 2.4.2) and they are much faster than the inverse decay of RHSN. In this case, the lepton state $|\ell\rangle$ in eq. (4.1) generated by the decays of RHSN loses coherence between its production and its washout in the inverse decay processes and gets projected into the flavor eigenstates $|\ell_\tau\rangle$ and $|\ell_\mu\rangle$ (and the third orthogonal state will be $|\ell_e\rangle$)¹. Thus in the washout through inverse decay of RHSN, the Higgs interacts with the lepton flavor eigenstate $|\ell_\alpha\rangle$ (instead of the coherent $|\ell\rangle$ state), and the corresponding washout is reduced by the flavor projector P_α defined in eq. (2.40). As a result flavor effects generally enhance the efficiency of leptogenesis by reducing the effective washout. Furthermore, in the absence of lepton flavor violating interactions, each lepton flavor can be treated as an independent species associated with its respective chemical potential.

The temperature regime for which the lepton flavor effects are important can be estimated using that the interaction rate for a charged lepton Yukawa coupling h_α can be approximated by [119, 120]

$$\Gamma_\alpha(T) \simeq 10^{-2} h_\alpha^2 T. \quad (4.2)$$

Requiring that $\Gamma_\alpha(T)$ is in equilibrium i.e. with interaction rate faster than the expansion rate of the Universe², $\Gamma_\alpha(T) > H(T)$, we obtain³

$$\Gamma_e(T) > H(T) \implies T \lesssim 4 \times 10^4 (1 + \tan^2 \beta) \text{ GeV}, \quad (4.3)$$

$$\Gamma_\mu(T) > H(T) \implies T \lesssim 2 \times 10^9 (1 + \tan^2 \beta) \text{ GeV}, \quad (4.4)$$

$$\Gamma_\tau(T) > H(T) \implies T \lesssim 5 \times 10^{11} (1 + \tan^2 \beta) \text{ GeV}. \quad (4.5)$$

Notice that if both μ and τ are in equilibrium, even if e is not, we still have to consider three flavors. In order for the top, bottom and tau Yukawa couplings

¹Since this argument and the following also apply to $|\tilde{\ell}\rangle$, to avoid repetition, we only talk about $|\ell\rangle$ from here onwards.

²A stronger and correct requirement as pointed out in refs. [32, 56] is to also have $\Gamma_\alpha(T)$ faster than the inverse decay rate of RHN (or RHSN in our case). However, as shown in ref. [56], for $M \lesssim 10^9$ GeV, we are always in the fully flavored regime.

³The dependence on $\tan \beta$ comes from the following: $h_\alpha^2 = \frac{m_\alpha^2}{v^2 \cos^2 \beta} = \frac{m_\alpha^2}{v^2} (1 + \tan^2 \beta)$.

not to become nonperturbatively large, we require $1 \lesssim \tan \beta \lesssim 65$. Hence for the temperature regime relevant for SL (i.e. $T \lesssim 10^9$ GeV), we are always in the three-flavor regime where we have to distinguish between the three lepton flavors $\alpha = e, \tau, \mu$.

The impact of flavor in thermal leptogenesis in the context of the standard seesaw leptogenesis has been investigated in much detail [28–32, 47, 55, 55–57, 88, 89, 103, 111, 121–126]. The relevant BEs including flavor effects were first introduced in ref. [28]. In ref. [30–32, 55] it was further analyzed how the BEs describing the asymmetries in flavor space have additional terms which can significantly affect the result for the final baryon asymmetry.

In this chapter we address the question of how flavor effects can affect the region of parameters in which successful leptogenesis in SL is possible, and in particular their impact on the required value of the L -violating soft bilinear B coupling.

4.2 Introducing Flavor Effects

4.2.1 Flavored CP asymmetries and reaction densities

The flavor effects in the CP asymmetries in SL come from the neutrino Yukawa couplings Y_α and the trilinear couplings A_α . In eq. (2.3) of Chapter 2, we have assumed a universal trilinear that is proportional to the Yukawa coupling $A_\alpha = AY_\alpha$. Here we will assume a general flavor structure where $A_\alpha = AZ_\alpha$ with

$$\begin{aligned}
 -\mathcal{L}_{\text{soft}} &= \widetilde{M}_{ij}^2 \widetilde{N}_i^* \widetilde{N}_j + \left(AZ_{i\alpha} \epsilon_{ab} \widetilde{N}_i \widetilde{\ell}_\alpha^a H_u^b + \frac{1}{2} B M_i \widetilde{N}_i \widetilde{N}_i + \text{h.c.} \right) \\
 &+ \frac{1}{2} \left(m_2 \overline{\widetilde{\lambda}_2^{\pm,0}} P_L \widetilde{\lambda}_2^{\pm,0} + m_1 \overline{\widetilde{\lambda}_1} P_L \widetilde{\lambda}_1 + \text{h.c.} \right). \quad (4.6)
 \end{aligned}$$

With this assumption, the physical phase changes from one $\phi_A = \arg(AB^*)$ as in eq. (2.7) to three

$$\phi_{A_\alpha} = \arg(AZ_\alpha Y_\alpha^* B^*), \quad (4.7)$$

and the CP asymmetries (2.42),(2.43) and (2.44) are modified to

$$\epsilon_\alpha^S(T) = -P_\alpha \frac{Z_\alpha}{Y_\alpha} \frac{A}{M} \sin \phi_{A_\alpha} \frac{4B\Gamma}{4B^2 + \Gamma^2} \Delta_{BF}(T), \quad (4.8)$$

$$\begin{aligned} \epsilon_\alpha^V(T) = & -P_\alpha \frac{3\alpha_2}{4} \frac{m_2}{M} \ln \frac{m_2^2}{m_2^2 + M^2} \Delta_{BF}(T) \\ & \times \left\{ \frac{Z_\alpha}{Y_\alpha} \frac{A}{M} [\sin \phi_{A_\alpha} \cos(2\phi_g) + \cos \phi_{A_\alpha} \sin(2\phi_g)] - \frac{B}{M} \sin(2\phi_g) \right\}, \end{aligned} \quad (4.9)$$

$$\begin{aligned} \epsilon_\alpha^I(T) = & P_\alpha \frac{Z_\alpha}{Y_\alpha} \frac{3\alpha_2}{2} \frac{A}{M} \frac{m_2}{M} \sin \phi_{A_\alpha} \cos(2\phi_g) \\ & \times \frac{\Gamma^2}{4B^2 + \Gamma^2} \ln \frac{m_2^2}{m_2^2 + M^2} \Delta_{BF}(T), \end{aligned} \quad (4.10)$$

where we have factored out all the CP-violating phases ϕ_{A_α} , $\phi_g \equiv \phi_{g_2}$ and all the parameters A , Z_α , Y_α etc. are assumed to be real and positive (unless explicitly stated in the text)⁴.

Taking into account that the neutrino Yukawa couplings can be chosen to be real the thermally averaged flavored decay and scattering rates verify (neglecting the zero temperature masses)

$$\gamma_X^\alpha = P_\alpha \gamma_X, \quad (4.11)$$

where the γ_X are defined in eqs. (2.109).

4.2.2 Flavor structure

Regarding the flavor structure of the soft terms relevant for flavored SL, we can distinguish two general possibilities:

1. *Universal soft terms.* This case is realized in supergravity and gauge mediated SUSY-breaking models (when the renormalization group running of the parameters is neglected), and in our notation corresponds to set

$$Z_\alpha = Y_\alpha. \quad (4.12)$$

In this *Universal Trilinear Scenario* (UTS) scenario, the only flavor structure arises from the Yukawa couplings and both the total CP asymmetries $\epsilon_\alpha =$

⁴Please refer to Appendix A for the phase convention we used.

$\epsilon_\alpha^S + \epsilon_\alpha^V + \epsilon_\alpha^I$ and the corresponding washout terms, that are generically denoted as W_α , are proportional to the same flavor projectors P_α , yielding:

$$\frac{\epsilon_e}{W_e} = \frac{\epsilon_\mu}{W_\mu} = \frac{\epsilon_\tau}{W_\tau}. \quad (4.13)$$

Furthermore, as seen in eq. (4.7) there is a unique phase for the trilinear couplings $\phi_{A_\alpha} = \phi_A = \arg(AB^*)$. Hence unlike in the case of seesaw leptogenesis induced by N decay [30–32], in this “minimal” SL scenario, it is not possible to have non-zero flavor asymmetries with a vanishing total CP asymmetry.

2. *General soft terms.* In this case the most general form for the soft terms is allowed, only subject to the phenomenological constraints from limits on flavor changing neutral currents (FCNC) and from lepton flavor violating (LFV) processes. The trilinear soft terms are not aligned with the corresponding Yukawa couplings, and eq. (4.13) does not hold. Studying this scenario can be rather involved due to the large dimensionality of the relevant parameter space. Therefore we will introduce a drastic simplification that, while it can still capture some of the main features of the general case, it allows to carry out an analysis in terms of the same number of independent parameters than in case 1.

Let us note that the CP asymmetries become flavor independent (except for the last term in eq. (4.9) if

$$Z_\alpha = \frac{\sum_\beta |Y_\beta|^2}{3Y_\alpha^*}, \quad (4.14)$$

where we have kept Z and Y explicitly as complex numbers. Eq. (4.14) yields $\epsilon_\alpha = \epsilon/3$ for each flavor, and from eq. (4.7) we see that, since $Z_\alpha Y_\alpha^*$ is real, also in this case there is a unique phase for the trilinear couplings $\phi_{A_\alpha} = \phi_A = \arg(AB^*)$. The normalization factor of $1/3$ in eq. (4.14) has been introduced so that both eq.(4.12) and eq. (4.14) yield the same total asymmetry $\sum_\alpha \epsilon_\alpha = \epsilon$. In what follows we will refer to this case as the *Simplified Misaligned Scenario* (SMS). Our SMS of course does not correspond to a completely general scenario, and for example, due to the reduction in the number of independent physical phases implied by eq. (4.14), it excludes the possibility of having flavor asymmetries of opposite signs, with $|\epsilon^\alpha| > |\epsilon|$ for some, or even

for all, flavors⁵. The reader should thus keep in mind that enhancements of the final lepton asymmetry even larger than the ones we will find within the SMS are certainly possible.

Finally, we would like to stress that both UTS and SMS scenarios are equivalent for the case of flavor equipartition: $P_e = P_\mu = P_\tau = 1/3$.

4.2.3 Lepton flavor equilibration interactions

In the temperature regime where all three lepton flavors are distinguishable and in the absence of LFV interactions, the lepton asymmetries stored in each of them are independent from each other. Hence it is possible to obtain an enhancement if the asymmetry stored in a particular lepton flavor is protected from the washout. However the presence of off-diagonal soft slepton masses could induce LFV interactions and if they are fast enough, they would equilibrate the asymmetries between the three lepton flavors and could diminish the aforementioned enhancement. In order to quantify this potentially destructive effect, in this section, we will discuss in detail the LFV interactions induced by off-diagonal soft slepton masses.

In the basis where charged lepton Yukawa couplings are diagonal, the soft slepton masses read

$$\mathcal{L}_{soft} \supset -\tilde{m}_{\alpha\beta}^2 \tilde{\ell}_\alpha^* \tilde{\ell}_\beta. \quad (4.15)$$

The off-diagonal soft slepton masses $\tilde{m}_{\alpha\beta}^2$, $\alpha \neq \beta$ affect the flavor composition of the slepton mass eigenstates so generically we can write

$$\tilde{\ell}_\alpha^{(int)} = R_{\alpha\beta} \tilde{\ell}_\beta, \quad (4.16)$$

where $R_{\alpha\beta}$ is a unitary rotation matrix. In this basis the corresponding slepton-gaugino interactions in eq. (2.6) become

$$\begin{aligned} \mathcal{L}_{\tilde{\lambda}, \tilde{\ell}} = & -g_2 (\sigma_\pm)_{ab} \overline{\tilde{\lambda}}_2^\pm P_L \ell_\alpha^a R_{\alpha\beta}^* \tilde{\ell}_\beta^{b*} - \frac{g_2}{\sqrt{2}} (\sigma_3)_{ab} \overline{\tilde{\lambda}}_2^0 P_L \ell_\alpha^a R_{\alpha\beta}^* \tilde{\ell}_\beta^{b*} \\ & - \frac{g_Y}{\sqrt{2}} \delta_{ab} \overline{\tilde{\lambda}}_1 Y_{\ell L} P_L \ell_\alpha^a R_{\alpha\beta}^* \tilde{\ell}_\beta^{b*} + \text{h.c.}, \end{aligned} \quad (4.17)$$

⁵In the most general scenario, it is of course possible to have null total CP asymmetry, see e.g. in ref. [108] where a scenario in flavored SL with null total CP asymmetry is studied.

The mixing matrix can be expressed in terms of the off-diagonal slepton masses as:

$$\begin{aligned}
R_{\alpha\beta} &\sim \delta_{\alpha\beta} + \frac{\tilde{m}_{\alpha\beta}^2}{h_i^2 T^2} \\
&= \delta_{\alpha\beta} + \frac{\tilde{m}_{\alpha\beta}^2 v^2 \cos^2 \beta}{m_\alpha^2 M^2} z^2,
\end{aligned} \tag{4.18}$$

where in the first line $h_\alpha > h_\beta$ is the relevant charged Yukawa coupling that determines at leading order the thermal mass splittings of the sleptons, v in the second line is the EW symmetry breaking VEV with $v^2 = v_u^2 + v_d^2 \simeq 174 \text{ GeV}$, $z \equiv \frac{M}{T}$ and $m_\alpha \equiv m_{\ell_\alpha}(T=0)$ is the zero temperature mass for the lepton ℓ_α . In what follows, for simplicity we construct the $R_{\alpha\beta}$ entries in such a way that they are flavor independent quantities. We assume $\tilde{m}_{\alpha\tau} = \tilde{m}_{od}$ (for $\alpha = e, \mu$) and $\tilde{m}_{e\mu} = \tilde{m}_{od} \frac{m_\mu}{m_\tau}$, where \tilde{m}_{od} , is a unique off-diagonal soft-mass parameter. We thus obtain for $(\alpha\beta) = (e\tau), (\mu\tau), (e\mu)$:

$$R_{\alpha\beta} \sim \delta_{\alpha\beta} + \frac{\tilde{m}_{od}^2 v^2 \cos^2 \beta}{m_\tau^2 M^2} z^2, \tag{4.19}$$

where m_τ is the mass of the tau lepton.

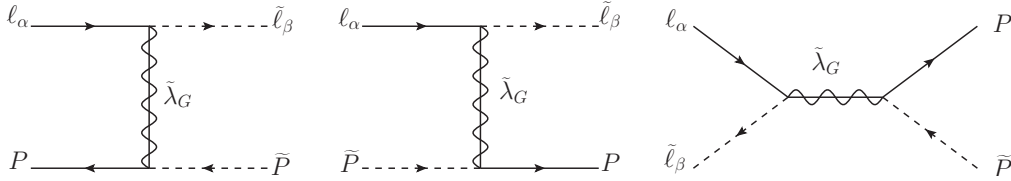


Figure 4.1: The lepton flavor violating lepton-slepton scatterings through the exchange of $SU(2)_L$ and $U(1)_Y$ gauginos $\tilde{\lambda}_G$.

The terms in eq. (4.17) induce LFV lepton-slepton scatterings through the exchange of $SU(2)_L$ and $U(1)_Y$ gauginos. There are two possible t-channel scatterings $\ell_\alpha \bar{P} \leftrightarrow \tilde{\ell}_\beta \tilde{P}^*$, $\ell_\alpha \tilde{P} \leftrightarrow \tilde{\ell}_\beta P$ and one s-channel scattering $\ell_\alpha \tilde{\ell}_\beta^* \leftrightarrow P \tilde{P}^*$ (we denote P as fermions and \tilde{P} as scalars) as shown in Figure 4.1. For processes mediated by $SU(2)_L$ gauginos $P = \ell, Q, \tilde{H}_{u,d}$, while when mediated by $U(1)_Y$ gaugino one must include the $SU(2)_L$ singlet states $P = e, u, d$ as

well. The corresponding reduced cross sections (defined in eq. (B.26)) read :

$$\begin{aligned}
\hat{\sigma}_{t1,G}^{\alpha\beta}(s) &= \sum_P \frac{g_G^4 |R_{\alpha\beta}|^2 \Pi_P^G}{8\pi} \left[\left(\frac{2m_{\lambda_G}^2}{s} + 1 \right) \ln \left| \frac{m_{\lambda_G}^2 + s}{m_{\lambda_G}^2} \right| - 2 \right], \\
\hat{\sigma}_{t2,G}^{\alpha\beta}(s) &= \sum_P \frac{g_G^4 |R_{\alpha\beta}|^2 \Pi_P^G}{8\pi} \left[\ln \left| \frac{m_{\lambda_G}^2 + s}{m_{\lambda_G}^2} \right| - \frac{s}{m_{\lambda_G}^2 + s} \right], \\
\hat{\sigma}_{s,G}^{\alpha\beta}(s) &= \sum_P \frac{g_G^4 |R_{\alpha\beta}|^2 \Pi_P^G}{16\pi} \left(\frac{s}{s - m_{\lambda_G}^2} \right)^2, \tag{4.20}
\end{aligned}$$

where Π_P^G counts the numbers of degrees of freedom of the particle P (isospin, quark flavors and color) involved in the scatterings mediated by the $SU(2)_L$ ($G = 2$) and $U(1)_Y$ ($G = Y$) gauginos respectively. In this last case the hypercharges $y_{\ell L}$ and y_P are also included in Π_P^Y . If the flavor changing scatterings in eq. (4.20) are fast enough, they will lead to *lepton flavor equilibration* (LFE), and damp all leptogenesis flavor effects [127]⁶.

The values of \tilde{m}_{od} for which this occurs can be estimated by comparing the LFE scattering rates and the $\Delta L = 1$ washout rates. Since the dominant $\Delta L = 1$ contribution arises from inverse decays, the terms to be compared are:

$$\begin{aligned}
\bar{\Gamma}_{\text{LFE}}(T) &\equiv \frac{\gamma_{\text{LFE}}(T)}{n_L^c(T)} \equiv \frac{1}{n_L^c(T)} \sum_{G,P} \Pi_P^G (\gamma_{t1,G}^{\alpha\beta} + \gamma_{t2,G}^{\alpha\beta} + \gamma_{s,G}^{\alpha\beta}) \\
&= \frac{1}{n_L^c(T)} \frac{T}{64\pi} \sum_G \int ds \sqrt{s} \mathcal{K}_1 \left(\frac{\sqrt{s}}{T} \right) \\
&\quad \times \left[\hat{\sigma}_{t1,G}^{\alpha\beta}(s) + \hat{\sigma}_{t2,G}^{\alpha\beta}(s) + \hat{\sigma}_{s,G}^{\alpha\beta}(s) \right], \tag{4.21}
\end{aligned}$$

$$\bar{\Gamma}_{\text{ID}}(T) \equiv \frac{\gamma_{\tilde{N}}(T)}{n_L^c(T)} = \frac{n_{\tilde{N}}^{eq}(T)}{n_L^c(T)} \frac{\mathcal{K}_1(z)}{\mathcal{K}_2(z)} \Gamma, \tag{4.22}$$

where the $\gamma_{x,G}^{\alpha\beta}$ with $(x = t1, t2, s)$ in the first line represent the thermally averaged LFE reactions for one degree of freedom of the P -particle⁷, $\mathcal{K}_{1,2}(z)$ are the modified Bessel function of the second kind of order 1 and 2, Γ is the zero temperature width eq. (2.12), and $n_{\tilde{N}}^{eq}$ is the equilibrium number density for \tilde{N} while $n_L^c = T^3/2$ is the relevant density factor appearing in the washouts

⁶See ref. [108] for some particular effects associated with lepton flavor violating processes in SL scenario with vanishing total CP asymmetry.

⁷The reader can refer to Appendix B.2.4 for additional details

(see next section for more details). In evaluating the reaction densities above we have not included the thermal masses, and we have neglected Pauli-blocking and stimulated emission as well as the relative motion of the particles with respect to the plasma.

LFE scattering reaction densities have a different T dependence than the Universe expansion rate H and the decay rates. While we have $H(T) \sim T^2$, for LFE processes we have $\bar{\Gamma}_{\text{LFE}} \sim T^{-3}$. This means that the ratio $\bar{\Gamma}_{\text{LFE}}/H \sim 1/T^5$, and thus once LFE reactions have attained thermal equilibrium, they will remain in thermal equilibrium also at lower temperatures. In contrast, $\bar{\Gamma}_{\text{ID}}$ first increases till reaching a maximum, but then decreases exponentially $\sim e^{-M/T}$ dropping out of equilibrium at temperatures not much below $T \sim M$. The relevant temperature where we should compare the rates of these interactions is when the inverse decay rate $\bar{\Gamma}_{\text{ID}}$ becomes slower than H , that is when the lepton asymmetry starts being generated from the out-of-equilibrium \tilde{N}_{\pm} decays. We define z_{dec} as $\bar{\Gamma}_{\text{ID}}(z_{dec}) = H(z_{dec})$. LFE is expected to be quite relevant for flavored leptogenesis when the following condition is verified:

$$\bar{\Gamma}_{\text{LFE}}(z_{dec}) \geq \bar{\Gamma}_{\text{ID}}(z_{dec}) = H(z_{dec}). \quad (4.23)$$

In this case, LFE processes are in equilibrium since the very onset of the era of out-of-equilibrium decays, and due to its temperature dependence it is guaranteed that they will remain in equilibrium until leptogenesis is over.

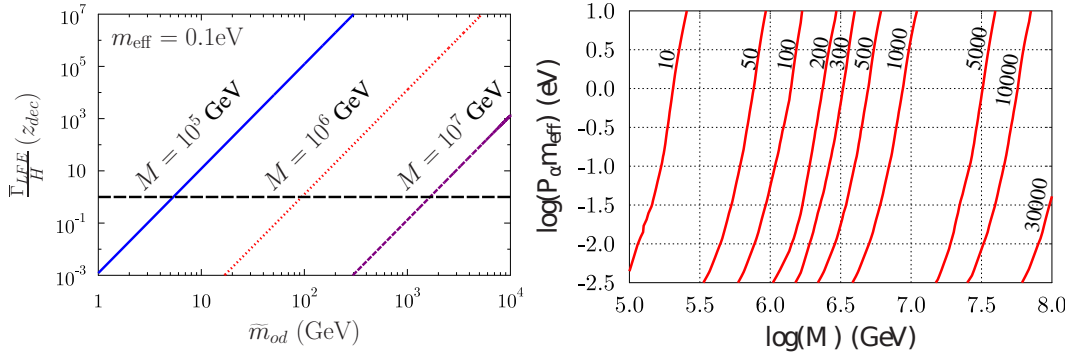


Figure 4.2: The top panel shows the ratio of $\bar{\Gamma}_{\text{LFE}}$ to the Hubble expansion rate H at z_{dec} as a function of \tilde{m}_{od} for $m_{\text{eff}} = 0.1$ eV and $\tan \beta = 30$ and three values of M . The bottom panel shows in the $(P_{\alpha} m_{\text{eff}}, M)$ plane, contours of constant values of \tilde{m}_{od} (in GeV) for which $\bar{\Gamma}_{\text{LFE}}(z_{dec}^{\alpha}) \geq P_{\alpha} \bar{\Gamma}_{\text{ID}}(z_{dec}^{\alpha})$.

In the top panel of Figure 4.2 we plot the ratio $\bar{\Gamma}_{\text{LFE}}(z_{\text{dec}})/H(z_{\text{dec}})$ as a function of \tilde{m}_{od} for $m_{\text{eff}} = 0.1$ eV, $\tan\beta = 30$, and for different values of M . From the figure we can read the characteristic value of \tilde{m}_{od} for which LFE becomes relevant. Notice that the dominant dependence on $\tan\beta \sim 1/\cos\beta$ ($\tan\beta \gg 1$) arises due to $v\cos\beta = v_d$ in eq. (4.19). Thus the results from other values of $\tan\beta$ can be easily read from the figure by rescaling $\tilde{m}_{od}^\beta = \tilde{m}_{od}^{\text{fig}}/(30\cos\beta)$.

Since we are interested in the dynamics of lepton flavors, to be more precise about LFE effects we should in fact consider the temperature z_{dec}^α at which the inverse decay rate for one specific flavor α goes out of equilibrium, that can be defined through $\bar{\Gamma}_{\text{ID}}^\alpha(z_{\text{dec}}^\alpha) = P_\alpha \bar{\Gamma}_{\text{ID}}(z_{\text{dec}}^\alpha) = H(z_{\text{dec}}^\alpha)$. Let's assume $P_a < P_b < P_c$ which implies $z_{\text{dec}}^a < z_{\text{dec}}^b < z_{\text{dec}}^c$. In other words, assuming that the lepton doublet ℓ_a is the most weakly coupled to \tilde{N}_\pm , $\bar{\Gamma}_{\text{ID}}^a$ will go out of equilibrium first, and then $\bar{\Gamma}_{\text{ID}}^b$ and $\bar{\Gamma}_{\text{ID}}^c$ will follow. Hence, for given values of m_{eff} and M , the minimum value $\tilde{m}_{od}^{\text{min}}$ for which LFE effects start being important is given by the following condition:

$$\bar{\Gamma}_{\text{LFE}}(z_{\text{dec}}^c) \simeq \bar{\Gamma}_{\text{ID}}^c(z_{\text{dec}}^c) \Rightarrow \text{determines } \tilde{m}_{od}^{\text{min}}. \quad (4.24)$$

For $\tilde{m}_{od} \ll \tilde{m}_{od}^{\text{min}}$ LFE effects can be neglected, since they will attain thermal equilibrium only after leptogenesis is over.

In the bottom panel in Figure 4.2, we plot in the plane of the flavored effective decay mass $P_\alpha m_{\text{eff}}$ and of the RHN mass M , various contours corresponding to different values of \tilde{m}_{od} for which $\bar{\Gamma}_{\text{LFE}}(z_{\text{dec}}^\alpha) = P_\alpha \bar{\Gamma}_{\text{ID}}(z_{\text{dec}}^\alpha)$. For a given value of M and m_{eff} , and for a given set of flavor projections $P_a < P_b < P_c$, $\tilde{m}_{od}^{\text{min}}$ is given by the value of the \tilde{m}_{od} curve for which the vertical line $x = M$ intersects the corresponding contour at $y_c = P_c m_{\text{eff}}$.

Furthermore, since $\bar{\Gamma}_{\text{LFE}}$ has a rather strong dependence on \tilde{m}_{od} ($\bar{\Gamma}_{\text{LFE}} \propto \tilde{m}_{od}^4$), one expects that the value $\tilde{m}_{od}^{\text{max}}$ for which LFE effects completely equilibrate the asymmetries in the different lepton flavors will not be much larger than $\tilde{m}_{od}^{\text{min}}$. Indeed our numerical results (see Section 4.4.4) show that $\tilde{m}_{od}^{\text{max}} \sim \mathcal{O}(5-10) \tilde{m}_{od}^{\text{min}}$. Clearly, as far as leptogenesis is concerned, larger values $\tilde{m}_{od} \gg \tilde{m}_{od}^{\text{max}} \sim \tilde{m}_{od}^{\text{min}}$ do not imply any modification in the numerical results with respect to what is obtained with $\tilde{m}_{od} = \tilde{m}_{od}^{\text{max}}$.

4.3 Flavored Boltzmann Equations

In refs. [30–32] the relevant equations including flavor effects associated to the charged-lepton Yukawas were derived in the density operator approach. One can define a density matrix for the difference of lepton and antileptons such that $\rho_{\alpha\alpha} = Y_{\Delta\ell_\alpha}$. As discussed in refs. [30–32] as long as we are in the regime in which a given set of the charged-lepton Yukawa interactions are out of equilibrium, one can restrict the general equation for the matrix density ρ to a subset of equations for the flavor diagonal directions $\rho_{\alpha\alpha}$. In the transition regimes in which a given Yukawa interaction is approaching equilibrium the off-diagonal entries of the density matrix cannot be neglected [32, 128]. However, as we will see below, for the case of SL, this is never the case.

There are additional flavor effects associated to the neutrino Yukawa couplings as discussed in ref. [46, 47] such as those arising from processes mediated by N_2 and \tilde{N}_2 (and N_3 and \tilde{N}_3). These effects are particularly important in seesaw resonant leptogenesis in which RHN of different “generations” are close in their masses. In leptogenesis with strong hierarchy among the masses of the different generations of RHN/RHSN one can neglect the neutrino Yukawa couplings in most of the parameter space, because the charged-lepton Yukawa rates are faster at the temperatures when the asymmetry is produced. In what follows we will work under this assumption and neglect flavor effects associated to the neutrino Yukawas.

Here for simplicity we will assume superequilibration as discussed in Section 2.4.2.2. Since we are in the flavored regime, instead of $Y_{L_{\text{tot}}}$ in eq. (2.111), we have to follow

$$Y_{L_{\text{tot}}}^\alpha \equiv Y_{\Delta\ell_\alpha} + Y_{\Delta\tilde{\ell}_\alpha}. \quad (4.25)$$

The BEs for RHN and RHSN are given by eqs. (2.103) and (2.104) which we list here again:

$$\begin{aligned} \dot{Y}_N &= - \left(\frac{Y_N}{Y_N^{\text{eq}}} - 1 \right) \left(\gamma_N + 4\gamma_t^{(0)} + 4\gamma_t^{(1)} + 4\gamma_t^{(2)} + 2\gamma_t^{(3)} + 4\gamma_t^{(4)} \right), \\ \dot{Y}_{\tilde{N}_{\text{tot}}} &= - \left(\frac{Y_{\tilde{N}_{\text{tot}}}}{Y_{\tilde{N}}^{\text{eq}}} - 2 \right) \left(\frac{\gamma_{\tilde{N}}}{2} + \gamma_{\tilde{N}}^{(3)} + 3\gamma_{22} + 2\gamma_t^{(5)} \right. \\ &\quad \left. + 2\gamma_t^{(6)} + 2\gamma_t^{(7)} + \gamma_t^{(8)} + 2\gamma_t^{(9)} \right). \end{aligned}$$

In writing the BEs for the evolution of flavored lepton asymmetries $Y_{L_{\text{tot}}^\alpha}$, it is most appropriate to follow the evolution of $B/3 - L_\alpha$ asymmetry $Y_{\Delta_\alpha} \equiv Y_{\Delta B}/3 - Y_{L_{\text{tot}}^\alpha} - Y_{\Delta e_R^\alpha}$ because $B/3 - L_\alpha$ is conserved by EW sphalerons and all other MSSM interactions (it is only violated by the interactions involving RHSN). Here we denote $Y_{\Delta e_R^\alpha}$ as the lepton asymmetry in the lepton singlet e_R^α . We have to consider $Y_{\Delta e_R^\alpha}$ because when charged lepton Yukawa interactions are not negligible, significant lepton asymmetry will be stored in e_R^α . We can write down the flavored BE for Y_{Δ_α} as follows⁸

$$\begin{aligned}
-\dot{Y}_{\Delta_\alpha} = & \epsilon_\alpha(T) \frac{\gamma_{\tilde{N}}}{2} \left(\frac{Y_{\tilde{N}_{\text{tot}}}}{Y_{\tilde{N}}^{eq}} - 2 \right) \\
& - \left[\frac{\gamma_{\tilde{N}}^\alpha}{2} + \frac{\gamma_N^\alpha}{2} + \gamma_{\tilde{N}}^{(3)\alpha} + \left(\frac{1}{2} \frac{Y_{\tilde{N}_{\text{tot}}}}{Y_{\tilde{N}}^{eq}} + 2 \right) \gamma_{22}^\alpha \right] \left(\frac{Y_{L_{\text{tot}}^\alpha}}{Y_c^{eq}} + \frac{Y_{H_{\text{tot}}}}{Y_c^{eq}} \right) \\
& - 2 \left(\gamma_t^{(1)\alpha} + \gamma_t^{(2)\alpha} + \gamma_t^{(4)\alpha} + \gamma_t^{(6)\alpha} + \gamma_t^{(7)\alpha} + \gamma_t^{(9)\alpha} \right) \frac{Y_{L_{\text{tot}}^\alpha}}{Y_c^{eq}} \\
& - \left[\left(2\gamma_t^{(0)} + \gamma_t^{(3)\alpha} \right) \frac{Y_N}{Y_N^{eq}} + \left(\gamma_t^{(5)\alpha} + \frac{1}{2} \gamma_t^{(8)\alpha} \right) \frac{Y_{\tilde{N}_{\text{tot}}}}{Y_{\tilde{N}}^{eq}} \right] \frac{Y_{L_{\text{tot}}^\alpha}}{Y_c^{eq}} \\
& - \left(2\gamma_t^{(0)\alpha} + \gamma_t^{(1)\alpha} + \gamma_t^{(3)\alpha} + \gamma_t^{(4)\alpha} + 2\gamma_t^{(5)\alpha} \right. \\
& \left. + \gamma_t^{(6)\alpha} + \gamma_t^{(7)\alpha} + \gamma_t^{(8)\alpha} + \gamma_t^{(9)\alpha} \right) \frac{Y_{H_{\text{tot}}}}{Y_c^{eq}} \\
& - \left[\left(\gamma_t^{(1)\alpha} + \gamma_t^{(2)\alpha} + \gamma_t^{(4)\alpha} \right) \frac{Y_N}{Y_N^{eq}} \right. \\
& \left. + \frac{1}{2} \left(\gamma_t^{(6)\alpha} + \gamma_t^{(7)\alpha} + \gamma_t^{(9)\alpha} \right) \frac{Y_{\tilde{N}_{\text{tot}}}}{Y_{\tilde{N}}^{eq}} \right] \frac{Y_{H_{\text{tot}}}}{Y_c^{eq}} \\
& - 84 \sum_{\beta \neq \alpha} \left(\gamma_{t1,2}^{\beta\alpha} + \gamma_{t2,2}^{\beta\alpha} + \gamma_{s,2}^{\beta\alpha} \right) \frac{Y_{L_{\text{tot}}^\alpha} - Y_{L_{\text{tot}}^\beta}}{Y_c^{eq}} \\
& - 76 \sum_{\beta \neq \alpha} \left(\gamma_{t1,Y}^{\beta\alpha} + \gamma_{t2,Y}^{\beta\alpha} + \gamma_{s,Y}^{\beta\alpha} \right) \frac{Y_{L_{\text{tot}}^\alpha} - Y_{L_{\text{tot}}^\beta}}{Y_c^{eq}}, \tag{4.26}
\end{aligned}$$

where $Y_{H_{\text{tot}}}$ is the total asymmetry for the H_u and \tilde{H}_u . The last two lines in eq. (4.26) correspond to the reaction densities for the LFE processes given in eq. (4.20), and play the role of controlling the effectiveness of the leptogenesis

⁸Please refer to Appendix B.2 for the derivations.

flavor effects⁹.

Compared to the unflavored BE (2.113), in addition to flavor, we have also taken into account the spectator effects [26, 27]: (s)quark and Higgs(ino) asymmetries which can all be written in term of $Y_{H_{\text{tot}}}$ (see Appendix B.2.5). These spectator effects as well as the sphaleron flavor mixing are taken into account by writing

$$Y_{L_{\text{tot}}}^{\alpha} = \sum_{\beta} A_{\alpha\beta} Y_{\Delta\beta}, \quad Y_{H_{\text{tot}}} = \sum_{\beta} C_{\beta} Y_{\Delta\beta}. \quad (4.27)$$

The values of the entries of the matrix A and of the vector C in eqs. (4.27) depend on the range of temperature, that is on the particular set of interactions that are in equilibrium when leptogenesis is taking place (see Appendix C for detailed discussions).

4.4 Results

4.4.1 Universal trilinear scenario (UTS)

In this section, we will discuss only the UTS scenario described in Section 4.2.1 with $Z_{\alpha} = Y_{\alpha}$ as in eq. (4.12). We parametrize the asymmetry generated by the decay of RHSN in a given flavor as

$$Y_{\Delta\alpha}(z \rightarrow \infty) = -2\eta_{\alpha} P_{\alpha} \bar{\epsilon} Y_{\tilde{N}}^{eq}(T \gg M), \quad (4.28)$$

where $\bar{\epsilon}$ is defined in eq. (2.115). Thus the final $B - L$ asymmetry can be written as

$$\begin{aligned} Y_{\Delta_{B-L}}^0 &= \sum_{\alpha} Y_{\Delta\alpha}(z \rightarrow \infty), \\ &= -2\eta_{\text{fla}} \bar{\epsilon} Y_{\tilde{N}}^{eq}(T \gg M), \end{aligned} \quad (4.29)$$

where we define

$$\eta_{\text{fla}} = \sum_{\alpha} \eta_{\alpha} P_{\alpha}. \quad (4.30)$$

According to our expressions for the CP asymmetries eqs. (4.8)–(4.10) and

⁹The reader can refer to Appendix B.2.4 for details on incorporating LFE into the BEs.

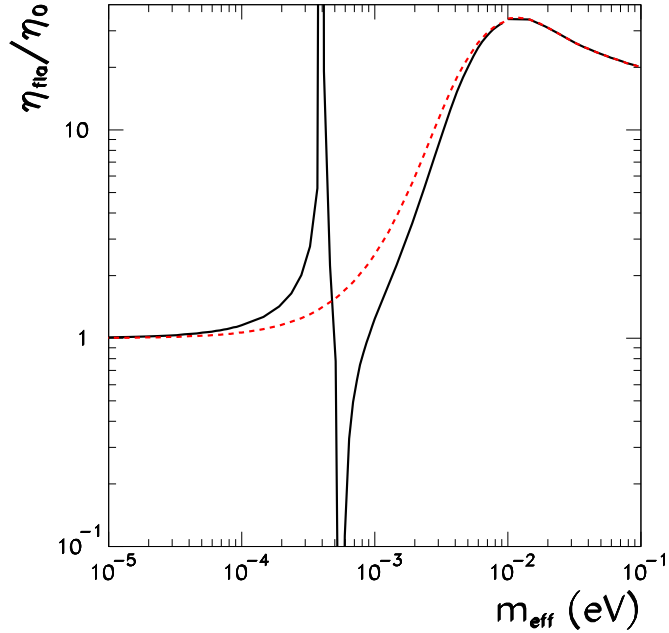


Figure 4.3: Efficiency factor $|\eta_{\text{fla}}/\eta_0|$ as a function of m_{eff} for $M = 10^7$ GeV and $\tan\beta = 30$. The two curves correspond to vanishing initial RHSN abundance (solid black curve) and thermal initial RHSN abundance, (dashed red curve).

to the general expression for the flavored reaction rates eq. (4.11), and neglecting for the time being LFE effects, η_{fla} depends on flavor via the flavor projector P_α . The final asymmetry produced also depends on the Yukawa couplings $\sum_\alpha Y_\alpha^2$ and on the heavy singlet mass M through the combination m_{eff} defined in eq. (2.95) (there is a residual mild dependence on M due to the running of the top Yukawa coupling).

In Figure 4.3 we plot $|\eta_{\text{fla}}/\eta_0|$ as a function of m_{eff} for $M = 10^7$ GeV and for $P_e = P_\mu = P_\tau = \frac{1}{3}$ as obtained from solving the BEs (2.103), (2.104) and (4.26) ignoring the LFE interactions (setting reactions in the last two lines of eq. (4.26) to zero) and the spectators (setting $C = (0, 0, 0)$ in the second

eq. (4.27)) and using the following A matrix as given in ref. [124]¹⁰

$$A = \begin{pmatrix} -\frac{93}{110} & \frac{6}{55} & \frac{6}{55} \\ \frac{3}{40} & -\frac{19}{30} & \frac{1}{30} \\ \frac{3}{40} & \frac{1}{30} & -\frac{19}{30} \end{pmatrix}, \quad (4.31)$$

Notice that this result applies to both UTS and SMS scenarios since we are in the case of flavor equipartition. We label η_0 the corresponding efficiency factor without considering flavor effects. As seen in the figure for these values of the flavor projectors P_α , and large m_{eff} (strong washout region), flavor effects can make leptogenesis more efficient by up to a factor of order 30. On the contrary flavor effects play no role for small m_{eff} (weak washout). This can be easily understood by adding the equations for the three flavor asymmetries, eq. (4.26). We get an equation which can be written as:

$$\dot{Y}_{\Delta_{B-L}} = - \left\{ \epsilon(T) \left(\frac{Y_{\tilde{N}_{\text{tot}}}}{Y_{\tilde{N}}^{eq}} - 2 \right) \frac{\gamma_{\tilde{N}}}{2} - \sum_{\alpha\beta} A_{\alpha\beta} P_\alpha \frac{Y_{\Delta_\alpha}}{Y_c^{eq}} W \right\}, \quad (4.32)$$

where we have defined the washout term

$$\begin{aligned} W &= \frac{\gamma_{\tilde{N}}}{2} + \frac{\gamma_N}{2} + \gamma_{\tilde{N}}^{(3)} + \frac{Y_{\tilde{N}_{\text{tot}}}}{Y_{\tilde{N}}^{eq}} \gamma_t^{(5)} + 2\gamma_t^{(6)} + 2\gamma_t^{(7)} + \frac{Y_N}{Y_N^{eq}} \gamma_t^{(3)} + 2\gamma_t^{(4)} \\ &+ \frac{1}{2} \frac{Y_{\tilde{N}_{\text{tot}}}}{Y_{\tilde{N}}^{eq}} \gamma_t^{(8)} + 2\gamma_t^{(9)} + 2 \frac{Y_N}{Y_N^{eq}} \gamma_t^{(0)} + 2\gamma_t^{(1)} + 2\gamma_t^{(2)} \\ &+ \left(2 + \frac{1}{2} \frac{Y_{\tilde{N}_{\text{tot}}}}{Y_{\tilde{N}}^{eq}} \right) \gamma_{22}, \end{aligned} \quad (4.33)$$

which can be directly compared with the unflavored equation eq. (2.113). We see that if we define $J_\alpha = Y_{\Delta_\alpha}/Y_{\Delta_{B-L}}$, eq. (4.32) is equivalent to eq. (2.113) with

$$W \rightarrow -W \times \sum_{\alpha\beta} A_{\alpha\beta} P_\alpha J_\beta \quad (4.34)$$

Thus flavor effects are unimportant when the W term in eq. (4.32) is much smaller than the source term which happens when m_{eff} is small enough (weak washout regime).

¹⁰Later in Section 4.4.2, we will use a A matrix which is more appropriate in the temperature range we are considering. It differs slightly from the one presented here.

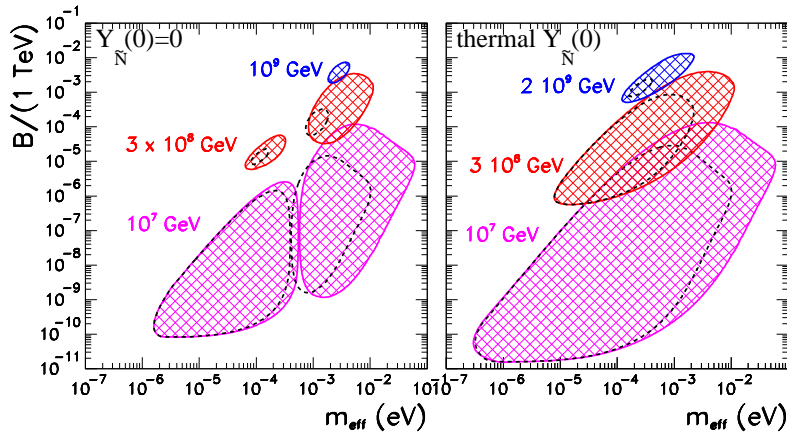


Figure 4.4: B, m_{eff} regions in which successful SL can be achieved when flavor effects are included with $P_e = P_\mu = P_\tau = 1/3$. We take $|\text{Im}A| = 10^3$ GeV and $\tan\beta = 30$ and different values of M as labeled in the figure. The dashed contours are the corresponding ones when flavor effects are not included. The two panels correspond to vanishing initial RHSN abundance (left) and thermal initial RHSN abundance (right).

We have verified that for UTS the equally distributed flavor composition $P_e = P_\mu = P_\tau = 1/3$ (so all flavor are in the same washout regime) gives an almost maximum flavor effect for $m_{\text{eff}} \lesssim 10^{-2}$ eV. Conversely for $m_{\text{eff}} \gtrsim 10^{-2}$ eV values, flavor effects lead to larger $B - L$ asymmetry for more asymmetric flavor compositions. In this case, the “optimum” flavor projection strongly depends on the value of m_{eff} . We will discuss more on this in Section 4.4.2.

Introducing the resulting η_{fla} in eqs. (4.29) and (2.116) we can easily quantify the allowed ranges of parameters for which enough asymmetry, $Y_{\Delta B}^0 \geq Y_B^{\text{CMB}}$ (see eq. (1.2)) [3], is generated. Considering only the CP asymmetry from mixing \bar{e}^S eq. (2.45), we plot in Figure 4.4 the range of parameters B and m_{eff} for which enough asymmetry is generated, $Y_{\Delta B}^0 \geq 8.54 \times 10^{-11}$ for the the equally distributed flavor composition $P_e = P_\mu = P_\tau = 1/3$. We show the ranges for several values of M and for the characteristic value of $|\text{Im}A| = 1$ TeV. The dashed contours are the corresponding ones when flavor effects are not included. The figure illustrates to what extent flavor effects can affect the ranges of B and M for which successful SL can be achieved. This is more quantitatively displayed in Figure 4.5 where we plot the baryon asymmetry

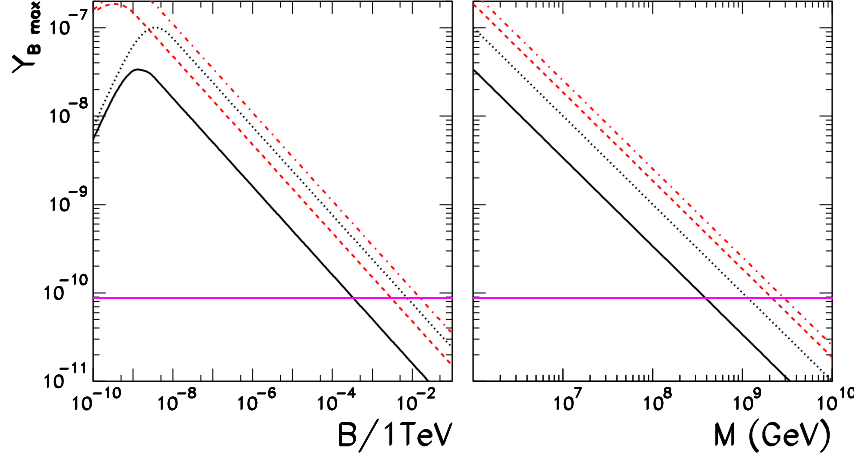


Figure 4.5: Maximum baryon asymmetry as a function of B (left) and M (right). The solid (dashed) lines are for no flavor effects and vanishing (thermal) initial RHSN abundance. The dotted (dash-dotted) lines are the corresponding asymmetries after including flavor effects with $P_e = P_\mu = P_\tau = 1/3$. The horizontal line correspond to the 1σ WMAP measurements in the Λ CDM model eq. (1.2).

that can be achieved for a give value of B (or M) maximized with respect to m_{eff} and M (or B) when flavor effects are included (for $P_e = P_\mu = P_\tau = 1/3$) compared to the corresponding one when they are neglected. From the figure we read that successful SL with (without) flavor effects considered requires $B \leq 8 \times 10^{-3}$ (3×10^{-4}) TeV and $M \leq \times 10^9$ (4×10^8) GeV for vanishing initial RHSN abundance and $B \leq 1.5 \times 10^{-2}$ (3×10^{-3}) TeV and $M \leq 3 \times 10^9$ (2×10^9) GeV for thermal initial RHSN abundance. Hence the flavor enhancement in UTS permits slightly larger values of the lepton-violating soft bilinear term B .

4.4.1.1 Gaugino contributions to the CP asymmetries

Next, we consider also the CP asymmetries from decay \bar{e}^V eq. (2.46) and interference \bar{e}^I eq. (2.47) which were first discussed in ref. [85]. For comparison, in Figure 4.6, we plot the resulting ranges for B and m_{eff} for the equally distributed flavor composition $P_e = P_\mu = P_\tau = 1/3$ and for $|A| = m_2 = 1$ TeV and $\tan \beta = 30$ for all three types of CP asymmetries eqs. (2.45)–(2.47). For

different values of the CP phases and M as explicitly given in the figure.

The upper panels in Figure 4.6 give the parametric regions for which the CP violation from pure mixing effects, $\bar{\epsilon}^S$, can produce the observed asymmetry as previously described in [25, 82, 83]. Due to the resonant nature of this contribution, these effects are only large enough for $B \sim \mathcal{O}(\Gamma)$ which leads to the well-known condition of the unconventionally small values of B and to the upper bound $M \lesssim 10^9$ GeV.

The central panels of Figure 4.6 give the corresponding regions for which CP violation from gaugino-induced vertex effects, $\bar{\epsilon}^V$, can produce the observed baryon asymmetry. Despite being higher order in δ_S and including a loop suppression factor, α_2 , this contribution can be relevant because it is dominant for conventional values of the B parameter. However, in order to overcome the loop and δ_S suppressions this contribution can only be sizable for lighter values of the RHSN masses $M \lesssim 10^6$ GeV (within the approximation used in this work: $\delta_S \ll 1$, $|A|, m_2 \sim \mathcal{O}(\text{TeV})$). The parameters chosen in the figure are such that the second term in eq. (2.46) dominates so that the allowed region depicts a lower bound on B . Conversely, when the first term in eq. (2.46) dominates, $\bar{\epsilon}^V$ becomes independent of B . In this case, for a given value of M and δ_S the produced baryon asymmetry can be sizable within the range of m_{eff} values for which η_{fla} is large enough. For example for $M = 10^5$ GeV, and $m_2 = |A| = 1$ TeV and $|\sin(\phi_A + 2\phi_g)| = 1$ with vanishing initial conditions

$$10^{-5} < \frac{m_{\text{eff}}}{\text{eV}} < 6.5 \times 10^{-4} \quad \text{or} \quad 8 \times 10^{-4} < \frac{m_{\text{eff}}}{\text{eV}} < 3 \times 10^{-2}, \quad (4.35)$$

where each range corresponds to a sign of the CP phase $\sin(\phi_A + 2\phi_g)$

Finally we show in the lower panels of Figure 4.6 the values of B and m_{eff} for which enough baryon asymmetry can be generated from the interference of mixing and vertex corrections $\bar{\epsilon}^I$, eq. (2.47). Generically $\bar{\epsilon}^I$ is subdominant to $\bar{\epsilon}^S$ since both involve the same CP phase $\sin(\phi_A)$ while $\bar{\epsilon}^I$ has additional δ_S and loop suppressions:

$$\frac{\bar{\epsilon}^I}{\bar{\epsilon}^S} = \frac{-3}{8} \alpha_2 \frac{m_2}{M} \ln \frac{m_2^2}{M^2 + m_2^2} \cos(2\phi_g) \frac{\Gamma}{B}. \quad (4.36)$$

Consequently as seen in the above equation and illustrated in the figure, $\bar{\epsilon}^I$ can only dominate for extremely low values of B ($B \ll \Gamma$) for which it becomes

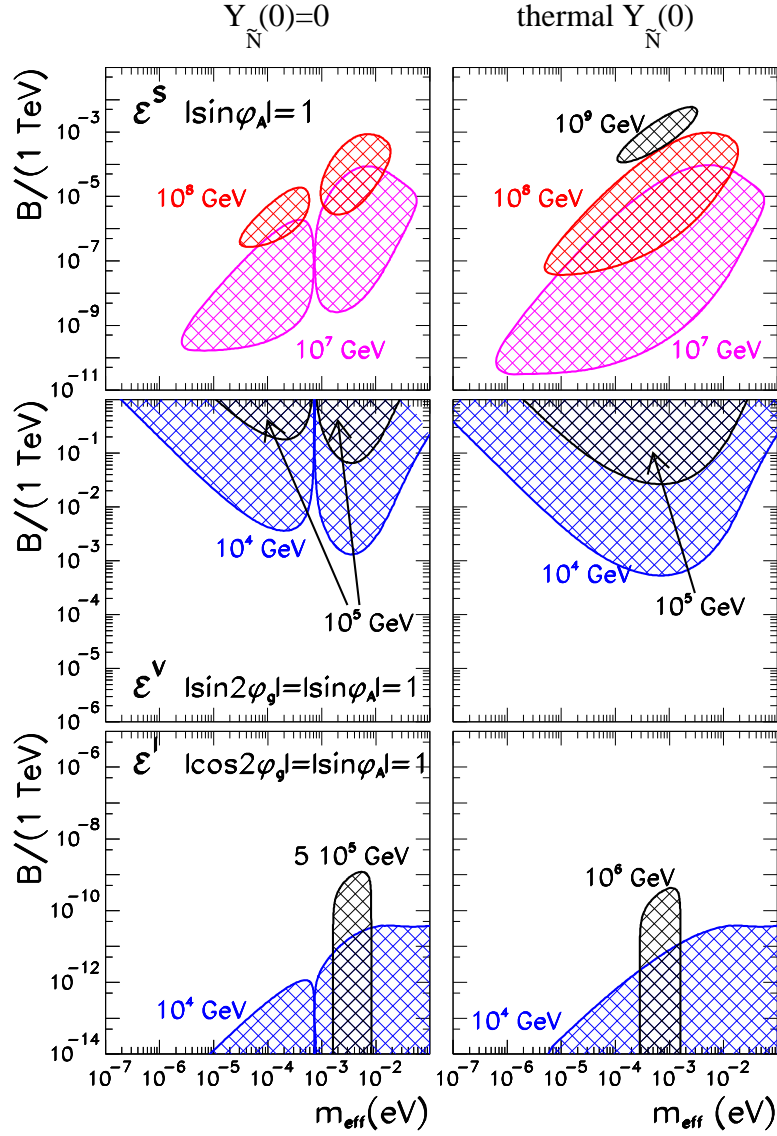


Figure 4.6: B, m_{eff} regions in which successful SL can be achieved when flavor effects are included with $P_e = P_\mu = P_\tau = 1/3$ and for different sources of CP violation. In all cases we take $|A| = m_2 = 10^3$ GeV and $\tan\beta = 30$ and different values of M and ϕ_A and ϕ_g as labeled in the figure (see text for details). The left (right) panels correspond to vanishing (thermal) initial RHSN abundance .

independent of B . Also we notice that for $M \lesssim 10^4$ GeV and $m_{\text{eff}} \gtrsim 10^{-2}$ eV the resulting baryon asymmetry generated by this contribution becomes independent of m_{eff} since the m_{eff}^2 dependence from Γ^2 cancels the approximate $1/m_{\text{eff}}^2$ dependence of η_{fla} in this strong washout regime.

4.4.2 Simplified misaligned scenario (SMS)

In this section, we will consider the SMS scenario discussed in Section 4.2.1 where $Z_\alpha = (\sum_\beta |Y_\beta|^2)/3Y_\alpha^*$ as in eq. (4.14). We note that these two scenarios: UTS and SMS are equivalent for the special case of flavor equipartition $P_e = P_\mu = P_\tau = 1/3$.

Here for simplicity, we only consider the CP asymmetry from mixing eq. (4.8). We parametrize the asymmetry generated by the decay of RHSN in a given flavor as

$$Y_{\Delta_\alpha}(z \rightarrow \infty) = -2\eta_\alpha \bar{\epsilon} Y_{\tilde{N}}^{eq}(T \gg M), \quad (4.37)$$

where $\bar{\epsilon} = \bar{\epsilon}^S$ eq. (2.45). Thus the final $B - L$ asymmetry can be written as

$$\begin{aligned} Y_{\Delta_{B-L}}^0 &= \sum_\alpha Y_{\Delta_\alpha}(z \rightarrow \infty), \\ &= -2\eta \bar{\epsilon} Y_{\tilde{N}}^{eq}(T \gg M), \end{aligned} \quad (4.38)$$

where we define

$$\eta = \sum_\alpha \eta_\alpha. \quad (4.39)$$

Notice that the η defined here is equivalent to the η_{fla} defined in eq. (4.30) for the UTS scenario.

The dependence of the efficiency factor on the flavor projectors P_α and on m_{eff} is shown in Figure 4.7. In generating these results, we have also taken

into account the spectator effects [26, 27] by using¹¹

$$A = \frac{2}{711} \begin{pmatrix} -221 & 16 & 16 \\ 16 & -221 & 16 \\ 16 & 16 & -221 \end{pmatrix}, \quad C = -\frac{8}{79} (1 \ 1 \ 1). \quad (4.40)$$

which is appropriate for $T \lesssim 10^5(1 + \tan^2 \beta)$ GeV when reactions mediated by the Yukawa couplings of all the three families are in equilibrium¹². The conditions under which the A and C are derived are given in Appendix C. Compared to the A and C presented in Appendix C.2, there is an additional factor of 6 in eqs. (4.40) because in this chapter we have define $Y_{L_{\text{tot}}^\alpha} = Y_{\Delta \ell_\alpha} + Y_{\Delta \tilde{\ell}_\alpha}$ and $Y_{H_{\text{tot}}} = Y_{\Delta H_u} + Y_{\Delta \tilde{H}_u}$ with the sum over $SU(2)_L$ degrees of freedom. The plot is shown for $M = 10^6$ GeV and $\tan \beta = 30$ although, as mentioned above, the efficiency is practically independent of M . As long as $\tan \beta$ is not very close to one, the dominant dependence on $\tan \beta$ arises via v_u as given in eq. (2.95) and it is therefore also rather mild. For $\tan \beta \sim \mathcal{O}(1)$ there is also an additional (very weak) dependence due to the associated change in the top Yukawa coupling.

From the top panel in Figure 4.7 we see that departure from the equipartition flavor case results in an enhancement of the efficiency, and that particularly large enhancements are possible for the SMS scenario. Note that the top line in the top panel of Figure 4.7 labeled $P_\tau = 0.99$ represents the maximum enhancement that can be obtained in the SMS (relaxing the constraint in eq. (4.14) that defines our SMS, larger enhancements are however possible). This is because for $P_\tau = 0.99$ both the asymmetries $Y_{\Delta e}$ and $Y_{\Delta \mu}$ are generated in the weak washout regime, that is, approximately within the same temperature range, and in the SMS this implies $\epsilon_e(T_e) \approx \epsilon_\mu(T_\mu)$. The related combined efficiency is then simply determined by $(P_e + P_\mu) m_{\text{eff}} \simeq m_*$ and is thus always maximal, independently of the individual values of P_e and

¹¹By using the A matrix in eq. (30) of ref. [124] or the A matrix presented here, the difference in the final efficiency is negligible. However by taking into account the spectators i.e. with nonzero C vector, there is an extra suppression of order $\mathcal{O}(1)$ in the efficiency in strong washout regime.

¹²Indeed we find that, within a given T regime, A and C for the MSSM and for the SM are the same up to a global factor 1/2 for C . This is expected to be so, since SUSY cannot alter the flavor distribution between the charges. This is in agreement with the analysis in ref. [106], but it disagrees with the A matrix given in ref. [124].

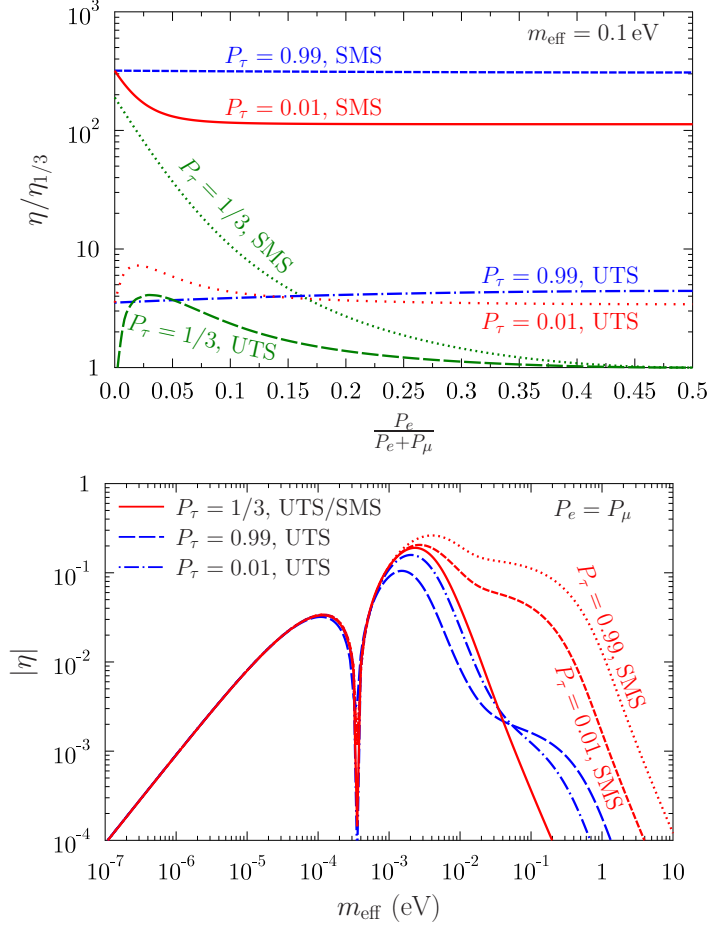


Figure 4.7: The dependence of the efficiency – normalized to the flavor equipartition case $P = (1/3, 1/3, 1/3)$ – on the values of the lepton flavor projections (top) and on m_{eff} (bottom). The figures correspond to $M = 10^6$ GeV and $\tan \beta = 30$.

P_μ , as is apparent from the figure.

The bottom panel of Figure 4.7 shows the dependence of the efficiency on m_{eff} in the flavor equipartition case and for two other sets of flavor projections. As it was discussed before, flavor effects become more relevant when the washouts get stronger. This is confirmed in this picture where it is seen that for the SMS scenario the possible enhancements quickly grow with m_{eff} . Note that in SL this dependence is even stronger than in standard leptogenesis. This is due to the fact that the flavored washout parameters $P_\alpha m_{\text{eff}}$ also determine the value of z_{dec}^α when the lepton asymmetry in the α flavor starts being generated, and since the CP asymmetry has a strong dependence on z ,

different values of P_e , P_μ , and P_τ imply that the corresponding flavor asymmetries are generated with different values of the CP asymmetry even when, as in the SMS, the fundamental quantity $\bar{\epsilon}$ is flavor independent. In summary, what happens is that the flavor that suffers the weakest washout is also the one for which inverse-decays go out of equilibrium earlier, and thus also the one for which the lepton asymmetry starts being generated when $\bar{\epsilon} \times \Delta_{BF}$ is larger. This realizes a very efficient scheme in which the flavor that is more weakly washed out has effectively the largest CP asymmetry, and this explains qualitatively the origin of the large enhancements that we have found. Furthermore, when $P_\alpha m_{\text{eff}} \ll m_*$ so that the inverse decay of flavor α never reaches equilibrium and the washout of the asymmetry Y_{Δ_α} is negligible, the maximum efficiency is reached.

We should however spend a word of caution for the reader about interpreting our numerical results in the weak washout regime and, for the SMS, also in the limit of extreme flavor hierarchies ($P_\alpha \rightarrow 0$). At high temperatures ($z < 1$) the Higgs bosons (higgsinos) develop a sufficiently large thermal mass to decay into sleptons (leptons) and sneutrinos. The new CP asymmetries associated with these decays could be particularly large [25], and thus sizable lepton flavor asymmetries could be generated at high temperatures. This type of thermal effects are not included in our analysis. Concerning the flavor decoupling limit within the SMS, clearly when $P_\alpha \rightarrow 0$ no asymmetry can be generated in the flavor α . However, in our SMS flavor asymmetries are defined to be independent of the projectors P and thus survive in the $P \rightarrow 0$ limit. On physical grounds, one would expect for example that when one decay branching ratio is suppressed, say, as $P < 10^{-5}$, the associated CP asymmetry will be at most of $\mathcal{O}(10^{-7})$ and thus irrelevant for leptogenesis. This means that for extreme flavor hierarchies, the SMS breaks down as a possible physical realization of SL, and thus in what follows we will restrict our considerations to a range of hierarchies $P \gtrsim 10^{-3}$.

As a result of our analysis, we find that for the SMS scenario with hierarchical Yukawa couplings, successful leptogenesis is possible even for $m_{\text{eff}} \gg \mathcal{O}(\text{eV})$. For example, as is shown in the right panel of Figure 4.7, for $P_e = P_\mu = 5 \times 10^{-3}$ and $m_{\text{eff}} \sim 5 \text{ eV}$, we obtain $|\eta| \sim 10^{-3}$, that yields the estimate

$$Y_{\Delta B}^0(\text{SMS}, P_e = P_\mu = 5 \times 10^{-3}, m_{\text{eff}} = 5 \text{ eV}) \sim 10^{-6} \times \bar{\epsilon}. \quad (4.41)$$

Thus we see that assuming a large, but still acceptable value of $\bar{\epsilon} \sim 10^{-4}$, SL can successfully generate the observed baryon asymmetry as quoted in eq. (1.2) [3] for values of m_{eff} that are about two orders of magnitude larger than what is found in the unflavored standard leptogenesis scenario.

4.4.3 Natural B values

We next explore the impact that flavor enhancements can have in relaxing the requirements on the values of B and M for successful SL with the CP asymmetry from mixing eq. (4.8). From eqs. (2.116), (4.38), (2.45), and (1.2), we find that the maximum value of B for given values of M and m_{eff} is:

$$B \leq \frac{\Gamma(m_{\text{eff}}, M)}{2} \frac{|\text{Im}A| C \eta(m_{\text{eff}})}{M Y_{B_{\text{obs}}}} \times \left[1 + \sqrt{1 - \left(\frac{M}{|\text{Im}A|} \frac{Y_{B_{\text{obs}}}}{C \eta(m_{\text{eff}})} \right)^2} \right], \quad (4.42)$$

where $C = \frac{16}{23} Y_{\tilde{N}}^{eq}(z \rightarrow 0)$, $\Gamma(m_{\text{eff}}, M)$ is given in eq. (2.12) and $\text{Im}A = A \sin \phi_A$. Thus we obtain

$$M \leq \frac{|\text{Im}A| C \eta(m_{\text{eff}})}{Y_B^{CMB}}, \quad (4.43)$$

$$B \leq \frac{3\sqrt{3}m_{\text{eff}}}{32\pi v^2} \left(\frac{|\text{Im}A| C \eta(m_{\text{eff}})}{Y_B^{CMB}} \right)^2, \quad (4.44)$$

where $\eta(m_{\text{eff}}) \equiv \eta(m_{\text{eff}}, P_\alpha, Z_\alpha)$ and we have neglected all residual dependence of η on M . As seen in the right panel of Figure 4.7, assuming the SMS and for sufficiently hierarchical P_α , $\eta(m_{\text{eff}})$ decreases first very mildly with m_{eff} and – once all the flavors have reached the strong washout regime– it decreases roughly as $\sim m_{\text{eff}}^{-2}$. Thus the product $m_{\text{eff}} \times \eta(m_{\text{eff}})^2$ first grows with m_{eff} till it reaches a maximum and then for sufficiently large m_{eff} it decreases $\sim m_{\text{eff}}^{-3}$. Therefore, for a fixed value of the projectors, the upper bound on B does not corresponds simply to the maximum allowed value of m_{eff} , but it has a more complicated dependence.

In Figure 4.8 we show the maximum values of B and M obtained for both the UTS and SMS cases as a function of the flavor projections. In order to

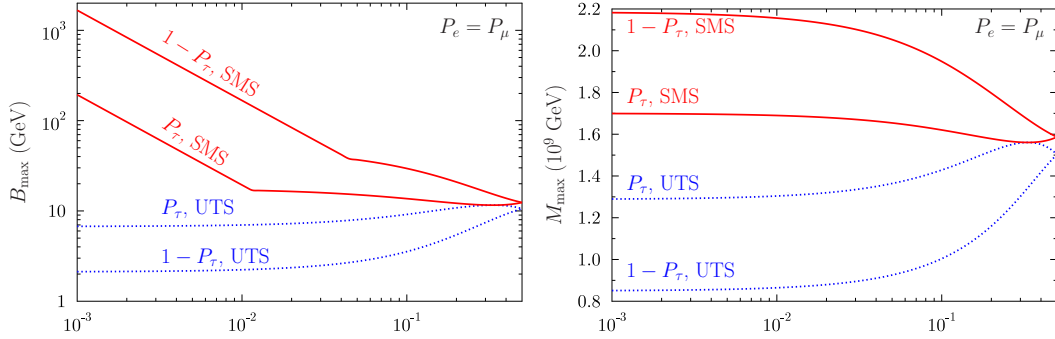


Figure 4.8: Maximum values of B and M which can lead to SL as a function of the flavor projections (we plot both as a function of P_τ or $1 - P_\tau$ for clarity when either P_τ or $1 - P_\tau$ is very small). The figure corresponds to $A \sin \phi_A = 1$ TeV and $\tan \beta = 30$.

have better resolution when either P_τ or $1 - P_\tau$ is very small, we plot them both as a function of P_τ or $1 - P_\tau$. In the figure we set $\text{Im}A = 1$ TeV. The figure illustrates that within the UTS, the parameter space for successful leptogenesis is very little modified by departing from the flavor equipartition case (that corresponds to the point where the UTS and SMS curves join). On the contrary, in the SMS case we find that with hierarchical flavor projections $1 - P_\tau \sim \text{few} \times 10^{-3}$ successful SL is allowed also with $B \sim \mathcal{O}(\text{TeV})$, that is for quite natural values of the bilinear term. As mentioned above, even for hierarchical projections the maximum allowed values of B and M do not correspond to the maximum allowed value of m_{eff} . In particular, for the range of flavor projections shown in the figure we obtain that the maximum values of B and M correspond to $m_{\text{eff}} \lesssim 2$ eV.

4.4.4 Lepton flavor equilibration and low energy constraints

We now turn to quantify the impact that the presence of LFE scatterings discussed in Section 4.2.3 can have on the enhancements we discussed previously. We plot in Figure 4.9 the dependence of the enhancement of the efficiency due to flavor effects, as a function of the off-diagonal slepton mass parameter \tilde{m}_{od} . As can be seen in the figure (and as it was expected from the discussion in the previous section) for any given value of M , LFE quickly becomes

efficient damping completely the lepton flavors enhancements of the efficiency within a very narrow range of values $\tilde{m}_{od}^{min} \leq \tilde{m}_{od} \leq \tilde{m}_{od}^{max}$. The figure is shown for $\tan \beta = 30$. Again, the dominant dependence on $\tan \beta$ arises due to $v_d = v \cos \beta$ in eq. (4.19). Results from other values of $\tan \beta$ can be easily read from the figure by rescaling $\tilde{m}_{od}^\beta = \tilde{m}_{od}^{fig}/(30 \cos \beta)$.

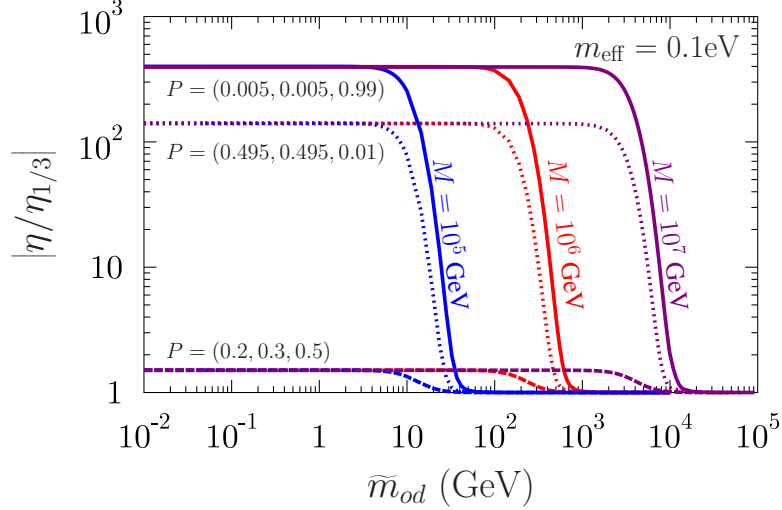


Figure 4.9: The dependence of the efficiency (normalized to the flavor equipartition case $P = (1/3, 1/3, 1/3)$) on the off-diagonal soft slepton mass parameter \tilde{m}_{od} , for different values of M and of the flavor projections (see text for details).

It is interesting to remark that while the efficiency $\eta(m_{\text{eff}})$ is practically insensitive to the particular value of M , as long as m_{eff} is held constant, this is not the case for the generalized efficiency η^{LFE} computed by accounting for LFE effects. Given the different scaling with the temperature of the $\bar{\Gamma}_{\text{LFE}}$ and $\bar{\Gamma}_{\text{ID}}$ rates, the precise temperature at which leptogenesis occurs is crucial. For example, we see from Figure 4.9 that for reasonable values $\tilde{m}_{od} \lesssim 200 \text{ GeV}$ and for $M \gtrsim 10^6 \text{ GeV}$, LFE is not effective, and the large enhancements of the efficiency due to flavor effects can survive, while for $M \lesssim 10^5 \text{ GeV}$ all flavor enhancements disappear.

It is interesting to compare the values of \tilde{m}_{od} for which the LFE does not occur with the existing bounds imposed from non-observation of flavor violation in leptonic decays. The question we want to address is the following: given the low energy constraints on \tilde{m}_{od} , what is the lower bound on the leptogenesis scale M for which large flavor enhancements of the lepton asymmetry

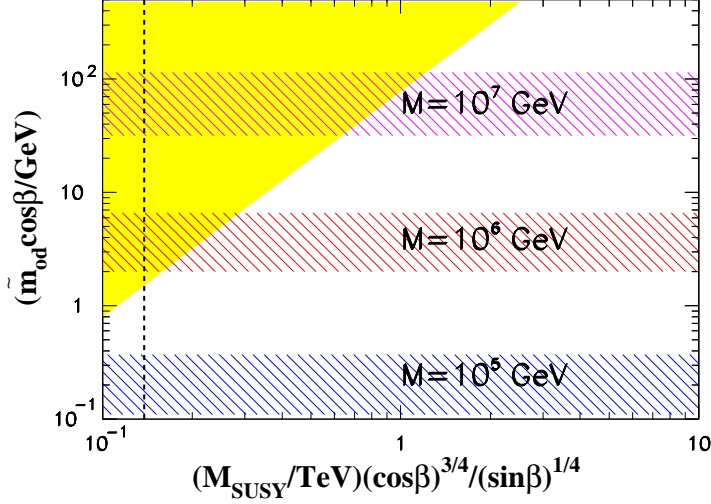


Figure 4.10: This figure shows the excluded region (shaded in yellow) of $\tilde{m}_{od} \cos \beta$ versus $m_{SUSY}(\cos \beta)^{3/4}/(\sin \beta)^{1/4}$ arising from the present bound on $BR(\mu \rightarrow e\gamma) \leq 1.2 \times 10^{-11}$, together with the minimum value of $\tilde{m}_{od} \cos \beta$ for which LFE effects start damping out flavor effects in SL. Three bands are shown corresponding to $M = 10^5$ GeV, $M = 10^6$ GeV and $M = 10^7$ GeV. The width of the bands represents the range associated with variations of $P_\alpha m_{\text{eff}}$ in the range 0.003 eV–10 eV, where P_α is the largest of the three flavor projections. The vertical dashed line represents the value of $m_{SUSY}/(\tan \beta)^{1/2}$ (for $\tan \beta = 1$) required to explain the discrepancy between the SM prediction and the measured value of a_μ . [129]

are not damped by LFE effects ?

Clearly the presence of a sizable \tilde{m}_{od} would induce various LFV decays, like for example $l_\alpha \rightarrow l_\beta \gamma$ with rate

$$\begin{aligned} \frac{BR(l_\alpha \rightarrow l_\beta \gamma)}{BR(l_\alpha \rightarrow l_\beta \nu_\alpha \bar{\nu}_\beta)} &\sim \frac{\alpha^3 \tan^2 \beta}{G_F^2 m_{SUSY}^8} \tilde{m}_{od}^4 \\ &\simeq 2.9 \times 10^{-19} \frac{\sin^2 \beta}{\cos^6 \beta} \left(\frac{\text{TeV}}{m_{SUSY}} \right)^8 \left(\cos^2 \beta \frac{\tilde{m}_{od}^2}{\text{GeV}^2} \right)^2, \end{aligned} \quad (4.45)$$

where m_{SUSY} is a generic SUSY scale for the gauginos and sleptons masses running in the LFV loop. We show in Figure 4.10 with a yellow shade, the excluded region of $\tilde{m}_{od} \cos \beta$ versus $m_{SUSY}(\cos \beta)^{3/4}/(\sin \beta)^{1/4}$ arising from the present bound $BR(\mu \rightarrow e\gamma) \leq 1.2 \times 10^{-11}$, together with the minimum value

of $\tilde{m}_{od} \cos \beta$ for which LFE effects start damping out flavor enhancements in SL. Three bands are shown respectively for $M = 10^5$ GeV, $M = 10^6$ GeV and $M = 10^7$ GeV. The width of the bands represents the range associated with variations of the effective flavored decay parameter $P_\alpha m_{\text{eff}}$ in the range $0.003 \text{ eV} - 10 \text{ eV}$, where P_α is the largest of the three flavor projections. For illustration we also show in the figure the characteristic SUSY scale that allows to explain the small discrepancy between the SM prediction and the measured value of the muon anomalous magnetic moment, a_μ . This value is $m_{SUSY}/(\tan \beta)^{\frac{1}{2}} = 141 \text{ GeV}$ [129], and the vertical dashed line in the picture corresponds to $\tan \beta = 1$. As seen in the figure, in this case the off-diagonal slepton masses are bound to be small enough to allow for flavor enhancements in SL for M as low as 10^6 GeV. For larger values of $\tan \beta$, even lower values of M are allowed.

4.5 Discussion and Conclusions

Given the temperature regimes in which SL can proceed $10^4 \text{ GeV} \lesssim T \lesssim 10^9 \text{ GeV}$, accounting for flavor effects is mandatory. We first studied this effect in Section 4.4.1 under the assumption of universality of the soft terms (UTS scenario). Such scenarios strongly constrain the possible flavor structures, and in particular imply that the flavored CP asymmetries must be proportional to the corresponding flavor dependent washouts, with the result that the larger is the CP asymmetry, the more efficient is the related washout. This compensating mechanism allows for only moderate $\sim \mathcal{O}(30)$ enhancements of the leptogenesis efficiency. Thus, within universal soft SUSY-breaking schemes, flavor effects can only moderately alleviate the fine tuning problem of the B parameter, and still do not allow for $B \sim m_{SUSY}$, that is what one would expect on the basis of naturalness considerations.

In Section 4.4.2 we show how this situation drastically changes if the assumption of universality for the soft terms is relaxed, which results in a generic situation in which the flavored CP asymmetries are not aligned with the respective washouts. Note that an analogous situation is generally realized within the standard flavored leptogenesis scenarios. To carry out our phenomenological analysis, while avoiding the proliferation of too many flavor-related

parameters, we have introduced a simplified non-universal scheme in which all the flavored CP asymmetries (evaluated at equal temperatures) are equal (and thus flavor independent) while the flavored washouts are allowed to be strongly hierarchical (SMS scenario). Here we stress that since the hierarchy in the washouts is controlled by the hierarchy in the neutrino Yukawa couplings, and given that we know that in the SM strong hierarchies in the Yukawa couplings are realized in the charged lepton sector as well as for the up- and down-type quark sectors, a strong hierarchy in the flavor dependent washouts can be considered as a natural possibility. As regards the amount of misalignment between the soft trilinear A terms and the corresponding neutrino Yukawa couplings Y_α , that eventually produces the misalignment between flavored CP asymmetries and washouts, due to our ignorance about the mechanism that breaks SUSY, any assumption is equally acceptable, provided that the existing limits on LFV processes are not violated.

Under these conditions, we have found that flavor effects can enhance the leptogenesis efficiency by more than two orders of magnitude with respect to the flavor equipartition case, defined as the situation in which all the flavored CP asymmetries and washouts are equal in magnitude. This result can then be translated into a several $\times 10^3$ enhancement with respect to the one-flavor approximation, which is sufficient to avoid the need for any additional enhancement from resonant conditions. Thus, the natural scale for the sneutrino mixing parameter $B \sim m_{SUSY}$ is eventually allowed. Curiously, the possibility of such large enhancements is directly related to the strong temperature dependence of the CP asymmetries: for the lepton flavors that are most weakly washed out, and for which inverse-decays go out of equilibrium first, the lepton asymmetry is generated at larger temperatures, that is precisely where the CP asymmetry is larger. Thus, relying only on the assumption of flavor misalignment and of hierarchical neutrino Yukawa couplings, a very efficient scheme in which the weaker is the washout, the larger is the corresponding CP asymmetry, is automatically realized, and this boosts the leptogenesis efficiency to the highest possible values.

Finally, we have also verified that LFE effects induced by off-diagonal soft slepton masses, subject to the bounds imposed from non-observation of flavor violation in leptonic decays, are ineffective for damping these flavor enhance-

ments.

Chapter 5

Non-superequilibration and R-genesis

5.1 Introduction

Early works on SM leptogenesis were carried out from the start within the unflavored effective theory. Quite likely this happened because the corresponding Lagrangian is much more simple than the full SM Lagrangian given that the number of relevant parameters is reduced to a few. The main virtue of subsequent studies on lepton flavor effects¹ was that of recognizing that for $T \lesssim 10^{12}$ GeV, the unflavored theory breaks down, and the new theory brings in new fundamental parameters which can give genuinely different answers for the amount of baryon asymmetry that is generated.

In supersymmetric leptogenesis the opposite happened: the effective theory that was generally used assumed fast particle-particle equilibration reaction and it is only appropriate for temperatures much lower than the typical temperatures $T \gg 10^8$ GeV in which leptogenesis can be successful. In fact only quite recently we clarified that in the relevant temperature range a completely different effective theory holds instead [69]. More specifically, before our work, it was always assumed (often implicitly) that lepton-slepton reactions like e.g. $\ell\ell \leftrightarrow \tilde{\ell}\tilde{\ell}$ that are induced by soft gaugino masses (see Figure 5.1), are in thermal equilibrium (see refs. [7, 25, 66] for examples of well known papers adopting this assumption). This implies equilibration between the lepton and

¹See the references in the Introduction of Chapter 4.

slepton chemical potentials as we have always assumed in the previous chapters (see Section 2.4.2.2). However, in general, in supersymmetric leptogenesis, superequilibration (SE) does not occur. In fact, the rates of interactions induced by SUSY-breaking scale (Λ_{susy}) parameters, like soft gaugino masses $m_{\tilde{g}}$ or the higgsino mixing parameter μ , are slower than the Universe expansion rate when $T \sim M$ (with M being the heavy neutrino mass, and M_{pl} below the Planck mass) if

$$\frac{\Lambda_{susy}^2}{M} \lesssim 25 \frac{M^2}{M_{pl}} \quad \Rightarrow \quad M \gtrsim 5 \times 10^7 \left(\frac{\Lambda_{susy}}{500 \text{ GeV}} \right)^{2/3} \text{ GeV}. \quad (5.1)$$

The effective theory appropriate for studying supersymmetric leptogenesis, in which the heavy Majorana masses certainly satisfy the bound eq. (5.1), is thus obtained by setting $m_{\tilde{g}}, \mu \rightarrow 0$. We analyzed the consequences of this in ref. [69] and they are far reaching. At $T \gtrsim 10^7$ GeV, besides the occurrence of non-superequilibration (NSE) effects, additional anomalous global symmetries that involve both $SU(2)_L$ and $SU(3)_c$ fermion representations emerge [130]. As a consequence, the EW and QCD sphaleron equilibrium conditions are modified with respect to the usual ones and, among other things, this also yields a different pattern of sphaleron induced lepton-flavor mixing [28, 30–32]. In addition, a new anomaly-free R -symmetry can be defined and the corresponding charge, being exactly conserved, provides a constraint on the particles density asymmetries that is not present in the SM. However, in ref. [69] we also concluded that, in spite of all these modifications, the resulting baryon asymmetry would not differ much from what was obtained in the usual supersymmetric type I seesaw scenario. Basically, this happens because in this case dropping the SE assumption and accounting for all the new effects only modifies spectator processes, while the overall amount of CP asymmetry that drives leptogenesis remains the same.

The most interesting scenario in which the appropriate effective theory not only yields far reaching qualitative differences but also very large quantitative effects, is in SL [82, 83] if it occurs above the SE threshold eq. (5.1). This is because of two main reasons:

(I) In SL there is a strong cancellation between the CP asymmetries for RHSN decays into scalars and into fermions $\epsilon \equiv \epsilon_s + \epsilon_f \simeq 0$. As we have shown,

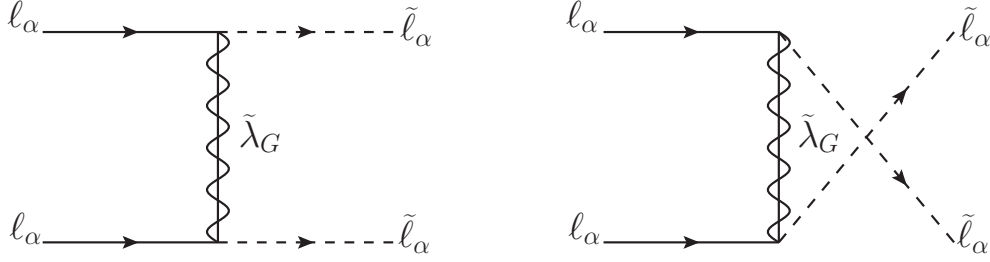


Figure 5.1: The lepton-slepton scatterings induced by soft gaugino masses $m_{\tilde{g}}$ through the exchange of $SU(2)_L$ and $U(1)_Y$ gauginos $\tilde{\lambda}_G$. Notice that the amplitude squared of these processes are proportional to $m_{\tilde{g}}^2$ and vanish in the limit of vanishing $m_{\tilde{g}}$.

at leading order, this cancellation is exact in the $T = 0$ limit, and ϵ gets lifted to an appreciable level only when thermal corrections are included [82, 83]. In the NSE regime however, the independent evolution of the scalar and leptonic density asymmetries implies that the corresponding efficiencies $\eta_{s,f}$ are different. When these different ‘weights’ are taken into account, the cancellation between the scalar and fermion contributions to the baryon asymmetry gets spoiled and a non-vanishing result is obtained even in the $\epsilon \equiv \epsilon_s + \epsilon_f \rightarrow 0$ limit. Indeed as we will see this effect can dominate over the ones due to thermal (or higher order) corrections to the CP asymmetries.

(II) Even more interestingly, in the high temperature effective theory two new global symmetries (a R -symmetry and a PQ -like symmetry) arise. While these symmetries are anomalous, two new anomaly free combinations of charges involving R and PQ can be defined. These new charges, that we denote as R_B and R_χ , are only (slowly) violated by sneutrino dynamics, that is by reactions of the third type (iii) in the classification given in Section 2.4.2, and thus their evolution must be followed by means of two new BEs. Because charge density asymmetries get mixed by EW sphalerons, these equations are coupled to the BEs that control the evolution of the $B - L$ asymmetry, and thus the dynamical evolution of R_B and R_χ affects its final value. What is important is that the CP violating sources for these two charges, that are respectively ϵ_s and $\epsilon_s - \epsilon_f$, are not suppressed by any kind of cancellation, and the corresponding density asymmetries remain large during leptogenesis. They act as source terms for $B - L$ that is thus driven to comparably large

values. As regards the final values of R_B and R_χ at the end of leptogenesis, they are instead irrelevant for the computation of the baryon asymmetry since, well before the temperature when the EW sphalerons are switched off, soft SUSY-breaking effects attain in-equilibrium rates, implying that R and PQ cease to be good symmetries also at the perturbative level. Thus, they decouple from the EW sphaleron processes that then reduce to the usual SM $B - L$ conserving form, that involves only quarks and leptons. The baryon asymmetry is then given only by $B - L$ conversion, according to the usual equation $B = \frac{8}{23}(B - L)$.

The effective theory appropriate for studying the generation of the baryon asymmetry when the heavy sneutrino masses satisfy the bound in eq. (5.1) is described in Section 5.2. We derive the equilibrium conditions and the relevant conservation laws that constrain the particle density asymmetries, we identify the new quasi-conserved charges, and we also compute the matrices that control the sphaleron induced lepton flavor mixing for two different sets of values of the electron and down-quark Yukawa couplings. In Section 5.3 we present the set of the *five* basic BEs, that is valid for numerical studies of SL at all temperatures, and in Section 5.3.1 we discuss a simple case in which the role played by the R_B and R_χ charge asymmetries is particularly transparent. In Section 5.4 we compute numerically the amount of baryon asymmetry that can be generated in SL within the NSE regime, and compare it to previous results based on the assumption of SE. Finally in Section 5.5 we present a simple explanation of the large numerical enhancements, we recap the main results and draw the conclusions.

5.2 Soft Leptogenesis Above the Superequilibration Temperature

We now discuss the early Universe effective theory appropriate for studying SL in the regime in which superequilibrating reactions like $\tilde{\ell}\tilde{\ell} \leftrightarrow \ell\ell$, that are induced by soft gaugino masses,

$$\mathcal{L}_{\tilde{\chi}} = -\frac{1}{2} \left(m_2 \overline{\tilde{\lambda}_2^{\pm,0}} P_L \tilde{\lambda}_2^{\pm,0} + m_1 \overline{\tilde{\lambda}_1} P_L \tilde{\lambda}_1 + \text{h.c.} \right), \quad (5.2)$$

	\tilde{g}	Q	u^c	d^c	ℓ	e^c	\tilde{H}_d	\tilde{H}_u	N^c
B	0	$\frac{1}{3}$	$-\frac{1}{3}$	$-\frac{1}{3}$	0	0	0	0	0
L	0	0	0	0	1	-1	0	0	0
PQ	0	0	-2	1	-1	2	-1	2	0
R f	1	-1	-3	1	-1	1	-1	3	-1
b	2	0	-2	2	0	2	0	4	0

Table 5.1: B , L , PQ and R charges for the particle supermultiplets that are labeled in the top row by their L-handed fermion component. Note that we use chemical potentials for the R-handed $SU(2)_L$ singlet fields u , d , e that have opposite charges with respect to the ones for u^c , d^c , e^c given in the table. The R charges for bosons are determined by $R(b) = R(f) + 1$.

and higgsino mixing transitions $\tilde{H}_u \leftrightarrow \overline{\tilde{H}_d}$, that are induced by the superpotential term

$$W_H = \mu \hat{H}_u \hat{H}_d, \quad (5.3)$$

do not occur. For simplicity, we assume equal masses for all the gauginos $m_1 = m_2 = m_{\tilde{g}}$ and that the supersymmetric higgsino mixing term also has approximately the same value: $\mu \simeq m_{\tilde{g}} = \Lambda_{susy}$. The regime we are interested here is defined by the condition given in eq. (5.1), that is the lower limit on the relevant temperatures is:

$$T \gtrsim 5 \cdot 10^7 \left(\frac{\Lambda_{susy}}{500 \text{ GeV}} \right)^{2/3} \text{ GeV}. \quad (5.4)$$

5.2.1 Anomalous and non-anomalous symmetries

The supersymmetric effective theory appropriate to study particle physics processes in the early Universe when the thermal bath temperature satisfies the condition eq. (5.4) is obtained by setting $m_{\tilde{g}}, \mu \rightarrow 0$ [130]. In this limit the theory gains two new $U(1)$ symmetries: $\mu \rightarrow 0$ yields a global symmetry of the Peccei-Quinn (PQ) type, and by setting also $m_{\tilde{g}} \rightarrow 0$ one additional global R -symmetry arises.

The charges of the various states under R and PQ , together with the

values of the other two global symmetries B and L are given in Table 5.1. Like L , also R and PQ are not symmetries of the seesaw superpotential terms $M\hat{N}^c\hat{N}^c + \lambda\hat{N}^c\hat{\ell}\hat{H}_u$, since it is not possible to find any charge assignment that would leave both terms invariant. In Table 5.1 we have fixed the charges of the heavy N^c supermultiplets in such a way that sneutrinos do not carry any charge. This has the advantage of ensuring that all the sneutrino bilinear terms, corresponding to the mass parameters M, \widetilde{M}, B , are invariant, and thus sneutrino mixing does not break any internal symmetry (this is because \widetilde{M}, B break SUSY). However, since $R(\hat{N}^c\hat{N}^c) = 0$, it follows that the mass term for the heavy Majorana neutrino breaks R by two units.²

All the four global symmetries B, L, PQ and R have mixed gauge anomalies with $SU(2)_L$, and R and PQ have also mixed gauge anomalies with $SU(3)_c$. Two linear combinations of R and PQ , having respectively only $SU(2)_L$ and $SU(3)_c$ mixed anomalies, have been identified in ref. [130]. They are:³

$$R_2 = R - 2PQ \quad (5.5)$$

$$R_3 = R - 3PQ. \quad (5.6)$$

The values of $R_{2,3}$ for the different states are given in Table 5.2. The authors of ref. [130] have also constructed the effective multi-fermions operators generated by the mixed anomalies:

$$\tilde{O}_{EW} = \Pi_\alpha (QQQ\ell_\alpha) \tilde{H}_u \tilde{H}_d \tilde{W}^4, \quad (5.7)$$

$$\tilde{O}_{QCD} = \Pi_i (QQQ u^c d^c)_i \tilde{g}^6. \quad (5.8)$$

Given that we have three charges R_2, B and L with mixed $SU(2)_L$ anomalies, it is then possible to define two anomaly free combinations. The most convenient are $B - L$ and

$$R_B = \frac{2}{3}B + R_2, \quad (5.9)$$

²Under R -symmetry the superspace Grassmann parameter transform as $\theta \rightarrow e^{i\alpha}\theta$. Invariance of $\int d\theta\theta = 1$ then requires $R(d\theta) = -1$. Then the chiral superspace integral of the superpotential $\int d\theta^2 W$ is invariant if $R(W) = 2$. By expanding a chiral supermultiplet in powers of θ it follows that the supermultiplet R charge equals the charge of the bosonic scalar component $R(b) = R(f) + 1$, and thus for the fermion bilinear term $R(\overline{N}_R^c N_L^c) = -2$.

³With respect to ref. [130], for definiteness we restrict ourselves to the case of three generations $N_g = 3$ and one pair of Higgs doublets $N_h = 1$, and we also normalize $R_{2,3}$ in such a way that $R_{2,3}(b) = R_{2,3}(f) + 1$.

	\tilde{g}	Q	u^c	d^c	ℓ	e^c	\tilde{H}_d	\tilde{H}_u	N^c	
R_2	f	1	-1	1	-1	1	-3	1	-1	-1
	b	2	0	2	0	2	-2	2	0	0
R_3	f	1	-1	3	-2	2	-5	2	-3	-1
	b	2	0	4	-1	3	-4	3	-2	0
R_B	f	1	$-\frac{7}{9}$	$\frac{7}{9}$	$-\frac{11}{9}$	1	-3	1	-1	-1
	b	2	$\frac{2}{9}$	$\frac{16}{9}$	$-\frac{2}{9}$	2	-2	2	0	0

Table 5.2: Charges for the fermionic and bosonic components of the SUSY multiplets under the R -symmetries defined in eqs.(5.5), (5.6) and (5.9). Supermultiplets are labeled in the top row by their L-handed fermion component. We use chemical potentials for the R-handed $SU(2)_L$ singlet fields u , d , e that have opposite charges with respect to the ones for u^c , d^c , e^c given in the table.

whose values are also given in Table 5.2. The fact that R_B does not contain any $B - L$ fragment, ensures that it will not enter in the final computation of the baryon asymmetry that will only depend on $B - L$. The fact that R_B is independent of L renders also easier writing a BE for its evolution.

The R_B values in Table 5.2 imply that the superpotential term $N^c \ell H_u$ has charge $R_B = 2$ and thus is invariant. It follows that sneutrinos decays into fermions conserve R_B . In contrast, the soft A term in eq. (2.3) responsible for sneutrinos decays into scalars violates R_B by 2 units, more precisely $\tilde{N}_\pm \rightarrow H_u \tilde{\ell}$ has $\Delta R_B = +2$ while $\tilde{N}_\pm \rightarrow H_u^* \tilde{\ell}^*$ has $\Delta R_B = -2$. As regards the heavy neutrinos, their mass term violates R_B by two units. Note that this is precisely like the case when one chooses to assign a lepton number -1 to the singlet neutrinos N . Accordingly, the decays of the heavy Majorana neutrino violate R_B by one unit: $N \rightarrow \ell H_u$, $\tilde{\ell} \tilde{H}_u$ have $\Delta R_B = +1$ and the decays to the CP conjugate states have $\Delta R_B = -1$. Since all R_B violating reactions have, by assumption, rates that are comparable to the Universe expansion rate, the evolution of this charge must then be tracked by means of a specific BE.

At temperatures satisfying the condition eq. (5.4) there is at least one other anomalous global symmetry, that we will denote by χ . It corresponds to $U(1)$ phase rotations of the u^c chiral multiplet that, for its fermionic component,

can be readily identified with chiral symmetry for the right-handed up-quark. In fact, above $T \sim 2 \times 10^6$ GeV, reactions mediated by h_u do not occur and the condition $h_u \rightarrow 0$ must be imposed, resulting in a new anomalous ‘chiral’ symmetry. In the $SU(3)_c$ sector we then have two anomalous symmetries R_3 and χ , and one anomaly free combination can be constructed. Assigning to the L -handed u_L^c supermultiplet a chiral charge $\chi = -1$ this combination has the form [69]

$$R_\chi = \chi_{u_L^c} + \kappa_{u_L^c} R_3, \quad (5.10)$$

where $\kappa_{u_L^c} = 1/3$. When the additional condition $h_d \rightarrow 0$ is imposed, a chiral symmetry arises also for the d^c supermultiplet. A second anomaly free R_χ symmetry can then be defined in a way completely analogous to eq. (5.10), with $\kappa_{d_L^c} = \kappa_{u_L^c} = 1/3$ [69]. As regards perturbative violations of R_χ , this charge inherits the same violations R_3 suffers. The soft A term in eq. (2.3) violates R_3 by one unit, and so do sneutrinos decays into scalars. Moreover, since $N^c \ell H_u$ has an overall charge $R_3 = 1$, a violation by one unit occurs also for sneutrinos decays into fermions. Correspondingly, we have $\Delta R_3 = +1$ for the decays $\tilde{N}, \tilde{N}^* \rightarrow H_u \tilde{\ell}, \tilde{H}_u \bar{\ell}$ and $\Delta R_3 = -1$ for $\tilde{N}, \tilde{N}^* \rightarrow \tilde{H}_u \ell, H_u^* \tilde{\ell}^*$. Of course, similarly to R_B , also the evolution of R_χ needs to be tracked by means of a BE.

5.2.2 Chemical equilibrium conditions and conservation laws

Because of the network of fast particle reactions occurring in the thermal bath, asymmetries generated in sneutrino decays spread around among the various particle species, and this can affect directly or indirectly leptogenesis processes. In principle there is one asymmetry for each particle degree of freedom. There are however several conditions and constraints that reduce the number of independent asymmetries to a few. The three types of reactions that have been classified in the introduction give rise to three different types of constraints and conditions, that need to be formulated in their own appropriate way⁴:

⁴These three types of reactions are first discussed in Section 2.4.2 and for reader’s convenience, we will go over them again here.

- (i) Constraints imposed by reactions whose rates are much faster than the Universe expansion have to be formulated in terms of chemical equilibrium conditions for the chemical potentials of incoming μ_I and final state particles μ_F :

$$\sum_I \mu_I = \sum_F \mu_F. \quad (5.11)$$

- (ii) Conservation laws that arise when all the reactions that violate some specific charge are much slower than the the Universe expansion have to be formulated in terms of particle number densities $\Delta n = n - \bar{n}$ and, for a generic charge Q , read:

$$Q = \sum_i Q_i \Delta n_i = \text{const}, \quad (5.12)$$

where Q_i is the charge of the i -particle species. We will always assume as initial conditions for leptogenesis that all particle asymmetries vanish, and thus we will put the constant value of eq. (5.12) equal to zero.

- (iii) Reactions with rates comparable with the Universe expansion have to be treated by means of appropriate dynamical equations. In this case, in order to reabsorb the dilution effects due to the Universe expansion, it is convenient to introduce as basic variables the number densities of particles per degree of freedom g normalized to the entropy density s (also known as *abundances*):

$$Y_{\Delta_i} = \frac{1}{g_i} \frac{\Delta n_i}{s}. \quad (5.13)$$

Clearly, μ_i , Δn_i and Y_{Δ_i} are all related to particles asymmetries. In particular, the number density asymmetries of particles for which a chemical potential can be defined are directly related with this chemical potential. For both bosons (b) and fermions (f) this relation acquires a particularly simple form in the relativistic limit $m_{b,f} \ll T$, and at first order in $\mu_{b,f}/T \ll 1$:

$$\Delta n_b = \frac{g_b}{3} T^2 \mu_b, \quad \Delta n_f = \frac{g_f}{6} T^2 \mu_f. \quad (5.14)$$

While we will always express the various constraints using the most appropriate quantities, eventually to solve for the large set of conditions in a closed form we will need to use a single set of variables. We will take this to be the set $\{Y_{\Delta_i}\}$, and will leave understood that our solutions to the constraining conditions are obtained after expressing μ_i and Δn_i in terms of this set, through eq. (5.14) and eq. (5.13).

5.2.2.1 General Constraints

We first list in items 1., 2. and 3. the conditions that surely hold in the temperature range $M_W \ll T \lesssim 10^{14}$ GeV. Conversely, some of the Yukawa coupling conditions given in items 4. and 5. will have to be dropped as the temperature is increased and the corresponding reactions go out of equilibrium. For simplicity of notations, in the following we denote the chemical potentials with the same notation that labels the corresponding field: $\phi \equiv \mu_\phi$.

- (1) At scales much higher than M_W , gauge fields have vanishing chemical potential $W = B = g = 0$ [51]. This also implies that all the particles belonging to the same $SU(2)_L$ or $SU(3)_c$ multiplets have the same chemical potential. For example $\phi(I_3 = +\frac{1}{2}) = \phi(I_3 = -\frac{1}{2})$ for a field ϕ that is a doublet of weak isospin \vec{I} , and similarly for color.
- (2) Denoting by \tilde{W}_R , \tilde{B}_R and \tilde{g}_R the right-handed winos, binos and gluinos chemical potentials, and by ℓ , Q ($\tilde{\ell}$, \tilde{Q}) the chemical potentials of the (s)lepton and (s)quarks left-handed doublets, the following reactions: $\tilde{Q} + \tilde{g}_R \rightarrow Q$, $\tilde{Q} + \tilde{W}_R \rightarrow Q$, $\tilde{\ell} + \tilde{W}_R \rightarrow \ell$, $\tilde{\ell} + \tilde{B}_R \rightarrow \ell$, imply that all gauginos have the same chemical potential:

$$-\tilde{g} = Q - \tilde{Q} = -\tilde{W} = \ell - \tilde{\ell} = -\tilde{B}, \quad (5.15)$$

where we have introduced \tilde{W} , \tilde{B} and \tilde{g} to denote the chemical potential of the *left-handed* gauginos. It follows that the chemical potentials of the SM particles are related to the chemical potential of their respective

superpartners as

$$\tilde{Q}, \tilde{\ell} = Q, \ell + \tilde{g} \quad (5.16)$$

$$H_{u,d} = \tilde{H}_{u,d} + \tilde{g} \quad (5.17)$$

$$\tilde{u}, \tilde{d}, \tilde{e} = u, d, e - \tilde{g}. \quad (5.18)$$

The last relation, in which $u, d, e \equiv u_R, d_R, e_R$ denote the R -handed $SU(2)_L$ singlets, follows e.g. from $\tilde{u}_L^c = u_L^c + \tilde{g}$ for the corresponding L -handed fields, together with $u_L^c = -u_R$, and from the analogous relation for the $SU(2)_L$ singlet squarks.

Eqs. (5.16)–(5.18) together with the vanishing of the chemical potentials of the gauge fields and the equality of the chemical potentials for all the gauginos, implies that we are left with 18 chemical potentials (or number density asymmetries) that we chose to be the ones of the fermionic states. They are 15 for the SM quarks and leptons, 2 for the up-type and down-type higgsinos, and 1 for the gauginos. These 18 quantities are further constrained by additional conditions.

- (3) Before EW symmetry breaking hypercharge is an exactly conserved quantity. Therefore for the total hypercharge of the Universe we have

$$y_{\text{tot}} = \sum_b \Delta n_b y_b + \sum_f \Delta n_f y_f = 0, \quad (5.19)$$

where $y_{b,f}$ denotes the hypercharge of the b -bosons or f -fermions. It is useful to rewrite explicitly this condition in terms of the rescaled density asymmetries per degree of freedom $\{Y_{\Delta_i}\}$ defined in eq. (5.13):

$$\sum_i (Y_{\Delta Q_i} + 2Y_{\Delta u_i} - Y_{\Delta d_i}) - \sum_\alpha (Y_{\Delta \ell_\alpha} + Y_{\Delta e_\alpha}) + Y_{\Delta \tilde{H}_u} - Y_{\Delta \tilde{H}_d} = 0. \quad (5.20)$$

- (4) When the reactions mediated by the leptons Yukawa couplings are faster than the Universe expansion rate, the following chemical equilibrium conditions are enforced:

$$\ell_\alpha - e_\alpha + \tilde{H}_d + \tilde{g} = 0, \quad (\alpha = e, \mu, \tau). \quad (5.21)$$

For $\alpha = e$ the corresponding Yukawa condition holds only as long as

$$T \lesssim 10^5(1 + \tan^2 \beta) \text{ GeV}, \quad (5.22)$$

when Yukawa reactions between the first generation left-handed $SU(2)_L$ lepton doublets ℓ_e and the right-handed singlets e are faster than the expansion [120, 131]. Note also that, as is discussed in refs. [92, 127], if the temperature is not too low lepton flavor equilibration induced by off-diagonal slepton soft masses will not occur. We assume that this is the case, and thus we take the three ℓ_α to be independent quantities.

- (5) Reactions mediated by the quarks Yukawa couplings enforce the following six chemical equilibrium conditions:

$$Q_i - u_i + \tilde{H}_u + \tilde{g} = 0, \quad (u_i = u, c, t), \quad (5.23)$$

$$Q_i - d_i + \tilde{H}_d + \tilde{g} = 0, \quad (d_i = d, s, b). \quad (5.24)$$

The up-quark Yukawa coupling maintains chemical equilibrium between the left and right handed up-type quarks up to $T \sim 2 \cdot 10^6 \text{ GeV}$. Note that when the Yukawa reactions of at least two families of quarks are in equilibrium, the mass basis is fixed for all the quarks and squarks. Intergeneration mixing then implies that family-changing charged-current transitions are also in equilibrium: $b_L \rightarrow c_L$ and $t_L \rightarrow s_L$ imply $Q_2 = Q_3$; $s_L \rightarrow u_L$ and $c_L \rightarrow d_L$ imply $Q_1 = Q_2$. Thus, up to temperatures $T \lesssim 10^{11} \text{ GeV}$, that are of the order of the charm Yukawa coupling equilibration temperature, the three quark doublets have the same chemical potential:

$$Q \equiv Q_3 = Q_2 = Q_1. \quad (5.25)$$

At higher temperatures, when only the third family is in equilibrium, we will have instead $Q \equiv Q_3 = Q_2 \neq Q_1$. Above $T \sim 10^{13}$ when (for moderate values of $\tan \beta$) also the τ and b -quark $SU(2)_L$ singlets decouple from their Yukawa reactions, all intergeneration mixing becomes negligible and $Q_3 \neq Q_2 \neq Q_1$.

5.2.2.2 Above the superequilibration temperature

Now, we will look at the condition specific for the temperature which satisfies eq. (5.4). We would like to stress that in this regime, the chemical potentials of particle ϕ and its superpartner $\tilde{\phi}$ are related by a non-vanishing gaugino chemical potential \tilde{g} as in eqs. (5.16)–(5.18). For definiteness, we fix the relevant values of the temperature around $T \sim 10^8$ GeV.

(6_{NSE}) In this regime, the reactions induced by the QCD and EW sphaleron multi-fermion operators eq. (5.7) and eq. (5.8) imply [130]⁵

$$3 \sum_i Q_i + \sum_\alpha \ell_\alpha + \tilde{H}_u + \tilde{H}_d + 4 \tilde{g} = 0, \quad (5.26)$$

$$2 \sum_i Q_i - \sum_i (u_i + d_i) + 6 \tilde{g} = 0. \quad (5.27)$$

In the above condition, we put the subscript ‘NSE’ on the numbering to emphasize that this condition applies only to the NSE regime.

At $T \sim 10^8$ GeV, Yukawa equilibrium for the up quark is never realized. For $\alpha = e$ and for the d -quark Yukawa equilibrium holds as long as $T \lesssim 10^5(1 + \tan^2 \beta)$ GeV [120, 131] and $T \lesssim 4 \cdot 10^6(1 + \tan^2 \beta)$ GeV respectively. Then, for $T \sim 10^8$ GeV both conditions hold only if $\tan \beta \gtrsim 35$, while they both do not hold if $\tan \beta \lesssim 5$. As we will discuss below, in the latter case the Yukawa equilibrium conditions get replaced by other two conditions, and thus the overall number of constraints does not change. Later in Section 5.2.3 and 5.2.4 we will present results for the large and small $\tan \beta$ cases, and since they do not differ much, we omit the corresponding results for the intermediate case $5 \lesssim \tan \beta \lesssim 35$.

Counting the number of additional conditions listed in items (3)–(5) and (6_{NSE}), we have 1 from global hypercharge neutrality, 8 from Yukawa equilibrium plus 2 due to quark intergenerational mixing, and 2 from the EW and QCD sphaleron equilibrium. This adds to a total of 13 constraints for the initial 18 variables, meaning that 5 quantities must be determined from dynamical evolution equations. These quantities can be chosen, for example, as the density-asymmetries of the three lepton flavors $Y_{\Delta \ell_\alpha}$, of the up-type higgsinos $Y_{\Delta \tilde{H}_u}$ and of the gauginos $Y_{\Delta \tilde{g}}$, where the last one allows to relate the

⁵Compare to the superequilibration sphaleron conditions (C.4) and (C.5).

previous four quantities to the corresponding densities asymmetries of their superpartners. This choice would be a natural one since these are the density asymmetries that ‘weight’ the various interactions entering the BEs for SL. However, the EW and QCD sphalerons reactions eq. (5.7) and eq. (5.8) imply fast changes of these asymmetries. A much more convenient choice is instead that of using appropriate linear combinations of the various asymmetries corresponding to anomaly free and quasi-conserved charges, where with ‘quasi-conserved’ we refer to charges that are not conserved only by the ‘slow’ sneutrino-related reactions. These quantities can be identified with the three flavored leptonic charges $B/3 - L_\alpha$ and with the two R_B and R_χ charges discussed in the previous section. In terms of the rescaled density asymmetries (asymmetry abundances) per degree of freedom they read:

$$Y_{\Delta_\alpha} = 6Y_{\Delta Q} + \sum_i (Y_{\Delta u_i} + Y_{\Delta d_i}) - 3(2Y_{\Delta\ell_\alpha} + Y_{\Delta e_\alpha}) - 2Y_{\Delta\tilde{g}}, \quad (5.28)$$

$$Y_{\Delta R_B} = -6Y_{\Delta Q} - \sum_i (13Y_{\Delta u_i} - 5Y_{\Delta d_i}) + \sum_\alpha (10Y_{\Delta\ell_\alpha} + 7Y_{\Delta e_\alpha}) + 68Y_{\Delta\tilde{g}} + 10Y_{\Delta\tilde{H}_d} - 2Y_{\Delta\tilde{H}_u}, \quad (5.29)$$

$$Y_{\Delta R_\chi} = 3(3Y_{\Delta u} - 2Y_{\Delta\tilde{g}}) + \frac{1}{3}Y_{\Delta R_3}, \quad (5.30)$$

where, in the last expression,

$$Y_{\Delta R_3} = -18Y_{\Delta Q} - 3 \sum_i (11Y_{\Delta u_i} - 4Y_{\Delta d_i}) + \sum_\alpha (16Y_{\Delta\ell_\alpha} + 13Y_{\Delta e_\alpha}) + 82Y_{\Delta\tilde{g}} + 16Y_{\Delta\tilde{H}_d} - 14Y_{\Delta\tilde{H}_u}. \quad (5.31)$$

The asymmetry abundances of the five charges in eqs. (5.28)-(5.30) then define the basis $Y_{\Delta_a} = \{Y_{\Delta_\alpha}, Y_{\Delta R_B}, Y_{\Delta R_\chi}\}$ in terms of which the five fermionic asymmetry abundances $Y_{\Delta\psi_a} = \{Y_{\Delta\ell_\alpha}, Y_{\Delta\tilde{g}}, Y_{\Delta\tilde{H}_u}\}$, that are the relevant ones for the SL processes, have to be expressed. We will do this by introducing a 5×5 A -matrix defined according to:

$$Y_{\Delta\psi_a} = A_{ab} Y_{\Delta_b}, \quad (5.32)$$

where the numerical values of A_{ab} are obtained from eqs. (5.28)-(5.30) subjected to the constraining conditions listed in items (3)–(5) and (6_{NSE}). Let us note at this point that the 3×5 submatrix $A_{\ell_\alpha b}$ for the lepton asymmetry abundances represents the generalization of the A matrix introduced in [28], $A_{\tilde{H}_u b}$ generalizes the Higgs C -vector first introduced in [27], and $A_{\tilde{g}b}$ generalizes the C -vector for the gauginos first introduced in ref. [69]. As regards the asymmetry abundances for the bosonic partners of ℓ_α and of \tilde{H}_u , they are simply given by: $A_{\tilde{\ell}_\alpha b} = 2(A_{\ell_\alpha b} + A_{\tilde{g}b})$ and $A_{H_u b} = 2(A_{\tilde{H}_u} + A_{\tilde{g}b})$.

5.2.3 Case I: Electron and down-quark Yukawa reactions in equilibrium

If the down-type Higgs vev is relatively small $v_d \ll v$, the values of the electron and down-quark masses are obtained for correspondingly large values of the h_d and h_e Yukawa couplings. For $v_u/v_d = \tan \beta \gtrsim 35$ we have a regime in which at $T \sim 10^8$ GeV, that is well above the NSE threshold eq. (5.4), both h_d and h_e related reactions are in equilibrium. In this case all the eight Yukawa conditions eqs. (5.21)-(5.23) hold. Solving for the densities-asymmetries $Y_{\Delta\psi_a} = \{Y_{\Delta\ell_\alpha}, Y_{\Delta\tilde{g}}, Y_{\Delta\tilde{H}_u}\}$ in terms of the charge-asymmetries $Y_{\Delta a} = \{Y_{\Delta\alpha}, Y_{\Delta R_B}, Y_{\Delta R_\chi}\}$ subject to the constraints in items 3 to 5, yields

$$A = \frac{1}{9 \times 827466} \begin{pmatrix} -788776 & 38690 & 38690 & -56295 & 41931 \\ 38690 & -788776 & 38690 & -56295 & 41931 \\ 38690 & 38690 & -788776 & -56295 & 41931 \\ 41913 & 41913 & 41913 & 124281 & 12798 \\ -102411 & -102411 & -102411 & 108108 & -335907 \end{pmatrix}. \quad (5.33)$$

5.2.4 Case II: Electron and down-quark Yukawa reactions out of equilibrium

If v_d is not much smaller than v_u , resulting in $\tan \beta \lesssim 5$, then both h_e and h_d are sufficiently small that at $T \sim 10^8$ GeV the related Yukawa reactions do not occur. In this case we have to set $h_d, h_e \rightarrow 0$ and the corresponding two Yukawa equilibrium conditions in eqs. (5.21)-(5.24) do not hold. However,

two conservation laws replace these conditions. $h_e \rightarrow 0$ implies that we gain a ‘chiral’ symmetry for the right-handed fermion and scalar electrons, ensuring that the total number-density asymmetry $\Delta n_e + \Delta n_{\bar{e}}$ is conserved. As usual, we assume that the constant value of this quantity vanishes, which in terms of the rescaled density asymmetries per degree of freedom implies:

$$Y_{\Delta e} - \frac{2}{3} Y_{\Delta \bar{g}} = 0. \quad (5.34)$$

For the right-handed down quark we could define an anomaly-free charge completely equivalent to $Y_{\Delta R_\chi}$ in eq. (5.30) but, given that in this regime all the dynamical equations are symmetric under the exchange $u \leftrightarrow d$, it is equivalent, and much more simple, to impose the condition

$$Y_{\Delta d} = Y_{\Delta u}. \quad (5.35)$$

The net result is that, with respect to the previous case, the total number of constraints is not changed, and again five quantities suffice to express the rescaled density asymmetries for all the fields. For the 5×5 A matrix defined in eq. (5.32) we obtain:

$$A = \frac{1}{9 \times 162332} \begin{pmatrix} -210531 & 21573 & 21573 & -12414 & 12483 \\ 8676 & -165529 & -3197 & -17958 & 29709 \\ 8678 & -3197 & -165529 & -17958 & 29709 \\ 7497 & 7299 & 7299 & 23634 & 4833 \\ -11322 & -18477 & -18477 & 23940 & -74385 \end{pmatrix}. \quad (5.36)$$

5.3 R-genesis Boltzmann Equations

In order to render clear the role played by the new charges ΔR_B and ΔR_χ and by NSE effects, in this section we introduce a simplified set of BEs including only decays and inverse decays of RHN and RHSN. However, for the numerical results that are discussed in the next section, we have used the more complete (and involved) set of equations described in Appendix B.2.6.

The evolution of the number density of the heavy states normalized to the

entropy density s is given by

$$\dot{Y}_N = - \left(\frac{Y_N}{Y_N^{eq}} - 1 \right) \gamma_N, \quad (5.37)$$

$$\dot{Y}_{\tilde{N}} = - \left(\frac{Y_{\tilde{N}_{\text{tot}}}}{Y_{\tilde{N}}^{eq}} - 2 \right) \frac{1}{2} \gamma_{\tilde{N}}, \quad (5.38)$$

where the time derivative is defined as $\dot{Y} = sH z \frac{dY}{dz}$ with $z = M/T$, and $H = H(z = 1)$ is the Hubble parameter at $T = M$. In eq. (5.37) γ_N represents the (thermal averaged) total decay width of the heavy neutrino N into particles and sparticles of all α -flavors $\gamma_N = \sum_{\alpha} \gamma_N^{\alpha}$ and Y_N^{eq} the N equilibrium abundance. For the RHSN, we denote with \tilde{N}_{tot} the sum of \tilde{N}_+ and \tilde{N}_- . Thus in eq. (5.38) $Y_{\tilde{N}_{\text{tot}}} = Y_{\tilde{N}_+} + Y_{\tilde{N}_-}$, while $Y_{\tilde{N}}^{eq}$ represents the equilibrium abundance of a single RHSN. For the reaction rates we have

$$\gamma_{\tilde{N}} = \gamma_{\tilde{N}_+} + \gamma_{\tilde{N}_-} = \sum_{p=s,f} \sum_{\alpha} \left(\gamma_{\tilde{N}_+}^{p\alpha} + \gamma_{\tilde{N}_-}^{p\alpha} \right), \quad (5.39)$$

where the p sum in the r.h.s of the last equality is over s -scalar and f -fermionic final states, while $\gamma_{\tilde{N}_+} = \gamma_{\tilde{N}_-} = \gamma_{\tilde{N}}/2$.

In writing down the evolution equations for the five charges $Y_{\Delta_{\alpha}}, Y_{\Delta_{RB}}, Y_{\Delta_{R\chi}}$ it is convenient to introduce a special notation for the scalar and fermionic asymmetry abundances (per degree of freedom) normalized to the respective equilibrium abundances $Y_s^{eq} = 2Y_f^{eq} = \frac{15}{4\pi^2 g_*}$:

$$\mathfrak{y}_{\Delta s, \Delta f} \equiv \frac{Y_{\Delta s, \Delta f}}{Y_{s, f}^{eq}}. \quad (5.40)$$

Using eqs. (5.14) and (5.13) together with (5.16) and (5.17) it is then easy to verify that

$$\mathfrak{y}_{\Delta \tilde{\ell}, \Delta H_u} = \mathfrak{y}_{\Delta \ell, \Delta \tilde{H}_u} + \mathfrak{y}_{\Delta \tilde{g}}. \quad (5.41)$$

Including only decays and inverse decays, the BEs for the flavor charge

$B/3 - L_\alpha$ asymmetries read:

$$\begin{aligned} \dot{Y}_{\Delta_\alpha} &= -\epsilon_\alpha^f(z) \left(\frac{Y_{\tilde{N}_{\text{tot}}} - 2}{Y_{\tilde{N}}^{eq}} - 2 \right) \frac{\gamma_{\tilde{N}}}{2} + (\mathcal{Y}_{\Delta\ell_\alpha} + \mathcal{Y}_{\Delta\tilde{H}_u}) \frac{\gamma_{\tilde{N}}^{f,\alpha}}{2} + (\mathcal{Y}_{\Delta\ell_\alpha} + \mathcal{Y}_{\Delta H_u}) \frac{\gamma_{\tilde{N}}^\alpha}{4} \\ &\quad - \epsilon_\alpha^s(z) \left(\frac{Y_{\tilde{N}_{\text{tot}}} - 2}{Y_{\tilde{N}}^{eq}} - 2 \right) \frac{\gamma_{\tilde{N}}}{2} + (\mathcal{Y}_{\Delta\tilde{\ell}_\alpha} + \mathcal{Y}_{\Delta H_u}) \frac{\gamma_{\tilde{N}}^{s,\alpha}}{2} + (\mathcal{Y}_{\Delta\tilde{\ell}_\alpha} + \mathcal{Y}_{\Delta\tilde{H}_u}) \frac{\gamma_{\tilde{N}}^\alpha}{4}. \end{aligned} \quad (5.42)$$

To write this expression in a more compact form, we define the total flavored CP asymmetry $\epsilon_\alpha = \epsilon_\alpha^f + \epsilon_\alpha^s$ and the total RHSN decay rate into α leptons and sleptons $\gamma_{\tilde{N}}^\alpha = \gamma_{\tilde{N}}^{f,\alpha} + \gamma_{\tilde{N}}^{s,\alpha}$. For quantities without a flavor index a sum over flavor will be understood, e.g.: $\gamma_{\tilde{N}} = \sum_\alpha \gamma_{\tilde{N}}^\alpha$ and $\epsilon_{f,s} = \sum_\alpha \epsilon_\alpha^{f,s}$. Furthermore, we can use eq. (5.41) to express the density asymmetries of the scalars in terms of the ones of the fermions, and to an excellent approximation we can write $\gamma_{\tilde{N}}^{s,\alpha} = \gamma_{\tilde{N}}^{f,\alpha 6}$. After the same notational simplifications are applied also to the BEs for $Y_{\Delta R_B}$ and $Y_{\Delta R_\chi}$, the following set is obtained:

$$\dot{Y}_{\Delta_\alpha} = -\epsilon_\alpha(z) \left(\frac{Y_{\tilde{N}_{\text{tot}}} - 2}{Y_{\tilde{N}}^{eq}} - 2 \right) \frac{\gamma_{\tilde{N}}}{2} + (\mathcal{Y}_{\Delta\ell_\alpha} + \mathcal{Y}_{\Delta\tilde{H}_u} + \mathcal{Y}_{\Delta\tilde{g}}) \frac{\gamma_{\tilde{N}}^\alpha + \gamma_{\tilde{N}}^\alpha}{2}, \quad (5.43)$$

$$\begin{aligned} \dot{Y}_{\Delta R_B} &= \epsilon^s(z) \left(\frac{Y_{\tilde{N}_{\text{tot}}} - 2}{Y_{\tilde{N}}^{eq}} - 2 \right) \gamma_{\tilde{N}} \\ &\quad - \sum_\alpha (\mathcal{Y}_{\Delta\ell_\alpha} + \mathcal{Y}_{\Delta\tilde{H}_u} + \mathcal{Y}_{\Delta\tilde{g}}) \frac{\gamma_{\tilde{N}}^\alpha + \gamma_{\tilde{N}}^\alpha}{2} - \mathcal{Y}_{\Delta\tilde{g}} \frac{\gamma_{\tilde{N}}}{2}, \end{aligned} \quad (5.44)$$

$$\dot{Y}_{\Delta R_\chi} = [\epsilon^s(z) - \epsilon^f(z)] \left(\frac{Y_{\tilde{N}_{\text{tot}}} - 2}{Y_{\tilde{N}}^{eq}} - 2 \right) \frac{\gamma_{\tilde{N}}}{6} - \mathcal{Y}_{\Delta\tilde{g}} \frac{\gamma_{\tilde{N}}}{6}. \quad (5.45)$$

It is possible, and formally straightforward, to add to these equations the appropriate terms that allow to extend their validity also in the SE regime, that is for sneutrino masses below the bound eq. (5.1). In order to do this, we denote by $\gamma_{\tilde{g}}^{\text{eff}}$ the set of gaugino-mediated reactions with chirality flip on the gaugino line that are responsible for processes that equilibrate particle-sparticle chemical potentials.⁷ We also denote by $\gamma_{\mu_{\tilde{H}}}^{\text{eff}}$ the set of reactions

⁶For $M \sim 10^8$ GeV, the soft terms corrections to this approximation $\gamma_{\tilde{N}}^s/\gamma_{\tilde{N}}^f - 1 = (A^2 - AB)/M^2$ can be safely neglected.

⁷Ref. [66] included a similar term γ_{MSSM} in the BEs for supersymmetric leptogenesis, corresponding to the thermally averaged cross section for the photino mediated process $e + e \leftrightarrow \tilde{e} + \tilde{e}$ computed in [132]. However, in the total cross section the only contributions

induced by the higgsino mixing parameter μ that enforce the chemical equilibrium condition $\tilde{H}_u + \tilde{H}_d = 0$. The thermally averaged rates for these reactions can be written in an approximated form as:

$$\frac{\gamma_{\tilde{g}}^{\text{eff}}}{n_f^{\text{eq}}} = \frac{m_{\tilde{g}}^2}{T}, \quad \frac{\gamma_{\mu_{\tilde{H}}}^{\text{eff}}}{n_f^{\text{eq}}} = \frac{\mu^2}{T}, \quad (5.46)$$

where n_f^{eq} is the equilibrium number density for one fermionic degree of freedom, while $m_{\tilde{g}}$ and μ in these equations have to be understood as effective mass parameters in which all coupling constants as well as reaction multiplicities are reabsorbed. Extension of the validity of eqs. (5.43)-(5.45) to the SE domain is then achieved by adding the following terms to the equations for R_B and R_χ :

$$\dot{Y}_{\Delta R_B}^{SE} = \left\{ \dot{Y}_{\Delta R_B} \right\} - \mathcal{Y}_{\Delta \tilde{g}} \gamma_{\tilde{g}}^{\text{eff}}, \quad (5.47)$$

$$\dot{Y}_{\Delta R_\chi}^{SE} = \left\{ \dot{Y}_{\Delta R_\chi} \right\} - \frac{1}{3} \mathcal{Y}_{\Delta \tilde{g}} \gamma_{\tilde{g}}^{\text{eff}} + \frac{1}{3} \left(\mathcal{Y}_{\Delta \tilde{H}_u} + \mathcal{Y}_{\Delta \tilde{H}_d} \right) \gamma_{\mu_{\tilde{H}}}^{\text{eff}}, \quad (5.48)$$

where the $\left\{ \dot{Y}_{\Delta R} \right\}$ above stand for the r.h.s of the corresponding equations (5.44) and (5.45). Note that since the R_B charge of the μ term is $R_B(H_u H_d) = 2$, μ conserves R_B and accordingly there is no term proportional to $\gamma_{\mu_{\tilde{H}}}^{\text{eff}}$ in eq. (5.47). Since higgsino equilibration involves also the density asymmetry $\mathcal{Y}_{\Delta \tilde{H}_d}$ we give below the corresponding C vectors to express it in terms of the basis of the charge-asymmetries:

$$\text{Case I : } C^{\tilde{H}_d} = \frac{1}{827466} (14237, 14237, 14237, 1260, -3915), \quad (5.49)$$

$$\text{Case II : } C^{\tilde{H}_d} = \frac{1}{3 \times 162332} (12469, 16768, 16768, 7056, -21924). \quad (5.50)$$

We have of course checked that by increasing the values of $m_{\tilde{g}}$ and μ , the results of integrating the set of BEs given by eq. (5.43) and eqs. (5.47)-(5.48) converge to the solutions of the usual BEs for the SE regime (see Appendix B.2.5).

that do not vanish in the $m_{\tilde{\gamma}} \rightarrow 0$ limit are those that, like e.g. $e_L^- + e_R^- \leftrightarrow \tilde{e}_L + \tilde{e}_R$, do not enforce SE. Superequilibrating reactions like $e_L^- + e_L^- \leftrightarrow \tilde{e}_L + \tilde{e}_L$ all vanish in the $m_{\tilde{\gamma}} \rightarrow 0$ limit.

5.3.1 NSE Regime: R-genesis in a simple case

To highlight the role played by the asymmetries of the two R charges, let us define a simple scenario, in which lepton flavor effects play basically no role and thus do not shadow the new effects. This scenario is defined by the following two conditions:

- We assume equal branching fractions for the decays of N and of \tilde{N}_\pm into the three lepton flavors, that is the P_α defined in eq. (2.40) are all equal to $\frac{1}{3}$ implying $\epsilon_\alpha = \frac{1}{3}\epsilon$ and $\gamma_{N,\tilde{N}}^\alpha = \frac{1}{3}\gamma_{N,\tilde{N}}$.
- We assume the regime described in Case I, Section 5.2.3, in which the Yukawa equilibrium condition for the electron holds, and thus the three lepton flavors are all treated on equal footing (see the 3×3 upper-left corner in the A -matrix eq. (5.33)). Given the previous condition, it is then useful to define a ‘flavor averaged’ lepton asymmetry as:

$$y_{\Delta\ell} = \frac{1}{3} \sum_{\alpha} y_{\Delta\ell_\alpha} \quad (5.51)$$

With these conditions, the three equations for the flavor charges eq. (5.43) can be resummed in closed form into a single equation for $B - L$ asymmetry:

$$\dot{Y}_{\Delta_{B-L}} = -\epsilon(z) \left(\frac{Y_{\tilde{N}_{\text{tot}}}}{Y_{\tilde{N}}^{\text{eq}}} - 2 \right) \frac{\gamma_{\tilde{N}}}{2} + (y_{\Delta\ell} + y_{\Delta\tilde{H}_u} + y_{\Delta\tilde{g}}) \frac{\gamma_N + \gamma_{\tilde{N}}}{2}, \quad (5.52)$$

yielding a reduced set of just 3 BEs. The 3×3 matrix relating $\{Y_{\Delta\ell}, Y_{\Delta\tilde{g}}, Y_{\Delta\tilde{H}_u}\}$ to the three charge-asymmetries $\{Y_{\Delta_{B-L}}, Y_{\Delta_{R_B}}, Y_{\Delta_{R_\chi}}\}$ can be readily evaluated from eq. (5.33):

$$A = \frac{1}{827466} \begin{pmatrix} -26348 & -6255 & 4659 \\ 4657 & 13809 & 1422 \\ -11379 & 12012 & -37323 \end{pmatrix}. \quad (5.53)$$

It is now easy to see that in the NSE regime we can rewrite the BEs as

$$\dot{Y}_{\Delta_{B-L}} = 3\dot{Y}_{\Delta_{R_\chi}} - \dot{Y}_{\Delta_{R_B}}, \quad (5.54)$$

$$\begin{aligned} \dot{Y}_{\Delta_{R_B}} &= \epsilon^s(z) \left(\frac{Y_{\tilde{N}_{\text{tot}}}}{Y_{\tilde{N}}^{\text{eq}}} - 2 \right) \gamma_{\tilde{N}} \\ &\quad - (\mathcal{Y}_{\Delta_\ell} + \mathcal{Y}_{\Delta_{\tilde{H}_u}} + \mathcal{Y}_{\Delta_{\tilde{g}}}) \frac{\gamma_N + \gamma_{\tilde{N}}}{2} - \mathcal{Y}_{\Delta_{\tilde{g}}} \frac{\gamma_{\tilde{N}}}{2}, \end{aligned} \quad (5.55)$$

$$\dot{Y}_{\Delta_{R_\chi}} = [\epsilon^s(z) - \epsilon^f(z)] \left(\frac{Y_{\tilde{N}_{\text{tot}}}}{Y_{\tilde{N}}^{\text{eq}}} - 2 \right) \frac{\gamma_{\tilde{N}}}{6} - \mathcal{Y}_{\Delta_{\tilde{g}}} \frac{\gamma_{\tilde{N}}}{6}, \quad (5.56)$$

since the difference in the r.h.s. of eq. (5.54) gives precisely eq. (5.52). Eq. (5.54) makes apparent how $Y_{\Delta_{R_\chi}}$ and $Y_{\Delta_{R_B}}$, that in the $T \rightarrow 0$ limit keep having non vanishing CP asymmetries, are sources of the $B-L$ asymmetry. This result is in fact completely general: the only role of the two conditions listed above is simply that of allowing to collapse the three equations for Δ_α into a single one for Δ_{B-L} , while maintaining the BEs in closed form. In particular, it holds also when scattering processes are included (see Appendix B.2.6) and independently of the particular NSE temperature regime (e.g. Case I and Case II) and flavor configuration. In short, in the NSE regime the evolution of Δ_{B-L} can be always obtained from the evolution of $3\Delta_{R_\chi} - \Delta_{R_B}$, and the final value of $Y_{\Delta_{B-L}}$ can be equally well obtained from summing the values of the flavor charges asymmetries $\sum_\alpha Y_{\Delta_\alpha}$ or from the final value of $3Y_{\Delta_{R_\chi}} - Y_{\Delta_{R_B}}$. The reason why this happens is simple: by using the definitions eqs. (5.9)-(5.10) together with eqs. (5.5)-(5.6) one obtains that $3R_\chi - R_B = \chi_{u_L^c} - \frac{2}{3}B - PQ$. Of course, only the PQ fragment of this charge is violated in sneutrinos interactions, and from Table 5.1 we see that this violation is precisely the same as for $B-L$ (e.g. for $\tilde{N} \rightarrow \ell \tilde{H}_u$ we have $\Delta(B-L) = -\Delta L = -\Delta(PQ) = -1$). Thus, regardless of the fact that $B-L$, R_B and R_χ are all independent charges, in the NSE regime the BE for $3Y_{\Delta_{R_\chi}} - Y_{\Delta_{R_B}}$ will always coincide with the BE for $Y_{\Delta_{B-L}} = \sum_\alpha Y_{\Delta_\alpha}$.

In our particularly simple case we can take a further step. Let us rewrite the density asymmetry $\mathcal{Y}_{\Delta_{\tilde{g}}}$ and the combination $(\mathcal{Y}_{\Delta_\ell} + \mathcal{Y}_{\Delta_{\tilde{H}_u}} + \mathcal{Y}_{\Delta_{\tilde{g}}})$ in the r.h.s of eqs. (5.55)-(5.56) in terms of $Y_{\Delta_{B-L}}$, $Y_{\Delta_{R_B}}$, $Y_{\Delta_{R_\chi}}$ by means of the A matrix Eq. (5.53). We can then replace $Y_{\Delta_{B-L}} \rightarrow 3Y_{\Delta_{R_\chi}} - Y_{\Delta_{R_B}}$ and, by using

$\gamma_N = \gamma_{\tilde{N}}$ we obtain:

$$3\dot{Y}_{\Delta R_\chi} = [\epsilon^s(z) - \epsilon^f(z)] \left(\frac{Y_{\tilde{N}_{\text{tot}}}}{Y_{\tilde{N}}^{\text{eq}}} - 2 \right) \frac{\gamma_{\tilde{N}}}{2} - \frac{1}{827466} (9152 Y_{\Delta R_B} + 15393 Y_{\Delta R_\chi}) \frac{\gamma_{\tilde{N}}}{2}, \quad (5.57)$$

$$\dot{Y}_{\Delta R_B} = 2 \epsilon^s(z) \left(\frac{Y_{\tilde{N}_{\text{tot}}}}{Y_{\tilde{N}}^{\text{eq}}} - 2 \right) \frac{\gamma_{\tilde{N}}}{2} - \frac{1}{827466} (114424 Y_{\Delta R_B} - 245511 Y_{\Delta R_\chi}) \frac{\gamma_{\tilde{N}}}{2}. \quad (5.58)$$

These two equations show that although the asymmetries produced in the two charges $3R_\chi$ and R_B tend to cancel at $T = 0$ when taking the difference, their respective washouts are quite different, and such a cancellation will never occur. In the general case flavor dynamics does not allow to collapse the set of BEs to just two equations, but still the same mechanism is at work: because of the different washouts, the difference between $3Y_{\Delta R_\chi}$ and $Y_{\Delta R_B}$ becomes of the same order of these density asymmetries, and so does $Y_{\Delta B-L}$. Perhaps surprisingly, we can then expect that by increasing the washouts from a strength of order weak up to (not too) large strengths, the final value of $B-L$ will increase. The numerical results in the next section confirm this picture.

In the SE regime instead, things proceed in a different way. Eqs. (5.47)-(5.48) show that the BEs for $Y_{\Delta R_\chi}$ and $Y_{\Delta R_B}$ acquire new washout terms, that are proportional to the SE rates, while on the contrary no analogous terms enter the BE for Y_{Δ_α} eq. (5.43) or for $Y_{\Delta_{B-L}}$ eq. (5.52). Thus, in the SE regime, eq. (5.54) does not hold. One can argue instead that, because of the SE washouts, the roles of Δ_{B-L} and of $3\Delta R_\chi - \Delta R_B$ get reversed, since now we have

$$3\dot{Y}_{\Delta R_\chi} - \dot{Y}_{\Delta R_B} = \dot{Y}_{\Delta_{B-L}} + \left(\mathfrak{y}_{\Delta \tilde{H}_u} + \mathfrak{y}_{\Delta \tilde{H}_d} \right) \gamma_{\mu_{\tilde{H}}}^{\text{eff}}. \quad (5.59)$$

In other words, since SE reactions conserve $B-L$ but violate the R and PQ charges, the only source of asymmetry surviving SE is the (thermally induced) $Y_{\Delta_{B-L}}$ asymmetry. Given that ΔR_χ and ΔR_B both contain ‘fragments’ that carry B number, they do not vanish in the SE limit, but are driven to values that are proportional to Δ_{B-L} . The constants of proportionality are determined by the chemical equilibrium and conservation law conditions ap-

appropriate for the specific regime and, for example, in Case I are given by $Y_{\Delta R_B} = -\frac{1}{3}Y_{\Delta B-L}$ and $Y_{\Delta R_\chi} = -\frac{3}{79}Y_{\Delta B-L}$.

5.4 Results

In this section we quantify the results that are obtained for the baryon asymmetry yield of SL when the effective theory described in the previous sections is used, and we confront them with what is obtained in the standard scenario, in which SE is assumed to hold at all temperatures. Our results are obtained by numerical integration of the BEs given in Appendix B.2.6 that also include various scattering processes. The comparative results for the SE case can be obtained in two formally different, but physically equivalent, ways. A first possibility is that of taking the limit $m_{\tilde{g}}, \mu \rightarrow \infty$ in the complete BEs (given, for example, in their basic form in eqs. (5.47)-(5.48)). A second possibility, that corresponds to usual treatments, is to solve only the three equations for the flavor charge-density asymmetries Y_{Δ_α} with the corresponding A matrix and C vectors obtained under the assumption of SE. For the two cases we are analyzing: Case I ($h_{e,d}$ Yukawa equilibrium) and Case II ($h_{e,d}$ Yukawa non-equilibrium), we give the corresponding matrices assuming SE in Appendix C in eqs. (C.8) and (C.10). Of course, we have verified that both procedures yield the same results.

Some of our results are presented in terms of an efficiency parameter η defined according to:

$$\eta \equiv \left| \frac{Y_{\Delta B-L}(z \rightarrow \infty)}{2 \bar{\epsilon} Y_{\tilde{N}}^{\text{eq}}(z \rightarrow 0)} \right|, \quad (5.60)$$

where $\bar{\epsilon}$ is defined in eq. (2.115) where for definiteness, we only consider the UTS scenario (Section 4.4.1) and only the CP asymmetry from mixing $\bar{\epsilon} = \bar{\epsilon}^S$ eq. (2.45). To single out the new effects that we want to quantify, all our results are obtained assuming a configuration of flavor equipartition, with all the flavor branching fractions eq. (2.40) equal: $P_\alpha = \frac{1}{3}$, so that flavor effects are basically switched off⁸. In all cases, the heavy sneutrino mass is held fixed at $M = 10^8$ GeV, that is above the temperature threshold for the validity of

⁸Notice that in this flavor equipartition scenario, both UTS and SMS scenarios discussed in Section 4.2.2 are the same.

the effective theory eq. (5.4). The values of the other relevant parameters are: $A = 1 \text{ TeV}$, $\phi_A = \frac{\pi}{2}$ and $\bar{\epsilon} = \frac{A}{M} = 10^{-5}$ that corresponds to a resonantly enhanced CP asymmetry in mixing $\bar{\epsilon}^S$ eq. (2.45). This is obtained for $2B \sim \Gamma \sim 2.6 \left(\frac{m_{\text{eff}}}{0.1 \text{ eV}}\right) \text{ GeV}$. As regards gaugino mass dependent contributions to the CP asymmetries from vertex corrections: $\bar{\epsilon}^V$ eq. (2.46) and $\bar{\epsilon}^I$ (2.47), they are suppressed by additional powers of Λ_{susy}/M . Given the large value of M that we are using, they remain irrelevant even in the cases labeled as the “ $m_{\tilde{g}} \rightarrow \infty$ limit”, since in practice $m_{\tilde{g}} \approx 10 \text{ TeV}$ is more than sufficient to enforce SE, and this is the value we are effectively using. Therefore, in our regime $\bar{\epsilon}$ is essentially determined only by CP violation in mixing.

We plot in Figure 5.2 the evolution of $Y_{\Delta_{B-L}}$ with increasing $z = M/T$. The solid (red) lines correspond to the full results obtained in the $m_{\tilde{g}}, \mu \rightarrow 0 \text{ GeV}$ limit, that is when particle-particle superequilibrating processes are completely switched off. The dashed (blue) lines give the results obtained in the same limit, but when all thermal corrections to the CP asymmetries are neglected, and $\epsilon^s = -\epsilon^f = \bar{\epsilon}/2$. From all the four panels we see that in the NSE regime neglecting thermal corrections is an excellent approximation that reproduces with very good accuracy the (sizable) final values of $Y_{\Delta_{B-L}}$. The dotted (black) lines give $Y_{\Delta_{B-L}}$ in the usual treatments which includes thermal corrections and also assumes SE, that in our treatment corresponds to taking the limit $m_{\tilde{g}}, \mu \rightarrow \infty$. Panels on the left side refer to Case I discussed in Section 5.2.3, panels on the right side are for Case II discussed in Section 5.2.4. We can see that the differences between the situations in which the $h_{e,d}$ Yukawa reactions are in equilibrium and when they are out of equilibrium are rather mild. Therefore in the following we will concentrate just on results for Case I. Upper and lower panels correspond instead to two different strength for the washout processes, parameterized respectively by $m_{\text{eff}} = 0.05 \text{ eV}$ and $m_{\text{eff}} = 0.20 \text{ eV}$. As it was expected from the analysis in the previous section, we see that the stronger the washouts, the larger is the gain in efficiency with respect to the SE scenario.

In Figure 5.3 we plot for Case I the efficiency η defined in eq. (5.60) as a function of the washout parameter m_{eff} . The red continuous line corresponds to $m_{\tilde{g}} = \mu = 100 \text{ GeV}$. We have chosen a non-zero value for these parameters because of phenomenological motivations, however we have checked that the re-

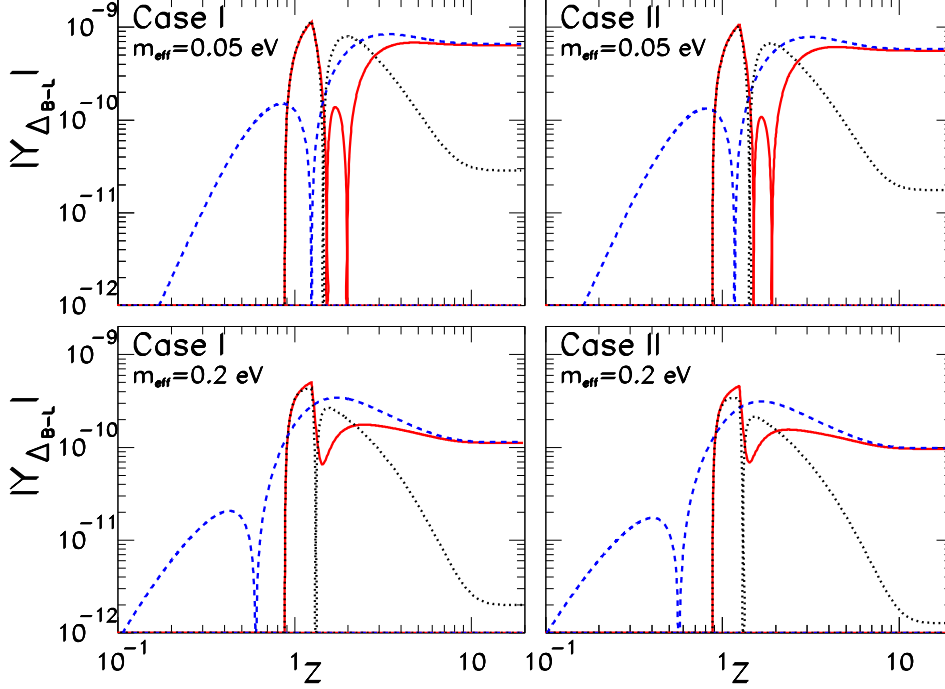


Figure 5.2: Evolution of $Y_{\Delta_{B-L}}$. The solid continuous (red) line depict the complete results in the $m_{\tilde{g}} = \mu \rightarrow 0$ limit. The dashed (blue) line correspond to the same limit but with all thermal corrections to the CP asymmetries neglected. The dotted (black) line gives $Y_{\Delta_{B-L}}$ with thermal effects when SE is assumed. Panels on the left and right sides are respectively for Case I ($h_{e,d}$ Yukawa equilibrium) and Case II ($h_{e,d}$ Yukawa non-equilibrium). Upper and lower panels are respectively for $m_{\text{eff}} = 0.05$ eV and $m_{\text{eff}} = 0.20$ eV.

sults are practically indistinguishable from those obtained in the $m_{\tilde{g}} = \mu \rightarrow 0$ limit and thus, in agreement with eq. (5.4), the evolution still occurs in the full NSE regime. The red dash-dotted line corresponds to $m_{\tilde{g}} = \mu = 500$ GeV. We can see that in this case SE rates start suppressing the efficiency, but are still far from attaining full thermal equilibrium. The black dotted line corresponds to the $m_{\tilde{g}}, \mu \rightarrow \infty$ limit of complete SE. We see that if SE is incorrectly assumed in temperature ranges where it does not occur, one could vastly underestimate the leptogenesis efficiency. The size of this underestimation is a fast increasing function of the washouts, and for particularly large

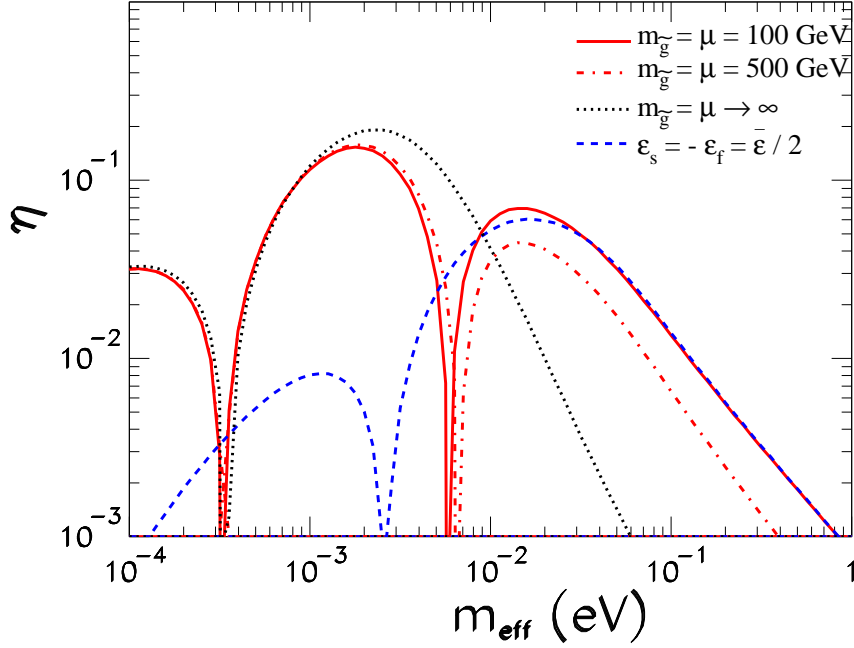


Figure 5.3: Efficiency factor η as a function of the washout parameter m_{eff} for Case I ($h_{e,d}$ Yukawa equilibrium) and different values of $m_{\tilde{g}} = \mu$. The red continuous line corresponds to the $m_{\tilde{g}} = \mu = 100$ GeV which is still in the full NSE regime, while the dashed blue line to the same limit but with thermal corrections neglected. The red dash-dotted line corresponds respectively to $m_{\tilde{g}} = \mu = 500$ GeV, and the black dotted line to SE with $m_{\tilde{g}}, \mu \rightarrow \infty$.

values of m_{eff} can reach the two orders of magnitude level. Let us also note that for $m_{\text{eff}} \gtrsim 6 \times 10^{-3}$ eV, the assumption of SE results in a baryon asymmetry of the wrong sign. Graphically, one can see this from the fact that at small values of m_{eff} the black dotted and red dash-dotted and continuous lines approximately overlap, and then change sign around $m_{\text{eff}} \sim 3 \times 10^{-4}$ eV. But around $m_{\text{eff}} \sim 6 \times 10^{-3}$ eV for the red dash-dotted and continuous lines there is another sign change. This marks the onset of R -genesis domination; therefore, from this point onward, baryogenesis does not proceed through leptogenesis, but rather through R -genesis.

In the same figure we have also plotted with the dashed blue continuous line

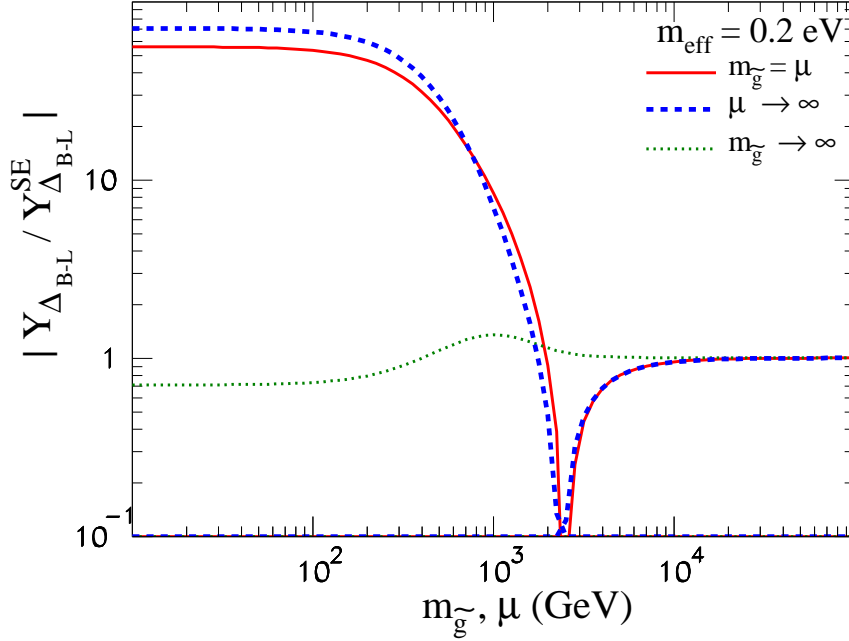


Figure 5.4: The final value of $Y_{\Delta_{B-L}}$ normalized to the SE result $Y_{\Delta_{B-L}}^{SE}$ as a function of $m_{\tilde{g}}$ and μ for Case I ($h_{e,d}$ Yukawa equilibrium) and $m_{\text{eff}} = 0.20$ eV. The red continuous line corresponds to varying simultaneously both parameters holding $m_{\tilde{g}} = \mu$. The blue dashed line corresponds to varying only $m_{\tilde{g}}$ in the limit $\mu \rightarrow \infty$. The green dotted line corresponds to varying only μ in the limit $m_{\tilde{g}} \rightarrow \infty$.

the NSE results in the approximation of neglecting all thermal corrections to the CP asymmetries. By comparing with the full results (red continuous line) we see that for $m_{\text{eff}} \gtrsim \text{few} \times 10^{-2}$ eV thermal corrections give negligible effects. We conclude that in the case of R -genesis, the zero temperature approximation yields quite reliable results.

In Figure 5.4 we plot the final value of $Y_{\Delta_{B-L}}$ as a function of different values of $m_{\tilde{g}}$ and μ , normalized for convenience to the value $Y_{\Delta_{B-L}}^{SE}$ obtained when SE is assumed. The results correspond again to Case I discussed in Section 5.2.3. In order to enhance the impact of the new effects, we have fixed the washout parameter to a rather large value $m_{\text{eff}} = 0.20$ eV. The red continuous line

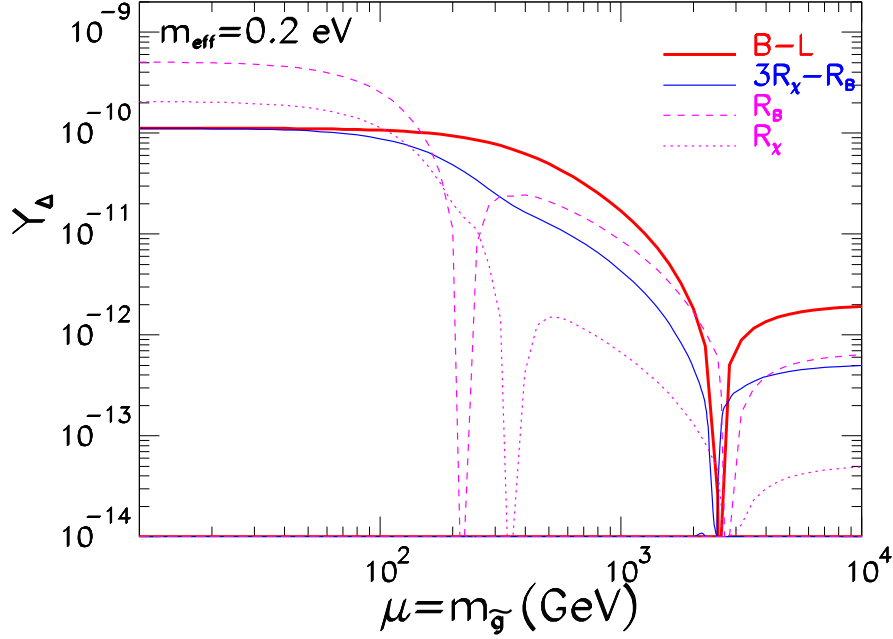


Figure 5.5: Final values of the charge density asymmetries as a function of $m_{\tilde{g}} = \mu$ for Case I ($h_{e,d}$ Yukawa equilibrium) and $m_{\text{eff}} = 0.20$ eV. Thick red line: $Y_{\Delta_{B-L}}$; thick blue line: $3Y_{\Delta_{R_x}} - Y_{\Delta_{R_B}}$; thin dashed purple line: $Y_{\Delta_{R_B}}$; thin dotted purple line: $Y_{\Delta_{R_x}}$.

corresponds to varying simultaneously both SE parameters keeping their values equal: $m_{\tilde{g}} = \mu$. We see that for $m_{\tilde{g}} = \mu \lesssim 1$ TeV the amount of $B - L$ asymmetry produced by SL can be up to two orders of magnitude larger (and of the opposite sign) with respect to what would be obtained in the usual approach with SE. SE effects start suppressing the asymmetry around $m_{\tilde{g}} = \mu \sim 1$ TeV. The asymmetry then changes sign around 3 TeV, that marks the transition from the R -genesis to the leptogenesis regime, and eventually around 5 TeV SE reactions attain complete thermal equilibrium and $Y_{\Delta_{B-L}}/Y_{\Delta_{B-L}}^{SE} \rightarrow 1$. It can be of some interest knowing what happens if only one of the two anomalous symmetries $U(1)_R$ or $U(1)_{PQ}$ were present. While we have not constructed such theories, our BEs are sufficiently general to allow exploring numerically also these cases. The corresponding results are also depicted in

Figure 5.4. The blue dashed line corresponds to the $U(1)_R$ -theory where $m_{\tilde{g}}$ is varied while $U(1)_{PQ}$ is broken.⁹ The green dotted line corresponds to the alternative $U(1)_{PQ}$ -theory in which $m_{\tilde{g}} \rightarrow \infty$ and only μ is varied. From these results we see that the real responsible of the large effects is the R -symmetry, while the effects of the PQ symmetry remains qualitatively more at the level of typical spectator effects. A theoretical justification of this behavior is not difficult to find, and we will discuss it in the following concluding section.

Some important aspects of the transition from R -genesis (NSE regime) to leptogenesis (SE regime) are highlighted in Figure 5.5, where we plot the final value of the relevant charge density-asymmetries as a function of $m_{\tilde{g}} = \mu$, assuming Case I and $m_{\text{eff}} = 0.20 \text{ eV}$. The thick solid red line corresponds to $Y_{\Delta_{B-L}}$, while the thin solid blue line corresponds to $3Y_{\Delta_{R_\chi}} - Y_{\Delta_{R_B}}$. The thin dashed and dotted purple lines display respectively $Y_{\Delta_{R_B}}$ and $Y_{\Delta_{R_\chi}}$. We see that up to $m_{\tilde{g}} = \mu \sim 100 \text{ GeV}$ we have $Y_{\Delta_{B-L}} \simeq 3Y_{\Delta_{R_\chi}} - Y_{\Delta_{R_B}}$ that is in agreement with Eq. (5.54), and thus implies that baryogenesis occurs almost only via R -genesis. As the soft SUSY-breaking parameters are increased, SE reactions begin to wash out efficiently $Y_{\Delta_{R_B}}$ and $Y_{\Delta_{R_\chi}}$ but the difference $3Y_{\Delta_{R_\chi}} - Y_{\Delta_{R_B}}$ still remains of the order of $Y_{\Delta_{B-L}}$, and R -genesis still gives the dominant contribution to baryogenesis.

Around $m_{\tilde{g}} = \mu \sim 3 \text{ TeV}$ all the charge asymmetries change simultaneously their sign. This is the benchmark of the onset of the regime in which leptogenesis dominates. The only relevant source for generating the density-asymmetries is now the (opposite-sign) thermally induced $B - L$ asymmetry, that is not affected by SE washouts, and that is feeding (small) asymmetries into all the other charges. In this regime $Y_{\Delta_{R_B}}$ and $Y_{\Delta_{R_\chi}}$ do not have anymore an independent dynamics, and can be simply computed in terms of $Y_{\Delta_{B-L}}$ yielding $Y_{\Delta_{R_B}} = -\frac{1}{3}Y_{\Delta_{B-L}}$ and $Y_{\Delta_{R_\chi}} = -\frac{3}{79}Y_{\Delta_{B-L}}$.

5.5 Discussion and Conclusions

In this chapter we have pointed out that in the temperature regime quantified by eq. (5.4), in which all reactions that depend on the soft gaugino masses

⁹Note that since μ breaks both symmetries, the case of the $U(1)_R$ -theory is somewhat academic. We include it to put in evidence the fundamental role of $U(1)_R$ in enhancing the baryon asymmetry.

do not occur, the early Universe effective theory includes a new R -symmetry. In SL, this R -symmetry is violated in the out of equilibrium interactions of neutrinos and sneutrinos. In particular, R -number CP asymmetries in heavy sneutrino decays can be defined, and constitute important quantities. In fact, given that R -symmetries do not commute with supersymmetry transformations, it is hardly surprising that no cancellation occurs between the R -number CP asymmetries for scalars and fermions. For this reason, a sizable density asymmetry for the R charge can develop in the thermal bath, and this asymmetry turns out to be the main responsible for the generation of the baryon asymmetry.

To keep higgsinos sufficiently light, in SUSY one needs to assume $\mu \sim m_{\tilde{g}}$, and thus when the gaugino masses are set to zero, one must set $\mu \rightarrow 0$ as well. In this limit the effective theory acquires another quasi-conserved global symmetry, that is a $U(1)_{PQ}$ symmetry of the Peccei-Quinn type. PQ is also violated in sneutrino interactions and thus it also has an associated CP asymmetry. However, since $U(1)_{PQ}$ is a bosonic symmetry that commutes with SUSY, the same cancellation between fermion/boson CP asymmetries occurring for lepton number also occurs for PQ . Accordingly, PQ does not play an equivalently important role in the generation of the baryon asymmetry.

In order to make more understandable the previous two remarks, let us start from the beginning, by listing the relevant global symmetries of the effective theory. For simplicity we concentrate on Case I ($h_{e,d}$ Yukawa equilibrium). Neglecting lepton flavor, that is irrelevant for the present discussion, these symmetries are: L , R , PQ , B and χ_{u^c} . The first three L , R , PQ are violated perturbatively in the interactions of the heavy sneutrinos, and all five symmetries are violated by non-perturbative sphaleron processes. In this paper, in carrying out our analysis, we have first identified the anomaly free combinations of the five charges, that are $B-L$, R_B and R_χ , and then we have written down the BEs to describe their evolution. Here, we want to sketch a different procedure. We first write a set of evolution equations for the five anomalous charges, that have the form:

$$\dot{Y}_{\Delta_Q} = \mathcal{S}_{\Delta_Q} + \mathcal{G}_{\Delta_Q} + \mathcal{G}_{\Delta_Q}^{NP}. \quad (5.61)$$

In this equation \mathcal{S} represent the source term for Y_{Δ} , \mathcal{G} is the (s)neutrino-related

washouts with all density-asymmetries and signs absorbed, and \mathcal{G}^{NP} represents the non-perturbative EW and/or QCD sphaleron reactions that violate Δ_Q . The latter are reactions of type (i), that is fast processes, that eventually will be convenient to eliminate in favor of chemical equilibrium conditions. Now, given that B and $\chi_{u_L^c}$ are good symmetries at the perturbative level, they have no CP-violating source term and $\mathcal{S}_{\Delta_B}, \mathcal{S}_{\Delta_\chi} = 0$ (they also do not have perturbative washouts, and $\mathcal{G}_{\Delta_B} \mathcal{G}_{\Delta_\chi} = 0$ too). The only source terms thus are $\mathcal{S}_{\Delta_L}, \mathcal{S}_{\Delta_{PQ}}$ and \mathcal{S}_{Δ_R} . However, as we already know, in the $T \rightarrow 0$ limit, for \mathcal{S}_{Δ_L} we have a cancellation between the fermion and scalar contributions: $\mathcal{S}_{\Delta_L}^f + \mathcal{S}_{\Delta_L}^s \rightarrow 0$. This straightforwardly implies that $\mathcal{S}_{\Delta_{PQ}}^f + \mathcal{S}_{\Delta_{PQ}}^s \rightarrow 0$ too, since the sneutrino processes contributing to the CP asymmetry for PQ are the same as for L : they are simply multiplied by the appropriate PQ charge that is, however, the same for fermion and scalar final states. For the R charge we have instead $\mathcal{S}_{\Delta_R} \propto R_f \cdot \mathcal{S}_{\Delta_L}^f + R_s \cdot \mathcal{S}_{\Delta_L}^s$, where $R_{f,s}$ are respectively the overall R -charges of the fermion and boson *two particle* final state, and thus satisfy $R_s = R_f + 2$. We then straightforwardly obtain that in the $T \rightarrow 0$ limit the R -charge source term does not vanish, and is given by $\mathcal{S}_{\Delta_R} \rightarrow 2\mathcal{S}_{\Delta_L}^s$. Fast in-equilibrium sphaleron processes enforce equilibrium conditions between particle densities carrying R charge, and those carrying a B and L numbers and, as a result, eventually baryon and lepton asymmetries roughly of the same order than the R charge-asymmetry develop. Eventually, with the decreasing of the temperature, gaugino mass related reactions will start occurring with in-equilibrium rates erasing any asymmetry in the R charge. It is important to notice that when the R -symmetry gets explicitly broken, generalized EW sphalerons reduce to the standard EW sphalerons and sphaleron induced multi-fermion operators decouple from gauginos,¹⁰ and reduce to their standard $B + L$ violating form. Since gaugino mass reactions as well as all other MSSM processes conserve $B - L$, the asymmetry initially generated through R -genesis will remain unaffected.

Now that we have identified where the large density asymmetries come from, we can complete our procedure by constructing suitable linear combinations of the five equations (5.61) for which the sphaleron terms \mathcal{G}^{NP} cancel

¹⁰We are concentrating here on the role and fate of the R -symmetry. However, given that eventually also the PQ symmetry gets explicitly broken, higgsinos decouple from sphalerons as well.

out. Since there are only two such terms, \mathcal{G}_{EW}^{NP} and \mathcal{G}_{QCD}^{NP} , we can construct three linear combinations in which only processes of type (iii) enter. These are the BEs for the three anomaly free charges that have been discussed at length in Section 5.2.1. The equilibrium conditions enforced by \mathcal{G}_{EW}^{NP} and \mathcal{G}_{QCD}^{NP} have to be imposed on the system, and to obtain the BEs in closed form, the various density-asymmetries appearing in the washout terms \mathcal{G} must be rotated into the densities of the anomaly free charges by means of the appropriate A matrix.

In this study, we have not formulated possible alternative effective theories in which for example only $\mu = 0$ is set to zero, that would correspond to an $U(1)_{PQ}$ -theory, or the alternative case of having just an $U(1)_R$ -theory. However, we have written down a set of BEs that are sufficiently general to allow exploring numerically the outcome of such scenarios. The corresponding results are resumed in Figure 5.4, and confirm the crucial role played by the R symmetry. In contrast, the effects ascribable to the new PQ symmetry arising in the $\mu \rightarrow 0$ limit, that as we have seen are not related with any new large CP violating source, remain of the typical size of spectator effects.

Chapter 6

Conclusions and Outlook

The matter-antimatter asymmetry of the Universe is one of the issues that the current Standard Model of particle physics cannot accommodate. While the supersymmetrized version of the type I seesaw has the virtue of having stable Higgs mass under radiative corrections, accommodating small active neutrino masses and generating baryon asymmetry of the universe through leptogenesis, it introduces serious tension between successful baryogenesis and the upper bound on the reheating temperature obtained from avoiding the overproduction of gravitinos (the so-called gravitino problem). Nevertheless, since supersymmetry has to be broken, the existence of soft supersymmetry-breaking terms provide possible new sources of CP violations for leptogenesis. This actually allows to lower the scale for successful leptogenesis and hence relaxes or completely avoids the gravitino problem.

In this thesis, we have studied leptogenesis from soft supersymmetry-breaking terms which is viable at the scale $10^4 \text{ GeV} \lesssim T \lesssim 10^9 \text{ GeV}$ termed soft leptogenesis [82, 83]. As seen in Chapter 2, soft leptogenesis is plagued by the problem of a congenital low efficiency, that is related to the cancellation between the asymmetries produced in fermions and bosons carrying lepton number. In particular, we have found that for all soft supersymmetry-breaking sources, an exact cancellation between the leading order asymmetries produced in the fermionic and scalar channels occurs at $T = 0$. Eventually, finite temperature corrections, that break supersymmetry and spoil the cancellation between the scalar and fermionic CP asymmetries, can rescue soft leptogenesis from a complete failure. It should be stressed the fact that lepton

number L commutes with supersymmetric transformations, that is that scalar and fermionic members of a supermultiplet have the same lepton number, plays a crucial role in enforcing the aforementioned CP asymmetry cancellation.

In Chapter 3, we have shown that quantum effects are most quantitatively important for extremely degenerate right-handed sneutrinos. In this case and in the strong washout regime quantum effects can enhance the absolute value of the produced asymmetry as well as induce a change of its sign. Nevertheless, altogether our results show that the parameter space to achieve successful soft leptogenesis are not substantially modified by the inclusion of these quantum effects.

In Chapter 4, we have shown that with the inclusion of lepton flavor effects, we obtain $\sim 10^3$ enhancement with respect to the one-flavor approximation, which is sufficient to avoid the need for any additional enhancement from resonant conditions. Thus, the natural scale for the right-handed sneutrino mixing parameter $B \sim m_{SUSY}$ is eventually allowed.

In Chapter 5, we have discovered a new possibility in which baryogenesis can proceed through R -genesis, that is the asymmetry can be first generated in the new R charge that appears in the effective theory for supersymmetry when the universe temperature is above $T \sim 10^7$ GeV, and then is transferred to baryons via generalized electroweak sphaleron interactions. In this scenario, contrary to common belief, a sizable baryon asymmetry is generated also when thermal effects are neglected.

In conclusion, supersymmetry offers different ways to explain the cosmic matter-antimatter asymmetry. The asymmetry could be directly generated in baryon number since, although severely constrained, there is still a narrow window in which electroweak baryogenesis could proceed. Alternatively, the asymmetry could be initially generated in lepton number, through supersymmetric leptogenesis if it occurs above $T \sim 10^9$ GeV although in this case, we have the gravitino problem as mentioned in first paragraph. At lower temperatures where the gravitino problem can be relaxed or completely avoided, baryogenesis could proceed through R -genesis if it occurs in the temperature range 10^7 GeV $\lesssim T \lesssim 10^9$ GeV. If it occurs in the temperature range 10^4 GeV $\lesssim T \lesssim 10^7$ GeV then the usual flavored soft leptogenesis will take over with an enhanced efficiency which allows a natural TeV scale for soft

supersymmetry-breaking parameters (in particular the right-handed sneutrino mixing parameter B).

If supersymmetry is discovered by the Large Hadron Collider, soft leptogenesis will become an attractive solution to the cosmic baryon asymmetry problem. Then a more careful study of the parameter space with the constraints from experimental measurement of soft terms is required to determine if soft leptogenesis is truly a viable model for baryogenesis.

Bibliography

- [1] Edward W. Kolb and Michael S. Turner. The Early Universe. *Front. Phys.*, 69:1–547, 1990.
- [2] W. M. Yao et al. Review of particle physics. *J. Phys.*, G33:1–1232, 2006.
- [3] J. Dunkley et al. Five-Year Wilkinson Microwave Anisotropy Probe (WMAP) Observations: Likelihoods and Parameters from the WMAP data. *Astrophys. J. Suppl.*, 180:306–329, 2009.
- [4] A. D. Sakharov. Violation of CP Invariance, C Asymmetry, and Baryon Asymmetry of the Universe. *Pisma Zh. Eksp. Teor. Fiz.*, 5:32–35, 1967.
- [5] Gerard 't Hooft. Symmetry breaking through Bell-Jackiw anomalies. *Phys. Rev. Lett.*, 37:8–11, 1976.
- [6] V. A. Kuzmin, V. A. Rubakov, and M. E. Shaposhnikov. On the Anomalous Electroweak Baryon Number Nonconservation in the Early Universe. *Phys. Lett.*, B155:36, 1985.
- [7] Sacha Davidson, Enrico Nardi, and Yosef Nir. Leptogenesis. *Phys. Rept.*, 466:105–177, 2008.
- [8] Nicola Cabibbo. Unitary Symmetry and Leptonic Decays. *Phys. Rev. Lett.*, 10:531–533, 1963.
- [9] Makoto Kobayashi and Toshihide Maskawa. CP Violation in the Renormalizable Theory of Weak Interaction. *Prog. Theor. Phys.*, 49:652–657, 1973.

- [10] V. A. Rubakov and M. E. Shaposhnikov. Electroweak baryon number non-conservation in the early Universe and in high-energy collisions. *Usp. Fiz. Nauk*, 166:493–537, 1996.
- [11] C. Jarlskog. Commutator of the Quark Mass Matrices in the Standard Electroweak Model and a Measure of Maximal CP Violation. *Phys. Rev. Lett.*, 55:1039, 1985.
- [12] M. B. Gavela, P. Hernandez, J. Orloff, and O. Pene. Standard Model CP-violation and Baryon asymmetry. *Mod. Phys. Lett.*, A9:795–810, 1994.
- [13] K. Jansen. Status of the Finite Temperature Electroweak Phase Transition on the Lattice. *Nucl. Phys. Proc. Suppl.*, 47:196–211, 1996.
- [14] H. Baer and X. Tata. Weak scale supersymmetry: From superfields to scattering events. Cambridge, UK: Univ. Pr. (2006) 537 p.
- [15] M. Drees, R. Godbole, and P. Roy. Theory and phenomenology of sparticles: An account of four-dimensional N=1 supersymmetry in high energy physics. Hackensack, USA: World Scientific (2004) 555 p.
- [16] Marcela S. Carena, M. Quiros, and C. E. M. Wagner. Opening the Window for Electroweak Baryogenesis. *Phys. Lett.*, B380:81–91, 1996.
- [17] A. Yu. Ignatiev, N. V. Krasnikov, V. A. Kuzmin, and A. N. Tavkhelidze. Universal CP Noninvariant Superweak Interaction and Baryon Asymmetry of the Universe. *Phys. Lett.*, B76:436–438, 1978.
- [18] D. Toussaint, S. B. Treiman, Frank Wilczek, and A. Zee. Matter - Antimatter Accounting, Thermodynamics, and Black Hole Radiation. *Phys. Rev.*, D19:1036–1045, 1979.
- [19] Motohiko Yoshimura. Unified Gauge Theories and the Baryon Number of the Universe. *Phys. Rev. Lett.*, 41:281–284, 1978.
- [20] Motohiko Yoshimura. Origin of Cosmological Baryon Asymmetry. *Phys. Lett.*, B88:294, 1979.

- [21] S. Weinberg. Cosmological Production of Baryons. *Phys. Rev. Lett.*, 42:850–853, 1979.
- [22] M. Fukugita and T. Yanagida. Baryogenesis Without Grand Unification. *Phys. Lett.*, B174:45, 1986.
- [23] Mu-Chun Chen. TASI 2006 Lectures on Leptogenesis. 2007.
- [24] Laura Covi, Nuria Rius, Esteban Roulet, and Francesco Vissani. Finite temperature effects on CP violating asymmetries. *Phys. Rev.*, D57:93–99, 1998.
- [25] G. F. Giudice, A. Notari, M. Raidal, A. Riotto, and A. Strumia. Towards a complete theory of thermal leptogenesis in the SM and MSSM. *Nucl. Phys.*, B685:89–149, 2004.
- [26] W. Buchmüller and M. Plümacher. Spectator processes and baryogenesis. *Phys. Lett.*, B511:74, 2001.
- [27] E. Nardi, Y. Nir, J. Racker, and E. Roulet. On Higgs and sphaleron effects during the leptogenesis era. *JHEP*, 01:068, 2006.
- [28] R. Barbieri, P. Creminelli, A. Strumia, and N. Tetradis. Baryogenesis through leptogenesis. *Nucl. Phys.*, B575:61–77, 2000.
- [29] T. Endoh, T. Morozumi, and Z. Xiong. Primordial lepton family asymmetries in seesaw model. *Prog. Theor. Phys.*, 111:123–149, 2004.
- [30] A. Abada, S. Davidson, A. Ibarra, F.X. Josse-Michaux, M. Losada, and A. Riotto. Flavour matters in leptogenesis. *JHEP*, 09:010, 2006.
- [31] Asmaa Abada, Sacha Davidson, Francois-Xavier Josse-Michaux, Marta Losada, and Antonio Riotto. Flavour Issues in Leptogenesis. *JCAP*, 0604:004, 2006.
- [32] Enrico Nardi, Yosef Nir, Esteban Roulet, and Juan Racker. The importance of flavor in leptogenesis. *JHEP*, 01:164, 2006.
- [33] E. Nardi, J. Racker, and E. Roulet. CP violation in scatterings, three body processes and the Boltzmann equations for leptogenesis. *JHEP*, 09:090, 2007.

- [34] Guy Engelhard, Yuval Grossman, Enrico Nardi, and Yosef Nir. The importance of N_2 leptogenesis. *Phys. Rev. Lett.*, 99:081802, 2007.
- [35] Stefan Antusch, Pasquale Di Bari, David A. Jones, and Steve F. King. A fuller flavour treatment of N_2 -dominated leptogenesis. 2010.
- [36] Peter Minkowski. $\mu \rightarrow e \gamma$ at a Rate of One Out of 1-Billion Muon Decays? *Phys. Lett.*, B67:421, 1977.
- [37] Murray Gell-Mann, Pierre Ramond, and Richard Slansky. Complex Spinors and Unified Theories. Print-80-0576 (CERN).
- [38] Tsutomu Yanagida. Horizontal gauge symmetry and masses of neutrinos. In Proceedings of the Workshop on the Baryon Number of the Universe and Unified Theories, Tsukuba, Japan, 13-14 Feb 1979.
- [39] Rabindra N. Mohapatra and Goran Senjanovic. Neutrino mass and spontaneous parity nonconservation. *Phys. Rev. Lett.*, 44:912, 1980.
- [40] B. Pontecorvo. Inverse beta processes and nonconservation of lepton charge. *Sov. Phys. JETP*, 7:172–173, 1958.
- [41] B. Pontecorvo. Mesonium and antimesonium. *Sov. Phys. JETP*, 6:429, 1957.
- [42] Ziro Maki, Masami Nakagawa, and Shoichi Sakata. Remarks on the unified model of elementary particles. *Prog. Theor. Phys.*, 28:870–880, 1962.
- [43] Laura Covi, Esteban Roulet, and Francesco Vissani. CP violating decays in leptogenesis scenarios. *Phys. Lett.*, B384:169–174, 1996.
- [44] Apostolos Pilaftsis. CP violation and baryogenesis due to heavy Majorana neutrinos. *Phys. Rev.*, D56:5431–5451, 1997.
- [45] Apostolos Pilaftsis and Thomas E. J. Underwood. Resonant leptogenesis. *Nucl. Phys.*, B692:303–345, 2004.
- [46] Apostolos Pilaftsis. Resonant tau leptogenesis with observable lepton number violation. *Phys. Rev. Lett.*, 95:081602, 2005.

- [47] Apostolos Pilaftsis and Thomas E. J. Underwood. Electroweak-scale resonant leptogenesis. *Phys. Rev.*, D72:113001, 2005.
- [48] Apostolos Pilaftsis. Electroweak Resonant Leptogenesis in the Singlet Majoron Model. *Phys. Rev.*, D78:013008, 2008.
- [49] J. A. Casas and A. Ibarra. Oscillating neutrinos and $\mu \rightarrow e, \gamma$. *Nucl. Phys.*, B618:171–204, 2001.
- [50] S. Davidson and A. Ibarra. A lower bound on the right-handed neutrino mass from leptogenesis. *Phys. Lett.*, B535:25, 2002.
- [51] Jeffrey A. Harvey and Michael S. Turner. Cosmological baryon and lepton number in the presence of electroweak fermion number violation. *Phys.Rev.*, D42:3344–3349, 1990.
- [52] M. C. Gonzalez-Garcia, Michele Maltoni, and Jordi Salvado. Updated global fit to three neutrino mixing: status of the hints of $\theta_{13} > 0$. *JHEP*, 04:056, 2010.
- [53] W. Buchmuller, P. Di Bari, and M. Plumacher. Cosmic microwave background, matter-antimatter asymmetry and neutrino masses. *Nucl. Phys.*, B643:367–390, 2002.
- [54] John R. Ellis and Martti Raidal. Leptogenesis and the violation of lepton number and CP at low energies. *Nucl. Phys.*, B643:229–246, 2002.
- [55] Steve Blanchet and Pasquale Di Bari. Flavor effects on leptogenesis predictions. *JCAP*, 0703:018, 2007.
- [56] S. Blanchet, P. Di Bari, and G. G. Raffelt. Quantum Zeno effect and the impact of flavor in leptogenesis. *JCAP*, 0703:012, 2007.
- [57] Oscar Vives. Flavoured leptogenesis: A successful thermal leptogenesis with $N(1)$ mass below 10^8 -GeV. *J. Phys. Conf. Ser.*, 171:012076, 2009.
- [58] T. Hambye, Y. Lin, A. Notari, M. Papucci, and A. Strumia. Constraints on neutrino masses from leptogenesis models. *Nucl. Phys.*, B695:169, 2004.

- [59] Pasquale Di Bari. Seesaw geometry and leptogenesis. *Nucl. Phys.*, B727:318–354, 2005.
- [60] Ernest Ma, Narendra Sahu, and Utpal Sarkar. Leptogenesis below the Davidson-Ibarra bound. *J. Phys.*, G32:L65–L68, 2006.
- [61] Heinz Pagels and Joel R. Primack. Supersymmetry, Cosmology and New TeV Physics. *Phys. Rev. Lett.*, 48:223, 1982.
- [62] Steven Weinberg. Cosmological Constraints on the Scale of Supersymmetry Breaking. *Phys. Rev. Lett.*, 48:1303, 1982.
- [63] M. Yu. Khlopov and Andrei D. Linde. Is It Easy to Save the Gravitino? *Phys. Lett.*, B138:265–268, 1984.
- [64] John R. Ellis, Jihn E. Kim, and Dimitri V. Nanopoulos. Cosmological Gravitino Regeneration and Decay. *Phys. Lett.*, B145:181, 1984.
- [65] John R. Ellis, Dimitri V. Nanopoulos, and Subir Sarkar. The Cosmology of Decaying Gravitinos. *Nucl. Phys.*, B259:175, 1985.
- [66] Michael Plumacher. Baryon asymmetry, neutrino mixing and supersymmetric SO(10) unification. *Nucl. Phys.*, B530:207–246, 1998.
- [67] Alessandro Strumia. Baryogenesis via leptogenesis. 2006.
- [68] P. Di Bari. Leptogenesis, neutrino mixing data and the absolute neutrino mass scale. 2004.
- [69] Chee Sheng Fong, M. C. Gonzalez-Garcia, Enrico Nardi, and J. Racker. Supersymmetric Leptogenesis. *JCAP*, 1012:013, 2010.
- [70] T. Moroi, H. Murayama, and Masahiro Yamaguchi. Cosmological constraints on the light stable gravitino. *Phys. Lett.*, B303:289–294, 1993.
- [71] M. Bolz, A. Brandenburg, and W. Buchmuller. Thermal Production of Gravitinos. *Nucl. Phys.*, B606:518–544, 2001.
- [72] Josef Pradler and Frank Daniel Steffen. Thermal Gravitino Production and Collider Tests of Leptogenesis. *Phys. Rev.*, D75:023509, 2007.

- [73] Josef Pradler and Frank Daniel Steffen. Constraints on the reheating temperature in gravitino dark matter scenarios. *Phys. Lett.*, B648:224–235, 2007.
- [74] Josef Pradler and Frank Daniel Steffen. Implications of Catalyzed BBN in the CMSSM with Gravitino Dark Matter. *Phys. Lett.*, B666:181–184, 2008.
- [75] Maxim Pospelov, Josef Pradler, and Frank Daniel Steffen. Constraints on Supersymmetric Models from Catalytic Primordial Nucleosynthesis of Beryllium. *JCAP*, 0811:020, 2008.
- [76] Josef Pradler and Frank Daniel Steffen. Thermal relic abundances of long-lived staus. *Nucl. Phys.*, B809:318–346, 2009.
- [77] Erich Holtmann, M. Kawasaki, Kazunori Kohri, and Takeo Moroi. Radiative decay of a long-lived particle and big-bang nucleosynthesis. *Phys. Rev.*, D60:023506, 1999.
- [78] Masahiro Kawasaki, Kazunori Kohri, and Takeo Moroi. Hadronic decay of late-decaying particles and big-bang nucleosynthesis. *Phys. Lett.*, B625:7–12, 2005.
- [79] Kazunori Kohri, Takeo Moroi, and Akira Yotsuyanagi. Big-bang nucleosynthesis with unstable gravitino and upper bound on the reheating temperature. *Phys. Rev.*, D73:123511, 2006.
- [80] Masahiro Kawasaki, Kazunori Kohri, Takeo Moroi, and Akira Yotsuyanagi. Big-Bang Nucleosynthesis and Gravitino. *Phys. Rev.*, D78:065011, 2008.
- [81] Lotfi Boubekur. Leptogenesis at low scale. 2002.
- [82] Yuval Grossman, Tamar Kashti, Yosef Nir, and Esteban Roulet. Leptogenesis from Supersymmetry Breaking. *Phys. Rev. Lett.*, 91:251801, 2003.
- [83] Giancarlo D’Ambrosio, Gian F. Giudice, and Martti Raidal. Soft leptogenesis. *Phys. Lett.*, B575:75–84, 2003.

- [84] Lotfi Boubekur, Thomas Hambye, and Goran Senjanovic. Low-scale leptogenesis and soft supersymmetry breaking. *Phys. Rev. Lett.*, 93:111601, 2004.
- [85] Yuval Grossman, Tamar Kashti, Yosef Nir, and Esteban Roulet. New ways to soft leptogenesis. *JHEP*, 11:080, 2004.
- [86] Yuval Grossman, Ryuichiro Kitano, and Hitoshi Murayama. Natural soft leptogenesis. *JHEP*, 06:058, 2005.
- [87] Chee Sheng Fong and M. C. Gonzalez-Garcia. On Gaugino Contributions to Soft Leptogenesis. *JHEP*, 03:073, 2009.
- [88] Andrea De Simone and Antonio Riotto. On Resonant Leptogenesis. *JCAP*, 0708:013, 2007.
- [89] Vincenzo Cirigliano, Andrea De Simone, Gino Isidori, Isabella Masina, and Antonio Riotto. Quantum Resonant Leptogenesis and Minimal Lepton Flavour Violation. *JCAP*, 0801:004, 2008.
- [90] Chee Sheng Fong and M. C. Gonzalez-Garcia. On Quantum Effects in Soft Leptogenesis. *JCAP*, 0808:008, 2008.
- [91] Chee Sheng Fong and M. C. Gonzalez-Garcia. Flavoured Soft Leptogenesis. *JHEP*, 06:076, 2008.
- [92] Chee Sheng Fong, M. C. Gonzalez-Garcia, Enrico Nardi, and J. Racker. Flavoured soft leptogenesis and natural values of the B term. 2010.
- [93] Chee Sheng Fong, M. C. Gonzalez-Garcia, and Enrico Nardi. Early Universe effective theories: The Soft Leptogenesis and R-Genesis Cases. 2010.
- [94] J. Garayoa, M. C. Gonzalez-Garcia, and N. Rius. Soft leptogenesis in the inverse seesaw model. *JHEP*, 02:021, 2007.
- [95] Giancarlo D’Ambrosio, Thomas Hambye, Andi Hektor, Martti Raidal, and Anna Rossi. Leptogenesis in the minimal supersymmetric triplet seesaw model. *Phys. Lett.*, B604:199–206, 2004.

- [96] Mu-Chun Chen and K. T. Mahanthappa. Lepton flavor violating decays, soft leptogenesis and SUSY SO(10). *Phys. Rev.*, D70:113013, 2004.
- [97] Eung Jin Chun and Stefano Scopel. Soft leptogenesis in Higgs triplet model. *Phys. Lett.*, B636:278–285, 2006.
- [98] Anibal D. Medina and Carlos E. M. Wagner. Soft leptogenesis in warped extra dimensions. *JHEP*, 12:037, 2006.
- [99] E. J. Chun and L. Velasco-Sevilla. SO(10) unified models and soft leptogenesis. *JHEP*, 08:075, 2007.
- [100] R. E. Cutkosky. Singularities and discontinuities of Feynman amplitudes. *J. Math. Phys.*, 1:429–433, 1960.
- [101] M. Plümacher. Baryogenesis and lepton number violation. *Z. Phys.*, C74:549, 1997.
- [102] M. C. Gonzalez-Garcia, Michele Maltoni, and Jordi Salvado. Robust Cosmological Bounds on Neutrinos and their Combination with Oscillation Results. *JHEP*, 08:117, 2010.
- [103] A. Anisimov, A. Broncano, and M. Plumacher. The CP-asymmetry in resonant leptogenesis. *Nucl. Phys.*, B737:176–189, 2006.
- [104] Chee Sheng Fong, M. C. Gonzalez-Garcia, and J. Racker. CP Violation from Scatterings with Gauge Bosons in Leptogenesis. *Phys. Lett.*, B697:463–470, 2011.
- [105] Daniel J. H. Chung, Bjorn Garbrecht, Michael. J. Ramsey-Musolf, and Sean Tulin. Supergauge interactions and electroweak baryogenesis. *JHEP*, 12:067, 2009.
- [106] Tomoyuki Inui, Tomoyasu Ichihara, Yukihiro Mimura, and Norisuke Sakai. Cosmological baryon asymmetry in supersymmetric Standard Models and heavy particle effects. *Phys. Lett.*, B325:392–400, 1994.
- [107] Daniel J. H. Chung, Bjorn Garbrecht, and Sean Tulin. The Effect of the Sparticle Mass Spectrum on the Conversion of B-L to B. *JCAP*, 0903:008, 2009.

- [108] Chee Sheng Fong and J. Racker. On fast CP violating interactions in leptogenesis. *JCAP*, 1007:001, 2010.
- [109] Eung Jin Chun. Late leptogenesis from radiative soft terms. *Phys. Rev.*, D69:117303, 2004.
- [110] Wilfried Buchmuller and Stefan Fredenhagen. Quantum mechanics of baryogenesis. *Phys. Lett.*, B483:217–224, 2000.
- [111] Andrea De Simone and Antonio Riotto. Quantum Boltzmann Equations and Leptogenesis. *JCAP*, 0708:002, 2007.
- [112] A. Anisimov, W. Buchmuller, M. Drewes, and S. Mendizabal. Leptogenesis from Quantum Interference in a Thermal Bath. *Phys. Rev. Lett.*, 104:121102, 2010.
- [113] A. Anisimov, W. Buchmuller, M. Drewes, and S. Mendizabal. Quantum Leptogenesis I. 2010.
- [114] M. Garny, A. Hohenegger, A. Kartavtsev, and M. Lindner. Systematic approach to leptogenesis in nonequilibrium QFT: vertex contribution to the CP-violating parameter. *Phys. Rev.*, D80:125027, 2009.
- [115] M. Garny, A. Hohenegger, A. Kartavtsev, and M. Lindner. Systematic approach to leptogenesis in nonequilibrium QFT: self-energy contribution to the CP-violating parameter. *Phys. Rev.*, D81:085027, 2010.
- [116] Vincenzo Cirigliano, Christopher Lee, Michael J. Ramsey-Musolf, and Sean Tulin. Flavoured Quantum Boltzmann Equations. *Phys. Rev.*, D81:103503, 2010.
- [117] Martin Beneke, Bjorn Garbrecht, Christian Fidler, Matti Herranen, and Pedro Schwaller. Flavoured Leptogenesis in the CTP Formalism. *Nucl. Phys.*, B843:177–212, 2011.
- [118] Steve Blanchet and Pasquale Di Bari. Leptogenesis beyond the limit of hierarchical heavy neutrino masses. *JCAP*, 0606:023, 2006.

- [119] Bruce A. Campbell, Sacha Davidson, John R. Ellis, and Keith A. Olive. On the baryon, lepton flavor and right-handed electron asymmetries of the Universe. *Phys. Lett.*, B297:118–124, 1992.
- [120] James M. Cline, Kimmo Kainulainen, and Keith A. Olive. Protecting the primordial baryon asymmetry from erasure by sphalerons. *Phys. Rev.*, D49:6394–6409, 1994.
- [121] T. Fujihara et al. Cosmological family asymmetry and CP violation. *Phys. Rev.*, D72:016006, 2005.
- [122] S. Pascoli, S. T. Petcov, and Antonio Riotto. Connecting Low Energy Leptonic CP-violation to Leptogenesis. *Phys. Rev.*, D75:083511, 2007.
- [123] S. Pascoli, S. T. Petcov, and Antonio Riotto. Leptogenesis and low energy CP violation in neutrino physics. *Nucl. Phys.*, B774:1–52, 2007.
- [124] S. Antusch, S. F. King, and A. Riotto. Flavour-dependent leptogenesis with sequential dominance. *JCAP*, 0611:011, 2006.
- [125] S. Antusch and A. M. Teixeira. Towards constraints on the SUSY seesaw from flavour- dependent leptogenesis. *JCAP*, 0702:024, 2007.
- [126] G. C. Branco, R. Gonzalez Felipe, and F. R. Joaquim. A new bridge between leptonic CP violation and leptogenesis. *Phys. Lett.*, B645:432–436, 2007.
- [127] D. Aristizabal Sierra, M. Losada, and E. Nardi. Lepton Flavor Equilibration and Leptogenesis. *JCAP*, 0912:015, 2009.
- [128] Andrea De Simone and Antonio Riotto. On the impact of flavour oscillations in leptogenesis. *JCAP*, 0702:005, 2007.
- [129] Sacha Davidson, Julia Garayoa, Federica Palorini, and Nuria Rius. CP Violation in the SUSY Seesaw: Leptogenesis and Low Energy. *JHEP*, 09:053, 2008.
- [130] Luis E. Ibanez and Fernando Quevedo. Supersymmetry protects the primordial baryon asymmetry. *Phys. Lett.*, B283:261–269, 1992.

- [131] James M. Cline, Kimmo Kainulainen, and Keith A. Olive. On the erasure and regeneration of the primordial baryon asymmetry by sphalerons. *Phys. Rev. Lett.*, 71:2372–2375, 1993.
- [132] Wai-Yee Keung and L. Littenberg. Test of Supersymmetry in e^-e^- collision. *Phys. Rev.*, D28:1067, 1983.
- [133] Anders Basboll and Steen Hannestad. Decay of heavy Majorana neutrinos using the full Boltzmann equation including its implications for leptogenesis. *JCAP*, 0701:003, 2007.
- [134] F. Hahn-Woernle, M. Plumacher, and Y. Y. Y. Wong. Full Boltzmann equations for leptogenesis including scattering. *JCAP*, 0908:028, 2009.
- [135] J. Garayoa, S. Pastor, T. Pinto, N. Rius, and O. Vives. On the full Boltzmann equations for Leptogenesis. *JCAP*, 0909:035, 2009.
- [136] E. W. Kolb and S. Wolfram. Baryon Number Generation in the Early Universe. *Nucl. Phys.*, B172:224, 1980.
- [137] James N. Fry, Keith A. Olive, and Michael S. Turner. Evolution of Cosmological Baryon Asymmetries. *Phys. Rev.*, D22:2953, 1980.

Appendix A

Phase Conventions and Feynman Rules

The relevant Lagrangian density for soft leptogenesis (SL) is given by

$$\begin{aligned}
-\mathcal{L}_{int+soft} = & \widetilde{M}_{ij}^2 \widetilde{N}_i^* \widetilde{N}_j + \frac{1}{2} M_i \overline{N}_i N_i \\
& + \left\{ \frac{1}{2} B M_i \widetilde{N}_i \widetilde{N}_i + \frac{1}{2} m_2 \overline{\widetilde{\lambda}}_2^{\pm,0} P_L \widetilde{\lambda}_2^{\pm,0} + \frac{1}{2} m_1 \overline{\widetilde{\lambda}}_1 P_L \widetilde{\lambda}_1 \right. \\
& + Y_{i\alpha} \epsilon_{ab} \left(M_i^* \widetilde{N}_i^* \widetilde{\ell}_\alpha^a H_u^b + \overline{\widetilde{H}}_u^{c,b} P_L \ell_\alpha^a \widetilde{N}_i + \overline{\widetilde{H}}_u^{c,b} P_L N_i \widetilde{\ell}_\alpha^a \right. \\
& \left. + \overline{N}_i P_L \ell_\alpha^a H_u^b + \frac{A Z_{i\alpha}}{Y_{i\alpha}} \widetilde{N}_i \widetilde{\ell}_\alpha^a H_u^b \right) \\
& + g_2 (\sigma_\pm)_{ab} \left(\overline{\widetilde{\lambda}}_2^\pm P_L \ell_\alpha^a \widetilde{\ell}_\alpha^{b*} + \overline{\widetilde{H}}_u^{c,a} P_L \widetilde{\lambda}_2^\pm H_u^{b*} \right) \\
& + \frac{g_2}{\sqrt{2}} (\sigma_3)_{ab} \left(\overline{\widetilde{\lambda}}_2^0 P_L \ell_\alpha^a \widetilde{\ell}_\alpha^{b*} + \overline{\widetilde{H}}_u^{c,a} P_L \widetilde{\lambda}_2^0 H_u^{b*} \right) \\
& \left. + \frac{g_Y}{\sqrt{2}} \delta_{ab} \left[\overline{\widetilde{\lambda}}_1 (y_{\ell L} P_L - y_{\ell R} P_R) \ell_\alpha^a \widetilde{\ell}_\alpha^{b*} + \overline{\widetilde{H}}_u^{c,a} P_L \widetilde{\lambda}_1 H_u^{b*} \right] + \text{h.c.} \right\}, \quad (\text{A.1})
\end{aligned}$$

where $i = 1, 2, \dots$ is the right-handed neutrino (RHN) generation indices, $\alpha, \beta = e, \mu, \tau$ the lepton flavor indices, $a = 0, 1$ the $SU(2)_L$ indices, $P_{L,R} = \frac{1}{2} (1 \mp \gamma_5)$ respectively the left and right chiral projectors and $\sigma_\pm = (\sigma_1 \pm i\sigma_2) / 2$ with σ_i being the Pauli matrices. Also, in eq. (A.1), g_2 and g_Y are respectively the $SU(2)_L$ and $U(1)_Y$ gauge couplings and $y_{\ell L} = -1$ and $y_{\ell R} = 2$ being respectively the hypercharges of the left- and right-handed (s)leptons.

We also define the Majorana fermions as follows: the RHN $N_i = \nu_{R_i} + (\nu_{R_i})^c$, the $SU(2)_L$ gauginos $\tilde{\lambda}_2^{\pm,0} = \tilde{\lambda}_{2L}^{\mp,0} + (\tilde{\lambda}_{2L}^{\pm,0})^c$ and the $U(1)_Y$ gaugino $\tilde{\lambda}_1 = \tilde{\lambda}_{1L} + (\tilde{\lambda}_{1L})^c$.

Here for simplicity, we will concentrate on SL arising from a single right-handed sneutrino (RHSN) generation $i = 1$ and in what follows we will drop that index ($Y_\alpha \equiv Y_{1\alpha}$, $Z_\alpha \equiv Z_{1\alpha}$, $B = B_{11}$, etc.). Now we rewrite the Lagrangian with the phases explicitly written out as follows:

$$\begin{aligned}
-\mathcal{L}_{int+soft} = & \left| \widetilde{M} \right|^2 \widetilde{N}^* \widetilde{N} + \frac{1}{2} |M| e^{2i\delta} \overline{N} N \\
& + \left\{ \frac{1}{2} |B| |M| e^{2i(\gamma+\delta)} \widetilde{N} \widetilde{N} + \frac{1}{2} |m_2| e^{2i\eta} \overline{\widetilde{\lambda}_2^{\pm,0}} P_L \widetilde{\lambda}_2^{\pm,0} + \frac{1}{2} |m_1| e^{2i\kappa} \overline{\widetilde{\lambda}_1} P_L \widetilde{\lambda}_1 \right. \\
& + |Y_\alpha| e^{i\zeta_\alpha} \epsilon_{ab} \left(e^{-2i\delta} |M| \widetilde{N}^* \widetilde{\ell}_\alpha^a H_u^b + \overline{\widetilde{H}_u^{c,b}} P_L \ell_\alpha^a \widetilde{N} + \overline{\widetilde{H}_u^{c,b}} P_L N \widetilde{\ell}_\alpha^a \right. \\
& \left. + \overline{N} P_L \ell_\alpha^a H_u^b + \frac{|A| |Z_\alpha|}{|Y_\alpha|} e^{i(\theta+\xi_\alpha-\zeta_\alpha)} \widetilde{N} \widetilde{\ell}_\alpha^a H_u^b \right) \\
& + g_2 (\sigma_\pm)_{ab} \left(\overline{\widetilde{\lambda}_2^\pm} P_L \ell_\alpha^a \widetilde{\ell}^{b*} + \overline{\widetilde{H}_u^{c,a}} P_L \widetilde{\lambda}_2^\pm H_u^{b*} \right) \\
& + \frac{g_2}{\sqrt{2}} (\sigma_3)_{ab} \left(\overline{\widetilde{\lambda}_2^0} P_L \ell_\alpha^a \widetilde{\ell}^{b*} + \overline{\widetilde{H}_u^{c,a}} P_L \widetilde{\lambda}_2^0 H_u^{b*} \right) \\
& \left. + \frac{g_Y}{\sqrt{2}} \delta_{ab} \left[\overline{\widetilde{\lambda}_1} (y_{\ell L} P_L - y_{\ell R} P_R) \ell_\alpha^a \widetilde{\ell}^{b*} + \overline{\widetilde{H}_u^{c,a}} P_L \widetilde{\lambda}_1 H_u^{b*} \right] + \text{h.c.} \right\}. \quad (\text{A.2})
\end{aligned}$$

Let us redefine the fields as follows

$$\begin{aligned}
e^{i\delta} \nu_R & \rightarrow \nu_R, \\
e^{i(\gamma+\delta)} \widetilde{N} & \rightarrow \widetilde{N}, \\
e^{i(\gamma-\delta+2\zeta_\alpha)/2} \widetilde{\ell}_\alpha & \rightarrow \widetilde{\ell}_\alpha, \\
e^{i(\gamma-\delta)/2} H_u & \rightarrow H_u, \\
e^{-i(\gamma+\delta-2\zeta_\alpha)/2} \ell_\alpha & \rightarrow \ell_\alpha, \\
e^{i(\gamma+\delta)/2} \widetilde{H}_u^c & \rightarrow \widetilde{H}_u^c. \quad (\text{A.3})
\end{aligned}$$

Then, we have

$$\begin{aligned}
-\mathcal{L}_{int+soft} &= \left| \widetilde{M} \right|^2 \widetilde{N}^* \widetilde{N} + \frac{1}{2} |M| \overline{N} N \\
&+ \left\{ \frac{1}{2} |B| |M| \widetilde{N} \widetilde{N} + \frac{1}{2} |m_2| e^{2i\eta} \overline{\widetilde{\lambda}}_2^a P_L \widetilde{\lambda}_2^a + \frac{1}{2} |m_1| e^{2i\kappa} \overline{\widetilde{\lambda}}_1 P_L \widetilde{\lambda}_1 \right. \\
&+ |Y_\alpha| \epsilon_{ab} \left(e^{-2i\delta} |M| \widetilde{N}^* \widetilde{\ell}_\alpha^a H_u^b + \overline{\widetilde{H}}_u^{c,b} P_L \ell_\alpha^a \widetilde{N} + \overline{\widetilde{H}}_u^{c,b} P_L N \widetilde{\ell}_\alpha^a \right. \\
&+ \overline{N} P_L \ell_\alpha^a H_u^b + \frac{|A| |Z_\alpha|}{|Y_\alpha|} e^{i(\theta + \xi_\alpha - \zeta_\alpha - 2\gamma)} \widetilde{N} \widetilde{\ell}_\alpha^a H_u^b \left. \right) \\
&+ g_2 e^{i\gamma} (\sigma_\pm)_{ab} \left(\overline{\widetilde{\lambda}}_2^\pm P_L \ell_\alpha^a \widetilde{\ell}_\alpha^{b*} + \overline{\widetilde{H}}_u^{c,a} P_L \widetilde{\lambda}_2^\pm H_u^{b*} \right) \\
&+ \frac{g_2}{\sqrt{2}} e^{i\gamma} (\sigma_3)_{ab} \left(\overline{\widetilde{\lambda}}_2^0 P_L \ell_\alpha^a \widetilde{\ell}_\alpha^{b*} + \overline{\widetilde{H}}_u^{c,a} P_L \widetilde{\lambda}_2^0 H_u^{b*} \right) \\
&+ \left. \frac{g_Y}{\sqrt{2}} e^{i\gamma} \delta_{ab} \left[\overline{\widetilde{\lambda}}_1 (y_{\ell L} P_L - y_{\ell R} P_R) \ell_\alpha^a \widetilde{\ell}_\alpha^{b*} + \overline{\widetilde{H}}_u^{c,a} P_L \widetilde{\lambda}_1 H_u^{b*} \right] + \text{h.c.} \right\}. \quad (\text{A.4})
\end{aligned}$$

We can further redefine the fields and show that there are only five unique phases. If we redefine the gaugino fields as follows

$$\begin{aligned}
e^{i\gamma} \widetilde{\lambda}_{2L}^{\pm,0} &\rightarrow \widetilde{\lambda}_{2L}^{\pm,0}, \\
e^{i\gamma} \widetilde{\lambda}_{1L} &\rightarrow \widetilde{\lambda}_{1L}, \quad (\text{A.5})
\end{aligned}$$

with the corresponding rephasing for $(\widetilde{\lambda}_{2L}^{\pm,0})^c$ and $(\widetilde{\lambda}_{1L})^c$, then the five remaining unique phases are

$$\begin{aligned}
\phi_{A_\alpha} &\equiv \arg(AZ_\alpha Y_\alpha^* B^*) = \theta + \xi_\alpha - \zeta_\alpha - 2\gamma, \\
\phi_{g_{m_2}} &\equiv \arg(m_2 B^*) = 2(\eta - \gamma), \\
\phi_{g_{m_1}} &\equiv \arg(m_1 B^*) = 2(\kappa - \gamma), \quad (\text{A.6})
\end{aligned}$$

where they can be assigned respectively to AZ_α , m_2 and m_1 .

On the other hand, from eq. A.4, if we redefine the gaugino fields as follows

$$\begin{aligned}
e^{i\eta} \widetilde{\lambda}_{2L}^{\pm,0} &\rightarrow \widetilde{\lambda}_{2L}^{\pm,0}, \\
e^{i\kappa} \widetilde{\lambda}_{1L} &\rightarrow \widetilde{\lambda}_{1L}, \quad (\text{A.7})
\end{aligned}$$

with the corresponding rephasing for $(\widetilde{\lambda}_{2L}^{\pm,0})^c$ and $(\widetilde{\lambda}_{1L})^c$, then the five re-

maining unique phases are

$$\begin{aligned}
\phi_{A_\alpha} &\equiv \arg(AZ_\alpha Y_\alpha^* B^*) = \theta + \xi_\alpha - \zeta_\alpha - 2\gamma, \\
\phi_{g_2} &\equiv \arg(Bm_2^*) = 2(\gamma - \eta), \\
\phi_{g_Y} &\equiv \arg(Bm_1^*) = 2(\gamma - \kappa),
\end{aligned} \tag{A.8}$$

where they can be assigned respectively to AZ_α , g_2 and g_Y .

Notice in the case of UTS where $Z_\alpha = Y_\alpha$ and SMS where $Z_\alpha = \frac{\sum_\beta |Y_\beta|^2}{3Y_\alpha^*}$ discussed in Chapter 4, we have $\xi_\alpha = \zeta_\alpha$ and hence ϕ_{A_α} reduce to one unique phase: $\phi_A \equiv \arg(AB^*) = \theta - 2\gamma$. In this thesis, we will adopt the phase convention as in eq. (A.8) together with the assumption of UTS or SMS where the only complex parameters are A , g_2 and g_Y . With this phase convention, we write down the vertex factors (for simplicity, we present them assuming $Z_\alpha = Y_\alpha$) associated with gauginos and RHSN (Feynman rules) as in Figure A.1 and A.2.

Figure A.1: Vertex factors involving $SU(2)_L$ and $U(1)_Y$ gauginos

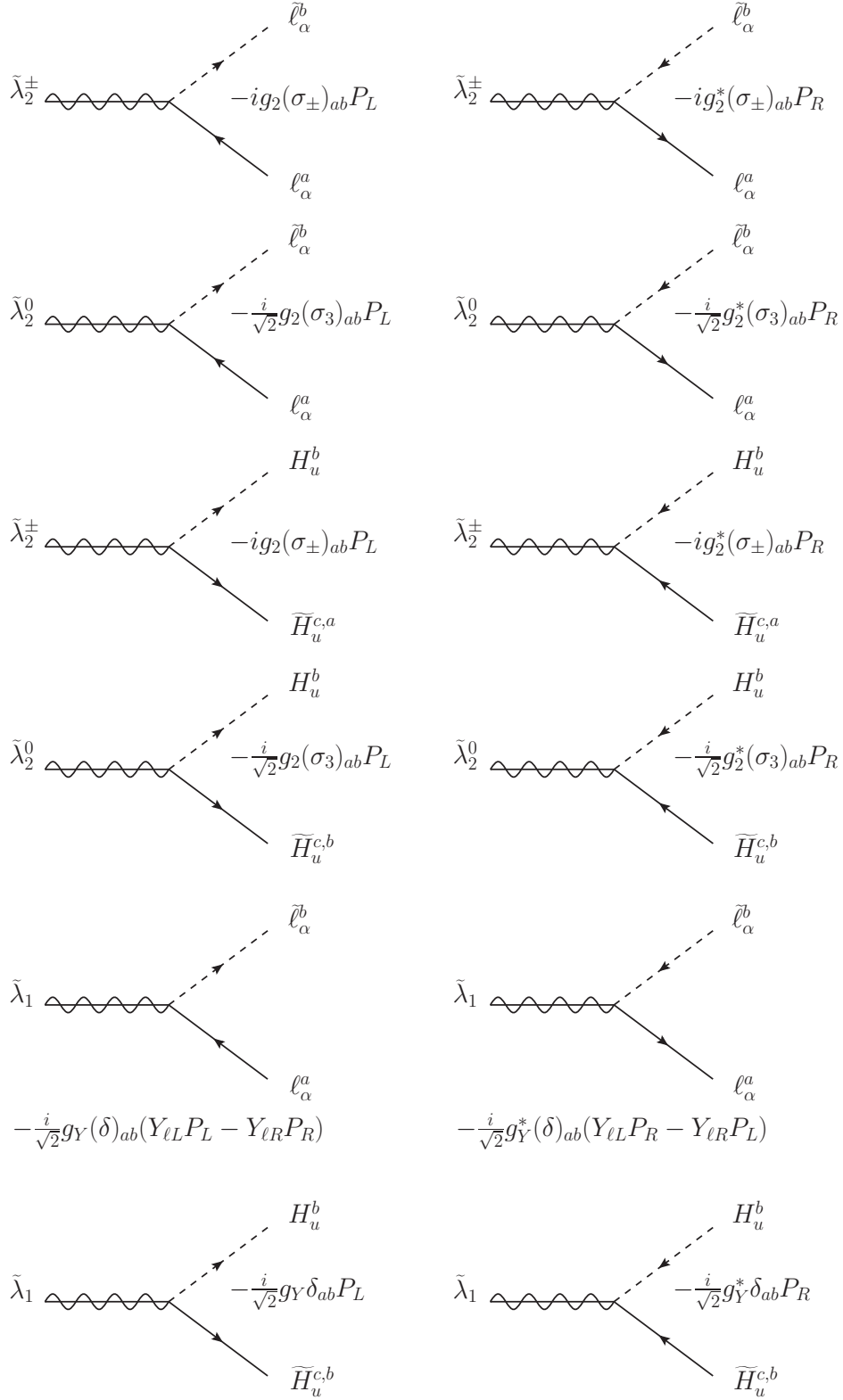
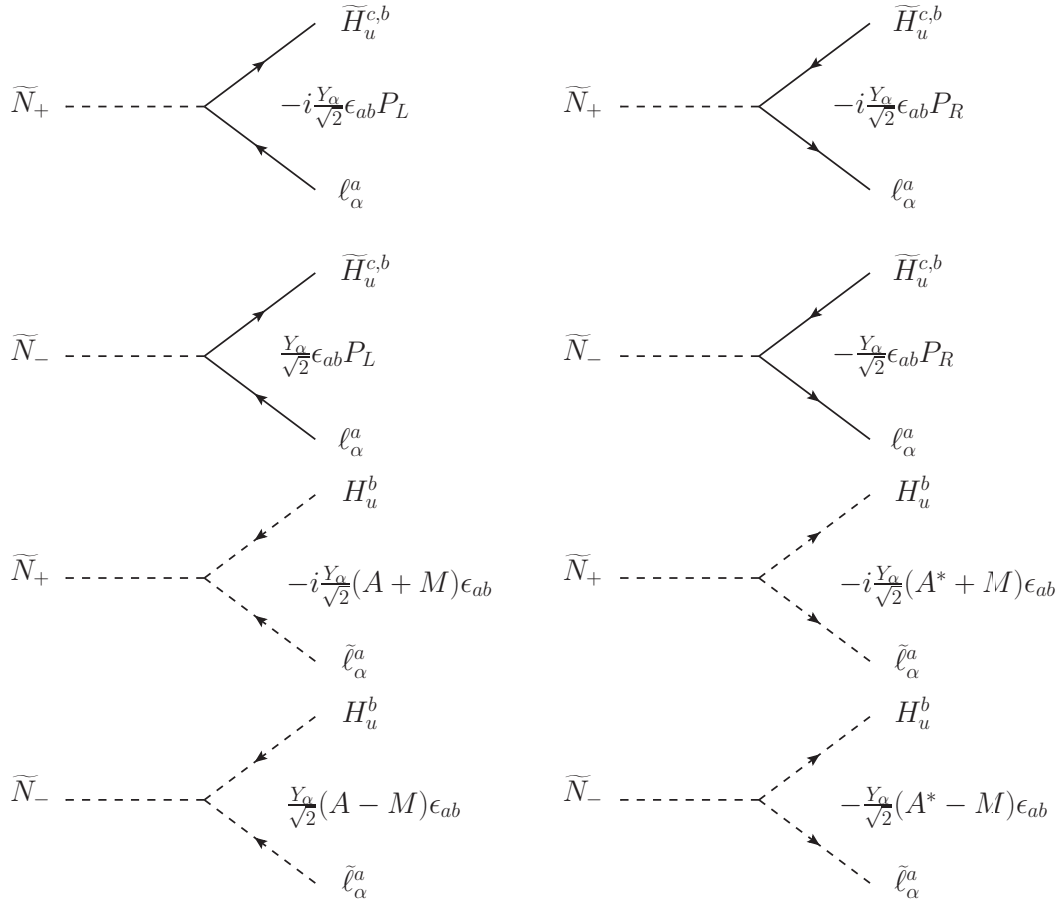


Figure A.2: Vertex factors involving \tilde{N}_\pm .



Appendix B

Boltzmann Equations

B.1 General Boltzman Equations

Our Universe is very well described by a spatially homogeneous and isotropic metric known as Robertson-Walker (RW) metric

$$ds^2 = dt^2 - R^2(t) \left[\frac{dr^2}{1 - kr^2} + r^2 d\theta^2 + r^2 \sin^2 \theta d\phi^2 \right], \quad (\text{B.1})$$

where (t, r, θ, ϕ) are comoving coordinates, $R(t)$ is the cosmic scale factor, and $k = 0, +1, -1$ describe spaces of zero, positive, or negative spatial curvature, respectively. For a general process $a + b + \dots \leftrightarrow i + j + \dots$ in the RW space, the Boltzmann equation (BE) for the phase-space distribution of the particle species a can be written as:

$$\frac{\partial f_a}{\partial t} - H |\vec{p}_a| \frac{\partial f_a}{\partial |\vec{p}_a|} = -\frac{1}{2E_a} C[f_a], \quad (\text{B.2})$$

where

$$C[f_a] \equiv \frac{1}{g_a} \sum_{b, \dots, i, j, \dots} \Lambda_{b, \dots}^{ij, \dots} \left[|\mathcal{M}(ab \dots \rightarrow ij \dots)|^2 f_a f_b \dots (1 + \eta_i f_i) (1 + \eta_j f_j) \dots \right. \\ \left. - |\mathcal{M}(ij \dots \rightarrow ab \dots)|^2 f_i f_j \dots (1 + \eta_a f_a) (1 + \eta_b f_b) \dots \right], \quad (\text{B.3})$$

where g_a is the number of spin degrees of freedom of particle a and

$$\Lambda_{b\dots}^{ij\dots} \equiv \int d\Pi_{b\dots} d\Pi_i d\Pi_{j\dots} (2\pi)^4 \delta^{(4)}(p_a + p_b + \dots - p_i - p_j - \dots),$$

$$d\Pi_x \equiv \frac{d^3 p_x}{(2\pi)^3 2E_x}. \quad (\text{B.4})$$

In eq. (B.3), $|\mathcal{M}_{ab\dots \rightarrow ij\dots}|^2$ is the squared amplitude summed over initial and final spin states and f_x is the distribution function of x with $\eta_x = \pm$ if x is a boson or fermion respectively. The factors $(1 \pm f_x)$ are known as Pauli-blocking (for x being fermion) and Bose-enhancement or stimulated emission (for x being boson) factors, respectively. In eq. B.2, the Hubble expansion rate of the Universe H in the radiation-dominated era is given by

$$H \equiv \frac{\dot{R}}{R} = \frac{2}{3} \sqrt{\frac{g_* \pi^3}{5}} \frac{T^2}{M_{pl}}, \quad (\text{B.5})$$

where $M_{pl} = 1.22 \times 10^{19}$ GeV is the Planck mass, g_* is the total number of relativistic degrees of freedom contributing to the energy density of the universe and can be written as

$$g_* = \sum_{i=\text{bosons}} g_i \left(\frac{T_i}{T}\right)^4 + \frac{7}{8} \sum_{i=\text{fermions}} g_i \left(\frac{T_i}{T}\right)^4. \quad (\text{B.6})$$

The relative factor of 7/8 accounts for the difference in Fermi-Dirac and Bose-Einstein statistics. In the SM, we have $g_* = 106.75$ while in the MSSM, we have $g_* = 228.75$.

Using the definition of the number density in terms of the phase space distribution

$$n_a = g_a \int \frac{d^3 p}{(2\pi)^3} f_a, \quad (\text{B.7})$$

and upon integration by parts, the BE (B.2) can be rewritten in the form

$$\frac{dn_a}{dt} + 3Hn_a = - \sum_{b,\dots,ij,\dots} [ab\dots \leftrightarrow ij\dots], \quad (\text{B.8})$$

where

$$\begin{aligned}
[ab\dots \leftrightarrow ij\dots] \equiv & \Lambda_{ab\dots}^{ij\dots} [|\mathcal{M}(ab\dots \rightarrow ij\dots)|^2 f_a f_b \dots (1 + \eta_i f_i) (1 + \eta_j f_j) \dots \\
& - |\mathcal{M}(ij\dots \rightarrow ab\dots)|^2 f_i f_j \dots (1 + \eta_a f_a) (1 + \eta_b f_b) \dots]. \quad (\text{B.9})
\end{aligned}$$

Notice that in writing the BE (B.8), we have implicitly assumed that the right hand side of this equation can also be written in term of n_a . However, without certain approximations, this cannot be done in general and we have to resort to the BE (B.2) and solve it in term of phase space distribution. In this thesis, we will make certain approximations that are described in Appendix B.2.2, that allow us to write the right hand side of eq. (B.8) in terms of number densities, and hence we can use the BE (B.8).

Notice that in the absence of interactions (i.e. the left hand side of eq. B.8 equals zero), the solution is $n_a \propto R^{-3}$ i.e. the density of particle is decreasing simply due to the expansion of the Universe. Since we are only interested in the effect of interactions, we would like to scale out the effect of the expansion of the Universe. In order to do so, we define the quantity called *abundance* i.e. the ratio of the particle density n_a to the entropy density s

$$Y_a \equiv \frac{n_a}{s}, \quad (\text{B.10})$$

where the entropy density s in the radiation dominated era is given by

$$s = \frac{2\pi^2}{45} g_{*s} T^3, \quad (\text{B.11})$$

where the entropy degrees of freedom g_{*s} is given by

$$g_{*s} = \sum_{i=\text{bosons}} g_i \left(\frac{T_i}{T}\right)^3 + \frac{7}{8} \sum_{i=\text{fermions}} g_i \left(\frac{T_i}{T}\right)^3. \quad (\text{B.12})$$

For the temperature regime relevant for leptogenesis i.e. $T \gtrsim T_{EW}$, all particle species have a common temperature, hence we always have $g_{*s} = g_*$ (see eq. (B.6)).

Using the conservation of entropy per comoving volume (i.e. $s R^3 = \text{con-}$

start), the left hand side of eq. (B.8) becomes

$$\frac{dn_a}{dt} + 3Hn_a = s\frac{dY_a}{dt}. \quad (\text{B.13})$$

Since the interaction term will often depend upon temperature rather than time, it is useful to replace the time t with the temperature T . In the radiation dominated era, we have $R \propto t^{-1/2}$, and from this relation we obtain

$$t = \frac{1}{2H}. \quad (\text{B.14})$$

We further define a convenient dimensionless parameter

$$z \equiv \frac{M}{T}, \quad (\text{B.15})$$

where M is any convenient mass scale. Using eq. (B.14) and eq. (B.15), we can rewrite eq. (B.13) as

$$s\frac{dY_a}{dt} = sHz\frac{dY_a}{dz}. \quad (\text{B.16})$$

Regarding the distribution functions in eqs. (B.9), for particles for which the elastic scatterings are much faster than the inelastic scatterings, we can assume that they are in kinetic equilibrium and have either Fermi-Dirac distribution (for fermions) or Bose-Einstein distribution (for bosons) given respectively by

$$\begin{aligned} f_{F,\bar{F}} &= \frac{1}{e^{(E_F \mp \mu_F)/T} + 1}, \\ f_{B,B^*} &= \frac{1}{e^{(E_B \mp \mu_B)/T} - 1}, \end{aligned} \quad (\text{B.17})$$

where μ 's are the chemical potentials and the “bar” or “star” refers to the corresponding antiparticles. We have the following useful identities

$$\begin{aligned} 1 - f_{F,\bar{F}} &= e^{(E_F \mp \mu_F)/T} f_{F,\bar{F}}, \\ 1 + f_{B,B^*} &= e^{(E_B \mp \mu_B)/T} f_{B,B^*}. \end{aligned} \quad (\text{B.18})$$

We also define the distribution with $\mu = 0$ as

$$\begin{aligned} f_{F,\bar{F}}^{eq} &= \frac{1}{e^{E_F/T} + 1}, \\ f_{B,B^*}^{eq} &= \frac{1}{e^{E_B/T} - 1}. \end{aligned} \quad (\text{B.19})$$

Assuming $\frac{\mu}{T} \ll 1$, we can expand the kinetic equilibrium distribution function in $\frac{\mu}{T}$ as

$$\begin{aligned} f_{F,\bar{F}} &= f_{F,\bar{F}}^{eq} \pm f_{F,\bar{F}}^{eq,2} e^{E_{F,\bar{F}}/T} \frac{\mu_F}{T} + \mathcal{O} \left[\left(\frac{\mu_F}{T} \right)^2 \right], \\ f_{B,B^*} &= f_{B,B^*}^{eq} \pm f_{B,B^*}^{eq,2} e^{E_{B,B^*}/T} \frac{\mu_B}{T} + \mathcal{O} \left[\left(\frac{\mu_B}{T} \right)^2 \right]. \end{aligned} \quad (\text{B.20})$$

At this point, we also define a thermally averaged reaction density as follows

$$\begin{aligned} \gamma(ab... \rightarrow ij...) &\equiv \Lambda_{ab...}^{ij...} |\mathcal{M}(ab... \rightarrow ij...)|^2 \\ &\quad \times f_a f_b \dots (1 + \eta_i f_i) (1 + \eta_j f_j) \dots, \end{aligned} \quad (\text{B.21})$$

and hence $[ab... \leftrightarrow ij...]$ in eqs. (B.9) can also be written as

$$[ab... \leftrightarrow ij...] = \gamma(ab... \rightarrow ij...) - \gamma(ij... \rightarrow ab...). \quad (\text{B.22})$$

In the following, we will show the results neglecting Pauli-blocking and Bose-enhancement factors and assuming that all the particles follow Maxwell-Boltzmann distribution $f = e^{-E/T}$, and that $|\mathcal{M}(ab... \rightarrow ij...)|^2$ does not depend on the relative motion of particles with respect to the plasma. Under this assumption, for a decay $N \rightarrow ij...$, eq. (B.21) reduces to

$$\gamma^{eq}(a \rightarrow ij...) = \gamma^{eq}(ij... \rightarrow a) = n_a^{eq} \frac{\mathcal{K}_1(z)}{\mathcal{K}_2(z)} \Gamma_a, \quad (\text{B.23})$$

where Γ_a is the decay width in the rest frame of a , \mathcal{K}_q is the modified Bessel function of the second kind of order q , and n_a^{eq} is the equilibrium number density of a given by

$$n_a^{eq} = g_a \int \frac{d^3 p_a}{(2\pi)^3} e^{-E_a/T} = \frac{g_a T^3}{\pi^2}. \quad (\text{B.24})$$

Under the same assumption, for a two-body scattering $ab \rightarrow ij$, eq. (B.21) reduces to

$$\gamma^{eq}(ab \rightarrow ij) = \frac{T}{64\pi^4} \int_{s_{\min}}^{\infty} ds \sqrt{s} \hat{\sigma}(s) \mathcal{K}_1\left(\frac{\sqrt{s}}{T}\right), \quad (\text{B.25})$$

where s is the center of mass energy squared, $s_{\min} = \max[(m_a + m_b)^2, (m_i + m_j)^2]$ and $\hat{\sigma}(s)$ is the *reduced cross section* which is related to the total cross section $\sigma(s)$ (summing over initial and final spin states) by

$$\begin{aligned} \hat{\sigma}(s) &\equiv \frac{2\lambda^2(s, m_a^2, m_b^2)}{2} \sigma(s), \\ &= \frac{1}{8\pi s} \int_{t_-}^{t_+} dt |\mathcal{M}(ab \rightarrow ij)|^2, \end{aligned} \quad (\text{B.26})$$

with

$$\lambda(a, b, c) \equiv \sqrt{(a - b - c)^2 - 4bc}, \quad (\text{B.27})$$

$$\begin{aligned} t_{\pm} &= \frac{m_a^2 - m_b^2 - m_i^2 + m_j^2}{4s} \\ &- \left[\sqrt{\frac{(s + m_a^2 - m_b^2)^2}{4s} - m_a^2} \mp \sqrt{\frac{(s + m_i^2 - m_j^2)^2}{4s} - m_i^2} \right]^2. \end{aligned} \quad (\text{B.28})$$

Next we describe the statistical factors which appear in general in the different type of reactions relevant for SL. They depend on whether we are dealing with reactions in which there is N or \tilde{N} in the external legs or not. If the right-handed neutrinos or sneutrinos are external states, we cannot assume kinetic equilibrium for all the states involved. Otherwise, if they are not external states, we can.

B.1.1 Particle a not in kinetic equilibrium and $\mu_a = 0$

Assuming that particles $b\dots ij\dots$ have kinetic equilibrium distributions with corresponding chemical potential $\mu_{b,\dots,ij,\dots}$, we have

$$\begin{aligned}
& f_i f_j \dots (1 + \eta_a f_a) (1 + \eta_b f_b) \dots \\
= & e^{-(E_i - \mu_i)/T} (1 + \eta_i f_i) e^{-(E_j - \mu_j)/T} \\
& \times (1 + \eta_j f_j) \dots (1 + \eta_a f_a) (1 + \eta_b f_b) \dots, \\
= & e^{(\mu_i + \mu_j + \dots)/T} (1 + \eta_i f_i) (1 + \eta_j f_j) \dots \\
& \times e^{-E_a/T} (1 + \eta_a f_a) e^{-\mu_b/T} e^{-(E_b - \mu_b)/T} (1 + \eta_b f_b) \dots, \\
= & e^{(\mu_i + \mu_j + \dots)/T} (1 + \eta_i f_i) (1 + \eta_j f_j) \dots f_a^{eq} \frac{1 + \eta_a f_a}{1 + \eta_a f_a^{eq}} \\
& \times e^{-(\mu_b + \mu_c + \dots)/T} f_b f_c \dots, \tag{B.29}
\end{aligned}$$

where we have used conservation of energy $E_a + E_b + \dots = E_i + E_j + \dots$ and the identities (B.18).

Substituting (B.29) into the right hand side of (B.8), we have

$$\begin{aligned}
& [ab\dots \leftrightarrow ij\dots] \\
= & \Lambda_{ab\dots}^{ij\dots} [|\mathcal{M}(ab\dots \rightarrow ij\dots)|^2 f_a f_b \dots (1 + \eta_i f_i) (1 + \eta_j f_j) \dots \\
& - |\mathcal{M}(ij\dots \rightarrow ab\dots)|^2 f_i f_j \dots (1 + \eta_a f_a) (1 + \eta_b f_b) \dots], \\
= & \Lambda_{ab\dots}^{ij\dots} [|\mathcal{M}(ab\dots \rightarrow ij\dots)|^2 f_a f_b \dots \\
& - |\mathcal{M}(ij\dots \rightarrow ab\dots)|^2 e^{(\mu_i + \mu_j + \dots)/T} f_a^{eq} \frac{1 + \eta_a f_a}{1 + \eta_a f_a^{eq}} e^{-(\mu_b + \mu_c + \dots)/T} f_b f_c \dots] \\
& \times (1 + \eta_i f_i) (1 + \eta_j f_j) \dots, \\
\equiv & \left[F_{ab\dots ij\dots} f_a f_b \dots - \overline{F_{ab\dots ij\dots}} e^{(\mu_i + \mu_j + \dots)/T} f_a^{eq} \frac{1 + \eta_a f_a}{1 + \eta_a f_a^{eq}} e^{-(\mu_b + \mu_c + \dots)/T} f_b f_c \dots \right] \\
& \times (1 + \eta_i f_i) (1 + \eta_j f_j) \dots, \tag{B.30}
\end{aligned}$$

where $F_{ab\dots ij\dots}$ and $\overline{F_{ab\dots ij\dots}}$ are shorthand notations with the following meaning:

$$\begin{aligned}
F_{ab\dots ij\dots}(\dots) & \equiv \Lambda_{ab\dots}^{ij\dots} |\mathcal{M}(ab\dots \rightarrow ij\dots)|^2(\dots), \\
\overline{F_{ab\dots ij\dots}}(\dots) & \equiv \Lambda_{ab\dots}^{ij\dots} |\mathcal{M}(ij\dots \rightarrow ab\dots)|^2(\dots). \tag{B.31}
\end{aligned}$$

Notice that CPT invariance implies $\overline{F_{ab\dots ij\dots}}(\dots) = F_{ab\dots ij\dots}(\dots)$.

Now by expanding $f_{b,\dots,i,j,\dots}$ in chemical potentials as in (B.20) and after some rearrangements, we have

$$\begin{aligned}
& [ab\dots \leftrightarrow ij\dots] \\
= & \left[F_{ab\dots ij\dots} f_a \left(f_b^{eq} + f_b^{eq,2} e^{E_b/T} \frac{\mu_b}{T} \right) \dots \right. \\
& - \overline{F_{ab\dots ij\dots}} f_a^{eq} \frac{1 + \eta_a f_a}{1 + \eta_a f_a^{eq}} f_b^{eq} f_c^{eq} \dots \left(1 + f_b^{eq} e^{E_b/T} \frac{\mu_b}{T} + f_c^{eq} e^{E_c/T} \frac{\mu_c}{T} + \dots \right) \\
& \left. - \overline{F_{ab\dots ij\dots}} \left(\frac{\mu_i + \mu_j + \dots}{T} - \frac{\mu_b + \mu_c + \dots}{T} \right) f_a^{eq} \frac{1 + \eta_a f_a}{1 + \eta_a f_a^{eq}} f_b^{eq} f_c^{eq} \dots \right] \\
& \times (1 + \eta_i f_i^{eq}) (1 + \eta_j f_j^{eq}) \dots \\
& + \left[F_{ab\dots ij\dots} f_a f_b^{eq} \dots - \overline{F_{ab\dots ij\dots}} f_a^{eq} \frac{1 + \eta_a f_a}{1 + \eta_a f_a^{eq}} f_b^{eq} f_c^{eq} \dots \right] \\
& \times (1 + \eta_i f_i^{eq}) (1 + \eta_j f_j^{eq}) \dots \\
& \times \left(\eta_i f_i^{eq} \frac{\mu_i}{T} + \eta_j f_j^{eq} \frac{\mu_j}{T} + \dots \right) + \mathcal{O} \left[\left(\frac{\mu}{T} \right)^2 \right], \tag{B.32}
\end{aligned}$$

where we have used the following identity

$$\begin{aligned}
(1 + \eta_i f_i) (1 + \eta_j f_j) \dots &= (1 + \eta_i f_i^{eq}) (1 + \eta_j f_j^{eq}) \dots \\
&\times \left(1 + \frac{\eta_i f_i^{eq,2} e^{E_i/T} \frac{\mu_i}{T}}{1 + \eta_i f_i^{eq}} + \frac{\eta_j f_j^{eq,2} e^{E_j/T} \frac{\mu_j}{T}}{1 + \eta_j f_j^{eq}} + \dots \right), \\
&= (1 + \eta_i f_i^{eq}) (1 + \eta_j f_j^{eq}) \dots \\
&\times \left(1 + \eta_i f_i^{eq} \frac{\mu_i}{T} + \eta_j f_j^{eq} \frac{\mu_j}{T} + \dots \right). \tag{B.33}
\end{aligned}$$

For example, making used of eq. (B.32) for the decay $a \rightarrow ij$ where a is out of kinetic equilibrium with $\mu_a = 0$, we have

$$\begin{aligned}
[a \leftrightarrow ij] &= \left[F_{aij} f_a - \overline{F_{aij}} f_a^{eq} \frac{1 + \eta_a f_a}{1 + \eta_a f_a^{eq}} - \overline{F_{aij}} \frac{\mu_i + \mu_j}{T} f_a^{eq} \frac{1 + \eta_a f_a}{1 + \eta_a f_a^{eq}} \right] \\
&\times (1 + \eta_i f_i^{eq}) (1 + \eta_j f_j^{eq}) \\
&+ \left[F_{aij} f_a - \overline{F_{aij}} f_a^{eq} \frac{1 + \eta_a f_a}{1 + \eta_a f_a^{eq}} \right] (1 + \eta_i f_i^{eq}) (1 + \eta_j f_j^{eq}) \\
&\times \left(\eta_i f_i^{eq} \frac{\mu_i}{T} + \eta_j f_j^{eq} \frac{\mu_j}{T} \right). \tag{B.34}
\end{aligned}$$

Applying eq. (B.32) for the scattering $ab \rightarrow ij$ where a is out of kinetic

equilibrium with $\mu_a = 0$, we have

$$\begin{aligned}
[ab \leftrightarrow ij] &= \left[\left(F_{abij} f_a - \overline{F_{abij}} f_a^{eq} \frac{1 + \eta_a f_a}{1 + \eta_a f_a^{eq}} \right) \left(1 + f_b^{eq} e^{E_b/T} \frac{\mu_b}{T} \right) \right. \\
&\quad \left. - \overline{F_{abij}} \left(\frac{\mu_i + \mu_j}{T} - \frac{\mu_b}{T} \right) f_a^{eq} \frac{1 + \eta_a f_a}{1 + \eta_a f_a^{eq}} \right] f_b^{eq} (1 + \eta_i f_i^{eq}) (1 + \eta_j f_j^{eq}) \\
&\quad + \left[F_{abij} f_a - \overline{F_{abij}} f_a^{eq} \frac{1 + \eta_a f_a}{1 + \eta_a f_a^{eq}} \right] f_b^{eq} (1 + \eta_i f_i^{eq}) (1 + \eta_j f_j^{eq}) \\
&\quad \times \left(\eta_i f_i^{eq} \frac{\mu_i}{T} + \eta_j f_j^{eq} \frac{\mu_j}{T} \right). \tag{B.35}
\end{aligned}$$

B.1.2 All particles in kinetic equilibrium with nonzero chemical potentials

Assuming that particles $ab\dots ij\dots$ have kinetic equilibrium distributions with corresponding chemical potential $\mu_{a,b,\dots,i,j,\dots}$, we have

$$\begin{aligned}
& f_i f_j \dots (1 + \eta_a f_a) (1 + \eta_b f_b) \dots \\
&= e^{-(E_i - \mu_i)/T} (1 + \eta_i f_i) e^{-(E_j - \mu_j)/T} (1 + \eta_j f_j) \dots (1 + \eta_a f_a) (1 + \eta_b f_b) \dots, \\
&= e^{(\mu_i + \mu_j + \dots)/T} (1 + \eta_i f_i) (1 + \eta_j f_j) \dots \\
&\quad \times e^{-\mu_a/T} e^{-(E_a - \mu_a)/T} (1 + \eta_a f_a) e^{-\mu_b/T} e^{-(E_b - \mu_b)/T} (1 + \eta_b f_b) \dots, \\
&= e^{(\mu_i + \mu_j + \dots)/T} (1 + \eta_i f_i) (1 + \eta_j f_j) \dots e^{-(\mu_a + \mu_b + \dots)/T} f_a f_b \dots, \tag{B.36}
\end{aligned}$$

where we have used conservation of energy $E_a + E_b + \dots = E_i + E_j + \dots$ and the identities (B.18).

Substituting (B.36) into the right hand side of (B.8), we have

$$\begin{aligned}
[ab\dots \leftrightarrow ij\dots] &= \Lambda_{ab\dots}^{ij\dots} \left[|\mathcal{M}(ab\dots \rightarrow ij\dots)|^2 f_a f_b \dots (1 + \eta_i f_i) (1 + \eta_j f_j) \dots \right. \\
&\quad \left. - |\mathcal{M}(ij\dots \rightarrow ab\dots)|^2 f_i f_j \dots (1 + \eta_a f_a) (1 + \eta_b f_b) \dots \right], \\
&= \Lambda_{ab\dots}^{ij\dots} \left[|\mathcal{M}(ab\dots \rightarrow ij\dots)|^2 f_a f_b \dots \right. \\
&\quad \left. - |\mathcal{M}(ij\dots \rightarrow ab\dots)|^2 e^{(\mu_i + \mu_j + \dots)/T} e^{-(\mu_a + \mu_b + \dots)/T} f_a f_b \dots \right] \\
&\quad \times (1 + \eta_i f_i) (1 + \eta_j f_j) \dots, \\
&= \left[F_{ab\dots ij\dots} - \overline{F_{ab\dots ij\dots}} e^{(\mu_i + \mu_j + \dots)/T} e^{-(\mu_a + \mu_b + \dots)/T} \right] f_a f_b \dots \\
&\quad \times (1 + \eta_i f_i) (1 + \eta_j f_j) \dots, \tag{B.37}
\end{aligned}$$

where we used the notations (B.31).

Now if we further expand $f_{a,b,\dots,i,j,\dots}$ in chemical potentials as in (B.20), we have

$$\begin{aligned}
& [ab\dots \leftrightarrow ij\dots] \\
= & \left(F_{ab\dots ij\dots} - \overline{F_{ab\dots ij\dots}} \right) \\
& \times \left(1 + f_a^{eq} e^{E_a/T} \frac{\mu_a}{T} + f_b^{eq} e^{E_b/T} \frac{\mu_b}{T} + \dots \right) f_a^{eq} f_b^{eq} \dots (1 + \eta_i f_i^{eq}) (1 + \eta_j f_j^{eq}) \dots \\
& - \overline{F_{ab\dots ij\dots}} \left(\frac{\mu_i + \mu_j + \dots}{T} - \frac{\mu_a + \mu_b + \dots}{T} \right) f_a^{eq} f_b^{eq} \dots \\
& \times (1 + \eta_i f_i^{eq}) (1 + \eta_j f_j^{eq}) \dots \\
& + \left(F_{ab\dots ij\dots} - \overline{F_{ab\dots ij\dots}} \right) f_a^{eq} f_b^{eq} \dots (1 + \eta_i f_i^{eq}) (1 + \eta_j f_j^{eq}) \dots \\
& \times \left(\eta_i f_i^{eq} \frac{\mu_i}{T} + \eta_j f_j^{eq} \frac{\mu_j}{T} + \dots \right) + \mathcal{O} \left[\left(\frac{\mu}{T} \right)^2 \right]. \tag{B.38}
\end{aligned}$$

For example, applying eq. (B.38) for a scattering process with $ab \leftrightarrow ij$ where all the particles are in kinetic equilibrium with nonzero chemical potentials, we have

$$\begin{aligned}
[ab \leftrightarrow ij] &= \left(F_{abij} - \overline{F_{abij}} \right) \left(1 + f_a^{eq} e^{E_a/T} \frac{\mu_a}{T} + f_b^{eq} e^{E_b/T} \frac{\mu_b}{T} \right) \\
&\times f_a^{eq} f_b^{eq} (1 + \eta_i f_i^{eq}) (1 + \eta_j f_j^{eq}) \\
&- \overline{F_{abij}} \left(\frac{\mu_i + \mu_j}{T} - \frac{\mu_a + \mu_b}{T} \right) \\
&\times f_a^{eq} f_b^{eq} (1 + \eta_i f_i^{eq}) (1 + \eta_j f_j^{eq}) \\
&+ \left(F_{abij} - \overline{F_{abij}} \right) f_a^{eq} f_b^{eq} (1 + \eta_i f_i^{eq}) (1 + \eta_j f_j^{eq}) \\
&\times \left(\eta_i f_i^{eq} \frac{\mu_i}{T} + \eta_j f_j^{eq} \frac{\mu_j}{T} \right). \tag{B.39}
\end{aligned}$$

B.1.3 Relation between chemical potential and particle density asymmetry

If we assume $\mu_{F,B}/T \ll 1$, from (B.20) we have

$$\begin{aligned}
f_{F+} - f_{F-} &= \frac{2e^{E_F/T}}{(e^{E_F/T} + 1)^2} \frac{\mu_F}{T} + \mathcal{O}\left[\left(\frac{\mu_F}{T}\right)^3\right], \\
&= 2(1 - f_F^{eq}) f_F^{eq} \frac{\mu_F}{T} + \mathcal{O}\left[\left(\frac{\mu_F}{T}\right)^3\right], \\
f_{B+} - f_{B-} &= \frac{2e^{E_B/T}}{(e^{E_B/T} - 1)^2} \frac{\mu_B}{T} + \mathcal{O}\left[\left(\frac{\mu_B}{T}\right)^3\right], \\
&= 2(1 + f_B^{eq}) f_B^{eq} \frac{\mu_B}{T} + \mathcal{O}\left[\left(\frac{\mu_B}{T}\right)^3\right].
\end{aligned} \tag{B.40}$$

Using eq. (B.7), we have that the difference between number densities of massless particles and antiparticles at leading order in chemical potentials is

$$\begin{aligned}
n_{\Delta F} &\equiv n_F - n_{\bar{F}} = \frac{g_F}{6} T^3 \frac{\mu_F}{T}, \\
n_{\Delta B} &\equiv n_B - n_{\bar{B}} = \frac{g_B}{3} T^3 \frac{\mu_B}{T}.
\end{aligned} \tag{B.41}$$

Normalizing the number density asymmetries $n_{\Delta F,B}$ to the entropy density s , $Y_{\Delta F,B} \equiv n_{\Delta F,B}/s$, we can rewrite the chemical potentials for massless fermions and bosons in terms of the asymmetries

$$\begin{aligned}
2\frac{\mu_F}{T} &= \frac{8\pi^2 g_s^*}{15g_F} Y_{\Delta F} \equiv \frac{Y_{\Delta F}}{Y_F^{eq}}, \\
2\frac{\mu_B}{T} &= \frac{4\pi^2 g_s^*}{15g_B} Y_{\Delta B} \equiv \frac{Y_{\Delta B}}{Y_B^{eq}},
\end{aligned} \tag{B.42}$$

where $Y_F^{eq} \equiv \frac{15g_F}{8\pi^2 g_s^*}$ and $Y_B^{eq} \equiv \frac{15g_B}{4\pi^2 g_s^*}$.

B.2 Boltzmann Equations for Soft Leptogenesis

Using the result from Appendix B.1, we will now derive the BEs for the number densities which describe the dynamics of SL. Because of the thermal-statistical

nature of the CP asymmetry in SL, in principle, the full treatment requires the use of the BEs for the particle distribution functions eq. (B.2) and not the integrated BEs for the number densities (equivalently the abundances) eq. (B.8).

In Appendix B.2.2.1, we will identify the minimum set of consistent assumptions that allow to keep the statistical factors that are required for SL, but that also allow to write the equations in terms of number densities.

In the following, we will first write down all the relevant unflavored BEs by keeping up to order $\mathcal{O}\left(\frac{\mu}{T}\right)$. After that, we will generalize to the flavored BEs.

B.2.1 Definitions

First, we define the thermally averaged decay reaction densities for right-handed sneutrinos \tilde{N}_\pm as

$$\begin{aligned}\gamma_{\tilde{N}_\pm}^f &\equiv \left(F_{\tilde{N}_\pm \tilde{H}_u \ell} + F_{\tilde{N}_\pm \overline{\tilde{H}_u \bar{\ell}}}\right) f_{\tilde{N}_\pm}^{eq} (1 - f_\ell^{eq}) \left(1 - f_{\tilde{H}_u}^{eq}\right), \\ \gamma_{\tilde{N}_\pm}^s &\equiv \left(F_{\tilde{N}_\pm H_u \tilde{\ell}} + F_{\tilde{N}_\pm H_u^* \tilde{\ell}^*}\right) f_{\tilde{N}_\pm}^{eq} \left(1 + f_{\tilde{\ell}}^{eq}\right) \left(1 + f_{H_u}^{eq}\right),\end{aligned}\quad (\text{B.43})$$

where the F 's are defined as in eq. (B.31). Let us also define the decay densities into scalars and fermions as follows

$$\begin{aligned}\gamma_{\tilde{N}}^f &\equiv \gamma_{\tilde{N}_+}^f + \gamma_{\tilde{N}_-}^f, \\ \gamma_{\tilde{N}}^s &\equiv \gamma_{\tilde{N}_+}^s + \gamma_{\tilde{N}_-}^s, \\ \gamma_{\tilde{N}} &\equiv \gamma_{\tilde{N}}^f + \gamma_{\tilde{N}}^s.\end{aligned}\quad (\text{B.44})$$

The CP asymmetries from \tilde{N}_\pm decays are defined as follows

$$\epsilon_\pm^f(T) \equiv \frac{\left(F_{\tilde{N}_\pm \tilde{H}_u \ell} - F_{\tilde{N}_\pm \overline{\tilde{H}_u \bar{\ell}}}\right) f_{\tilde{N}_\pm}^{eq} (1 - f_\ell^{eq}) \left(1 - f_{\tilde{H}_u}^{eq}\right)}{\gamma_{\tilde{N}}}, \quad (\text{B.45})$$

$$\epsilon_\pm^s(T) \equiv \frac{\left(F_{\tilde{N}_\pm H_u \tilde{\ell}} - F_{\tilde{N}_\pm H_u^* \tilde{\ell}^*}\right) f_{\tilde{N}_\pm}^{eq} \left(1 + f_{\tilde{\ell}}^{eq}\right) \left(1 + f_{H_u}^{eq}\right)}{\gamma_{\tilde{N}}}, \quad (\text{B.46})$$

and

$$\begin{aligned}
\epsilon^f(T) &\equiv \epsilon_+^f(T) + \epsilon_-^f(T), \\
\epsilon^s(T) &\equiv \epsilon_+^s(T) + \epsilon_-^s(T), \\
\epsilon(T) &\equiv \epsilon^f(T) + \epsilon^s(T).
\end{aligned} \tag{B.47}$$

For simplicity, we neglect CP asymmetries in scatterings (see Section 2.4.2.1 for discussion and references therein). Next, we define the decay reaction densities of right-handed neutrino N as

$$\begin{aligned}
\gamma_N^f &\equiv 2F_{NH_u\ell}f_N^{eq}(1-f_\ell^{eq})(1+f_{H_u}^{eq}), \\
\gamma_N^s &\equiv 2F_{N\tilde{H}_u\tilde{\ell}}f_N^{eq}\left(1+f_{\tilde{\ell}}^{eq}\right)\left(1-f_{\tilde{H}_u}^{eq}\right), \\
\gamma_N &\equiv \gamma_N^f + \gamma_N^s.
\end{aligned} \tag{B.48}$$

We also define the reaction densities for the interactions from the scalar potential as

$$\begin{aligned}
\gamma_{\tilde{N}_i}^{(3)} &\equiv F_{\tilde{N}_i\tilde{\ell}\tilde{u}\tilde{Q}^*}f_{\tilde{N}_i}^{eq}\left(1+f_{\tilde{\ell}}^{eq}\right)\left(1+f_{\tilde{u}}^{eq}\right)\left(1+f_{\tilde{Q}}^{eq}\right), \\
\gamma_{22_i} &\equiv F_{\tilde{N}_i\tilde{\ell}\tilde{u}^*\tilde{Q}}f_{\tilde{N}_i}^{eq}f_{\tilde{\ell}}^{eq}\left(1+f_{\tilde{u}}^{eq}\right)\left(1+f_{\tilde{Q}}^{eq}\right), \\
&= F_{\tilde{N}_i\tilde{Q}\tilde{\ell}\tilde{u}}f_{\tilde{N}_i}^{eq}f_{\tilde{Q}}^{eq}\left(1+f_{\tilde{u}}^{eq}\right)\left(1+f_{\tilde{\ell}}^{eq}\right), \\
&= F_{\tilde{N}_i\tilde{u}^*\tilde{\ell}\tilde{Q}^*}f_{\tilde{N}_i}^{eq}f_{\tilde{u}}^{eq}\left(1+f_{\tilde{\ell}}^{eq}\right)\left(1+f_{\tilde{Q}}^{eq}\right).
\end{aligned} \tag{B.49}$$

In addition we define their sum as

$$\begin{aligned}
\gamma_{\tilde{N}}^{(3)} &\equiv \gamma_{\tilde{N}_+}^{(3)} + \gamma_{\tilde{N}_-}^{(3)}, \\
\gamma_{22} &\equiv \gamma_{22_+} + \gamma_{22_-}.
\end{aligned} \tag{B.50}$$

Ignoring the thermal masses, we define the reaction densities for scatterings

of RHN and RHSN with top and stop respectively as follows

$$\begin{aligned}
\gamma_t^{(0)} &\equiv F_{N\tilde{\ell}Q\tilde{u}^*} f_N^{eq} f_{\tilde{\ell}}^{eq} (1 - f_Q^{eq}) (1 + f_{\tilde{u}}^{eq}), \\
&= F_{N\tilde{\ell}\tilde{Q}\tilde{u}} f_N^{eq} f_{\tilde{\ell}}^{eq} (1 + f_{\tilde{Q}}^{eq}) (1 - f_u^{eq}), \\
\gamma_t^{(1)} &\equiv F_{N\tilde{Q}\tilde{\ell}^*\tilde{u}^*} f_N^{eq} f_{\tilde{Q}}^{eq} (1 + f_{\tilde{\ell}}^{eq}) (1 + f_{\tilde{u}}^{eq}), \\
&= F_{Nu\tilde{\ell}^*\tilde{Q}} f_N^{eq} f_u^{eq} (1 + f_{\tilde{\ell}}^{eq}) (1 + f_{\tilde{Q}}^{eq}), \\
\gamma_t^{(2)} &\equiv F_{N\tilde{u}\tilde{\ell}^*Q} f_N^{eq} f_{\tilde{u}}^{eq} (1 + f_{\tilde{\ell}}^{eq}) (1 - f_Q^{eq}), \\
&= F_{N\tilde{Q}^*\tilde{\ell}^*\tilde{u}} f_N^{eq} f_{\tilde{Q}}^{eq} (1 + f_{\tilde{\ell}}^{eq}) (1 - f_u^{eq}), \\
\gamma_t^{(3)} &\equiv F_{N\ell Q\bar{u}} f_N^{eq} f_{\ell}^{eq} (1 - f_Q^{eq}) (1 - f_u^{eq}), \\
\gamma_t^{(4)} &\equiv F_{Nu\bar{\ell}Q} f_N^{eq} f_u^{eq} (1 - f_{\ell}^{eq}) (1 - f_Q^{eq}), \\
&= F_{N\bar{Q}\bar{\ell}\bar{u}} f_N^{eq} f_Q^{eq} (1 - f_{\ell}^{eq}) (1 - f_u^{eq}),
\end{aligned} \tag{B.51}$$

and

$$\begin{aligned}
\gamma_{t\pm}^{(5)} &\equiv F_{\tilde{N}_{\pm}\ell Q\tilde{u}^*} f_{\tilde{N}_{\pm}}^{eq} f_{\ell}^{eq} (1 - f_Q^{eq}) (1 + f_{\tilde{u}}^{eq}), \\
&= F_{\tilde{N}_{\pm}\tilde{\ell}\tilde{Q}\tilde{u}} f_{\tilde{N}_{\pm}}^{eq} f_{\tilde{\ell}}^{eq} (1 + f_{\tilde{Q}}^{eq}) (1 - f_u^{eq}), \\
\gamma_{t\pm}^{(6)} &\equiv F_{\tilde{N}_{\pm}\tilde{u}^*\tilde{\ell}Q} f_{\tilde{N}_{\pm}}^{eq} f_{\tilde{u}}^{eq} (1 - f_{\ell}^{eq}) (1 - f_Q^{eq}), \\
&= F_{\tilde{N}_{\pm}\tilde{Q}^*\tilde{\ell}\bar{u}} f_{\tilde{N}_{\pm}}^{eq} f_{\tilde{Q}}^{eq} (1 - f_{\ell}^{eq}) (1 - f_u^{eq}), \\
\gamma_{t\pm}^{(7)} &\equiv F_{N_{\pm}\ell Q\bar{u}} f_{N_{\pm}}^{eq} f_{\ell}^{eq} (1 - f_Q^{eq}) (1 - f_u^{eq}), \\
\gamma_{t\pm}^{(8)} &\equiv F_{N_{\pm}u\bar{\ell}Q} f_{N_{\pm}}^{eq} f_u^{eq} (1 - f_{\ell}^{eq}) (1 - f_Q^{eq}), \\
&= F_{N_{\pm}\bar{Q}\bar{\ell}\bar{u}} f_{N_{\pm}}^{eq} f_Q^{eq} (1 - f_{\ell}^{eq}) (1 - f_u^{eq}), \\
\gamma_{t\pm}^{(9)} &\equiv F_{N_{\pm}u\bar{\ell}Q} f_{N_{\pm}}^{eq} f_u^{eq} (1 - f_{\ell}^{eq}) (1 - f_Q^{eq}), \\
&= F_{N_{\pm}\bar{Q}\bar{\ell}\bar{u}} f_{N_{\pm}}^{eq} f_Q^{eq} (1 - f_{\ell}^{eq}) (1 - f_u^{eq}).
\end{aligned} \tag{B.52}$$

We also define their sum as

$$\gamma_t^{(n)} \equiv \gamma_{t+}^{(n)} + \gamma_{t-}^{(n)} \quad \text{for } n = 5, \dots, 9. \tag{B.53}$$

Finally, we define the reaction densities for gaugino exchange which will

result in superequilibration

$$\gamma_{\tilde{g}}^{\text{eff}} \equiv F_{\ell\tilde{\ell}\tilde{\ell}} f_{\ell}^{\text{eq},2} \left(1 + f_{\tilde{\ell}}^{\text{eq}}\right)^2. \quad (\text{B.54})$$

Notice that all the reaction densities defined above are summed over $SU(2)_L$ components. In the next section, all the number densities on the right hand side of the BEs of leptons and sleptons will be defined as summed over $SU(2)_L$ as well e.g. $Y_{\ell} = Y_e + Y_{\nu_e}$.

B.2.2 Derivations of unflavored Boltzmann equations

In this section, we first introduce the following notations

$$\begin{aligned} [ab \leftrightarrow ij]_+ &\equiv [ab \leftrightarrow ij] + [\bar{a}\bar{b} \leftrightarrow \bar{i}\bar{j}], \\ [ab \leftrightarrow ij]_- &\equiv [ab \leftrightarrow ij] - [\bar{a}\bar{b} \leftrightarrow \bar{i}\bar{j}]. \end{aligned} \quad (\text{B.55})$$

The BE for the right-handed neutrino N can be written down as follows

$$\begin{aligned} sHz \frac{dY_N}{dz} &= - [N \leftrightarrow \tilde{H}_u \tilde{\ell}]_+ - [N \leftrightarrow H_u \ell]_+ \\ &\quad - [N \tilde{\ell} \leftrightarrow Q \tilde{u}^*]_+ - [N \tilde{\ell} \leftrightarrow \tilde{Q} \bar{u}]_+ - [N \bar{Q} \leftrightarrow \tilde{\ell}^* \tilde{u}^*]_+ \\ &\quad - [N u \leftrightarrow \tilde{\ell}^* \tilde{Q}]_+ - [N \tilde{u} \leftrightarrow \tilde{\ell}^* Q]_+ - [N \tilde{Q}^* \leftrightarrow \tilde{\ell}^* \bar{u}]_+ \\ &\quad - [N \ell \leftrightarrow Q \bar{u}]_+ - [N u \leftrightarrow \bar{\ell} Q]_+ - [N \bar{Q} \leftrightarrow \bar{\ell} \bar{u}]_+, \\ &= 2\tilde{F}_N \left(\frac{f_N}{f_N^{\text{eq}}} - \frac{1-f_N}{1-f_N^{\text{eq}}} \right) + 2F_N \left(\frac{f_N}{f_N^{\text{eq}}} - \frac{1-f_N}{1-f_N^{\text{eq}}} \right) \\ &\quad + (4F^{(0)} + 4F^{(1)} + 4F^{(2)} + 2F^{(3)} + 4F^{(4)}) \\ &\quad \times \left(\frac{f_N}{f_N^{\text{eq}}} - \frac{1-f_N}{1-f_N^{\text{eq}}} \right), \end{aligned} \quad (\text{B.56})$$

where we have used the following shorthand notations:

$$\begin{aligned} \tilde{F}_N(\dots) &\equiv F_{N\tilde{H}_u\tilde{\ell}} f_N^{\text{eq}} \left(1 + f_{\tilde{\ell}}^{\text{eq}}\right) \left(1 - f_{\tilde{H}_u}^{\text{eq}}\right) (\dots), \\ F_N(\dots) &\equiv F_{NH_u\ell} f_N^{\text{eq}} \left(1 - f_{\ell}^{\text{eq}}\right) \left(1 + f_{H_u}^{\text{eq}}\right) (\dots). \end{aligned} \quad (\text{B.57})$$

For the top and stop scatterings, we ignore the thermal masses and hence

we have the following relations

$$\begin{aligned}
F^{(0)}(\dots) &\equiv F_{N\tilde{Q}\tilde{u}^*} f_N^{eq} f_{\tilde{\ell}}^{eq} (1 - f_Q^{eq}) (1 + f_{\tilde{u}}^{eq}) (\dots), \\
&= F_{N\tilde{Q}\tilde{u}} f_N^{eq} f_{\tilde{\ell}}^{eq} (1 + f_{\tilde{Q}}^{eq}) (1 - f_u^{eq}) (\dots), \\
F^{(1)}(\dots) &\equiv F_{N\tilde{Q}\tilde{\ell}^*\tilde{u}^*} f_N^{eq} f_{\tilde{Q}}^{eq} (1 + f_{\tilde{\ell}}^{eq}) (1 + f_{\tilde{u}}^{eq}) (\dots), \\
&= F_{N\tilde{u}\tilde{\ell}^*\tilde{Q}} f_N^{eq} f_u^{eq} (1 + f_{\tilde{\ell}}^{eq}) (1 + f_{\tilde{Q}}^{eq}) (\dots), \\
F^{(2)}(\dots) &\equiv F_{N\tilde{u}\tilde{\ell}^*Q} f_N^{eq} f_{\tilde{u}}^{eq} (1 + f_{\tilde{\ell}}^{eq}) (1 - f_Q^{eq}) (\dots), \\
&= F_{N\tilde{Q}\tilde{\ell}^*\tilde{u}} f_N^{eq} f_{\tilde{Q}}^{eq} (1 + f_{\tilde{\ell}}^{eq}) (1 - f_u^{eq}) (\dots), \\
F^{(3)}(\dots) &\equiv F_{N\tilde{\ell}Q\tilde{u}} f_N^{eq} f_{\tilde{\ell}}^{eq} (1 - f_Q^{eq}) (1 - f_u^{eq}) (\dots), \\
F^{(4)}(\dots) &\equiv F_{N\tilde{u}\tilde{\ell}Q} f_N^{eq} f_u^{eq} (1 - f_{\tilde{\ell}}^{eq}) (1 - f_Q^{eq}) (\dots), \\
&= F_{N\tilde{Q}\tilde{\ell}u} f_N^{eq} f_{\tilde{Q}}^{eq} (1 - f_{\tilde{\ell}}^{eq}) (1 - f_u^{eq}) (\dots). \tag{B.58}
\end{aligned}$$

The BE for the right-handed sneutrino \tilde{N}_{\pm} can be written down as follows

$$\begin{aligned}
sHz \frac{dY_{\tilde{N}_{\pm}}}{dz} &= - \left[\tilde{N}_{\pm} \leftrightarrow \tilde{H}_u \ell \right]_+ - \left[\tilde{N}_{\pm} \leftrightarrow H_u \tilde{\ell} \right]_+ - \left[\tilde{N}_{\pm} \leftrightarrow \tilde{\ell} \tilde{u} \tilde{Q}^* \right]_+ \\
&\quad - \left[\tilde{N}_{\pm} \tilde{\ell} \leftrightarrow \tilde{u}^* \tilde{Q} \right]_+ - \left[\tilde{N}_{\pm} \tilde{Q} \leftrightarrow \tilde{\ell} \tilde{u} \right]_+ - \left[\tilde{N}_{\pm} \tilde{u} \leftrightarrow \tilde{\ell}^* \tilde{Q} \right]_+ \\
&\quad - \left[\tilde{N}_{\pm} \ell \leftrightarrow Q \tilde{u}^* \right]_+ - \left[\tilde{N}_{\pm} \ell \leftrightarrow \tilde{Q} \tilde{u} \right]_+ - \left[\tilde{N}_{\pm} \tilde{u} \leftrightarrow \tilde{\ell} Q \right]_+ \\
&\quad - \left[\tilde{N}_{\pm} \tilde{Q}^* \leftrightarrow \tilde{\ell} \tilde{u} \right]_+ - \left[\tilde{N}_{\pm} \tilde{Q} \leftrightarrow \tilde{\ell} \tilde{u}^* \right]_+ - \left[\tilde{N}_{\pm} u \leftrightarrow \tilde{\ell} \tilde{Q} \right]_+ \\
&\quad - \left[\tilde{N}_{\pm} \tilde{\ell}^* \leftrightarrow \tilde{Q} u \right]_+ - \left[\tilde{N}_{\pm} Q \leftrightarrow \tilde{\ell} u \right]_+ - \left[\tilde{N}_{\pm} \tilde{u} \leftrightarrow \tilde{\ell} \tilde{Q} \right]_+, \\
&= - \left(F_{\tilde{N}_{\pm}} + \tilde{F}_{\tilde{N}_{\pm}} + 2\tilde{F}_{\tilde{N}_{\pm}}^{(3)} + 6F_{22\pm} \right) \left(\frac{f_{\tilde{N}_{\pm}}}{f_{\tilde{N}_{\pm}}^{eq}} - \frac{1 + f_{\tilde{N}_{\pm}}}{1 + f_{\tilde{N}_{\pm}}^{eq}} \right) \\
&\quad - 2 \left(2F_{\pm}^{(5)} + 2F_{\pm}^{(6)} + 2F_{\pm}^{(7)} + F_{\pm}^{(8)} + 2F_{\pm}^{(9)} \right) \\
&\quad \times \left(\frac{f_{N_{\pm}}}{f_{N_{\pm}}^{eq}} - \frac{1 + f_{\tilde{N}_{\pm}}}{1 + f_{\tilde{N}_{\pm}}^{eq}} \right), \tag{B.59}
\end{aligned}$$

where we have dropped terms of order $\mathcal{O}(\epsilon \frac{\mu}{T})$, and we have used the following

shorthand notations

$$\begin{aligned}
F_{\tilde{N}_\pm}(\dots) &\equiv \left(F_{\tilde{N}_\pm \tilde{H}_u \ell} + F_{\tilde{N}_\pm \overline{\tilde{H}_u \tilde{\ell}}} \right) f_{\tilde{N}_\pm}^{eq} (1 - f_\ell^{eq}) \left(1 - f_{\tilde{H}_u}^{eq} \right) (\dots), \\
\tilde{F}_{\tilde{N}_\pm}(\dots) &\equiv \left(F_{\tilde{N}_\pm H_u \tilde{\ell}} + F_{\tilde{N}_\pm H_u^* \tilde{\ell}^*} \right) f_{\tilde{N}_\pm}^{eq} \left(1 + f_{\tilde{\ell}}^{eq} \right) \left(1 + f_{H_u}^{eq} \right) (\dots), \\
\tilde{F}_{\tilde{N}_\pm}^{(3)}(\dots) &\equiv F_{\tilde{N}_\pm \tilde{\ell} \tilde{Q}^*} f_{\tilde{N}_\pm}^{eq} \left(1 + f_{\tilde{\ell}}^{eq} \right) \left(1 + f_{\tilde{u}}^{eq} \right) \left(1 + f_{\tilde{Q}}^{eq} \right) (\dots). \quad (\text{B.60})
\end{aligned}$$

We ignore thermal masses and use the following relations

$$\begin{aligned}
F_{22_\pm}(\dots) &\equiv F_{\tilde{N}_\pm \tilde{\ell} \tilde{u}^* \tilde{Q}} f_{\tilde{N}_\pm}^{eq} f_{\tilde{\ell}}^{eq} (1 + f_{\tilde{u}}^{eq}) \left(1 + f_{\tilde{Q}}^{eq} \right) (\dots), \\
&= F_{\tilde{N}_\pm \tilde{Q} \tilde{\ell} \tilde{u}} f_{\tilde{N}_\pm}^{eq} f_{\tilde{Q}}^{eq} (1 + f_{\tilde{u}}^{eq}) \left(1 + f_{\tilde{\ell}}^{eq} \right) (\dots), \\
&= F_{\tilde{N}_\pm \tilde{u}^* \tilde{\ell} \tilde{Q}^*} f_{\tilde{N}_\pm}^{eq} f_{\tilde{u}}^{eq} \left(1 + f_{\tilde{\ell}}^{eq} \right) \left(1 + f_{\tilde{Q}}^{eq} \right) (\dots), \quad (\text{B.61})
\end{aligned}$$

and

$$\begin{aligned}
F_{\pm}^{(5)}(\dots) &\equiv F_{\tilde{N}_\pm \ell \tilde{Q} \tilde{u}^*} f_{\tilde{N}_\pm}^{eq} f_\ell^{eq} (1 - f_Q^{eq}) (1 + f_{\tilde{u}}^{eq}) (\dots), \\
&= F_{\tilde{N}_\pm \ell \tilde{Q} \tilde{u}} f_{\tilde{N}_\pm}^{eq} f_\ell^{eq} \left(1 + f_{\tilde{Q}}^{eq} \right) (1 - f_u^{eq}) (\dots), \\
F_{\pm}^{(6)}(\dots) &\equiv F_{\tilde{N}_\pm \tilde{u}^* \tilde{\ell} \tilde{Q}} f_{\tilde{N}_\pm}^{eq} f_{\tilde{u}}^{eq} (1 - f_\ell^{eq}) (1 - f_Q^{eq}) (\dots), \\
&= F_{\tilde{N}_\pm \tilde{Q}^* \tilde{\ell} \tilde{u}} f_{\tilde{N}_\pm}^{eq} f_{\tilde{Q}}^{eq} (1 - f_\ell^{eq}) (1 - f_u^{eq}) (\dots), \\
F_{\pm}^{(7)}(\dots) &\equiv F_{N_\pm \ell \tilde{Q} \tilde{u}} f_{N_\pm}^{eq} f_\ell^{eq} (1 - f_Q^{eq}) (1 - f_u^{eq}) (\dots), \\
F_{\pm}^{(8)}(\dots) &\equiv F_{N_\pm u \tilde{\ell} \tilde{Q}} f_{N_\pm}^{eq} f_u^{eq} (1 - f_\ell^{eq}) (1 - f_Q^{eq}) (\dots), \\
&= F_{N_\pm \tilde{Q} \tilde{\ell} \tilde{u}} f_{N_\pm}^{eq} f_{\tilde{Q}}^{eq} (1 - f_\ell^{eq}) (1 - f_u^{eq}) (\dots), \\
F_{\pm}^{(9)}(\dots) &\equiv F_{N_\pm u \tilde{\ell} \tilde{Q}} f_{N_\pm}^{eq} f_u^{eq} (1 - f_\ell^{eq}) (1 - f_Q^{eq}) (\dots), \\
&= F_{N_\pm \tilde{Q} \tilde{\ell} \tilde{u}} f_{N_\pm}^{eq} f_{\tilde{Q}}^{eq} (1 - f_\ell^{eq}) (1 - f_u^{eq}) (\dots). \quad (\text{B.62})
\end{aligned}$$

The BE for the lepton asymmetry $Y_{\Delta\ell} \equiv Y_\ell - Y_{\tilde{\ell}}$ can be written down as

follows

$$\begin{aligned}
sHz \frac{dY_{\Delta\ell}}{dz} &= \sum_{i=\pm} \left[\tilde{N}_i \leftrightarrow \tilde{H}_u \ell \right]_- - \sum_{ij} \left[\tilde{H}_u \ell \leftrightarrow ij \right]_-^{\text{sub}} \\
&+ [N \leftrightarrow H_u \ell]_- - [\ell \ell \leftrightarrow \tilde{\ell} \tilde{\ell}]_- \\
&- [N \ell \leftrightarrow Q \bar{u}]_- - [Nu \leftrightarrow \bar{\ell} Q]_- - [N \bar{Q} \leftrightarrow \bar{\ell} \bar{u}]_- \\
&- \sum_{i=\pm} \left(\left[\tilde{N}_i \ell \leftrightarrow Q \tilde{u}^* \right]_- + \left[\tilde{N}_i \ell \leftrightarrow \tilde{Q} \bar{u} \right]_- + \left[\tilde{N}_i \tilde{u} \leftrightarrow \bar{\ell} Q \right]_- \right. \\
&\left. + \left[\tilde{N}_i \tilde{Q}^* \leftrightarrow \bar{\ell} \bar{u} \right]_- + \left[\tilde{N}_i \bar{Q} \leftrightarrow \bar{\ell} \tilde{u}^* \right]_- + \left[\tilde{N}_i u \leftrightarrow \bar{\ell} \tilde{Q} \right]_- \right), \\
&= \sum_{i=\pm} \left\{ \left(F_{\tilde{N}_i \tilde{H}_u \ell} - F_{\tilde{N}_i \tilde{H}_u \bar{\ell}} \right) f_{\tilde{N}_i}^{eq} (1 - f_\ell^{eq}) (1 - f_{\tilde{H}_u}^{eq}) \left(\frac{f_{\tilde{N}_i}}{f_{\tilde{N}_i}^{eq}} - \frac{1 + f_{\tilde{N}_i}}{1 + f_{\tilde{N}_i}^{eq}} \right) \right. \\
&- F_{\tilde{N}_i} \left[\frac{f_{\tilde{N}_i}}{f_{\tilde{N}_i}^{eq}} f_\ell^{eq} + \frac{1 + f_{\tilde{N}_i}}{1 + f_{\tilde{N}_i}^{eq}} (1 - f_\ell^{eq}) \right] \frac{\mu_\ell}{T} \\
&- F_{\tilde{N}_i} \left[\frac{f_{\tilde{N}_i}}{f_{\tilde{N}_i}^{eq}} f_{\tilde{H}_u}^{eq} + \frac{1 + f_{\tilde{N}_i}}{1 + f_{\tilde{N}_i}^{eq}} (1 - f_{\tilde{H}_u}^{eq}) \right] \frac{\mu_{\tilde{H}_u}}{T} \left. \right\} \\
&- 2F_N \left[\frac{f_N}{f_N^{eq}} f_\ell^{eq} + \frac{1 - f_N}{1 - f_N^{eq}} (1 - f_\ell^{eq}) \right] \frac{\mu_\ell}{T} \\
&- 2F_N \left[-\frac{f_N}{f_N^{eq}} f_{H_u}^{eq} + \frac{1 - f_N}{1 - f_N^{eq}} (1 + f_{H_u}^{eq}) \right] \frac{\mu_{H_u}}{T} \\
&+ 4F_{\ell \tilde{\ell} \tilde{\ell}} \left(\frac{\mu_{\tilde{\ell}}}{T} - \frac{\mu_\ell}{T} \right) f_\ell^{eq,2} \left(1 + f_\ell^{eq} \right)^2 + S_t + W_{\Delta L=2}. \quad (\text{B.63})
\end{aligned}$$

In the above, $\sum_{ij} \left[\tilde{H}_u \ell \leftrightarrow ij \right]_-^{\text{sub}}$ refers to the sum of all possible $\Delta L = 2$ scatterings $\tilde{H}_u \ell \leftrightarrow ij$ and in particular, if they involve an exchange of \tilde{N}_\pm in the s-channel, the on-shell contributions $\tilde{H}_u \ell \leftrightarrow \tilde{N}_\pm \leftrightarrow ij$ are subtracted to avoid double counting. The $\Delta L = 2$ scatterings $\tilde{H}_u \ell \leftrightarrow ij$ with t- and u-channel exchange of \tilde{N}_\pm , and the leftover off-shell contribution for s-channel exchange of \tilde{N}_\pm are all collected in $W_{\Delta L=2}$. The detailed subtraction procedure is given in Section B.2.3. In the numerical calculation, we ignore $W_{\Delta L=2}$ since it is subdominant in the temperature range we are exploring ($T \lesssim 10^9$ GeV).

The top and stop scattering terms S_t in eq. (B.63) are given by

$$\begin{aligned}
S_t = & -2F^{(3)} \left[\frac{f_N}{f_N^{eq}} (1 - f_\ell^{eq}) + \frac{1 - f_N}{1 - f_N^{eq}} f_\ell^{eq} \right] \frac{\mu_\ell}{T} \\
& -4F^{(4)} \left[\frac{f_N}{f_N^{eq}} f_\ell^{eq} + \frac{1 - f_N}{1 - f_N^{eq}} (1 - f_\ell^{eq}) \right] \frac{\mu_\ell}{T} \\
& +2 \left(F^{(3)} + F^{(4)} \right) \left[\frac{f_N}{f_N^{eq}} f_Q^{eq} + \frac{1 - f_N}{1 - f_N^{eq}} (1 - f_Q^{eq}) \right] \frac{\mu_Q}{T} \\
& +2F^{(4)} \left[\frac{f_N}{f_N^{eq}} (1 - f_Q^{eq}) + \frac{1 - f_N}{1 - f_N^{eq}} f_Q^{eq} \right] \frac{\mu_Q}{T} \\
& - \sum_{i=\pm} \left\{ 4F_i^{(5)} \left[\frac{f_{\tilde{N}_i}}{f_{\tilde{N}_i}^{eq}} (1 - f_\ell^{eq}) + \frac{1 + f_{\tilde{N}_i}}{1 + f_{\tilde{N}_i}^{eq}} f_\ell^{eq} \right] \frac{\mu_\ell}{T} \right. \\
& +4 \left(F_i^{(6)} + F_i^{(7)} \right) \left[\frac{f_{\tilde{N}_i}}{f_{\tilde{N}_i}^{eq}} f_\ell^{eq} + \frac{1 + f_{\tilde{N}_i}}{1 + f_{\tilde{N}_i}^{eq}} (1 - f_\ell^{eq}) \right] \frac{\mu_\ell}{T} \\
& -2 \left(F_i^{(5)} + F_i^{(6)} \right) \left[\frac{f_{\tilde{N}_i}}{f_{\tilde{N}_i}^{eq}} f_Q^{eq} + \frac{1 + f_{\tilde{N}_i}}{1 + f_{\tilde{N}_i}^{eq}} (1 - f_Q^{eq}) \right] \frac{\mu_Q}{T} \\
& -2F_i^{(7)} \left[\frac{f_{\tilde{N}_i}}{f_{\tilde{N}_i}^{eq}} (1 - f_Q^{eq}) + \frac{1 + f_{\tilde{N}_i}}{1 + f_{\tilde{N}_i}^{eq}} f_Q^{eq} \right] \frac{\mu_Q}{T} \\
& -2 \left(F_i^{(5)} + F_i^{(7)} \right) \left[-\frac{f_{\tilde{N}_i}}{f_{\tilde{N}_i}^{eq}} f_{\tilde{Q}}^{eq} + \frac{1 + f_{\tilde{N}_i}}{1 + f_{\tilde{N}_i}^{eq}} (1 + f_{\tilde{Q}}^{eq}) \right] \frac{\mu_{\tilde{Q}}}{T} \\
& \left. -2F_i^{(6)} \left[\frac{f_{\tilde{N}_i}}{f_{\tilde{N}_i}^{eq}} (1 + f_{\tilde{Q}}^{eq}) - \frac{1 + f_{\tilde{N}_i}}{1 + f_{\tilde{N}_i}^{eq}} f_{\tilde{Q}}^{eq} \right] \frac{\mu_{\tilde{Q}}}{T} \right\} \\
& - (Q \rightarrow u) - (\tilde{Q} \rightarrow \tilde{u}), \tag{B.64}
\end{aligned}$$

where in the last line $(Q \rightarrow u)$ and $(\tilde{Q} \rightarrow \tilde{u})$ denote respectively the terms in which Q is replaced by u and \tilde{Q} is replaced by \tilde{u} .

The BE for the slepton asymmetry $Y_{\Delta\tilde{\ell}} \equiv Y_{\tilde{\ell}} - Y_{\tilde{\ell}^*}$ can be written down as

follows

$$\begin{aligned}
sHz \frac{dY_{\Delta\tilde{\ell}}}{dz} &= \sum_{i=\pm} \left[\tilde{N}_+ \leftrightarrow H_u \tilde{\ell} \right]_- - \sum_{ij} \left[H_u \tilde{\ell} \leftrightarrow ij \right]_-^{\text{sub}} \\
&+ \left[N \leftrightarrow \tilde{H}_u \tilde{\ell} \right]_- + \left[\ell\ell \leftrightarrow \tilde{\ell}\tilde{\ell} \right]_- \\
&+ \sum_i \left(\left[\tilde{N}_i \leftrightarrow \tilde{\ell}\tilde{u}\tilde{Q}^* \right]_- + \left[\tilde{N}_i \tilde{\ell}^* \leftrightarrow \tilde{u}\tilde{Q}^* \right]_- \right. \\
&+ \left. \left[\tilde{N}_i \tilde{Q} \leftrightarrow \tilde{\ell}\tilde{u} \right]_- + \left[\tilde{N}_i \tilde{u}^* \leftrightarrow \tilde{\ell}\tilde{Q}^* \right]_- \right) \\
&- \left[N\tilde{\ell} \leftrightarrow Q\tilde{u}^* \right]_- - \left[N\tilde{\ell} \leftrightarrow \tilde{Q}\tilde{u} \right]_- - \left[N\tilde{Q} \leftrightarrow \tilde{\ell}^* \tilde{u}^* \right]_- \\
&- \left[Nu \leftrightarrow \tilde{\ell}^* \tilde{Q} \right]_- - \left[N\tilde{u} \leftrightarrow \tilde{\ell}^* Q \right]_- - \left[N\tilde{Q}^* \leftrightarrow \tilde{\ell}^* \tilde{u} \right]_- \\
&+ \sum_i \left(\left[\tilde{N}_i \tilde{\ell}^* \leftrightarrow \tilde{Q}u \right]_- + \left[\tilde{N}_i Q \leftrightarrow \tilde{\ell}u \right]_- + \left[\tilde{N}_i \tilde{u} \leftrightarrow \tilde{\ell}\tilde{Q} \right]_- \right), \\
&= \sum_{i=\pm} \left\{ \left(F_{\tilde{N}_i H_u \tilde{\ell}} - F_{\tilde{N}_i H_u^* \tilde{\ell}^*} \right) f_{\tilde{N}_i}^{eq} \left(1 + f_{\tilde{\ell}}^{eq} \right) \left(1 + f_{H_u}^{eq} \right) \left(\frac{f_{\tilde{N}_i}}{f_{\tilde{N}_i}^{eq}} - \frac{1 + f_{\tilde{N}_i}}{1 + f_{\tilde{N}_i}^{eq}} \right) \right. \\
&- \tilde{F}_{\tilde{N}_i} \left[-\frac{f_{\tilde{N}_i}}{f_{\tilde{N}_i}^{eq}} f_{\tilde{\ell}}^{eq} + \frac{1 + f_{\tilde{N}_i}}{1 + f_{\tilde{N}_i}^{eq}} \left(1 + f_{\tilde{\ell}}^{eq} \right) \right] \frac{\mu_{\tilde{\ell}}}{T} \\
&- \tilde{F}_{\tilde{N}_i} \left[-\frac{f_{\tilde{N}_i}}{f_{\tilde{N}_i}^{eq}} f_{H_u}^{eq} + \frac{1 + f_{\tilde{N}_i}}{1 + f_{\tilde{N}_i}^{eq}} \left(1 + f_{H_u}^{eq} \right) \right] \frac{\mu_{H_u}}{T} \left. \right\} \\
&- 2F_N \left[-\frac{f_N}{f_N^{eq}} f_{\tilde{\ell}}^{eq} + \frac{1 - f_N}{1 - f_N^{eq}} \left(1 + f_{\tilde{\ell}}^{eq} \right) \right] \frac{\mu_{\tilde{\ell}}}{T} \\
&- 2F_N \left[-\frac{f_N}{f_N^{eq}} f_{\tilde{H}_u}^{eq} + \frac{1 - f_N}{1 - f_N^{eq}} \left(1 - f_{\tilde{H}_u}^{eq} \right) \right] \frac{\mu_{\tilde{H}_u}}{T} \\
&- 4F_{\ell\tilde{\ell}\tilde{\ell}} \left(\frac{\mu_{\tilde{\ell}}}{T} - \frac{\mu_{\ell}}{T} \right) f_{\ell}^{eq,2} \left(1 + f_{\tilde{\ell}}^{eq} \right)^2 + \tilde{S}_t + S_{22} + \tilde{W}_{\Delta L=2}, \quad (\text{B.65})
\end{aligned}$$

where the interactions from scalar potential S_{22} are given by

$$\begin{aligned}
S_{22} = & \sum_i \left\{ 2\tilde{F}_{\tilde{N}_i}^{(3)} \left[\frac{f_{\tilde{N}_i}}{f_{\tilde{N}_i}^{eq}} f_{\tilde{\ell}}^{eq} - \frac{1 + f_{\tilde{N}_i}}{1 + f_{\tilde{N}_i}^{eq}} (1 + f_{\tilde{\ell}}^{eq}) \right] \frac{\mu_{\tilde{\ell}}}{T} \right. \\
& - 2F_{22_i} \left[\frac{f_{\tilde{N}_i}}{f_{\tilde{N}_i}^{eq}} (1 - f_{\tilde{\ell}}^{eq}) + \frac{1 + f_{\tilde{N}_i}}{1 + f_{\tilde{N}_i}^{eq}} (2 + f_{\tilde{\ell}}^{eq}) \right] \frac{\mu_{\tilde{\ell}}}{T} \\
& - 2\tilde{F}_{\tilde{N}_i}^{(3)} \left[\frac{f_{\tilde{N}_\pm}}{f_{\tilde{N}_\pm}^{eq}} f_{\tilde{Q}}^{eq} - \frac{1 + f_{\tilde{N}_\pm}}{1 + f_{\tilde{N}_\pm}^{eq}} (1 + f_{\tilde{Q}}^{eq}) \right] \frac{\mu_{\tilde{Q}}}{T} \\
& \left. + 2F_{22_i} \left[\frac{f_{\tilde{N}_i}}{f_{\tilde{N}_i}^{eq}} (1 - f_{\tilde{Q}}^{eq}) + \frac{1 + f_{\tilde{N}_i}}{1 + f_{\tilde{N}_i}^{eq}} (2 + f_{\tilde{Q}}^{eq}) \right] \frac{\mu_{\tilde{Q}}}{T} \right\} \\
& - (\tilde{Q} \rightarrow \tilde{u}), \tag{B.66}
\end{aligned}$$

and the top and stop scatterings terms \tilde{S}_t are given by

$$\begin{aligned}
\tilde{S}_t = & -4F^{(0)} \left[\frac{f_N}{f_N^{eq}} (1 + f_{\tilde{\ell}}^{eq}) - \frac{1 - f_N}{1 - f_N^{eq}} f_{\tilde{\ell}}^{eq} \right] \frac{\mu_{\tilde{\ell}}}{T} \\
& - 4(F^{(1)} + F^{(2)}) \left[-\frac{f_N}{f_N^{eq}} f_{\tilde{\ell}}^{eq} + \frac{1 - f_N}{1 - f_N^{eq}} (1 + f_{\tilde{\ell}}^{eq}) \right] \frac{\mu_{\tilde{\ell}}}{T} \\
& + 2F^{(0)} \left[\frac{f_N}{f_N^{eq}} f_{\tilde{Q}}^{eq} + \frac{1 - f_N}{1 - f_N^{eq}} (1 - f_{\tilde{Q}}^{eq}) \right] \frac{\mu_Q}{T} \\
& + 2F^{(1)} \left[\frac{f_N}{f_N^{eq}} (1 - f_{\tilde{Q}}^{eq}) + \frac{1 - f_N}{1 - f_N^{eq}} f_{\tilde{Q}}^{eq} \right] \frac{\mu_Q}{T} \\
& + 2(F^{(0)} + F^{(1)}) \left[-\frac{f_N}{f_N^{eq}} f_{\tilde{Q}}^{eq} + \frac{1 - f_N}{1 - f_N^{eq}} (1 + f_{\tilde{Q}}^{eq}) \right] \frac{\mu_{\tilde{Q}}}{T} \\
& + 2F^{(2)} \left[\frac{f_N}{f_N^{eq}} (1 + f_{\tilde{Q}}^{eq}) - \frac{1 - f_N}{1 - f_N^{eq}} f_{\tilde{Q}}^{eq} \right] \frac{\mu_{\tilde{Q}}}{T} \\
& - \sum_{i=\pm} \left\{ 2F_i^{(8)} \left[\frac{f_{\tilde{N}_i}}{f_{\tilde{N}_i}^{eq}} (1 + f_{\tilde{\ell}}^{eq}) - \frac{1 + f_{\tilde{N}_i}}{1 + f_{\tilde{N}_i}^{eq}} f_{\tilde{\ell}}^{eq} \right] \frac{\mu_{\tilde{\ell}}}{T} \right. \\
& + 4F_i^{(9)} \left[-\frac{f_{\tilde{N}_i}}{f_{\tilde{N}_i}^{eq}} f_{\tilde{\ell}}^{eq} + \frac{1 + f_{\tilde{N}_i}}{1 + f_{\tilde{N}_i}^{eq}} (1 + f_{\tilde{\ell}}^{eq}) \right] \frac{\mu_{\tilde{\ell}}}{T} \\
& - 2F_i^{(8)} \left[\frac{f_{\tilde{N}_i}}{f_{\tilde{N}_i}^{eq}} f_{\tilde{Q}}^{eq} + \frac{1 + f_{\tilde{N}_i}}{1 + f_{\tilde{N}_i}^{eq}} (1 - f_{\tilde{Q}}^{eq}) \right] \frac{\mu_Q}{T} \\
& \left. - 2F_i^{(9)} \left[\frac{f_{\tilde{N}_i}}{f_{\tilde{N}_i}^{eq}} + \frac{1 + f_{\tilde{N}_i}}{1 + f_{\tilde{N}_i}^{eq}} \right] \frac{\mu_Q}{T} \right\} - (Q \rightarrow u) - (\tilde{Q} \rightarrow \tilde{u}). \tag{B.67}
\end{aligned}$$

In eq. B.65, the $\Delta L = 2$ scatterings $H_u \tilde{\ell} \leftrightarrow ij$ with t- and u-channel exchange of \tilde{N}_\pm , and the leftover off-shell contribution for s-channel exchange of \tilde{N}_\pm are all collected in $\widetilde{W}_{\Delta L=2}$. For the detailed subtraction procedure, please refer to Section B.2.3. As mentioned previously, we will ignore $\widetilde{W}_{\Delta L=2}$ since it is negligible in the temperature range we are exploring ($T \lesssim 10^9$ GeV).

B.2.2.1 Approximations: integrated Boltzmann equations

An analysis of the BEs derived above shows that in order to be able to write them in the integrated form as equations for the number densities, we have to make the following assumptions:

$$\begin{aligned} \frac{1 + \eta_a f_a}{1 + \eta_a f_a^{eq}} &\rightarrow 1, \\ \eta_i f_i^{eq} \frac{\mu_i}{T} &\rightarrow 0, \end{aligned} \tag{B.68}$$

where a refers to N or \tilde{N}_\pm . The approximations above are equivalent to ignoring the chemical potentials in the quantum statistical factors i.e. the Fermi-blocking and Bose-enhancement factors. In addition, we also have to assume that N and \tilde{N}_\pm are in kinetic equilibrium namely

$$\begin{aligned} \frac{f_N}{f_N^{eq}} &= \frac{Y_N}{Y_N^{eq}}, \\ \frac{f_{\tilde{N}_\pm}}{f_{\tilde{N}_\pm}^{eq}} &= \frac{Y_{\tilde{N}_\pm}}{Y_{\tilde{N}_\pm}^{eq}}, \end{aligned} \tag{B.69}$$

where

$$\begin{aligned} Y_N^{eq} &= \frac{45g_N}{4\pi^4 g_s^*} \frac{M^2}{T^2} \mathcal{K}_2\left(\frac{M}{T}\right), \\ Y_{\tilde{N}_\pm}^{eq} &= \frac{45g_{\tilde{N}}}{4\pi^4 g_s^*} \frac{M_\pm^2}{T^2} \mathcal{K}_2\left(\frac{M_\pm}{T}\right), \end{aligned} \tag{B.70}$$

with $\mathcal{K}_2(x)$ the modified Bessel function of second kind. Both expressions in eq. (B.70) were obtained by assuming Maxwell-Boltzmann distribution. Here $g_N = 2$ since it is a massive fermion and $g_{\tilde{N}} = 1$ since it is a massive scalar.

The approximations (B.69) are justified as long as we are in the strong

washout regime where the distributions of N and \tilde{N}_\pm are close to kinetic equilibrium. In refs. [133–135], the full BEs are considered and it is shown that the integrated BEs are a very good approximation in the strong washout regime. In particular, ref. [135] has studied SL using full BEs and showed that the difference between using the full BEs and the integrated BEs is negligible in the strong washout regime but the difference can be up to one order of magnitude in the weak washout regime. In this thesis, for simplicity, we are going to use approximations (B.68) and (B.69) which enable us to write down the following set of integrated BEs

$$sHz \frac{dY_N}{dz} = - \left(\frac{Y_N}{Y_N^{eq}} - 1 \right) \times \left(\gamma_N + 4\gamma_t^{(0)} + 4\gamma_t^{(1)} + 4\gamma_t^{(2)} + 2\gamma_t^{(3)} + 4\gamma_t^{(4)} \right), \quad (\text{B.71})$$

$$sHz \frac{dY_{\tilde{N}_\pm}}{dz} = - \left(\gamma_{\tilde{N}_\pm}^f + \gamma_{\tilde{N}_\pm}^s \right) \left(\frac{Y_{\tilde{N}_\pm}}{Y_{\tilde{N}_\pm}^{eq}} - 1 \right) - 2 \left(\gamma_{\tilde{N}_\pm}^{(3)} + 3\gamma_{22\pm} \right) \left(\frac{Y_{\tilde{N}_\pm}}{Y_{\tilde{N}_\pm}^{eq}} - 1 \right) - 2 \left(2\gamma_{t\pm}^{(5)} + 2\gamma_{t\pm}^{(6)} + 2\gamma_{t\pm}^{(7)} + \gamma_{t+}^{(8)} + 2\gamma_{t\pm}^{(9)} \right) \left(\frac{Y_{\tilde{N}_\pm}}{Y_{\tilde{N}_\pm}^{eq}} - 1 \right), \quad (\text{B.72})$$

$$sHz \frac{dY_{\Delta\ell}}{dz} = \epsilon_+^f(T) \gamma_{\tilde{N}} \left(\frac{Y_{\tilde{N}_+}}{Y_{\tilde{N}_+}^{eq}} - 1 \right) + \epsilon_-^f(T) \gamma_{\tilde{N}} \left(\frac{Y_{\tilde{N}_-}}{Y_{\tilde{N}_-}^{eq}} - 1 \right) - \frac{1}{2} \gamma_{\tilde{N}}^f \left(2\frac{\mu_\ell}{T} + 2\frac{\mu_{\tilde{H}_u}}{T} \right) - \frac{1}{2} \gamma_N^f \left(2\frac{\mu_\ell}{T} + 2\frac{\mu_{H_u}}{T} \right) - \left[\gamma_t^{(3)} \frac{Y_N}{Y_N^{eq}} + 2\gamma_t^{(4)} + 2 \sum_{i=\pm} \left(\gamma_{ti}^{(6)} + \gamma_{ti}^{(7)} + \gamma_{ti}^{(5)} \frac{Y_{\tilde{N}_i}}{Y_{\tilde{N}_i}^{eq}} \right) \right] \frac{2\mu_\ell}{T} + \left[\left(\gamma_t^{(3)} + \gamma_t^{(4)} \right) + \gamma_t^{(4)} \frac{Y_N}{Y_N^{eq}} + \sum_{i=\pm} \left(\gamma_{ti}^{(5)} + \gamma_{ti}^{(6)} + \gamma_{ti}^{(7)} \frac{Y_{\tilde{N}_i}}{Y_{\tilde{N}_i}^{eq}} \right) \right] \times \frac{2(\mu_Q - \mu_u)}{T} + \sum_{i=\pm} \left(\gamma_{ti}^{(5)} + \gamma_{ti}^{(7)} + \gamma_{ti}^{(6)} \frac{Y_{\tilde{N}_i}}{Y_{\tilde{N}_i}^{eq}} \right) \frac{2(\mu_{\tilde{Q}} - \mu_{\tilde{u}})}{T} + 2\gamma_{\ell\ell\tilde{\ell}} \left(2\frac{\mu_{\tilde{\ell}}}{T} - 2\frac{\mu_\ell}{T} \right) + W_{\Delta L=2}, \quad (\text{B.73})$$

$$\begin{aligned}
sHz \frac{dY_{\Delta\tilde{\ell}}}{dz} &= \epsilon_+^s(T) \gamma_{\tilde{N}} \left(\frac{Y_{\tilde{N}_+}}{Y_{\tilde{N}_+}^{eq}} - 1 \right) + \epsilon_-^s(T) \gamma_{\tilde{N}} \left(\frac{Y_{\tilde{N}_-}}{Y_{\tilde{N}_-}^{eq}} - 1 \right) \\
&- \frac{1}{2} \gamma_{\tilde{N}}^s \left(2 \frac{\mu_{\tilde{\ell}}}{T} + 2 \frac{\mu_{H_u}}{T} \right) - \frac{1}{2} \gamma_{\tilde{N}}^s \left(2 \frac{\mu_{\tilde{\ell}}}{T} + 2 \frac{\mu_{\tilde{H}_u}}{T} \right) \\
&- \gamma_{\tilde{N}}^{(3)} 2 \frac{\mu_{\tilde{\ell}} - \mu_{\tilde{Q}} + \mu_{\tilde{u}}}{T} - 2\gamma_{22} 2 \frac{\mu_{\tilde{\ell}} - \mu_{\tilde{Q}} + \mu_{\tilde{u}}}{T} \\
&- \sum_i \gamma_{22i} \frac{Y_{\tilde{N}_i}}{Y_{\tilde{N}_i}^{eq}} 2 \frac{\mu_{\tilde{\ell}} - \mu_{\tilde{Q}} + \mu_{\tilde{u}}}{T} \\
&- \left[2\gamma_t^{(0)} \frac{Y_N}{Y_N^{eq}} + 2 \left(\gamma_t^{(1)} + \gamma_t^{(2)} \right) + \sum_{i=\pm} \left(\gamma_{ti}^{(8)} \frac{Y_{\tilde{N}_i}}{Y_{\tilde{N}_i}^{eq}} + 2\gamma_{ti}^{(9)} \right) \right] \frac{2\mu_{\tilde{\ell}}}{T} \\
&+ \left[\gamma_t^{(0)} + \gamma_t^{(1)} \frac{Y_N}{Y_N^{eq}} + \sum_{i=\pm} \left(\gamma_{ti}^{(8)} + \gamma_{ti}^{(9)} + \gamma_{ti}^{(9)} \frac{Y_{\tilde{N}_i}}{Y_{\tilde{N}_i}^{eq}} \right) \right] \frac{2(\mu_{\tilde{Q}} - \mu_{\tilde{u}})}{T} \\
&+ \left(\gamma_t^{(0)} + \gamma_t^{(1)} + \gamma_t^{(2)} \frac{Y_N}{Y_N^{eq}} \right) \frac{2(\mu_{\tilde{Q}} - \mu_{\tilde{u}})}{T} \\
&- \frac{1}{2} \gamma_N^2 \left(2 \frac{\mu_{\tilde{\ell}}}{T} - 2 \frac{\mu_{\tilde{H}_u}}{T} \right) + 2\gamma_{\ell\ell\tilde{\ell}} \left(2 \frac{\mu_{\tilde{\ell}}}{T} - 2 \frac{\mu_{\tilde{\ell}}}{T} \right) + \widetilde{W}_{\Delta L=2}. \quad (\text{B.74})
\end{aligned}$$

In the above, all the γ 's are the thermally averaged reaction densities defined in Appendix B.2.1. Here however, we would like to stress that for simplicity, in the numerical calculations, we have ignored the Fermi-blocking and Bose-enhancement factors that appear in the thermally averaged reaction densities defined in Appendix B.2.1¹. The effects are not expected to be larger than the results obtained in ref. [135].

To further simplify the BEs, we can make the following approximations

$$\begin{aligned}
Y_{\tilde{N}_+}^{eq} &\approx Y_{\tilde{N}_-}^{eq} \equiv Y_{\tilde{N}}^{eq}, \\
Y_{\tilde{N}_+} &\approx Y_{\tilde{N}_-} \equiv \frac{1}{2} Y_{\tilde{N}_{\text{tot}}}, \\
\gamma_{\tilde{N}_+}^f + \gamma_{\tilde{N}_+}^s &\approx \gamma_{\tilde{N}_-}^f + \gamma_{\tilde{N}_-}^s \approx \frac{\gamma_{\tilde{N}}}{2}. \quad (\text{B.75})
\end{aligned}$$

The approximations above are justified if the mass splitting is small $B \ll M$. Then, we can sum up the BEs for \tilde{N}_+ and \tilde{N}_- (B.72) and also rewrite the BEs

¹We only include the Pauli-blocking and Bose-enhancement factors and the relevant thermal masses in the CP asymmetry evaluation which is crucial to lift the cancellation between the scalar and fermionic CP asymmetries.

for $Y_{\Delta\ell}$ and $Y_{\Delta\tilde{\ell}}$ as follows

$$sHz \frac{dY_{\tilde{N}_{\text{tot}}}}{dz} = - \left(\frac{\gamma_{\tilde{N}}}{2} + \gamma_{\tilde{N}}^{(3)} + 3\gamma_{22} + 2\gamma_t^{(5)} + 2\gamma_t^{(6)} + 2\gamma_t^{(7)} + \gamma_t^{(8)} + 2\gamma_t^{(9)} \right) \times \left(\frac{Y_{\tilde{N}_{\text{tot}}}}{Y_{\tilde{N}}^{eq}} - 2 \right), \quad (\text{B.76})$$

$$\begin{aligned} sHz \frac{dY_{\Delta\ell}}{dz} = & \epsilon^f(T) \frac{\gamma_{\tilde{N}}}{2} \left(\frac{Y_{\tilde{N}_{\text{tot}}}}{Y_{\tilde{N}}^{eq}} - 2 \right) - \frac{\gamma_{\tilde{N}}^f}{2} \left(2\frac{\mu_\ell}{T} + 2\frac{\mu_{\tilde{H}_u}}{T} \right) \\ & - \frac{1}{2}\gamma_N^f \left(2\frac{\mu_\ell}{T} + 2\frac{\mu_{H_u}}{T} \right) \\ & - \left(\gamma_t^{(3)} \frac{Y_N}{Y_N^{eq}} + 2\gamma_t^{(4)} + 2\gamma_t^{(6)} + 2\gamma_t^{(7)} + \gamma_t^{(5)} \frac{Y_{\tilde{N}_{\text{tot}}}}{Y_{\tilde{N}}^{eq}} \right) \frac{2\mu_\ell}{T} \\ & + \left(\gamma_t^{(3)} + \gamma_t^{(4)} + \gamma_t^{(4)} \frac{Y_N}{Y_N^{eq}} + \gamma_t^{(5)} + \gamma_t^{(6)} + \frac{1}{2}\gamma_t^{(7)} \frac{Y_{\tilde{N}_{\text{tot}}}}{Y_{\tilde{N}}^{eq}} \right) \frac{2(\mu_Q - \mu_u)}{T} \\ & + \left(\gamma_t^{(5)} + \gamma_t^{(7)} + \frac{1}{2}\gamma_t^{(6)} \frac{Y_{\tilde{N}_{\text{tot}}}}{Y_{\tilde{N}}^{eq}} \right) \frac{2(\mu_{\tilde{Q}} - \mu_{\tilde{u}})}{T} \\ & + 2\gamma_{\ell\tilde{\ell}\tilde{\ell}} \left(2\frac{\mu_{\tilde{\ell}}}{T} - 2\frac{\mu_\ell}{T} \right) + W_{\Delta L=2}, \quad (\text{B.77}) \end{aligned}$$

$$\begin{aligned}
sHz \frac{dY_{\Delta\tilde{\ell}}}{dz} &= \epsilon^s (T) \frac{\gamma_{\tilde{N}}}{2} \left(\frac{Y_{\tilde{N}_{\text{tot}}}}{Y_{\tilde{N}}^{eq}} - 2 \right) - \frac{\gamma_{\tilde{N}}^s}{2} \left(2 \frac{\mu_{\tilde{\ell}}}{T} + 2 \frac{\mu_{H_u}}{T} \right) \\
&\quad - \frac{1}{2} \gamma_N^s \left(2 \frac{\mu_{\tilde{\ell}}}{T} + 2 \frac{\mu_{\tilde{H}_u}}{T} \right) - \gamma_{\tilde{N}}^{(3)} 2 \frac{\mu_{\tilde{\ell}} - \mu_{\tilde{Q}} + \mu_{\tilde{u}}}{T} \\
&\quad - \gamma_{22} \left(\frac{1}{2} \frac{Y_{\tilde{N}_{\text{tot}}}}{Y_{\tilde{N}}^{eq}} + 2 \right) 2 \frac{\mu_{\tilde{\ell}} - \mu_{\tilde{Q}} + \mu_{\tilde{u}}}{T} \\
&\quad - \left(2\gamma_t^{(0)} \frac{Y_N}{Y_N^{eq}} + 2\gamma_t^{(1)} + 2\gamma_t^{(2)} + \frac{1}{2} \gamma_t^{(8)} \frac{Y_{\tilde{N}_{\text{tot}}}}{Y_{\tilde{N}}^{eq}} + 2\gamma_t^{(9)} \right) \frac{2\mu_{\tilde{\ell}}}{T} \\
&\quad + \left(\gamma_t^{(0)} + \gamma_t^{(1)} \frac{Y_N}{Y_N^{eq}} + \gamma_t^{(8)} + \gamma_t^{(9)} + \frac{1}{2} \gamma_t^{(9)} \frac{Y_{\tilde{N}_{\text{tot}}}}{Y_{\tilde{N}}^{eq}} \right) \frac{2(\mu_{\tilde{Q}} - \mu_u)}{T} \\
&\quad + \left(\gamma_t^{(0)} + \gamma_t^{(1)} + \gamma_t^{(2)} \frac{Y_N}{Y_N^{eq}} \right) \frac{2(\mu_{\tilde{Q}} - \mu_{\tilde{u}})}{T} \\
&\quad - 2\gamma_{\ell\tilde{\ell}\tilde{\ell}} \left(2 \frac{\mu_{\tilde{\ell}}}{T} - 2 \frac{\mu_{\ell}}{T} \right) + \widetilde{W}_{\Delta L=2}. \tag{B.78}
\end{aligned}$$

In order to solve the BEs (B.77) and (B.78) in a closed form, we need to express all chemical potentials $\mu_{Q,\tilde{Q},u,\tilde{u},H_u,\tilde{H}_u}$ in terms of $\mu_{\ell,\tilde{\ell}}$ and then relate it to the lepton and slepton asymmetries through the relations (B.42).

For example, using the equilibrium condition of top Yukawa interactions eqs. (B.105), we can actually eliminate the (s)quark chemical potentials which appear in the BEs in term of only the Higgs(ino) ones

$$\begin{aligned}
\mu_Q - \mu_u &= \mu_{H_u}, \\
\mu_{\tilde{Q}} - \mu_{\tilde{u}} &= \mu_{H_u} - 2\mu_{\tilde{H}_u}. \tag{B.79}
\end{aligned}$$

In Appendix B.2.5, we will further simplify the BEs (B.77) and (B.78) in a closed form for the superequilibrium scenario, and in Appendix B.2.6 for non-superequilibrium scenario.

B.2.3 Subtracted $2 \leftrightarrow 2$ scatterings

It is well-known that if we naively write down the BE for lepton or slepton asymmetry without taking into account the $2 \leftrightarrow 2$ scatterings, we would generate lepton or slepton asymmetry even in thermal equilibrium, in contradiction with one of the Sakharov's conditions. This inconsistency is due to

the following. Although the $2 \leftrightarrow 2$ scatterings are processes of higher order $\mathcal{O}(Y^4)$ (compared to the decays or inverse decays which are of $\mathcal{O}(Y^2)$), the CP asymmetries of the subtracted rates are of the same order than that of the decays[136, 137] and hence cannot be ignored.

Using (B.39), we can write down the term $\left[\widetilde{H}_u \ell \leftrightarrow ij \right]_-^{\text{sub}}$ which appears in BE (B.63) as follows

$$\begin{aligned}
& \left[\widetilde{H}_u \ell \leftrightarrow ij \right]^{\text{sub}} \\
= & \left(F_{\widetilde{H}_u \ell ij} - \overline{F_{\widetilde{H}_u \ell ij}} \right)^{\text{sub}} \left(1 + f_\ell^{\text{eq}} e^{E_\ell/T} \frac{\mu_\ell}{T} + f_{\widetilde{H}_u}^{\text{eq}} e^{E_{\widetilde{H}_u}/T} \frac{\mu_{\widetilde{H}_u}}{T} \right) \\
& \times f_\ell^{\text{eq}} f_{\widetilde{H}_u}^{\text{eq}} (1 + \eta_i f_i^{\text{eq}}) (1 + \eta_j f_j^{\text{eq}}) \\
& - \overline{F_{\widetilde{H}_u \ell ij}}^{\text{sub}} \left(\frac{\mu_i + \mu_j}{T} - \frac{\mu_\ell + \mu_{\widetilde{H}_u}}{T} \right) f_\ell^{\text{eq}} f_{\widetilde{H}_u}^{\text{eq}} (1 + \eta_i f_i^{\text{eq}}) (1 + \eta_j f_j^{\text{eq}}) \\
& + \left(F_{\widetilde{H}_u \ell ij} - \overline{F_{\widetilde{H}_u \ell ij}} \right)^{\text{sub}} f_\ell^{\text{eq}} f_{\widetilde{H}_u}^{\text{eq}} (1 + \eta_i f_i^{\text{eq}}) (1 + \eta_j f_j^{\text{eq}}) \\
& \times \left(\eta_i f_i^{\text{eq}} \frac{\mu_i}{T} + \eta_j f_j^{\text{eq}} \frac{\mu_j}{T} \right), \tag{B.80}
\end{aligned}$$

and

$$\begin{aligned}
& \left[\widetilde{H}_u \bar{\ell} \leftrightarrow ij \right]^{\text{sub}} \\
= & \left(F_{\widetilde{H}_u \bar{\ell} ij} - \overline{F_{\widetilde{H}_u \bar{\ell} ij}} \right)^{\text{sub}} \left(1 - f_\ell^{\text{eq}} e^{E_\ell/T} \frac{\mu_\ell}{T} - f_{\widetilde{H}_u}^{\text{eq}} e^{E_{\widetilde{H}_u}/T} \frac{\mu_{\widetilde{H}_u}}{T} \right) \\
& \times f_\ell^{\text{eq}} f_{\widetilde{H}_u}^{\text{eq}} (1 + \eta_i f_i^{\text{eq}}) (1 + \eta_j f_j^{\text{eq}}) \\
& - \overline{F_{\widetilde{H}_u \bar{\ell} ij}}^{\text{sub}} \left(\frac{\mu_i + \mu_j}{T} + \frac{\mu_\ell + \mu_{\widetilde{H}_u}}{T} \right) f_\ell^{\text{eq}} f_{\widetilde{H}_u}^{\text{eq}} (1 + \eta_i f_i^{\text{eq}}) (1 + \eta_j f_j^{\text{eq}}) \\
& + \left(F_{\widetilde{H}_u \bar{\ell} ij} - \overline{F_{\widetilde{H}_u \bar{\ell} ij}} \right)^{\text{sub}} f_\ell^{\text{eq}} f_{\widetilde{H}_u}^{\text{eq}} (1 + \eta_i f_i^{\text{eq}}) (1 + \eta_j f_j^{\text{eq}}) \\
& \times \left(\eta_i f_i^{\text{eq}} \frac{\mu_i}{T} + \eta_j f_j^{\text{eq}} \frac{\mu_j}{T} \right). \tag{B.81}
\end{aligned}$$

From eqs. (B.80) and (B.81) and assuming CPT invariance, we have

$$\begin{aligned}
& \sum_{ij} \left\{ \left[\widetilde{H}_u \ell \leftrightarrow ij \right]^{\text{sub}} - \left[\widetilde{H}_u \bar{\ell} \leftrightarrow ij \right]^{\text{sub}} \right\} \\
= & \sum_{ij} \left\{ 2 \left(F_{\widetilde{H}_u \ell ij} - \overline{F_{\widetilde{H}_u \ell ij}} \right)^{\text{sub}} f_\ell^{eq} f_{\widetilde{H}_u}^{eq} (1 + \eta_i f_i^{eq}) (1 + \eta_j f_j^{eq}) \right. \\
& + \left(\overline{F_{\widetilde{H}_u \ell ij}} - F_{\widetilde{H}_u \bar{\ell} ij} \right)^{\text{sub}} \frac{\mu_i + \mu_j}{T} f_\ell^{eq} f_{\widetilde{H}_u}^{eq} (1 + \eta_i f_i^{eq}) (1 + \eta_j f_j^{eq}) \\
& + \left(\overline{F_{\widetilde{H}_u \ell ij}} + F_{\widetilde{H}_u \bar{\ell} ij} \right)^{\text{sub}} \frac{\mu_\ell + \mu_{\widetilde{H}_u}}{T} f_\ell^{eq} f_{\widetilde{H}_u}^{eq} (1 + \eta_i f_i^{eq}) (1 + \eta_j f_j^{eq}) \\
& + 2 \left(F_{\widetilde{H}_u \ell ij} - \overline{F_{\widetilde{H}_u \ell ij}} \right)^{\text{sub}} f_\ell^{eq} f_{\widetilde{H}_u}^{eq} (1 + \eta_i f_i^{eq}) (1 + \eta_j f_j^{eq}) \\
& \left. \times \left(\eta_i f_i^{eq} \frac{\mu_i}{T} + \eta_j f_j^{eq} \frac{\mu_j}{T} \right) \right\}. \tag{B.82}
\end{aligned}$$

For the $\widetilde{H}_u \ell \leftrightarrow ij$ with the exchange of \widetilde{N}_\pm in s-channel, the subtracted rate can be rewritten as follows

$$\begin{aligned}
& \sum_{ij} \left(F_{\widetilde{H}_u \ell ij}^s - \overline{F_{\widetilde{H}_u \ell ij}^s} \right)^{\text{sub}} (1 + \eta_i f_i^{eq}) (1 + \eta_j f_j^{eq}) \\
= & \sum_{ij,k} \left[F_{\widetilde{H}_u \ell ij}^s - F_{\widetilde{H}_u \ell \widetilde{N}_k} (1 + f_{\widetilde{N}_k}) \text{Br}(\widetilde{N}_k \rightarrow ij) \right. \\
& \left. - \overline{F_{\widetilde{H}_u \ell ij}^s} + \overline{F_{\widetilde{H}_u \ell \widetilde{N}_k}} (1 + f_{\widetilde{N}_k}) \text{Br}(\widetilde{N}_k \rightarrow ij) \right] \\
& \times (1 + \eta_i f_i^{eq}) (1 + \eta_j f_j^{eq}), \\
= & \sum_{ij} \left(F_{\widetilde{H}_u \ell ij}^s - F_{\widetilde{H}_u \bar{\ell} ij}^s \right) (1 + \eta_i f_i^{eq}) (1 + \eta_j f_j^{eq}) \\
& + \sum_k \left(F_{\widetilde{N}_k \widetilde{H}_u \ell} - F_{\widetilde{N}_k \widetilde{H}_u \bar{\ell}} \right) (1 + f_{\widetilde{N}_k}), \tag{B.83}
\end{aligned}$$

where $\text{Br}(\widetilde{N}_k \rightarrow ij)$ is the branching ratio for the corresponding process and we have used the unitary condition

$$\sum_a \text{Br}(\widetilde{N}_k \rightarrow ij) (1 + \eta_i f_i^{eq}) (1 + \eta_j f_j^{eq}) = 1. \tag{B.84}$$

In eq. (B.83), since the CP asymmetry of any process is always of higher order in the couplings with respect to the corresponding tree level process [136], $\left(F_{\widetilde{H}_u \ell ij}^s - F_{\widetilde{H}_u \bar{\ell} ij}^s \right)$ will be of order of $\mathcal{O}(Y^6)$. Hence, we will ignore this term

and eq. (B.83) becomes

$$\begin{aligned}
& \sum_{ij} \left(F_{\tilde{H}_u \ell ij}^s - \overline{F_{\tilde{H}_u \ell ij}^s} \right)^{\text{sub}} (1 + \eta_i f_i^{eq}) (1 + \eta_j f_j^{eq}) \\
&= \sum_k \left(F_{\tilde{N}_k \tilde{H}_u \ell} - F_{\tilde{N}_k \overline{\tilde{H}_u \ell}} \right) \left(1 + f_{\tilde{N}_k} \right). \tag{B.85}
\end{aligned}$$

Substituting eq. (B.85) into eq. (B.82) and ignoring the term of order $\mathcal{O}(\epsilon \frac{\mu}{T})$, we have

$$\begin{aligned}
\sum_{ij} \left[\tilde{H}_u \ell \leftrightarrow ij \right]_-^{\text{sub}} &= 2 \sum_k \left(F_{\tilde{N}_k \tilde{H}_u \ell} - F_{\tilde{N}_k \overline{\tilde{H}_u \ell}} \right) \frac{1 + f_{\tilde{N}_k}}{1 + f_{\tilde{N}_k}^{eq}} \\
&\quad \times f_{\tilde{N}_k}^{eq} (1 - f_\ell^{eq}) \left(1 - f_{\tilde{H}_u}^{eq} \right) - W_{\Delta L=2}, \tag{B.86}
\end{aligned}$$

where we have used the identity $f_\ell^{eq} f_{\tilde{H}_u}^{eq} = \frac{f_{\tilde{N}_k}^{eq}}{1 + f_{\tilde{N}_k}^{eq}} (1 - f_\ell^{eq}) (1 - f_{\tilde{H}_u}^{eq})$ and

$$\begin{aligned}
W_{\Delta L=2} &= - \sum_{ij} \left(F_{\tilde{H}_u \ell ij} + F_{\overline{\tilde{H}_u \ell} ij} \right)^{\text{sub}} \frac{\mu_\ell + \mu_{\tilde{H}_u}}{T} \\
&\quad \times f_\ell^{eq} f_{\tilde{H}_u}^{eq} (1 + \eta_i f_i^{eq}) (1 + \eta_j f_j^{eq}). \tag{B.87}
\end{aligned}$$

Following the same procedure as above, we obtain

$$\begin{aligned}
\sum_{ij} \left[H_u \tilde{\ell} \leftrightarrow ij \right]_-^{\text{sub}} &= 2 \sum_k \left(F_{\tilde{N}_k H_u \tilde{\ell}} - F_{\tilde{N}_k H_u^* \tilde{\ell}^*} \right) \frac{1 + f_{\tilde{N}_k}}{1 + f_{\tilde{N}_k}^{eq}} \\
&\quad \times f_{\tilde{N}_k}^{eq} \left(1 + f_{\tilde{\ell}}^{eq} \right) \left(1 + f_{H_u}^{eq} \right) - \widetilde{W}_{\Delta L=2}, \tag{B.88}
\end{aligned}$$

where

$$\begin{aligned}
\widetilde{W}_{\Delta L=2} &\equiv - \sum_{ij} \left(F_{H_u \tilde{\ell} ij} + F_{H_u^* \tilde{\ell}^* ij} \right)^{\text{sub}} \frac{\mu_{\tilde{\ell}} + \mu_{H_u}}{T} \\
&\quad \times f_{\tilde{\ell}}^{eq} f_{H_u}^{eq} (1 + \eta_i f_i^{eq}) (1 + \eta_j f_j^{eq}). \tag{B.89}
\end{aligned}$$

B.2.4 Lepton flavor and lepton flavor equilibration

We can readily generalize the unflavored BE (B.77) and (B.78) to the flavored ones with (s)lepton flavor α as follows

$$\begin{aligned}
sHz \frac{dY_{\Delta\ell_\alpha}}{dz} &= \epsilon_\alpha^f(T) \frac{\gamma_{\tilde{N}}}{2} \left(\frac{Y_{\tilde{N}_{\text{tot}}}}{Y_{\tilde{N}}^{\text{eq}}} - 2 \right) - \frac{\gamma_{\tilde{N}}^{f,\alpha}}{2} \left(2\frac{\mu_{\ell_\alpha}}{T} + 2\frac{\mu_{\tilde{H}_u}}{T} \right) \\
&\quad - \frac{1}{2} \gamma_{\tilde{N}}^{f,\alpha} \left(2\frac{\mu_{\ell_\alpha}}{T} + 2\frac{\mu_{H_u}}{T} \right) \\
&\quad - \left(\gamma_t^{(3)\alpha} \frac{Y_N}{Y_N^{\text{eq}}} + 2\gamma_t^{(4)\alpha} + 2\gamma_t^{(6)\alpha} + 2\gamma_t^{(7)\alpha} + \gamma_t^{(5)\alpha} \frac{Y_{\tilde{N}_{\text{tot}}}}{Y_{\tilde{N}}^{\text{eq}}} \right) \frac{2\mu_{\ell_\alpha}}{T} \\
&\quad + \left(\gamma_t^{(3)\alpha} + \gamma_t^{(4)\alpha} + \gamma_t^{(4)\alpha} \frac{Y_N}{Y_N^{\text{eq}}} + \gamma_t^{(5)\alpha} + \gamma_t^{(6)\alpha} + \frac{1}{2} \gamma_t^{(7)\alpha} \frac{Y_{\tilde{N}_{\text{tot}}}}{Y_{\tilde{N}}^{\text{eq}}} \right) \frac{2(\mu_Q - \mu_u)}{T} \\
&\quad + \left(\gamma_t^{(5)\alpha} + \gamma_t^{(7)\alpha} + \frac{1}{2} \gamma_t^{(6)\alpha} \frac{Y_{\tilde{N}_{\text{tot}}}}{Y_{\tilde{N}}^{\text{eq}}} \right) \frac{2(\mu_{\tilde{Q}} - \mu_{\tilde{u}})}{T} \\
&\quad + 2\gamma_{\tilde{g}}^{\text{eff},\alpha} \left(2\frac{\mu_{\tilde{\ell}_\alpha}}{T} - 2\frac{\mu_{\ell_\alpha}}{T} \right) + W_{\Delta L=2}^\alpha, \tag{B.90}
\end{aligned}$$

$$\begin{aligned}
sHz \frac{dY_{\Delta\tilde{\ell}_\alpha}}{dz} &= \epsilon_\alpha^s(T) \frac{\gamma_{\tilde{N}}}{2} \left(\frac{Y_{\tilde{N}_{\text{tot}}}}{Y_{\tilde{N}}^{\text{eq}}} - 2 \right) - \frac{\gamma_{\tilde{N}}^{s,\alpha}}{2} \left(2\frac{\mu_{\tilde{\ell}_\alpha}}{T} + 2\frac{\mu_{H_u}}{T} \right) \\
&\quad - \frac{1}{2} \gamma_{\tilde{N}}^{s,\alpha} \left(2\frac{\mu_{\tilde{\ell}_\alpha}}{T} + 2\frac{\mu_{\tilde{H}_u}}{T} \right) - \gamma_{\tilde{N}}^{(3)\alpha} 2\frac{\mu_{\tilde{\ell}_\alpha} - \mu_{\tilde{Q}} + \mu_{\tilde{u}}}{T} \\
&\quad - \gamma_{22}^\alpha \left(\frac{1}{2} \frac{Y_{\tilde{N}_{\text{tot}}}}{Y_{\tilde{N}}^{\text{eq}}} + 2 \right) 2\frac{\mu_{\tilde{\ell}_\alpha} - \mu_{\tilde{Q}} + \mu_{\tilde{u}}}{T} \\
&\quad - \left(2\gamma_t^{(0)\alpha} \frac{Y_N}{Y_N^{\text{eq}}} + 2\gamma_t^{(1)\alpha} + 2\gamma_t^{(2)\alpha} + \frac{1}{2} \gamma_t^{(8)\alpha} \frac{Y_{\tilde{N}_{\text{tot}}}}{Y_{\tilde{N}}^{\text{eq}}} + 2\gamma_t^{(9)\alpha} \right) \frac{2\mu_{\tilde{\ell}_\alpha}}{T} \\
&\quad + \left(\gamma_t^{(0)\alpha} + \gamma_t^{(1)\alpha} \frac{Y_N}{Y_N^{\text{eq}}} + \gamma_t^{(8)\alpha} + \gamma_t^{(9)\alpha} + \frac{1}{2} \gamma_t^{(9)\alpha} \frac{Y_{\tilde{N}_{\text{tot}}}}{Y_{\tilde{N}}^{\text{eq}}} \right) \frac{2(\mu_Q - \mu_u)}{T} \\
&\quad + \left(\gamma_t^{(0)\alpha} + \gamma_t^{(1)\alpha} + \gamma_t^{(2)\alpha} \frac{Y_N}{Y_N^{\text{eq}}} \right) \frac{2(\mu_{\tilde{Q}} - \mu_{\tilde{u}})}{T} \\
&\quad - 2\gamma_{\tilde{g}}^{\text{eff}} \left(2\frac{\mu_{\tilde{\ell}_\alpha}}{T} - 2\frac{\mu_{\ell_\alpha}}{T} \right) + \tilde{W}_{\Delta L=2}^\alpha. \tag{B.91}
\end{aligned}$$

Lepton Flavor Equilibrating Interactions

The off-diagonal soft slepton masses induce lepton flavor violating interactions through the exchange of $SU(2)_L$ gauginos $\tilde{\lambda}_2^a$ and $U(1)_Y$ gaugino $\tilde{\lambda}_1$ (see the Lagrangian (4.17)), and this can result in lepton flavor equilibration. There are two t-channel scatterings $l_\alpha \bar{P} \leftrightarrow \tilde{l}_\beta \tilde{P}^*$, $l_\alpha \tilde{P} \leftrightarrow \tilde{l}_\beta P$ and one s-channel scattering $l_\alpha \tilde{l}_\beta^* \leftrightarrow P \tilde{P}$ as shown in Figure 4.1. We denote fermions as P and scalars as \tilde{P} . For processes mediated by $SU(2)_L$ gauginos $P = \ell, Q, \tilde{H}_{u,d}$, while when mediated by $U(1)_Y$ gaugino one must include the $SU(2)_L$ singlet states $P = e, u, d$ as well. Using (B.39), we have in general

$$\begin{aligned}
\left[l_\alpha P \leftrightarrow \tilde{l}_\beta \tilde{P} \right]_- &= -2 \overline{F_{l_\alpha P \tilde{l}_\beta \tilde{P}}} |R_{\alpha\beta}|^2 \left(\frac{\mu_{\tilde{l}_\beta} + \mu_{\tilde{P}}}{T} - \frac{\mu_{l_\alpha} + \mu_P}{T} \right) \\
&\quad f_{l_\alpha}^{eq} f_{\tilde{P}}^{eq} \left(1 + f_{\tilde{l}_\beta}^{eq} \right) \left(1 + f_{\tilde{P}}^{eq} \right), \\
\left[l_\alpha \tilde{P} \leftrightarrow \tilde{l}_\beta P \right]_- &= -2 \overline{F_{l_\alpha \tilde{P} \tilde{l}_\beta P}} |R_{\alpha\beta}|^2 \left(\frac{\mu_{\tilde{l}_\beta} + \mu_P}{T} - \frac{\mu_{l_\alpha} + \mu_{\tilde{P}}}{T} \right) \\
&\quad f_{l_\alpha}^{eq} f_{\tilde{P}}^{eq} \left(1 + f_{\tilde{l}_\beta}^{eq} \right) \left(1 - f_{\tilde{P}}^{eq} \right), \\
\left[l_\alpha \tilde{l}_\beta^* \leftrightarrow P \tilde{P} \right]_- &= -2 \overline{F_{l_\alpha \tilde{l}_\beta^* P \tilde{P}}} |R_{\alpha\beta}|^2 \left(\frac{\mu_P + \mu_{\tilde{P}}}{T} - \frac{\mu_{l_\alpha} - \mu_{\tilde{l}_\beta}}{T} \right) \\
&\quad f_{l_\alpha}^{eq} f_{\tilde{l}_\beta}^{eq} \left(1 - f_P^{eq} \right) \left(1 + f_{\tilde{P}}^{eq} \right), \tag{B.92}
\end{aligned}$$

where the factor of two comes from the corresponding CP processes (CP violation is irrelevant in here and is neglected). Each $l_\alpha \tilde{l}_\beta$ – gaugino vertex involves a unitary matrix $R_{\alpha\beta}$. Hence, to simplify the expressions, in what follows we will use the property of unitary matrix:

$$\begin{aligned}
\sum_{\beta} |R_{\alpha\beta}|^2 &= \delta_{\alpha\alpha}, \quad \text{no sum over } \alpha \\
\sum_{\alpha,\beta} |R_{\alpha\beta}|^2 &= 3. \tag{B.93}
\end{aligned}$$

Notice that in eq. (B.92) we have explicitly factored out the rotation matrices $|R_{\alpha\beta}|^2$ and hence, if we ignore the zero temperature lepton and slepton masses, $\overline{F_{l_\alpha P \tilde{l}_\beta \tilde{P}}}(\dots)$, $\overline{F_{l_\alpha \tilde{P} \tilde{l}_\beta P}}(\dots)$ and $\overline{F_{l_\alpha \tilde{l}_\beta^* P \tilde{P}}}(\dots)$ are flavor independent. If $P \tilde{P}$ are for example $l_\zeta \tilde{l}_\eta$, then we will have an additional factor of $|R_{\zeta\eta}|^2$. With the same approximation the distributions $f_{l_\alpha}^{eq}$ and $f_{\tilde{l}_\alpha}^{eq}$ are also flavor indepen-

dent. Hence from now on, we will drop the flavor index for all quantities which do not depend on flavor.

For simplicity, we keep the thermal masses only for $SU(2)_L$ and $U(1)_Y$ gauginos, $m_{\tilde{\lambda}_2}$ and $m_{\tilde{\lambda}_Y}$ respectively. With this approximations, we can define the flavor independent lepton flavor equilibration reaction densities (where we factor out e.g. $|R_{\alpha\beta}|^2$) as follows

$$\begin{aligned}\gamma_{t1,G} &\equiv \overline{F_{\ell P \tilde{\ell} \tilde{P}}}(g_G) f_\ell^{eq} f_P^{eq} \left(1 + f_{\tilde{\ell}}^{eq}\right) \left(1 + f_{\tilde{P}}^{eq}\right), \\ \gamma_{t2,G} &\equiv \overline{F_{\ell \tilde{P} \tilde{\ell} P}}(g_G) f_\ell^{eq} f_{\tilde{P}}^{eq} \left(1 + f_{\tilde{\ell}}^{eq}\right) \left(1 - f_P^{eq}\right), \\ \gamma_{s,G} &\equiv \overline{F_{\tilde{\ell}^* P \tilde{P}}}(g_G) f_\ell^{eq} f_{\tilde{\ell}}^{eq} \left(1 - f_P^{eq}\right) \left(1 + f_{\tilde{P}}^{eq}\right),\end{aligned}\quad (\text{B.94})$$

where $G = 2, Y$ for the scatterings mediated by the $SU(2)_L$ and $U(1)_Y$ gauginos respectively and (g_G) means that the gauge coupling which appear in the corresponding amplitude is either g_2 or g_Y .

For example, let us consider the scatterings with $P = \ell$ and ℓ_α as the particle of which we would like to track the evolution of its abundance. We have

$$\begin{aligned}\sum_{g\ell,\zeta,\beta,\eta} \left[\ell_\alpha \bar{\ell}_\zeta \leftrightarrow \tilde{\ell}_\beta \tilde{\ell}_\eta^* \right]_- &= -2\Pi_\ell \sum_{\zeta,\beta,\eta} \gamma_{t1,G} |R_{\alpha\beta}|^2 |R_{\zeta\eta}|^2 \\ &\quad \times \left(\frac{\mu_{\tilde{\ell}_\beta} - \mu_{\tilde{\ell}_\eta} - \mu_{\ell_\alpha} - \mu_{\ell_\zeta}}{T} \right) \\ &= -2\Pi_\ell \gamma_{t1,G} \\ &\quad \times \left(3 \sum_\beta |R_{\alpha\beta}|^2 \frac{\mu_{\tilde{\ell}_\beta} - \mu_{\ell_\alpha}}{T} + \sum_\zeta \frac{\mu_{\ell_\zeta} - \mu_{\tilde{\ell}_\zeta}}{T} \right),\end{aligned}\quad (\text{B.95})$$

$$\begin{aligned}\sum_{g\ell,\zeta,\beta,\eta} \left[\ell_\alpha \tilde{\ell}_\zeta \leftrightarrow \tilde{\ell}_\beta \ell_\eta \right]_- &= -2\Pi_\ell \sum_{\zeta,\beta,\eta} \gamma_{t2,G} |R_{\alpha\beta}|^2 |R_{\zeta\eta}|^2 \\ &\quad \left(\frac{\mu_{\tilde{\ell}_\beta} + \mu_{\ell_\eta} - \mu_{\ell_\alpha} + \mu_{\tilde{\ell}_\zeta}}{T} \right) \\ &= -2\Pi_\ell \gamma_{t2,G} \\ &\quad \times \left(3 \sum_\beta |R_{\alpha\beta}|^2 \frac{\mu_{\tilde{\ell}_\beta} - \mu_{\ell_\alpha}}{T} + \sum_\zeta \frac{\mu_{\ell_\zeta} - \mu_{\tilde{\ell}_\zeta}}{T} \right),\end{aligned}\quad (\text{B.96})$$

$$\begin{aligned}
\sum_{g\ell,\zeta,\beta,\eta} \left[\ell_\alpha \tilde{\ell}_\beta^* \leftrightarrow \tilde{\ell}_\zeta^* \ell_\eta \right]_- &= -2\Pi_\ell \sum_{\zeta,\beta,\eta} \gamma_{s,G} |R_{\alpha\beta}|^2 |R_{\zeta\eta}|^2 \\
&\quad \left(\frac{\mu_{\ell_\eta} - \mu_{\tilde{\ell}_\zeta}}{T} - \frac{\mu_{\ell_\alpha} - \mu_{\tilde{\ell}_\beta}}{T} \right) \\
&= -2\Pi_\ell \gamma_{s,G} \\
&\quad \times \left(3 \sum_\beta |R_{\alpha\beta}|^2 \frac{\mu_{\tilde{\ell}_\beta} - \mu_{\ell_\alpha}}{T} + \sum_\zeta \frac{\mu_{\ell_\zeta} - \mu_{\tilde{\ell}_\zeta}}{T} \right). \quad (\text{B.97})
\end{aligned}$$

In the above, Π_ℓ is a factor from summing over isospin degrees of freedom of leptons and sleptons, and for the scatterings mediated by $\tilde{\lambda}_2^0$ we have $\Pi_\ell = 3$. This can be understood as follows. For a scattering with the exchange of $\tilde{\lambda}_2^+$, all the external particles involved are fixed. Hence, we only have one contribution. Similarly, we have another contribution from the exchange of $\tilde{\lambda}_2^-$. For the scattering with the exchange of $\tilde{\lambda}_2^0$, we have four possible diagrams for each process. For example in the first process we have $\nu_L \bar{\nu}_L \rightarrow \tilde{\nu}_L \tilde{\nu}_L^*$, $\nu_L \bar{\nu}_L \rightarrow \tilde{\ell}_L^- \tilde{\ell}_L^{*-}$, $\ell_L^- \bar{\ell}_L^- \rightarrow \tilde{\nu}_L \tilde{\nu}_L^*$ and $\ell_L^- \bar{\ell}_L^- \rightarrow \tilde{\ell}_L^- \tilde{\ell}_L^{*-}$. However, the contribution is only $\frac{1}{4}$ from each diagram due to the factor of $\frac{1}{\sqrt{2}}$ in the Lagrangian (see (4.17)). Hence, in total we have a factor of $1 + 1 + 4 \times \frac{1}{4} = 3$.

Notice that in eqs. (B.95)–(B.95), since $\tilde{\ell}_\alpha - \ell_\alpha = \mu_{\tilde{g}}$, the equal flavor chemical potentials always cancel as expected (soft slepton masses can only induce lepton flavor violating interactions and not superequilibration). Hence eqs. (B.95)–(B.95) simply become

$$\sum_{g\ell,\zeta,\beta,\eta} \left[\ell_\alpha \bar{\ell}_\zeta \leftrightarrow \tilde{\ell}_\beta \tilde{\ell}_\eta^* \right]_- = -6\Pi_\ell \gamma_{t1,G} \sum_{\beta \neq \alpha} |R_{\alpha\beta}|^2 \frac{\mu_{\tilde{\ell}_\beta} - \mu_{\ell_\alpha}}{T}, \quad (\text{B.98})$$

$$\sum_{g\ell,\zeta,\beta,\eta} \left[\ell_\alpha \tilde{\ell}_\zeta \leftrightarrow \tilde{\ell}_\beta \ell_\eta \right]_- = -6\Pi_\ell \gamma_{t2,G} \sum_{\beta \neq \alpha} |R_{\alpha\beta}|^2 \frac{\mu_{\tilde{\ell}_\beta} - \mu_{\ell_\alpha}}{T}, \quad (\text{B.99})$$

$$\sum_{g\ell,\zeta,\beta,\eta} \left[\ell_\alpha \tilde{\ell}_\beta^* \leftrightarrow \tilde{\ell}_\zeta^* \ell_\eta \right]_- = -6\Pi_\ell \gamma_{s,G} \sum_{\beta \neq \alpha} |R_{\alpha\beta}|^2 \frac{\mu_{\tilde{\ell}_\beta} - \mu_{\ell_\alpha}}{T}. \quad (\text{B.100})$$

Similarly, we can calculate the scatterings with $P = Q, \tilde{H}_{u,d}$ for processes mediated by $SU(2)_L$ gauginos and $P = Q, \tilde{H}_{u,d}, e, u, d$ for processes mediated by $U(1)_Y$ gaugino. Altogether, we find these additional terms to the BEs of

$Y_{\Delta\ell_\alpha}$ and $Y_{\Delta\tilde{\ell}_\alpha}$ as follows

$$\begin{aligned}
sHz \frac{dY_{\Delta\ell_\alpha}}{dz} &\supset -42 (\gamma_{t1,2} + \gamma_{t2,2} + \gamma_{s,2}) \sum_{\beta \neq \alpha} 2 |R_{\alpha\beta}|^2 \frac{\mu_{\ell_\alpha} - \mu_{\tilde{\ell}_\beta}}{T} \\
&\quad -38 (\gamma_{t1,Y} + \gamma_{t2,Y} + \gamma_{s,Y}) \sum_{\beta \neq \alpha} 2 |R_{\alpha\beta}|^2 \frac{\mu_{\ell_\alpha} - \mu_{\tilde{\ell}_\beta}}{T}, \\
sHz \frac{dY_{\Delta\tilde{\ell}_\alpha}}{dz} &\supset -42 (\gamma_{t1,2} + \gamma_{t2,2} + \gamma_{s,2}) \sum_{\beta \neq \alpha} 2 |R_{\alpha\beta}|^2 \frac{\mu_{\tilde{\ell}_\alpha} - \mu_{\ell_\beta}}{T} \\
&\quad -38 (\gamma_{t1,Y} + \gamma_{t2,Y} + \gamma_{s,Y}) \sum_{\beta \neq \alpha} 2 |R_{\alpha\beta}|^2 \frac{\mu_{\tilde{\ell}_\alpha} - \mu_{\ell_\beta}}{T}. \quad (\text{B.101})
\end{aligned}$$

The reduced cross sections for the lepton flavor equilibration interactions (ignoring the quantum statistical factors) are given as follows

$$\begin{aligned}
\hat{\sigma}_{t1,G}(s) &= \frac{g_G^4}{8\pi} \left[\left(\frac{2m_{\lambda_G}^2}{s} + 1 \right) \ln \left| \frac{m_{\lambda_G}^2 + s}{m_{\lambda_G}^2} \right| - 2 \right], \\
\hat{\sigma}_{t2,G}(s) &= \frac{g_G^4}{8\pi} \left[\ln \left| \frac{m_{\lambda_G}^2 + s}{m_{\lambda_G}^2} \right| - \frac{s}{m_{\lambda_G}^2 + s} \right], \\
\hat{\sigma}_{s,G}(s) &= \frac{g_G^4}{16\pi} \left(\frac{s}{s - m_{\lambda_G}^2} \right)^2, \quad (\text{B.102})
\end{aligned}$$

where the gaugino thermal mass is $m_{\lambda_G}^2 = (9/2) g_G^2 T^2$. Notice that in the above, we have not included the factor involving the unitary rotation matrix $|R_{\alpha\beta}|^2$, in order to define the reduced cross sections in a flavor independent way. This factor is explicitly shown in the BE (B.101).

B.2.5 Boltzmann equations in the superequilibration regime

In the superequilibration regime, the BEs which describe the evolution of RHN and RHSN are still given respectively by the eqs. (B.71) and (B.76).

In the following we will simplify the BEs for lepton and slepton asymmetries eqs. (B.90) and (B.91) and show that in this regime, we can in fact sum them up into one single BE.

For $T \lesssim 10^7$ GeV, superequilibration occurs if SUSY-breaking terms are large enough. For example for superequilibration induced by gaugino interac-

tions we would need

$$T \lesssim 5 \times 10^7 \left(\frac{m_{1/2}}{500 \text{ GeV}} \right)^{2/3}, \quad (\text{B.103})$$

where $m_{1/2}$ is the gaugino Majorana mass. If we assume $m_{1/2} = \mathcal{O}(\text{TeV})$, these processes will be in equilibrium for $T \lesssim 8 \times 10^7 \text{ GeV}$ which implies the equilibration between particle-particle chemical potentials

$$\mu_\phi = \mu_{\tilde{\phi}}. \quad (\text{B.104})$$

From the equilibrium of top Yukawa interactions, we have the following relations

$$-\mu_Q + \mu_{\tilde{u}} = \mu_{\tilde{H}_u}, \quad -\mu_Q + \mu_u = \mu_{H_u}, \quad -\mu_{\tilde{Q}} + \mu_u = \mu_{\tilde{H}_u}. \quad (\text{B.105})$$

Using (B.104) and (B.105), we obtain

$$\begin{aligned} \mu_{\tilde{Q}} - \mu_{\tilde{u}} &= -\mu_{\tilde{H}_u} = -\mu_{H_u}, \\ \mu_Q - \mu_u &= -\mu_{\tilde{H}_u} = -\mu_{H_u}. \end{aligned} \quad (\text{B.106})$$

Hence, we can sum up BEs (B.90) and (B.91) and write down a single BE

for $Y_{L_{\text{tot}}}^\alpha \equiv Y_{\Delta\ell_\alpha} + Y_{\Delta\tilde{\ell}_\alpha}$ as follows

$$\begin{aligned}
sHz \frac{dY_{L_{\text{tot}}}^\alpha}{dz} = & \epsilon_\alpha(T) \frac{\gamma_{\tilde{N}}}{2} \left(\frac{Y_{\tilde{N}_{\text{tot}}}}{Y_{\tilde{N}}^{eq}} - 2 \right) - \frac{\gamma_{\tilde{N}}^\alpha}{2} \left(2 \frac{\mu_{\ell_\alpha}}{T} + 2 \frac{\mu_{H_u}}{T} \right) \\
& - \left[\frac{1}{2} \gamma_N^\alpha + \gamma_{\tilde{N}}^{(3)\alpha} + \gamma_{22}^\alpha \left(\frac{1}{2} \frac{Y_{\tilde{N}_{\text{tot}}}}{Y_{\tilde{N}}^{eq}} + 2 \right) \right] \left(2 \frac{\mu_{\ell_\alpha}}{T} + 2 \frac{\mu_{H_u}}{T} \right) \\
& - \left(\gamma_t^{(3)\alpha} \frac{Y_N}{Y_N^{eq}} + 2\gamma_t^{(4)\alpha} + 2\gamma_t^{(6)\alpha} + 2\gamma_t^{(7)\alpha} + \gamma_t^{(5)\alpha} \frac{Y_{\tilde{N}_{\text{tot}}}}{Y_{\tilde{N}}^{eq}} \right) \frac{2\mu_{\ell_\alpha}}{T} \\
& - \left(2\gamma_t^{(0)\alpha} \frac{Y_N}{Y_N^{eq}} + 2\gamma_t^{(1)\alpha} + 2\gamma_t^{(2)\alpha} + \frac{1}{2} \gamma_t^{(8)\alpha} \frac{Y_{\tilde{N}_{\text{tot}}}}{Y_{\tilde{N}}^{eq}} + 2\gamma_t^{(9)\alpha} \right) \frac{2\mu_{\ell_\alpha}}{T} \\
& - \left(\gamma_t^{(3)\alpha} + \gamma_t^{(4)\alpha} + \gamma_t^{(4)\alpha} \frac{Y_N}{Y_N^{eq}} + \gamma_t^{(6)\alpha} + \frac{1}{2} \gamma_t^{(7)\alpha} \frac{Y_{\tilde{N}_{\text{tot}}}}{Y_{\tilde{N}}^{eq}} \right) \frac{2\mu_{H_u}}{T} \\
& - \left(2\gamma_t^{(5)\alpha} + \gamma_t^{(7)\alpha} + \frac{1}{2} \gamma_t^{(6)\alpha} \frac{Y_{\tilde{N}_{\text{tot}}}}{Y_{\tilde{N}}^{eq}} \right) \frac{2\mu_{H_u}}{T} \\
& - \left(\gamma_t^{(1)\alpha} \frac{Y_N}{Y_N^{eq}} + \gamma_t^{(8)\alpha} + \gamma_t^{(9)\alpha} + \frac{1}{2} \gamma_t^{(9)\alpha} \frac{Y_{\tilde{N}_{\text{tot}}}}{Y_{\tilde{N}}^{eq}} \right) \frac{2\mu_{H_u}}{T} \\
& - \left(2\gamma_t^{(0)\alpha} + \gamma_t^{(1)\alpha} + \gamma_t^{(2)\alpha} \frac{Y_N}{Y_N^{eq}} \right) \frac{2\mu_{H_u}}{T} + W_{\Delta L=2}^\alpha + \widetilde{W}_{\Delta L=2}^\alpha \\
& - 84 (\gamma_{t1,2} + \gamma_{t2,2} + \gamma_{s,2}) \sum_{\beta \neq \alpha} 2 |R_{\alpha\beta}|^2 \frac{\mu_{\ell_\alpha} - \mu_{\ell_\beta}}{T} \\
& - 76 (\gamma_{t1,Y} + \gamma_{t2,Y} + \gamma_{s,Y}) \sum_{\beta \neq \alpha} 2 |R_{\alpha\beta}|^2 \frac{\mu_{\ell_\alpha} - \mu_{\ell_\beta}}{T}, \quad (\text{B.107})
\end{aligned}$$

where in the last two lines, we have included the lepton flavor equilibration interactions.

Using eqs. (B.42), we have

$$\frac{2\mu_{\ell_\alpha}}{T} = \frac{Y_{\Delta\ell_\alpha}}{2Y_\ell^{eq}}, \quad \frac{2\mu_{H_u}}{T} = \frac{Y_{\Delta H_u}}{2Y_{H_u}^{eq}}, \quad (\text{B.108})$$

where $2Y_\ell^{eq} = Y_{H_u}^{eq} = \frac{15}{4\pi^2 g_s^*}$ since $g_{H_u} = g_\ell = 1$. Notice that since $Y_{\Delta\ell_\alpha}$ and $Y_{\Delta H_u}$ are the asymmetry abundances summed over $SU(2)_L$ degrees of freedom, we take this into account by multiplying a factor of 2 to Y_ℓ^{eq} and $Y_{H_u}^{eq}$ in eqs. (B.108). Under superequilibration $Y_{\Delta B} = 2Y_{\Delta F}$, then we have $Y_{L_{\text{tot}}}^\alpha \equiv Y_{\Delta\ell_\alpha} + Y_{\Delta\tilde{\ell}_\alpha} = 3Y_{\Delta\ell_\alpha}$ and $Y_{H_{\text{tot}}} \equiv Y_{\Delta H_u} + Y_{\Delta\tilde{H}_u} = \frac{3}{2}Y_{\Delta\tilde{H}_u}$. With these,

we can rewrite eqs. (B.108) as follows

$$\frac{2\mu_{\ell_\alpha}}{T} = \frac{Y_{L_{\text{tot}}}^\alpha}{Y_c^{eq}}, \quad \frac{2\mu_{H_u}}{T} = \frac{Y_{H_{\text{tot}}}}{Y_c^{eq}}, \quad (\text{B.109})$$

where $Y_c^{eq} \equiv \frac{45}{4\pi^2 g_s^*}$.

Finally the BE (B.107) becomes

$$\begin{aligned} sHz \frac{dY_{L_{\text{tot}}}^\alpha}{dz} = & \epsilon_\alpha(T) \frac{\gamma_{\tilde{N}}}{2} \left(\frac{Y_{\tilde{N}_{\text{tot}}}}{Y_{\tilde{N}}^{eq}} - 2 \right) \\ & - \left[\frac{\gamma_{\tilde{N}}^\alpha}{2} + \frac{\gamma_N^\alpha}{2} + \gamma_{\tilde{N}}^{(3)\alpha} + \left(\frac{1}{2} \frac{Y_{\tilde{N}_{\text{tot}}}}{Y_{\tilde{N}}^{eq}} + 2 \right) \gamma_{22}^\alpha \right] \left(\frac{Y_{L_{\text{tot}}}^\alpha}{Y_c^{eq}} + \frac{Y_{H_{\text{tot}}}}{Y_c^{eq}} \right) \\ & - 2 \left(\gamma_t^{(1)\alpha} + \gamma_t^{(2)\alpha} + \gamma_t^{(4)\alpha} + \gamma_t^{(6)\alpha} + \gamma_t^{(7)\alpha} + \gamma_t^{(9)\alpha} \right) \frac{Y_{L_{\text{tot}}}^\alpha}{Y_c^{eq}} \\ & - \left[\left(2\gamma_t^{(0)} + \gamma_t^{(3)\alpha} \right) \frac{Y_N}{Y_N^{eq}} + \left(\gamma_t^{(5)\alpha} + \frac{1}{2} \gamma_t^{(8)\alpha} \right) \frac{Y_{\tilde{N}_{\text{tot}}}}{Y_{\tilde{N}}^{eq}} \right] \frac{Y_{L_{\text{tot}}}^\alpha}{Y_c^{eq}} \\ & - \left(2\gamma_t^{(0)\alpha} + \gamma_t^{(1)\alpha} + \gamma_t^{(3)\alpha} + \gamma_t^{(4)\alpha} + 2\gamma_t^{(5)\alpha} \right. \\ & \quad \left. + \gamma_t^{(6)\alpha} + \gamma_t^{(7)\alpha} + \gamma_t^{(8)\alpha} + \gamma_t^{(9)\alpha} \right) \frac{Y_{H_{\text{tot}}}}{Y_c^{eq}} \\ & - \left[\left(\gamma_t^{(1)\alpha} + \gamma_t^{(2)\alpha} + \gamma_t^{(4)\alpha} \right) \frac{Y_N}{Y_N^{eq}} + \frac{1}{2} \left(\gamma_t^{(6)\alpha} + \gamma_t^{(7)\alpha} + \gamma_t^{(9)\alpha} \right) \frac{Y_{\tilde{N}_{\text{tot}}}}{Y_{\tilde{N}}^{eq}} \right] \frac{Y_{H_{\text{tot}}}}{Y_c^{eq}} \\ & - 84 \sum_{\beta \neq \alpha} \left(\gamma_{t1,2}^{\beta\alpha} + \gamma_{t2,2}^{\beta\alpha} + \gamma_{s,2}^{\beta\alpha} \right) \frac{Y_{L_{\text{tot}}}^\alpha - Y_{L_{\text{tot}}}^\beta}{Y_c^{eq}} \\ & - 76 \sum_{\beta \neq \alpha} \left(\gamma_{t1,Y}^{\beta\alpha} + \gamma_{t2,Y}^{\beta\alpha} + \gamma_{s,Y}^{\beta\alpha} \right) \frac{Y_{L_{\text{tot}}}^\alpha - Y_{L_{\text{tot}}}^\beta}{Y_c^{eq}}, \quad (\text{B.110}) \end{aligned}$$

where we have absorbed the factor $|R_{\alpha\beta}|^2$ into the definition of lepton flavor equilibration reaction densities $\gamma_{x,G}^{\beta\alpha} = |R_{\alpha\beta}|^2 \gamma_{x,G}$. Notice that we have also dropped the terms $W_{\Delta L=2}^\alpha$ and $\widetilde{W}_{\Delta L=2}^\alpha$ which we are neglecting in our numerical evaluation.

Instead of following the evolution of the flavored lepton asymmetries $Y_{L_{\text{tot}}}^\alpha$ as in eq. (B.110), it is more appropriate to follow the evolution of $Y_{\Delta_\alpha} \equiv Y_{\Delta B}/3 - Y_{\Delta L}^\alpha$ because $B/3 - L_\alpha$ is conserved by EW sphalerons and all other MSSM interactions. Here we denote $Y_{\Delta L}^\alpha \equiv Y_{L_{\text{tot}}}^\alpha + Y_{\Delta e_R^\alpha}$ and $Y_{\Delta e_R^\alpha}$ is the lepton asymmetry in the lepton singlet e_R^α . We have to consider $Y_{\Delta e_R^\alpha}$ because

when charged lepton Yukawa interactions are not negligible, significant lepton asymmetry will be stored in e_R^α . Since EW sphalerons violate both L and B , we can write down the BEs for $Y_{\Delta L^\alpha}$ and $Y_{\Delta B}$

$$\frac{dY_{\Delta L^\alpha}}{dz} = \frac{dY_{L_{\text{tot}}^\alpha}}{dz} + \frac{dY_{L^\alpha}^{EW}}{dz}, \quad (\text{B.111})$$

$$\frac{dY_{\Delta B}}{dz} = \frac{dY_{\Delta B}^{EW}}{dz}, \quad (\text{B.112})$$

where we have included the B and L violating sources from EW sphalerons. Since $B/3 - L_\alpha$ is conserved by EW sphalerons, we have

$$\frac{1}{3} \frac{dY_{\Delta B}^{EW}}{dz} - \frac{dY_{L^\alpha}^{EW}}{dz} = 0. \quad (\text{B.113})$$

Taking the difference of eqs. (B.111) and (B.112) with the proper factor of $1/3$ and using eq. (B.113), we arrive at

$$\frac{dY_{\Delta\alpha}}{dz} = -\frac{dY_{L_{\text{tot}}^\alpha}}{dz}, \quad (\text{B.114})$$

where we can clearly see that the only $B/3 - L_\alpha$ -violating sources are from the RNSN decays.

In order to solve the BE (B.114), we need to relate $Y_{L_{\text{tot}}^\alpha}$ and $Y_{H_{\text{tot}}}$ to $Y_{\Delta\alpha}$. Using the chemical equilibrium conditions and conservation laws, they can be related as follows

$$Y_{L_{\text{tot}}^\alpha} = \sum_{\beta} A_{\alpha\beta} Y_{\Delta\beta}, \quad Y_{H_{\text{tot}}} = \sum_{\beta} C_{\beta} Y_{\Delta\beta}.$$

The values of the entries of the matrix A and of the vector C above depend on the range of temperature, that is on the particular set of interactions that are in equilibrium when leptogenesis is taking place and are presented in Appendix C.

B.2.6 Boltzmann equations in the non-superequilibration regime

Here we present the BEs that must be used for numerical studies of SL when the heavy sneutrino masses satisfy the condition eq. (5.1). We also include the SE reactions $\gamma_{\tilde{g}}^{\text{eff}}$ and $\gamma_{\mu_{\tilde{H}}}^{\text{eff}}$ defined in eq. (5.46), that extend the validity of our BEs to all temperatures.

The BEs which describe the evolution of RHN and RHSN are still given respectively by the eqs. (B.71) and (B.76).

For the evolution of the flavor charges Y_{Δ_α} , we have

$$sH z \frac{dY_{\Delta_\alpha}}{dz} = - \left(E_\alpha + \tilde{E}_\alpha \right), \quad (\text{B.115})$$

where

$$\begin{aligned} E_\alpha &= \epsilon_\alpha^f(z) \frac{\gamma_{\tilde{N}}}{2} \left(\frac{Y_{\tilde{N}_{\text{tot}}}}{Y_{\tilde{N}}^{\text{eq}}} - 2 \right) - \frac{\gamma_{\tilde{N}}^{f,\alpha}}{2} (\mathfrak{y}_{\Delta\ell_\alpha} + \mathfrak{y}_{\Delta\tilde{H}_u}) - \frac{1}{4} \gamma_N^\alpha (\mathfrak{y}_{\Delta\ell_\alpha} + \mathfrak{y}_{\Delta H_u}) \\ &\quad - \left(\gamma_t^{(3)\alpha} \frac{Y_N}{Y_N^{\text{eq}}} + 2\gamma_t^{(4)\alpha} + 2\gamma_t^{(6)\alpha} + 2\gamma_t^{(7)\alpha} + \gamma_t^{(5)\alpha} \frac{Y_{\tilde{N}_{\text{tot}}}}{Y_{\tilde{N}}^{\text{eq}}} \right) \mathfrak{y}_{\Delta\ell_\alpha} \\ &\quad - \left(\gamma_t^{(3)\alpha} + \gamma_t^{(4)\alpha} + \gamma_t^{(4)\alpha} \frac{Y_N}{Y_N^{\text{eq}}} + \gamma_t^{(5)\alpha} + \gamma_t^{(6)\alpha} + \frac{1}{2} \gamma_t^{(7)\alpha} \frac{Y_{\tilde{N}_{\text{tot}}}}{Y_{\tilde{N}}^{\text{eq}}} \right) \mathfrak{y}_{\Delta H_u} \\ &\quad - \left(\gamma_t^{(5)k} + \gamma_t^{(7)k} + \frac{1}{2} \gamma_t^{(6)k} \frac{Y_{\tilde{N}_{\text{tot}}}}{Y_{\tilde{N}}^{\text{eq}}} \right) (2\mathfrak{y}_{\Delta\tilde{H}_u} - \mathfrak{y}_{\Delta H_u}) \\ &\quad + \gamma_{\tilde{g}}^{\text{eff}} (\mathfrak{y}_{\Delta\tilde{\ell}_\alpha} - \mathfrak{y}_{\Delta\ell_\alpha}), \end{aligned} \quad (\text{B.116})$$

and

$$\begin{aligned}
\tilde{E}_\alpha &= \epsilon_\alpha^s(z) \frac{\gamma_{\tilde{N}}}{2} \left(\frac{Y_{\tilde{N}_{\text{tot}}}}{Y_{\tilde{N}}^{eq}} - 2 \right) - \frac{\gamma_{\tilde{N}}^{s,\alpha}}{2} (\mathcal{Y}_{\Delta\tilde{\ell}_\alpha} + \mathcal{Y}_{\Delta H_u}) - \frac{1}{4} \gamma_{\tilde{N}}^\alpha (\mathcal{Y}_{\Delta\tilde{\ell}_\alpha} + \mathcal{Y}_{\Delta\tilde{H}_u}) \\
&- \left(\gamma_{\tilde{N}}^{(3)\alpha} + \frac{1}{2} \gamma_{22}^\alpha \frac{Y_{\tilde{N}_{\text{tot}}}}{Y_{\tilde{N}}^{eq}} + 2\gamma_{22}^\alpha \right) (\mathcal{Y}_{\Delta\tilde{\ell}_\alpha} + 2\mathcal{Y}_{\Delta\tilde{H}_u} - \mathcal{Y}_{\Delta H_u}) \\
&- \left(2\gamma_t^{(0)\alpha} \frac{Y_N}{Y_N^{eq}} + 2\gamma_t^{(1)\alpha} + 2\gamma_t^{(2)\alpha} + \frac{1}{2} \gamma_t^{(8)\alpha} \frac{Y_{\tilde{N}_{\text{tot}}}}{Y_{\tilde{N}}^{eq}} + 2\gamma_t^{(9)k} \right) \mathcal{Y}_{\Delta\tilde{\ell}_\alpha} \\
&- \left(\gamma_t^{(0)\alpha} + \gamma_t^{(1)\alpha} \frac{Y_N}{Y_N^{eq}} + \gamma_t^{(8)\alpha} + \gamma_t^{(9)\alpha} + \frac{1}{2} \gamma_t^{(9)\alpha} \frac{Y_{\tilde{N}_{\text{tot}}}}{Y_{\tilde{N}}^{eq}} \right) \mathcal{Y}_{\Delta H_u} \\
&- \left(\gamma_t^{(0)\alpha} + \gamma_t^{(1)\alpha} + \gamma_t^{(2)\alpha} \frac{Y_N}{Y_N^{eq}} \right) (2\mathcal{Y}_{\Delta\tilde{H}_u} - \mathcal{Y}_{\Delta H_u}) \\
&- \gamma_{\tilde{g}}^{\text{eff}} (\mathcal{Y}_{\Delta\tilde{\ell}_\alpha} - \mathcal{Y}_{\Delta\ell_\alpha}). \tag{B.117}
\end{aligned}$$

The \mathcal{Y}_Δ appearing in these equations are defined in eq. (5.40), while the SE reaction rate $\gamma_{\tilde{g}}^{\text{eff}}$ has been defined in eq. (5.46). For the decay reaction densities we have:

$$\begin{aligned}
\gamma_{\tilde{N}}^{s,\alpha} &= \gamma_{\tilde{N}}^{f,\alpha} \left(1 + \frac{A^2}{M^2} - \frac{AB}{M^2} \right), \\
\gamma_{\tilde{N}}^\alpha &\equiv \gamma_{\tilde{N}}^{f,\alpha} + \gamma_{\tilde{N}}^{s,\alpha}, \tag{B.118}
\end{aligned}$$

where A and B are taken to be real. For values $M \sim 10^8$ GeV the higher order terms in the soft parameters can be safely neglected.

The scattering processes considered are

Reaction	ΔR_B	ΔR_3
$\gamma_{22}^\alpha \equiv \gamma \left(\tilde{N}_\pm \tilde{l}_\alpha \leftrightarrow \tilde{Q} \tilde{u}^* \right) = \gamma \left(\tilde{N}_\pm \tilde{Q}^* \leftrightarrow \tilde{l}_\alpha^* \tilde{u}^* \right) = \gamma \left(\tilde{N}_\pm \tilde{u} \leftrightarrow \tilde{l}_\alpha^* \tilde{Q} \right)$	0	1
$\gamma_{\tilde{N}}^{(3)\alpha} \equiv \gamma \left(\tilde{N}_\pm \leftrightarrow \tilde{u}^* \tilde{l}_\alpha^* \tilde{Q} \right)$	0	1
$\gamma_t^{(0)\alpha} \equiv \gamma \left(N \tilde{l}_\alpha \leftrightarrow Q \tilde{u}^* \right) = \gamma \left(N \tilde{l}_\alpha \leftrightarrow \tilde{Q} \bar{u} \right)$	-1	0
$\gamma_t^{(1)\alpha} \equiv \gamma \left(N \bar{Q} \leftrightarrow \tilde{l}_\alpha^* \tilde{u}^* \right) = \gamma \left(N u \leftrightarrow \tilde{l}_\alpha^* \tilde{Q} \right)$	-1	0
$\gamma_t^{(2)\alpha} \equiv \gamma \left(N \tilde{u} \leftrightarrow \tilde{l}_\alpha^* Q \right) = \gamma \left(N \tilde{Q}^* \leftrightarrow \tilde{l}_\alpha^* \bar{u} \right)$	-1	0
$\gamma_t^{(3)\alpha} \equiv \gamma \left(N l_\alpha \leftrightarrow Q \bar{u} \right)$	-1	0
$\gamma_t^{(4)\alpha} \equiv \gamma \left(N u \leftrightarrow \bar{l}_\alpha Q \right) = \gamma \left(N \bar{Q} \leftrightarrow \bar{l}_\alpha \bar{u} \right)$	-1	0
$\gamma_t^{(5)\alpha} \equiv \gamma \left(\tilde{N}_\pm l_\alpha \leftrightarrow Q \tilde{u}^* \right) = \gamma \left(\tilde{N}_\pm l_\alpha \leftrightarrow \tilde{Q} \bar{u} \right)$	0	1
$\gamma_t^{(6)\alpha} \equiv \gamma \left(\tilde{N}_\pm \tilde{u} \leftrightarrow \bar{l}_\alpha Q \right) = \gamma \left(\tilde{N}_\pm \tilde{Q}^* \leftrightarrow \bar{l}_\alpha \bar{u} \right)$	0	1
$\gamma_t^{(7)\alpha} \equiv \gamma \left(\tilde{N}_\pm \bar{Q} \leftrightarrow \bar{l}_\alpha \tilde{u}^* \right) = \gamma \left(\tilde{N}_\pm u \leftrightarrow \bar{l}_\alpha \tilde{Q} \right)$	0	1
$\gamma_t^{(8)\alpha} \equiv \gamma \left(\tilde{N}_\pm \tilde{l}_\alpha^* \leftrightarrow \bar{Q} u \right)$	2	1
$\gamma_t^{(9)\alpha} \equiv \gamma \left(\tilde{N}_\pm Q \leftrightarrow \tilde{l}_\alpha u \right) = \gamma \left(\tilde{N}_\pm \bar{u} \leftrightarrow \tilde{l}_\alpha \bar{Q} \right)$	2	1

where for convenience we have listed the corresponding changes of the R-charges in each process. The reduced cross sections for the processes listed above can be found in ref. [66]. The BEs above do not include the CP asymmetries of top and stop scatterings as discussed in Section 2.4.2.1.

The BEs for the evolution of R_B and R_χ , defined in eqs. (5.9)-(5.10), are:

$$sH z \frac{dY_{\Delta R_B}}{dz} = \sum_\alpha \left(2\tilde{F}_\alpha + F_\alpha \right) - \gamma_{\tilde{g}}^{\text{eff}} \mathcal{Y}_{\Delta \tilde{g}}, \quad (\text{B.119})$$

$$sH z \frac{dY_{\Delta R_\chi}}{dz} = \frac{1}{3} \sum_\alpha \left(\tilde{G}_\alpha - G_\alpha \right) - \frac{\gamma_{\tilde{g}}^{\text{eff}}}{3} \mathcal{Y}_{\Delta \tilde{g}} + \frac{\gamma_{\mu_{\tilde{H}}}^{\text{eff}}}{3} \left(\mathcal{Y}_{\Delta \tilde{H}_u} + \mathcal{Y}_{\Delta \tilde{H}_d} \right), \quad (\text{B.120})$$

where again the SE rates $\gamma_{\tilde{g}}^{\text{eff}}$ and $\gamma_{\mu_{\tilde{H}}}^{\text{eff}}$ have been also included. F_α and \tilde{F}_α are

given by:

$$\begin{aligned}
F_\alpha &= -\frac{1}{4}\gamma_N^\alpha (\mathfrak{y}_{\Delta l_\alpha} + \mathfrak{y}_{\Delta H_u}) \\
&\quad - \left(\gamma_t^{(3)\alpha} \frac{Y_N}{Y_N^{eq}} + 2\gamma_t^{(4)\alpha} \right) \mathfrak{y}_{\Delta l_\alpha} \\
&\quad - \left(\gamma_t^{(3)\alpha} + \gamma_t^{(4)\alpha} + \gamma_t^{(4)\alpha} \frac{Y_N}{Y_N^{eq}} \right) \mathfrak{y}_{\Delta H_u}, \tag{B.121}
\end{aligned}$$

and

$$\begin{aligned}
\tilde{F}_\alpha &= \epsilon_\alpha^s(z) \frac{\gamma_{\tilde{N}}}{2} \left(\frac{Y_{\tilde{N}_{\text{tot}}}}{Y_{\tilde{N}}^{eq}} - 2 \right) - \frac{\gamma_{\tilde{N}}^{s,\alpha}}{2} (\mathfrak{y}_{\Delta \tilde{l}_\alpha} + \mathfrak{y}_{\Delta H_u}) - \frac{1}{8}\gamma_N^\alpha (\mathfrak{y}_{\Delta \tilde{l}_\alpha} + \mathfrak{y}_{\Delta \tilde{H}_u}) \\
&\quad - \left(\gamma_t^{(0)\alpha} \frac{Y_N}{Y_N^{eq}} + \gamma_t^{(1)\alpha} + \gamma_t^{(2)\alpha} + \frac{1}{2}\gamma_t^{(8)\alpha} \frac{Y_{\tilde{N}_{\text{tot}}}}{Y_{\tilde{N}}^{eq}} + 2\gamma_t^{(9)\alpha} \right) \mathfrak{y}_{\Delta \tilde{l}_\alpha} \\
&\quad - \left(\frac{1}{2}\gamma_t^{(0)\alpha} + \frac{1}{2}\gamma_t^{(1)\alpha} \frac{Y_N}{Y_N^{eq}} + \gamma_t^{(8)\alpha} + \gamma_t^{(9)\alpha} + \frac{1}{2}\gamma_t^{(9)\alpha} \frac{Y_{\tilde{N}_{\text{tot}}}}{Y_{\tilde{N}}^{eq}} \right) \mathfrak{y}_{\Delta H_u} \\
&\quad - \frac{1}{2} \left(\gamma_t^{(0)\alpha} + \gamma_t^{(1)\alpha} + \gamma_t^{(2)\alpha} \frac{Y_N}{Y_N^{eq}} \right) (2\mathfrak{y}_{\Delta \tilde{H}_u} - \mathfrak{y}_{\Delta H_u}). \tag{B.122}
\end{aligned}$$

For G_α and \tilde{G}_α we have:

$$\begin{aligned}
G_\alpha &= \epsilon_\alpha^f(z) \frac{\gamma_{\tilde{N}}}{2} \left(\frac{Y_{\tilde{N}_{\text{tot}}}}{Y_{\tilde{N}}^{eq}} - 2 \right) - \frac{\gamma_{\tilde{N}}^{f,\alpha}}{2} (\mathfrak{y}_{\Delta l_\alpha} + \mathfrak{y}_{\Delta \tilde{H}_u}) \\
&\quad - \left(2\gamma_t^{(6)\alpha} + 2\gamma_t^{(7)\alpha} + \gamma_t^{(5)\alpha} \frac{Y_{\tilde{N}_{\text{tot}}}}{Y_{\tilde{N}}^{eq}} \right) \mathfrak{y}_{\Delta l_\alpha} \\
&\quad - \left(\gamma_t^{(5)\alpha} + \gamma_t^{(6)\alpha} + \frac{1}{2}\gamma_t^{(7)\alpha} \frac{Y_{\tilde{N}_{\text{tot}}}}{Y_{\tilde{N}}^{eq}} \right) \mathfrak{y}_{\Delta H_u} \\
&\quad - \left(\gamma_t^{(5)\alpha} + \gamma_t^{(7)\alpha} + \frac{1}{2}\gamma_t^{(6)\alpha} \frac{Y_{\tilde{N}_{\text{tot}}}}{Y_{\tilde{N}}^{eq}} \right) (2\mathfrak{y}_{\Delta \tilde{H}_u} - \mathfrak{y}_{\Delta H_u}), \tag{B.123}
\end{aligned}$$

and

$$\begin{aligned}
\tilde{G}_\alpha &= \epsilon_\alpha^s(z) \frac{\gamma_{\tilde{N}}}{2} \left(\frac{Y_{\tilde{N}_{\text{tot}}}}{Y_{\tilde{N}}^{\text{eq}}} - 2 \right) - \frac{\gamma_{\tilde{N}}^{s,\alpha}}{2} (\mathfrak{y}_{\Delta\tilde{\ell}_\alpha} + \mathfrak{y}_{\Delta H_u}) \\
&+ \left(\gamma_{\tilde{N}}^{(3)\alpha} + \frac{1}{2} \gamma_{22}^\alpha \frac{Y_{\tilde{N}_{\text{tot}}}}{Y_{\tilde{N}}^{\text{eq}}} + 2\gamma_{22}^\alpha \right) (\mathfrak{y}_{\Delta\tilde{\ell}_\alpha} + 2\mathfrak{y}_{\Delta\tilde{H}_u} - \mathfrak{y}_{\Delta H_u}) \\
&- \left(\frac{1}{2} \gamma_t^{(8)\alpha} \frac{Y_{\tilde{N}_{\text{tot}}}}{Y_{\tilde{N}}^{\text{eq}}} + 2\gamma_t^{(9)\alpha} \right) \mathfrak{y}_{\Delta\tilde{\ell}_\alpha} \\
&- \left(\gamma_t^{(8)\alpha} + \gamma_t^{(9)\alpha} + \frac{1}{2} \gamma_t^{(9)\alpha} \frac{Y_{\tilde{N}_{\text{tot}}}}{Y_{\tilde{N}}^{\text{eq}}} \right) \mathfrak{y}_{\Delta H_u}. \tag{B.124}
\end{aligned}$$

The density asymmetries of the five charges in the BEs (B.115), (B.119) and (B.120) define the basis $Y_{\Delta_a} = \{Y_{\Delta_\alpha}, Y_{\Delta R_B}, Y_{\Delta R_\chi}\}$ in terms of which the five fermionic density-asymmetries $Y_{\Delta\psi_a} = \{Y_{\Delta\ell_\alpha}, Y_{\Delta\tilde{g}}, Y_{\Delta\tilde{H}_u}\}$, that are the relevant ones for the SL processes, have to be expressed. In fact, they can be related by 5×5 A -matrix defined according to:

$$Y_{\Delta\psi_a} = A_{ab} Y_{\Delta_b},$$

where the numerical values of A_{ab} are presented in Section 5.2.2.2.

As we have explained, with the inclusion of $\gamma_{\tilde{g}}^{\text{eff}}$ and $\gamma_{\mu_{\tilde{H}}}^{\text{eff}}$ our BEs are valid at all temperatures. To verify this, we have compared the results obtained with the complete BEs given above, with what is obtained by integrating the set of BEs specific for the SE regime, that reduce to the equations for the neutrino and sneutrino abundances eq. (B.71) and eq. (B.76) plus the three equations for the flavor charges eq. (B.115). Of course, one also has to use the A^ℓ matrices and $C^{\tilde{H}_u}$ vectors appropriate for the SE limits of the two cases that we have been studying (recalling also that $A^{\tilde{\ell}} = 2A^\ell$ and $C^{H_u} = 2C^{\tilde{H}_u}$). For the two cases we are analyzing: Case I ($h_{e,d}$ Yukawa equilibrium) and Case II ($h_{e,d}$ Yukawa non-equilibrium), the corresponding matrices are given in Appendix C in eqs. (C.8) and (C.10).

Appendix C

Conditions in the Superequilibration Regime

On top of the conditions 1. to 5. listed in Section 5.2.2.1, at relatively low temperatures, additional conditions from reactions in chemical equilibrium hold which we will list them here. For simplicity of notations, in the following we denote the chemical potentials with the same notation that labels the corresponding field: $\phi \equiv \mu_\phi$.

6_{SE}. Equilibration of the particle-antiparticle chemical potentials $\mu_\phi = \mu_{\tilde{\phi}}$ (generally referred as *superequilibration* (SE) or superequilibrium [107]) is ensured when reactions like $\tilde{\ell}\tilde{\ell} \leftrightarrow \ell\ell$ are faster than the Universe expansion rate. These reactions are induced by gaugino interactions, but since they require a gaugino chirality flip they turn out to be proportional to its soft mass $m_{\tilde{g}}^2$, and can be neglected in the limit $m_{\tilde{g}} \rightarrow 0$.

Furthermore, since the μ parameter of the $\mu\hat{H}_u\hat{H}_d$ superpotential term is expected to be of the order of the soft gaugino masses, it is reasonable to consider in the same temperature range also the effect of the higgsino mixing term, which implies that the sum of the up- and down- higgsino chemical potentials vanishes. The rates of the corresponding reactions, given approximately by $\Gamma_{\tilde{g}} \sim m_{\tilde{g}}^2/T$ and $\Gamma_\mu \sim \mu^2/T$, are faster than the Universe expansion rate up to temperatures

$$T \lesssim 5 \cdot 10^7 \left(\frac{m_{\tilde{g}}, \mu}{500 \text{ GeV}} \right)^{2/3} \text{ GeV}. \quad (\text{C.1})$$

For example the fast lepton-slepton scattering $\tilde{\ell}\tilde{\ell} \leftrightarrow \ell\ell$ together with fast gaugino scattering $\tilde{\ell} \leftrightarrow \ell + \tilde{g}$ (eq. (5.16)) imply

$$\tilde{g} = 0. \quad (\text{C.2})$$

We can also see that the vanishing of gaugino chemical potential eq. (C.2) together with other fast gaugino scatterings like $\tilde{Q} \leftrightarrow Q + \tilde{g}$, $H_{u,d} \leftrightarrow \tilde{H}_{u,d} + \tilde{g}$ and $\tilde{u}, \tilde{d}, \tilde{e} = u, d, e - \tilde{g}$ (see eqs. (5.16)–(5.18)) imply equilibration of the particle-sparticle chemical potentials $\mu_\phi = \mu_{\tilde{\phi}}$ (i.e. superequilibration).

On the other hand, fast $\tilde{H}_u \leftrightarrow \tilde{H}_d$ enforces the condition:

$$\tilde{H}_u + \tilde{H}_d = 0. \quad (\text{C.3})$$

7_{SE}. Up to temperatures given by (C.1) the MSSM has the same global anomalies than the SM, that are the EW $SU(2)_L-U(1)_{B+L}$ mixed anomaly and the QCD chiral anomaly. They generate the effective operators $O_{EW} = \Pi_\alpha(QQQ\ell_\alpha)$ and $O_{QCD} = \Pi_i(QQu_{Li}^c d_{Li}^c)$. Above the EW phase transition reactions induced by these operators are in thermal equilibrium, and the corresponding conditions read (compared to the non-superequilibration sphaleron conditions (5.26) and (5.27)):

$$9Q + \sum_\alpha \ell_\alpha = 0 \quad (\text{C.4})$$

$$6Q - \sum_i (u_i + d_i) = 0, \quad (\text{C.5})$$

where we have used the same chemical potential for the three quark doublets (eq.(5.25)), which is always appropriate in the SE regime below the limit (C.1).

C.1 Flavor charges

Eqs. (5.21) and (5.23)–(5.25), together with the SE conditions (C.2)–(C.3), the two anomaly conditions (C.4)–(C.5) and the hypercharge neutrality condition

(5.20), give $11 + 2 + 2 + 1 = 16$ constraints for the 18 chemical potentials. Note however that there is one redundant constraint, that we take to be the QCD sphaleron condition, since by summing up eqs. (5.23) and (5.24) and taking into account (5.25), (C.2), and (C.3) we obtain precisely eq. (C.5). Therefore, like in the SM, we have three independent chemical potentials, that could be taken to be the ones corresponding to the leptons doublets. Another choice, that is more useful in leptogenesis, is to define three linear combinations of the chemical potentials corresponding to the $SU(2)_L$ anomaly free flavor charges $B/3 - L_\alpha$. The reason is that these charges, being anomaly free and perturbatively conserved by the low energy MSSM Lagrangian, evolve *slowly* because the corresponding symmetries are violated only by the heavy Majorana neutrino dynamics. Their evolution is thus determined by reactions belonging to type (iii), and needs to be computed by means of three independent Boltzmann equations. In terms of the quantity defined in (5.13) the density of the $B/3 - L_\alpha$ charge asymmetry normalized to the entropy density can be written as $Y_{\Delta_\alpha} \equiv Y_{\Delta B}/3 - Y_{\Delta L_\alpha}$:

$$Y_{\Delta_\alpha} = 3 \left[\frac{1}{3} \sum_i (2Y_{\Delta Q_i} + Y_{\Delta u_i} + Y_{\Delta d_i}) - (2Y_{\Delta \ell_\alpha} + Y_{\Delta e_\alpha}) - \frac{2}{3} Y_{\Delta \tilde{g}} \right]. \quad (\text{C.6})$$

The expression above is completely general and holds in all temperature regimes, including the NSE regime (see Section 5.2). Note that \tilde{g} in the equation above cancels for the quarks but not for the leptons, and thus in the NSE, in which the gaugino chemical potential does not vanish, when the Y_{Δ_α} charges are expressed just in terms of the number density asymmetries of the fermions, $Y_{\Delta \tilde{g}}$ also contributes.

In eq. (C.6) we have left in clear some numerical factors: the overall factor of 3 adds the contributions of scalars (that is twice that of fermions), the factor of 2 in front of the $Y_{\Delta Q_i}$ and $Y_{\Delta \ell_\alpha}$ accounts for the $SU(2)_L$ gauge multiplicity, while the color factor compensates against the the quark baryon number $B = 1/3$.

The density asymmetries of the doublet leptons and higgsinos, that weight the washout terms in the Boltzmann equations, can now be expressed in terms of the anomaly free charges by means of the A matrix and C vectors introduced

respectively in ref. [28] and ref. [32] that are defined as:

$$Y_{\Delta\ell_\alpha} = A_{\alpha\beta}^\ell Y_{\Delta\beta}, \quad Y_{\Delta\tilde{H}_{u,d}} = C_\alpha^{\tilde{H}_{u,d}} Y_{\Delta\alpha}. \quad (\text{C.7})$$

Here and in the following we will give results for the A and C matrices for the fermion states. We recall that in the SE regime the density asymmetry of a scalar boson that is in chemical equilibrium with its fermionic partner is given simply by $Y_{\Delta b} = 2 Y_{\Delta f}$ with the factor of 2 from statistics.

C.2 All Yukawa reactions in equilibrium

Assuming moderate values of $\tan\beta$, at temperatures below the limit in eq. (5.22), A and C are given by¹

$$A^\ell = \frac{1}{9 \times 237} \begin{pmatrix} -221 & 16 & 16 \\ 16 & -221 & 16 \\ 16 & 16 & -221 \end{pmatrix},$$

$$C^{\tilde{H}_u} = -C^{\tilde{H}_d} = \frac{-4}{237} (1, 1, 1). \quad (\text{C.8})$$

Note that since in this regime the chemical potentials for the scalars and leptons degrees of freedom of each chiral multiplet equilibrate, the analogous results for $Y_{\Delta\ell_\alpha} + Y_{\Delta\bar{\ell}_\alpha}$ can be obtained by simply multiplying the A matrix in eq.(C.8) by a factor of 3. This gives the same A matrix obtained in the non-supersymmetric case in the same regime (see e.g. eq.(4.13) in ref. [32]). The C matrix (multiplied by the same factor of 3) differs from the non-supersymmetric result by a factor 1/2. This is because after substituting $\tilde{H}_d = -\tilde{H}_u$ (see eq.(C.3)) all the chemical potential conditions are formally the same than in the SM with \tilde{H}_u identified with the chemical potential of the scalar Higgs, but since C expresses the result for number densities, in the SM a factor of 2 from boson statistics appears for the SM Higgs. This agrees with the analysis in ref. [106], and is a general result that holds for supersymmetry within the SE regime.

¹To compare with the corresponding matrix obtained in the non-superequilibrium regime see eq. (5.33).

C.3 Electron and up-quark Yukawa reactions out of equilibrium

Raising the temperature above $10^5(1 + \tan^2 \beta)$ GeV the interactions mediated by the electron Yukawa h_e are not able to maintain equilibrium, and one condition in eq. (5.21) for $\alpha = e$ is lost. However, since in the effective theory at this temperature one can set $h_e \rightarrow 0$, one global symmetry is gained. This corresponds in the fermion sector to chiral symmetry for the R-handed electron, that in the present case translates into a symmetry under phase rotations of the e chiral multiplet that holds in the limit of unbroken supersymmetry. Conservation of the corresponding charge ensures that $\Delta n_e + \Delta n_{\tilde{e}} = 3\Delta n_e$ is constant, and since leptogenesis aims to explain dynamically the generation of a lepton asymmetry we set this constant to zero, so that the R-handed electron chemical potential is $e = 0$. In this way the chemical equilibrium condition that is lost is replaced by a new condition implied by the conservation of a global charge, and three independent chemical potentials (or alternatively the three non-anomalous charges (C.6)) are still sufficient to describe all the density asymmetries of the thermodynamic system. At temperatures above $T \sim 2 \cdot 10^6$ GeV interactions mediated by the up-quark Yukawa coupling h_u drop out of equilibrium. In this case however, by setting $h_u \rightarrow 0$ no new symmetry is obtained, since chiral symmetry for the R-handed quarks is anomalous and the corresponding charge is not conserved by fast QCD sphaleron interactions. However, after dropping the first condition in eq. (5.23) for $u_i = u$, the QCD sphaleron condition eq. (C.5) ceases to be a redundant constraint, with the result that also in this case no new chemical potentials are needed to determine all the particle density asymmetries. In this case, the A and C are given by

$$\begin{aligned}
 A^\ell &= \frac{1}{3 \times 2886} \begin{pmatrix} -1221 & 156 & 156 \\ 111 & -910 & 52 \\ 111 & 52 & -910 \end{pmatrix}, \\
 C^{\tilde{H}_u} &= -C^{\tilde{H}_d} = \frac{-1}{2886} (37, 52, 52).
 \end{aligned} \tag{C.9}$$

C.4 First generation Yukawa reactions out of equilibrium

Let us now consider what happens at temperatures $T \gtrsim 4 \cdot 10^6 (1 + \tan^2 \beta)$ GeV, when also the d -quark Yukawa coupling can be set to zero (in order to remain within the SE regime we assume $\tan \beta \sim 1$). In this case the equilibrium dynamics is symmetric under the exchange $u \leftrightarrow d$ (both chemical potentials enter only the QCD sphaleron condition eq. (C.5) with equal weights) and so must be any physical solution of the set of constraints. Thus, the first condition in eq. (5.24) can be replaced by the condition $d = u$, and again three independent quantities suffice to determine all the particle density asymmetries. The corresponding result is² :

$$\begin{aligned}
 A^\ell &= \frac{1}{3 \times 2148} \begin{pmatrix} -906 & 120 & 120 \\ 75 & -688 & 28 \\ 75 & 28 & -688 \end{pmatrix}, \\
 C^{\tilde{H}_u} &= -C^{\tilde{H}_d} = \frac{-1}{2148} (37, 52, 52),
 \end{aligned} \tag{C.10}$$

that agree with what is obtained in non-supersymmetric leptogenesis (see eq. (4.12) of ref. [32]) after the factor 1/2 for the higgsinos discussed below eq. (C.8) is accounted for.

²To compare with the corresponding matrix obtained in the non-superequilibration regime see eq. (5.36).